ZooKeys 810: 1–18 (2018)
doi: 10.3897/zookeys.810.26910
http://zookeys.pensoft.net

RESEARCH ARTICLE

A peer-reviewed open-access journal
ZooKeys
Launched to accelerate biodiversity research

Prionospio from the coast of the Iberian Peninsula, with the description of two new species (Annelida, Spionidae)

Víctor Hugo Delgado-Blas[1], Óscar Díaz-Díaz[2,3], José M. Viéitez[4]

1 *Universidad de Quintana Roo, División de Ciencias e Ingeniería, Chetumal, Quintana Roo, 77010, México* **2** *Postgrado en Ciencias Marinas-Instituto Oceanográfico de Venezuela, Universidad de Oriente, Cumaná, Sucre, Venezuela* **3** *FAUNAMAR LTDA, Consultorías Medio Ambientales e Investigación Marina, Santiago, Chile* **4** *Departamento de Ciencias de la Vida, Universidad de Alcalá, 28871, Alcalá de Henares, Spain*

Corresponding author: *V.H. Delgado-Blas* (vhdblas@hotmail.com; blas@uqroo.edu.mx)

Academic editor: *Chris Glasby* | Received 29 May 2018 | Accepted 7 November 2018 | Published 20 December 2018

http://zoobank.org/CC6F3E3E-A8C4-44DD-8CA9-5A14DC7FAAFD

Citation: Delgado-Blas VH, Díaz-Díaz Ó, Viéitez JM (2018) *Prionospio* from the coast of the Iberian Peninsula, with the description of two new species (Annelida, Spionidae). ZooKeys 810: 1–18. https://doi.org/10.3897/zookeys.810.26910

Abstract

Five species of *Prionospio* Malmgren, 1867, each with four pairs of branchiae, are studied from coast of the Iberian Peninsula. Two of these species, *Prionospio cristaventralis* **sp. n.** and *P. parapari* **sp. n.,** are new to science, whereas *P. caspersi* Laubier, 1962*, P. fallax* Söderström, 1920, and *P. ehlersi* Fauvel, 1928 have been previously recorded. *Prionospio cristaventralis* **sp. n.** is characterized by having ventral crests present on chaetigers XI–XIX, dorsal crests and low crests on chaetigers X–XXXIV, triangular neuropodial postchaetal lamellae with pointed ventral edges on chaetiger II, oval neuropodial lamellae on chaetiger III, digitiform pinnules on the posterior face of the first and fourth pairs, and branchial pairs II and III are triangular. *Prionospio parapari* **sp. n.** is characterized by having rounded neuropodial postchaetal lamellae on chaetiger I, digitiform pinnules on the posterior face of the first and fourth pairs, branchial pairs II and III are cirriform, low dorsal crests on chaetigers VIII–IX, and oval neuropodial lamellae with enlarged dorsal edges on chaetiger III. A key is given to all *Prionospio* species with four pairs of branchiae known from the Iberian Peninsula coastline.

Keywords

key to species, morphology, Polychaeta, spionids, systematics, taxonomy

Introduction

Prionospio was established by Malmgren (1867) for *P. steenstrupi* Malmgren, 1867, a spionid species with branchiae on chaetigers II–V, the first and fourth pairs of which are pinnate, and the second and third pairs apinnate. With the discovery of additional species, the diagnosis of the genus was widened to include species with different branchial shapes and arrangements, with the chaetiger upon which the branchiae first arise being particularly relevant. Variability has thus increased, making *Prionospio* a very heterogeneous genus with about 100 species (Sigvaldadóttir 1998). As a result, several authors have suggested that some of these should be reclassified into new genera and/or subgenera (Foster 1971, Blake and Kudenov 1978, Maciolek 1985, Wilson 1990, Sigvaldadóttir 1998).

So far *Prionospio caspersi* Laubier, 1962, *P. fallax* Södreström, 1920, and *P. ehlersi* Fauvel, 1928 have been recorded from the Iberian Peninsula: the former from Catalonia (Desbruyères et al. 1972) and from off Aveiro (Ravara and Moreira 2013); the second from several localities on the Portuguese coast (Quintino and Gentil 1987; Quintino et al. 1989; Dexter 1992; Pardal et al. 1992; Gil and Sardá 1999, Ravara and Moreira 2013) and the third from the Bay of Biscay (Aguirrezabalaga and Cebeiro 2005), from Coruña (Amoureux 1972, López Jamar and González 1986), from off Aveiro and off Porto (Amoureux 1974, Pardal et al. 1992), and from the South western continental shelf of Portugal (Gil 2011). In this study, we examined material deposited in the Museo Nacional de Ciencias Naturales de Madrid previously identified as *P. caspersi* and *P. fallax*.

Following the careful comparison between the redescription of *P. fallax* by Sigvaldadóttir and Mackie (1993), redescription of *P. ehlersi* by Mackie and Hartley (1990) as well as the original description of *P. caspersi*, we describe two new species: *P. cristaventralis* sp. n. and *P. parapari* sp. n. An identification key and a map with type localities are provided for all known *Prionospio* species with four branchial pairs from the coastline of the Iberian Peninsula (Fig. 1).

Materials and methods

The material examined belongs to the collections maintained at the Museo Nacional de Ciencias Naturales de Madrid, Spain (**MNCNM**) and the Alcalá de Henares University, Spain, as well as the personal collection of J Parapar at the University of La Coruña, Spain. Type specimens of the two newly described species are deposited in the MNCNM. For each species, the location where the specimens were collected is indicated in their respective sections.

All material was fixed in 10% formaldehyde in sea water and preserved and stored in 70% ethanol. In order to examine some morphological characters, specimens were dipped first into water and then into methyl green solution for staining. The color fades quickly when specimens are returned to the alcohol solution (Warren et al. 1994). Specimens were measured with a millimeter ruler: body widths refer to the maximum postbranchial body width (including parapodia but not chaetae) at about chaetiger VIII. The eye color mentioned in the descriptions of the species was based on preserved organisms.

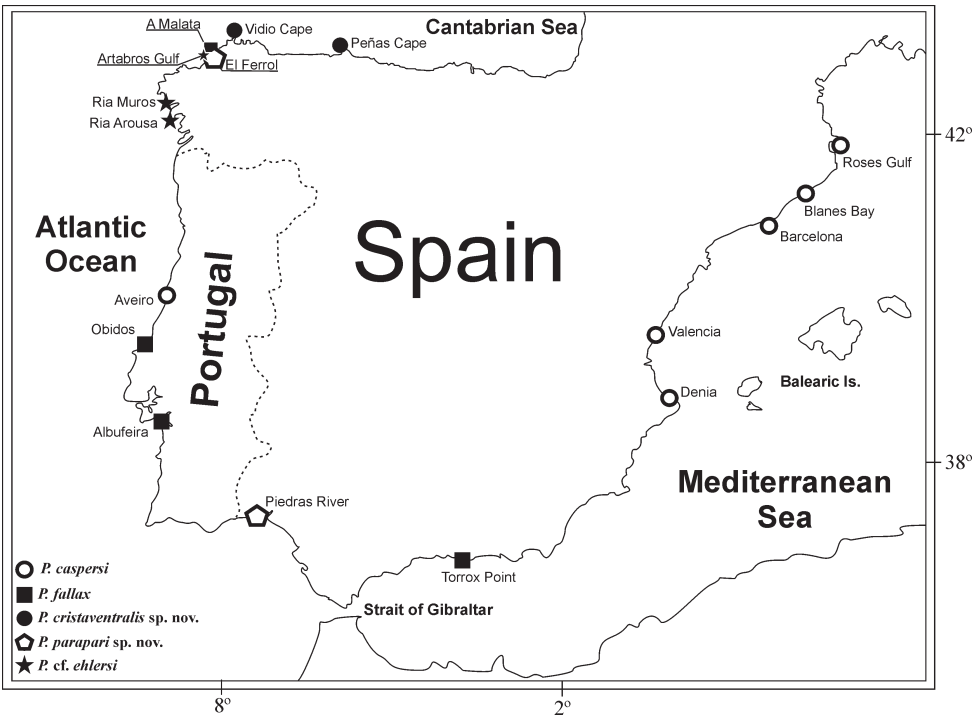

Figure 1. Collection localities of *Prionospio* species from the Iberian Peninsula.

Systematic section

Spionidae Grube, 1850
***Prionospio* Malmgren, 1867 sensu stricto**

Type species. *Prionospio steenstrupi* Malmgren, 1867, by monotypy.

Prionospio caspersi Laubier, 1962

Prionospio caspersi Laubier, 1962:135–148, figs 1–3.
Prionospio (*Prionospio*) *caspersi*: Imajima 1990: 111–114, figs 4–5; Dagli and Çinar 2009: 3.

Material examined. Mediterranean Sea. Valencia: 3 specimens (MNCNM 16.01/4313), 39°43'16"N, 0°10'37"W, coll. G San Martín, April 1998. 1 specimen (MNCNM 16.01/9834), Denia, Alicante, 38°51'17"N, 0°5'37"E, coll. G San Martín, December 1997. 1 specimen (MNCNM 16.01/9836), Denia, Alicante, 38°51'17"N, 0°5'37"E, coll G San Martín, December 1997.

Description. Incomplete specimens, 5.5–8.5 mm long for 30–50 chaetigers, 0.5 mm wide. Prostomium triangular, slightly truncate to convex anteriorly, poste-

riorly tapered, with narrow caruncle extending to posterior edge of chaetiger I. Two pairs of small black subdermal eyes. Peristomium short, fused dorsally with chaetiger I. Four pairs of branchiae present on chaetigers II–V; pairs 1–3 apinnate, densely ciliated laterally; pair four with numerous digitiform pinnules, on lateral and posterior faces of stems, and naked, smooth distal tips. Notopodial postchaetal lamellae largest in branchial region, lamellae triangular; neuropodial lamellae lanceolate; high dorsal crest across dorsum on chaetiger VII. Sabre chaetae from chaetiger XI, neuropodial hooded hooks from chaetigers XVI–XVII; notopodial hooded hooks from chaetigers XXXII–XXXIII. All hooks with one tooth above main tooth.

Remarks. The specimens examined in this study agree with the original and subsequent descriptions of the species (Laubier 1962, Imajima 1990, Dagli and Çinar 2009). However, there is a slight difference between our specimens and Dagli and Çinar's specimens: the sabre chaetae were reported as present from chaetiger X by Dagli and Çinar (2009) whereas they first appear on chaetiger XI in our specimens. There are a few further differences between the specimens examined here and the description given by Imajima (1990). Imajima (1990) described the prostomium as being broadly flared anteriorly, with a slight medial indentation and unilimbate chaetae, whereas the specimens in this study have a narrower prostomium that is slightly truncate to convex anteriorly, with bilimbate chaetae. Due, to these morphological differences, the identity of the specimens recorded as *P. caspersi* from Japan by Imajima (1990) should be verified.

Habitat. *Zostera marina*, sand, muddy sand, depth 3–68 m.

Distribution. Mediterranean Sea: Italy, Venetian Lagoon (type locality); Southern coast of Turkey; Black Sea; Iberian coasts: Aveiro (Portugal), Catalonia, Valencia, Denia (Alicante); Pacific Ocean: Japan.

Prionospio cf. *ehlersi* Fauvel, 1928

Figure 2A–R

Material examined. Atlantic Ocean. Galicia: 4 specimens (MNCNM 16.01/18424), Ría de Arousa, La Coruña, GA EBS 250, VERTIDOS 04, 42°36'23"N, 8°53'20"W, 26 September 2004, coll. J Parapar; 6 specimens (MNCNM 16.01/18425), GA EBS 200, VERTIDOS 04, 42°36'22"N, 8°52'20"W, 26 September 2004, coll. J Parapar; 17 specimens (MNCNM 16.01/18426), shelf and upper slope off the Artabro Gulf: GA AT 110–4, 43°29'15"N, 8°28'41"W, 25 September 2004, coll. J Parapar; 1 specimen (MNCNM 16.01/18427), DIVA-Artabria 2003: EBS 250, 43°40'14"N, 8°44'3"W, 12 September 2003, coll. J Parapar; 3 specimens (MNCNM 16.01/18428), EBS 1 200E, 43°43'40"N, 8°36'49"W, 12 September 2003, coll. J Parapar; 2 specimens (MNCNM 16.01/18429), EBS 200, 43°43'40"N, 8°36'49"W, 12 September 2003, coll. J Parapar; 25 specimens (MNCNM 16.01/18430), EBS 200, 43°43'40"N, 8°36'49"W, 12 September 2003, coll. J Parapar; 23 specimens (MNCNM 16.01/18431), EB5 200, 43°43'40"N, 8°36'49"W; 3 specimens (MNCNM 16.01/18432), EBS 150 W, 43°31'36"N, 8°43'56"W; 14 September 2003, coll. J Parapar.

Description. Incomplete specimens, 3.0–11.0 mm long, with 13–40 chaetigers, 0.6–1.0 mm wide. Posterior fragment 9.0 mm long for 26 chaetigers, 0.8 mm wide. Color in alcohol pale white. Some specimens with oocytes on chaetigers XXX–XXXIV.

Prostomium bottle-shaped, rounded anteriorly (Fig. 2A, A', B), posteriorly tapered, with short, narrow caruncle extending to anterior edge of chaetiger II; caruncle with large triangular nuchal organs on either side (Fig. 2A', B). Two pairs of black subdermal eyes, arranged in a trapezoid; anterior pair small, rounded, posterior pair small, crescent-shaped; one paratype without eyes (Fig. 2A, A', B). Palps lost, except in one specimen with palps inserted anterior to nuchal organs: left palp in process of regeneration, with a short basal sheath (Fig. 2C). Peristomium short, collar-like, surrounding prostomium, partially fused dorsally with very large oval notopodial lamellae on chaetiger I (Fig. 2A, B). Neuropodial postchaetal lamellae on chaetiger I small, rounded (Fig. 2A, A', B), smaller than notopodial lamellae. Eversible, sac-like proboscis.

Four pairs of branchiae present on chaetigers II–V, first pair longest and thickest (Fig. 2D); sometimes first and fourth pairs equal in length or fourth pair slightly longer than first. First pair with long, dense digitiform pinnules on lateral and posterior faces, continuing to tip; central stem of branchial pair 1 pinnate, cylindrical, very thick and with a blunt tip (Fig. 2A, D). Pairs 2–4 apinnate; pairs 2 and 3 triangular, thick (Fig. 2D, E), slightly expanded distally, with rounded tips, densely ciliated laterally, shorter than notopodial lamellae and pinnate pair. Pair 4 cirriform (Fig. 2D), basally united by a short, moderate dorsal cord-shape (Fig. 2D); branchiae subequal to, or longer than, notopodial lamellae; some specimens with regenerating branchiae.

Notopodial postchaetal lamellae subtriangular, short on chaetiger II (Fig. 2A, B, D); lamellae on chaetigers III–VII triangular with wide bases (Fig. 2A, B, D); larger and wider on chaetigers III– IV, with long, triangular tips (Fig. 2A, B, E) (in some specimens, the notopodial lamellae on chaetigers III–IV touch each other). Lamellae gradually becoming smaller, rounder and more dorsally directed on chaetiger VIII (Fig. 2F); lamellae on chaetiger XIX subtriangular and becoming angular with ventrally-directed process. Subsequent lamellae progressively decreasing in size, and becoming rounded and wider with ventrally pointed edges (Fig. 2G). Lamellae on posterior chaetigers oval. Notopodial postchaetal lamellae united across dorsum, forming a low dorsal crest, starting on chaetiger VI (Fig. 2D) and continuing as a very low fold or large crest (in large specimens) (Fig. 2H) up to almost end of body. Ventral and dorsal edges of notopodial and neuropodial lamellae touching or overlapping (Fig. 2I) from chaetigers VII–X, up to about chaetiger XX. Anterior notopodial prechaetal lamellae low, rounded; posterior lamellae rudimentary.

Anterior neuropodial postchaetal lamellae large, rounded on chaetiger II (Fig. 2B); very large, more angular and dorsally directed on chaetiger III (Fig. 2E); oval on chaetigers IV–XV (Fig. 2J); subsequent neuropodial lamellae small, rounded up to end of body. Neuropodial prechaetal lamellae low in branchial region (Fig. 2F, J), thereafter increasing in size; some specimens with small ventral rounded lobe like extensions of

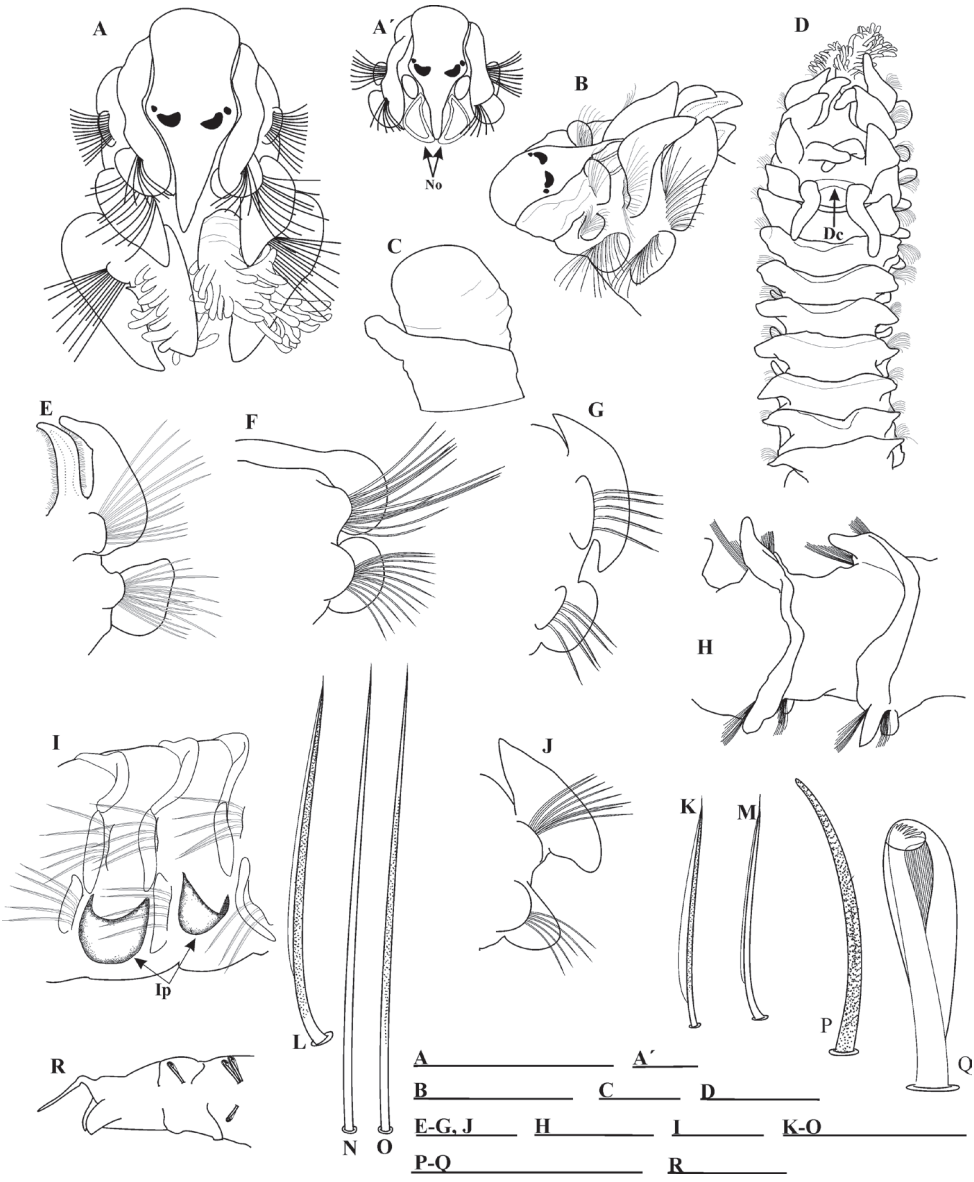

Figure 2. *Prionospio* cf. *ehlersi*: **A** Anterior end, dorsal view **A'** Prostomium and detail of nuchal organ **B** anterior end, dorso-lateral view **C** detail of palp showing the short basal sheath **D** anterior end, dorsal view **E** parapodium and branchia of chaetiger 3 **F** parapodium of chaetiger VIII **G** parapodium of posterior chaetiger **H** dorsal crest on middle chaetigers **I** interpodial pouches **J** parapodium of chaetiger V **K** unilimbate notopodial chaeta from anterior row of chaetigers I ,II **L** notopodial capillary chaeta from posterior row of chaetigers I, II **M** smooth, unilimbate, middle notopodial capillary from middle chaetigers **N** long, smooth, alimbate posterior capillary **O** slightly granulated, alimbate capillary from middle chaetigers **P** sabre chaeta **Q** neuropodial hooded hook **R** pygidium, lateral view. Abbreviations: Dorsal cord (Dc), Nuchal organ (No), Interpodial pouches (Ip). Scale bars: 0.9 mm (**A, B, D, H, R**); 0.25 mm (**A'**); 0.07 mm (**C**); 0.5 mm (**E–G, I, J**); 0.04 mm (**K–O, P, Q**).

neuropodial prechaetal lamellae on middle chaetigers, rudimentary on posterior chaetigers. Interparapodial pouches (Fig. 2I) from chaetigers IV–V up to end of fragments, non-reticulated; interparapodial pouches fused with neuropodial prechaetal lamellae.

Notopodial capillaries on chaetigers I–II arranged in two rows, with short, slender, slightly granulated and unilimbate chaetae (Fig. 2K); posterior row longer than anterior one. Notopodial capillaries on chaetigers III–XIII arranged in three rows, anterior row shortest; dorsal chaetae very long and acute (Fig. 2L), ventral chaetae very short and acute; capillaries on middle chaetigers smooth, unilimbate (Fig. 2M); posterior capillaries long, smooth, alimbate (Fig. 2N). Anterior neuropodial chaetigers with granulated, unilimbate capillaries arranged in two rows, anterior row much shorter than the posterior one; capillaries on middle chaetigers slightly granulated, alimbate (Fig. 2O); capillaries on posterior chaetigers smooth, alimbate. Neuropodial sabre chaetae from chaetigers XVII–XX up to two per parapodium, each chaeta long, stout, heavily granulated, alimbate (Fig. 2P). Neuropodial hooded hooks (Fig. 2Q) from chaetigers XVIII–XX, up to 15 per fascicle; notopodial hooded hooks not observed up to chaetiger XL (present in a posterior fragment up to 10 per fascicle); hooks with six pairs of small teeth (Fig. 2Q) above thick, blunt main tooth, and a large principal hood; hooks also appear to possess very striated secondary hoods, producing a feathered effect below main tooth (Fig. 2Q).

Pygidium with one long median cirrus and two short, rounded, lateral lobes (Fig. 2R).

Remarks. *Prionospio* cf. *ehlersi* is very similar to the original and subsequent descriptions of *P. ehlersi* (Fauvel 1928, Mackie and Hartley 1990), in that both describe the same prostomial shape, branchial arrangement, and hooded hook structure, and all have interparapodial pouches. However, specimens of this study differ from *P. ehlersi* in that the former have oval (rather than triangular to subtriangular) notopodial lamellae on chaetiger I, the neuropodial lamellae on chaetigers IV–V are oval (rather than rounded), and the second and third branchial pairs are triangular and thick (rather than expanded or swollen distally), a dorsal cord-shape (rather than low crest) on chaetiger V is present, and the sabre chaetae in *P.* cf. *ehlersi* are alimbate (rather than sheathed). Mackie and Hartley (1990) reported a variation in the shape of chaetiger I notopodial postchaetal lamellae, and so considered this unimportant. They also noted some parapodial variation around chaetiger XVIII–XX. They did not mention the oval anterior neuropodial postchaetal lamellae, however, Fauvel (1928, fig. 1b) shows a chaetiger IV with neuropodial lamella very similar to that in this study (Fig. 2J). We consider that these differences are important, but we consider it premature to erect a new species with these specimens, without being able to first compare them with Fauvel's syntype material. The syntypes are deposited at the Museum National d'Histoire Naturelle, Paris under MNHN A438, A449. However, the material cannot be sent abroad for re-examination.

Type locality. Ría de Arousa (La Coruña, Galicia, Spain).

Distribution. Atlantic Ocean. Galicia: Ría de Arousa, La Coruña, shelf and upper slope off the Artabro Gulf, Spain.

Prionospio fallax Söderström, 1920

Prionospio fallax Söderström, 1920: 235–237, figs 135, 144–145; Sigvaldadóttir and Mackie 1993: 207–211, figs 3–5, tables 1–2.

Material examined. Atlantic Ocean, La Coruña: 1 specimen (MNCNM 16.01/15809), A Malata, Ría de Ferrol, 43°29'30"N, 8°14'40"W, coll. J Parapar, 26 October 2000; Mediterranean Sea. Andalucia: 2 specimens (MNCNM 16.01/8756), Punta Torrox, Malaga, 36°43'33"N, 3°57'28"W, coll. G San Martín, February 1995.

Description. Incomplete specimens, 4.5–6.5 mm long for 39–49 chaetigers, 0.5 mm wide. Prostomium bottle-shaped, truncated anteriorly with lateral edges rounded, posteriorly tapered, with a long, blunt caruncle extending to anterior edge of chaetiger II. Two pairs of brown eyes, arranged in a trapezoid; anterior pair small, rounded; posterior pair large, reniform. Four pairs of branchiae present on chaetigers II–V; pairs 1 and 4 equal in size with sparse lateral digitiform pinnules and long naked distal tips; pairs 2 and 3 apinnate, triangular with dense lateral ciliation and sharply pointed tips; shorter than pinnate pairs. Noto- and neuropodial postchaetal lamellae smallest on chaetiger I, rounded in both rami; notopodial lamellae foliaceous, largest on chaetigers III–IV; progressively decreasing in size through chaetigers V–X, becoming rounded. Neuropodial postchaetal lamellae largest in branchial region; lamellae large, subtriangular, ventrally pointed on chaetiger II; those of chaetiger III with dorsally pointed tip; rounded on middle chaetigers, becoming rather inconspicuous on posterior chaetigers. High dorsal crest on chaetiger VII only; no crests on following chaetigers. Interparapodial pouches absent. Sabre chaetae from chaetiger X, up to two per fascicle; neuropodial hooded hooks from chaetigers XII–XIV; notopodial hooded hooks from chaetigers XL–XLIII; hooks multidentate with three to four pairs of small teeth above main tooth and secondary hood.

Remarks. These specimens match the redescription given by Sigvaldadóttir and Mackie (1993), except that we found some specimens with eyes and others without eyes; one specimen had a single large brown eyespot. Possibly, the variation is due to the preservation of the specimens.

Habitat. Silty (mud with much detritus) sediments, depth 25–140 m.

Distribution. Northeast Atlantic, from northern Scotland (Shetland Islands) to the Mediterranean.

Prionospio cristaventralis sp. n.

http://zoobank.org/892F5C2D-3F46-4923-94C3-C8FB2DC99A42
Figure 3A–Q

Material examined. Atlantic Ocean. Cantabrian Sea: **Holotype** (MNCNM 16.01/3983), Between Cabo Vidio and Cabo de Peñas, Asturias, Z2 D59, depth 25.6

m, 43°33'30"N, 6°7'1"W, colls. G San Martin and R Acuña Castroviejo, 1998. 1 **paratype** (MNCNM 16.01/3984), depth 34.5 m, 43°33'30"N, 6°7'1"W, colls. G San Martin and R Acuña Castroviejo. 1 **paratype** (MNCNM 16.01/3985), depth 24 m, 43°33'30"N, 6°7'1"W, colls. G San Martin and R Acuña Castroviejo, 1998. 1 **paratype** (MNCNM 16.01/3986), depth 34 m, 43°33'30"N, 6°7'1"W, colls. G San Martin and R Acuña Castroviejo, 1998.

Description. Holotype incomplete, 18 mm long with 34 chaetigers, 1.1 mm wide. Paratypes incomplete, 12.0–13.0 mm long, 22–23 chaetigers, 0.9–1.1 mm wide. Color in alcohol pale white. Prostomium bottle-shaped, broadly rounded, flared anteriorly (Fig. 3A), flattened dorso-ventrally on anterior margin (Fig. 3B), posteriorly tapered, with long, narrow caruncle extending to the posterior edge of chaetiger II, with U-shaped nuchal organs on both sides (Fig. 3A). Two pairs of black subdermal eyes in a trapezoidal arrangement; anterior pair small, rounded, posterior pair very large, crescent-shaped (Fig. 3A, B). Palps lost. Peristomium short, collar-like, surrounding the prostomium, not fused dorsally, with moderate, oval notopodial lamellae on chaetiger I (Fig. 3A–C). Neuropodial postchaetal lamellae on chaetiger I large, oval with ventral edge elongated (Fig. 3A–C), much larger than the notopodial lamellae; notopodial and neuropodial prechaetal lamellae lacking on chaetiger I.

Four pairs of long branchiae present on chaetigers II–V (Fig. 3A, B), first pair longest (Fig. 3B). Pairs 1 and 4 with long, slender, dense digitiform pinnules on posterior face of stems (Fig. 3A, B); branchiae with very long, naked, smooth distal tips, pinnulated basally; pinnule distribution similar on both pairs; pinnules long, slender, blunt in middle and basal regions of branchiae. Pairs 2 and 3 apinnate, triangular, broad, with short pointed tips, densely ciliated laterally (Fig. 3A, B), subequal in length, shorter than pinnate pairs, but slightly longer than notopodial lamellae. Pairs 3 and 4 each united basally by low crest across dorsum (Fig. 3A).

Notopodial postchaetal lamellae on chaetigers II–VII foliaceous with wide bases (Fig. 3A–C), distal halves narrow and elongated; larger and wider on chaetigers III and IV, with long, pointed tips; becoming more oval on chaetigers VIII–X (holotype X) (Fig. 3B, D); lamellae progressively decreasing in size and becoming subtriangular on chaetigers XV– XIX, assuming a more angular form with a ventrally-directed process (Fig. 3E). Subsequent lamellae progressively decreasing in size, and becoming subtriangular (Fig. 3F). Notopodial postchaetal lamellae united across dorsum of chaetigers X and XI forming high dorsal crests (Fig. 3G); on chaetigers XII–XXII/XXXIV (end fragment) forming low dorsal crests. Ventral edges of notopodial lamellae and dorsal edges of neuropodial lamellae not touching on any chaetigers (Fig. 3B–D). Notopodial prechaetal lamellae very large in anterior region, basally fused with notopodial postchaetal lamellae (Fig. 3A, B, D); prechaetal lamellae on chaetigers XI–XV and subsequent lamellae progressively decreasing in size, split, and becoming rounder and smaller (Fig. 3E).

Neuropodial postchaetal lamellae large, triangular, with ventrally-directed process, enlarged on chaetiger II (Fig. 3B); neuropodial lamellae oval on chaetigers III-IX

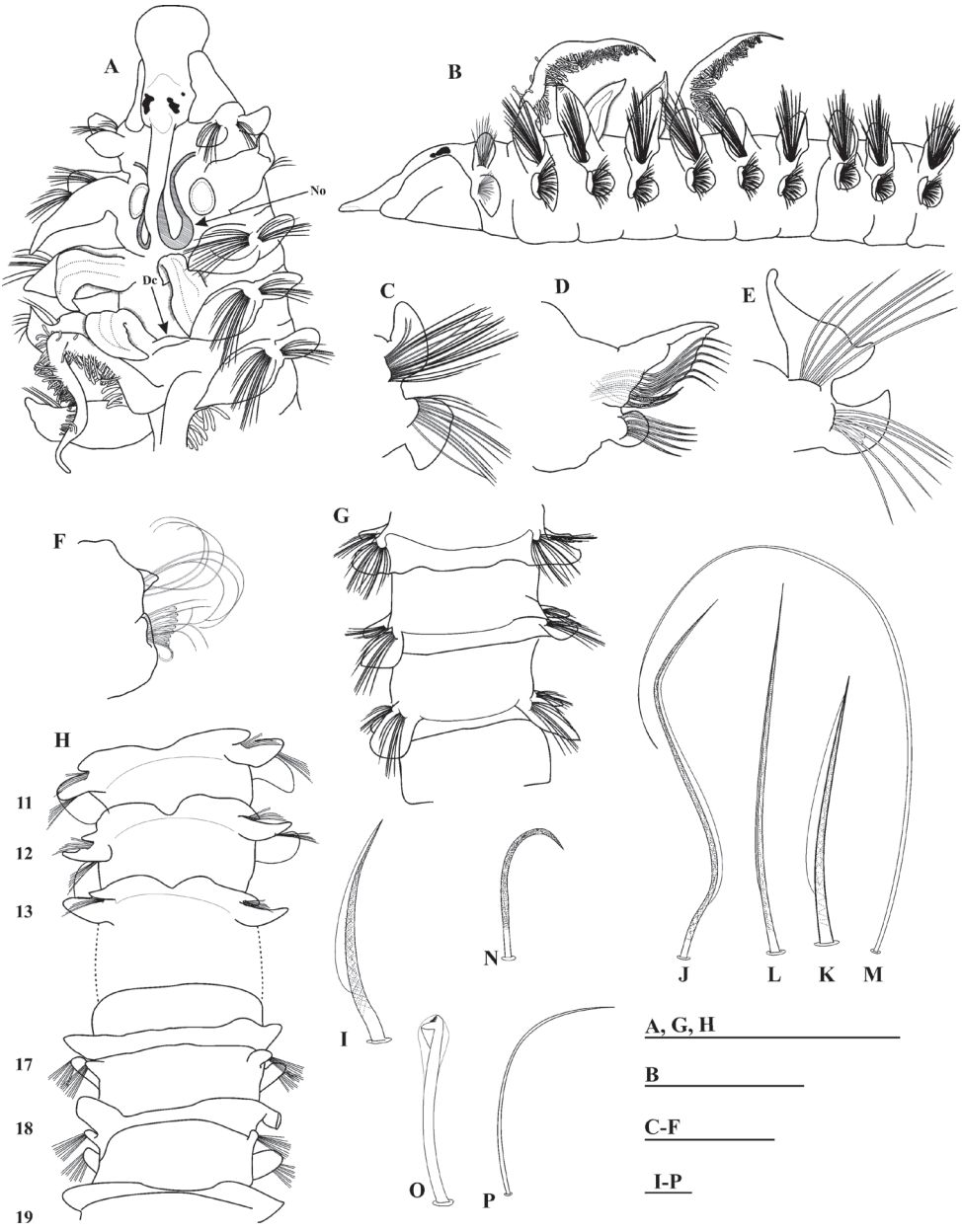

Figure 3. *Prionospio cristaventralis* sp. n. (Holotype MNCNM 16.01/3983: **A, B, G** Paratype MNCNM 16.01/3984: **C, D, E, H, I**): **A** Anterior end, dorso-lateral view **B** anterior end, lateral view **C** Parapodium of chaetiger I (paratype) **D** Parapodium of chaetigers X **E** parapodium of chaetigers 15 **F** parapodium of posterior chaetiger **G** dorsal crest **H** ventral crest **I** short, granulated, unilimbate, notopodial capillary chaeta from anterior row **J** granulated, unilimbate, notopodial capillary chaeta from posterior row of anterior chaetigers **K** short, granulated, unilimbate, notopodial capillary chaeta from anterior row of middle chaetigers **L** granulated, unilimbate, notopodial capillary chaeta from posterior row of middle chaetigers **M** very long, smooth, slender, alimbate, notopodial capillary chaeta from posterior chaetigers **N** sabre chaeta **O** neuropodial hooded hook **P** companion, thin, alimbate capillary chaeta. Abbreviations: Dorsal crest (Dc), Nuchal organ (No). Scale bars: 1 mm (**A, B, G, H**); 0.4 mm (**C–F**); 0.001 mm (**I–P**).

(Fig. 3B), small and rounded on chaetigers X–XIII (Fig. 3D), thereafter, becoming triangular with long, pointed tips (Fig. 3E); subsequent neuropodial lamellae more small (Fig. 3F). Anterior neuropodial prechaetal lamellae short (Fig. 3B, D), progressively increasing in size, becoming rounded and very large on chaetigers XI–XII, connected through well-developed ventral crests forming U-shaped depressions at midline (Fig. 3H); large crests continuing through chaetigers XV–XIX (Fig. 3H); subsequent chaetigers without ventral crests. Interparapodial pouches lacking.

Notopodial capillaries on chaetigers I–V arranged in two rows: anterior row short, heavily granulated, unilimbate (wide limbation), very acute (Fig. 3I); posterior row longer, thinner, more heavily granulated (Fig. 3J); capillaries arranged in three rows on chaetiger VI, similar to anterior chaetae. Notopodial capillaries in middle chaetigers arranged in two rows: anterior row short, granulated, unilimbate (Fig. 3K); posterior row granulated, unilimbate, with very long and pointed tips (Fig. 3L); posterior chaetigers with very long, slender, smooth, alimbate chaetae (Fig. 3M). Neuropodial capillaries on chaetigers I–V arranged in two rows; neuropodial capillaries on chaetigers VI–X arranged in three rows; all capillaries with same structure as notopodial chaetae. Sabre chaetae in neuropodia from chaetiger X, one per fascicle, each chaeta stout, distinctly curved, basally smooth, heavily granulated medially and distally, without sheaths (Fig. 3N). Neuropodial hooded hooks (Fig. 3O) from chaetiger XV, up to 10 per fascicle, accompanied by thin, alimbate capillaries (Fig. 3P). All hooks with six pairs of small teeth above large main tooth, and short, small secondary hoods (Fig. 3O). Notopodial hooded hooks not present on incomplete XXXIV-chaetiger holotype.

Pygidium missing.

Remarks. *Prionospio cristaventralis* sp n. is similar to *P. multicristata* Hutchings & Rainer, 1979, *P. nirripa* Wilson, 1990, *P. nielseni* Hylleberg & Nateewathana, 1991, *P. cornuta* Hylleberg & Nateewathana, 1991, and *P. paradisea* Imajima, 1990 in that all show the same prostomial shape and neuropodial postchaetal lamellae on chaetigers II–III. However, *P. cristaventralis* sp. n. differs from these species due to the presence of ventral crests and dorsal crests limited to chaetigers X–XI, and low dorsal crests on chaetigers XII–XXII/XXXIV (end fragment) compared to low dorsal crests from chaetigers VII to XXV-XXX in *P. multicristata*, low dorsal crests from X–XIII to XX-VIII–XXXVII in *P. nirripa*, *P. nielseni* and *P. cornuta* and high crests from X to LX in *P. paradisea*. *Prionospio cristaventralis* sp. n. is also similar to *P. pacifica* Zhou & Li, 2009 in that both species have dorsal and ventral crests or folds. However, *P. cristaventralis* sp. n. can be distinguished from *P. pacifica* by having a prostomium that is rounded anteriorly (instead of being truncate), dorsal crests on chaetigers IV–V (instead of lacking such crests), and ventral crests on chaetigers XI–XIX (instead of only on chaetiger IX). The presence of ventral crests appears to be a unique feature of these two species.

Etymology. The specific name is from the Latin *crista* meaning crests and *ventralis* meaning ventral.

Type locality. Between Cabo Vidio and Cabo de Peñas, Asturias, Spain.

Habitat. Specimens were collected in shallow water (24–34.5 m depth).

Distribution. Atlantic Ocean. Cantabrian Sea: Between Cabo Vidio and Cabo de Peñas, Asturias, Spain.

***Prionospio parapari* sp. n.**
http://zoobank.org/EFF7C0D4-5E43-4E9D-9BF6-CB12DB8226BE
Figure 4A–Z

Material examined. Atlantic Ocean. **Holotype** (MNCNM 16.01/18433), Mouth of Piedras River, Huelva: St. D24, 37°12'53"N, 7°7'8"W, coll. L Lopez-Serrano, March 1988. 8 **Paratypes** (anterior fragments) (MNCNM 16.01/18434), St. D22, 37°12'42"N, 7°9'8"W, coll. L Lopez-Serrano, November 1987; 6 **paratypes** (MNCNM 16.01/18435), St. D24, 37°12'53"N, 7°7'8"W, coll. L Lopez-Serrano, March 1988; 2 **paratypes** (MNCNM 16.01/18436), St. D25, 37°12'53"N, 7°7'57"W, coll. L López-Serrano, March 1988; 2 **paratypes** and anterior fragments (MNCNM 16.01/18437), St. D29, 37°6'50"N, 7°4'0"W, coll. L Lopez-Serrano, May 1988; 1 **paratype** and 4 anterior fragments (MNCNM 16.01/18438), St. D38, 37°12'45"N, 7°5'57"W, coll. L Lopez-Serrano, November 1988. Coruña: 1 **paratype** (MNCNM 16.01/12588), Ria de Ferrol, Batel Bay, 1 February 2010, coll. J Parapar; 1 **paratype** (MNCNM 16.01/12569), coll. J Parapar; 64 **paratypes** (MNCNM 16.01/125701); 1 **paratype** (MNCNM 16.01/12572), 43°29'9"N, 08°15'15"W; 1 **paratype** (MNCNM 16.01/12573), 43°29'31"N, 8°10'44"W; 6 **paratypes** (MNCNM 16.01/12574), 43°27'38"N, 08°12'14"W; 5 **paratypes** (MNCNM 16.01/12577), 43°28'51"N, 8°11'13"W; 4 **paratypes** (MNCNM 16.01/12578); 2 **paratypes** (MNCNM 16.01/12579); 1 **paratype** (MNCNM 16.01/12580), 43°29'7"N, 8°10'19"W; 1 **paratype** (MNCNM 16.01/12582), 43°28'46"N, 8°11'45"W; 1 **paratype** (MNCNM 16.01/12583), 43°28'31"N, 8°12'14"W; 1 **paratype** (MNCNM 16.01/12589), 43°28'2"N, 8°16'37"W; 6 **paratypes** (MNCNM 16.01/12575), 43°28'51"N, 8°15'15"W; 1 **paratype** (MNCNM 16.01/15810); 1 paratype (MNCNM 16.01/15802); 1 **paratype** (MNCNM 16.01/15800); 1 **paratype** (MNCNM 16.01/15811), Ria de Ferrol, Laxe Bay, coll. J Parapar; Ria de Ferrol, Redonda Point, coll. J Parapar.

Description. Holotype complete, 18.0 mm long with 62 chaetigers, 0.4 mm wide. Complete paratypes, 17.0–21.0 mm long with 47–68 chaetigers, 0.2–0.8 mm wide. Incomplete paratypes, 4.0–12.5 mm long with 14–61 chaetigers, 0.2–0.5 mm wide. Color in alcohol pale white. Prostomium bottle-shaped, truncated and narrow anteriorly, widening in mid-region (Fig. 4A), posteriorly tapered, with long, blunt caruncle extending to anterior edge of chaetiger II (Fig. 4A); caruncle with large V-shaped nuchal organs on either side (Fig. 4A, B). Two pairs of brown-black subdermal eyes (holotype brown), arranged in a trapezoid; anterior pair small, posterior pair very large, both pairs crescent-shaped (Fig. 4A, B) (one specimen lacks eyes). Palps lost. Peristomium moderate in size, collar-like, surrounding prostomium, fused dorsally with large, rounded notopodial lamellae on chaetiger I (Fig. 4A, C). Neuropodial postchaetal lamellae on chaetiger I large, rounded (Fig. 4C), less than half the size of notopodial lamellae.

Four pairs of branchiae present on chaetigers II–V (Fig. 4B, C); first pair longer than fourth pair, up to 1 time and a half longer than the fourth pair. Pairs 1 and 4 with long, slender, dense digitiform pinnules arranged along posterior face of the stems, pinnules thick, long, blunt in middle region of branchiae (Fig. 3B); branchiae with very long, naked, smooth, distal tips (Fig. 4B). Pairs 2 and 3 apinnate, cirriform, long,

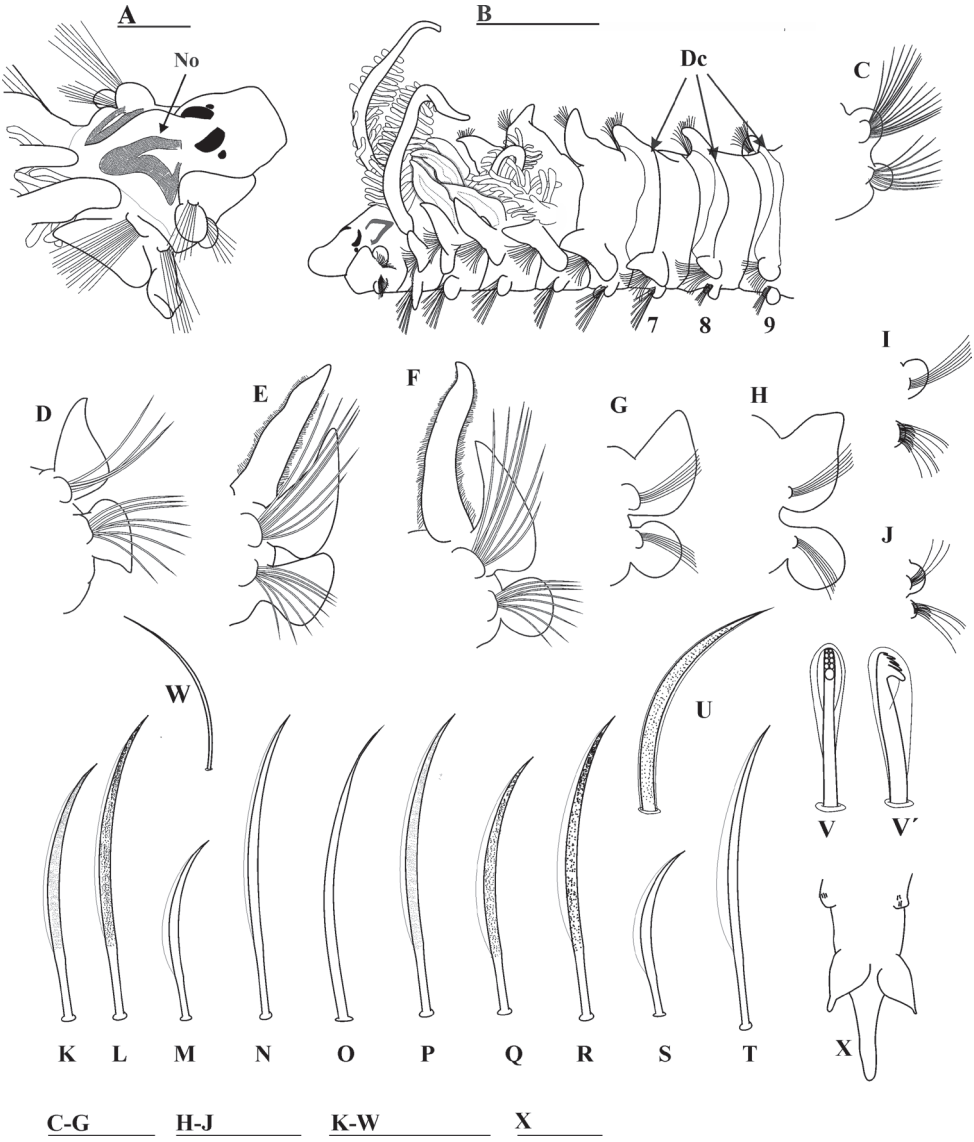

Figure 4. *Prionospio parapari* sp. n. (Holotype MNCNM 16.01/18433: **A, C, L** Paratype MNCNM 16.01/18434: **B**): **A** Anterior end, dorso-lateral view **B** anterior end, dorso-lateral view, showing dorsal crest and crest **C** parapodium of first chaetiger **D–H** parapodium of chaetigers II–VI, frontal view (**D** and **G** with branchiae removed) **I** chaetiger from middle-posterior region **J** chaetiger from posterior region **K** heavily granulated, unilimbate notochaeta from anterior row of anterior chaetigers **L** heavily granulated, unilimbate notochaeta from posterior row of anterior chaetigers **M** unilimbate notochaeta from anterior row of middle chaetigers **N** unilimbate notochaeta from posterior row of middle chaetigers **O** smooth, alimbate chaeta on posterior notopodia **P** slightly granulated, unilimbate neurochaeta from posterior row of anterior chaetiger **Q, R** heavily granulated, unilimbate chaeta from chaetigers II–IX **S,T** smooth, unilimbate neurochaetae from anterior and posterior rows, respectively **U** sabre chaeta **V,V'** neuropodial hooded hooks **W** alternating alimbate capillaries **X** pygidium, ventral view. Abbreviations: Nuchal organ (No), Dorsal crest (Dc). Scale bars: 0.2 mm (**A**); 0.5 mm (**B, X**); 0.4 mm (**G–J**); 0.03 mm (**K–W**).

densely ciliated laterally, with pointed tips (Fig. 4E, F); subequal in length, up to 3 times shorter than pinnate pairs, but longer than notopodial lamellae (Fig. 4B, E, F).

Notopodial postchaetal lamellae triangular and slender on chaetigers II–VI (Fig. 4D–H); largest on chaetigers III–IV, with short triangular tips (Fig. 4E, F); becoming wider on chaetigers V–VI (Fig. 4G, H) and thereafter progressively decreasing in size; small, rounded on middle and posterior chaetigers (Fig. 4I, J). Notopodial lamellae united across dorsum, forming a high dorsal crest on chaetiger VII and low dorsal crests on chaetigers VIII–IX (Fig. 4A); some specimens without dorsal crests on chaetiger IX, subsequent chaetigers lacking crests. Ventral and dorsal edges of notopodial and neuropodial lamellae touch only on chaetiger III (Fig. 4E). Notopodial prechaetal lamellae moderate and oval in branchial region (Fig. 4E–G), not basally fused with notopodial postchaetal lamellae, inconspicuous thereafter (Fig. 4H–J).

Anterior neuropodial postchaetal lamellae rounded (Fig. 4C, F–H) throughout, except on chaetigers II–III; lamella on chaetiger II triangular, large, with ventral edge enlarged, pointed (Fig. 4D); lamella on chaetiger III oval with dorsal edge enlarged (Fig. 4E); second and third pairs larger than other neuropodial lamellae; subsequent neuropodial lamellae small and rounded on middle chaetigers (Fig. 4I), and rounded lobes on posterior chaetigers (Fig. 4J). Neuropodial prechaetal lamellae low in anterior region (Fig. 4C–H), rudimentary throughout. Interparapodial pouches lacking. All anterior and middle notopodial chaetae arranged in two rows. Notochaetae on chaetigers I–IX heavily granulated, unilimbate (Fig. 4K, L); posterior row longer, more heavily granulated (Fig. 4L) than anterior row (Fig. K); both rows of chaetae on middle notopodia thin, smooth, unilimbate (Fig. 4M, N); anterior row shorter (up to half) (Fig. 4M) than posterior row (Fig. 4N); posterior notopodia with smooth, alimbate chaetae (Fig. 4O) arranged in one row. All neuropodial capillaries arranged in two rows; capillaries on chaetiger I slightly granulated, unilimbate (Fig. 4P); chaetigers II–IX with heavily granulated, unilimbate neurochaetae (Fig. 4Q, R); posterior row more heavily granulated (Fig. 4R), with limbation wider than for notochaetae. Neurochaetae smooth, unilimbate on subsequent chaetigers, those on anterior row up to three times shorter and wider (Fig. 4S) than those on posterior row; limbation of posterior row wider than that of the anterior one (Fig. 4T); chaetae on posterior neuropodia arranged in one row. Neuropodial sabre chaetae from chaetigers X–XII (holotype X), up to two per fascicle, each chaeta stout, curved, heavily granulated, bilimbate (Fig. 4U). Neuropodial hooded hooks (Fig. 4V, V') from chaetigers XI–XV (holotype XIII), up to eight per fascicle, alternating with long, thin, alimbate capillaries (Fig. 4W). Notopodial hooded hooks on chaetigers XXIX–XXXVIII (holotype XXXIII), up to six per fascicle, alternating with up to two thin, alimbate capillaries, hooks on posterior chaetigers longer than those on middle chaetigers; all hooks with four pairs of small teeth above main tooth, and large secondary hoods (Fig. 4V, V').

Pygidium with one long median cirrus and two short, lateral lobes (Fig. 4X).

Remarks. *Prionospio parapari* sp. n. is very similar to *P. fallax* in having a prostomium that is truncated on the anterior margin, a neuropodial postchaetal lamellae on chaetiger II being the same shape, and a high dorsal crest on chaetiger 7. However, *P. parapari* sp. n. can be distinguished from *P. fallax* as redescribed by Sigvaldadóttir and

Mackie (1993), by the former having rounded (rather than rectangular) postchaetal neuropodial lamellae on chaetiger I, the first pair of branchiae longer than fourth (rather than of equal size), and with dense digitiform (rather than sparse lateral) pinnules arranged along the posterior face of the stems on branchiae 1 and 4, and cirriform (rather than subtriangular) second and third branchial pairs. In addition, the low dorsal crests in *P. parapari* sp. n. are present on chaetigers VIII–IX while in *P. fallax* they are absent; the neuropodium on chaetiger III in *P. parapari* sp. n. is oval with an enlarged dorsal edge whilst in *P. fallax* it is subtriangular and dorsally pointed; and the sabre chaetae in *P. parapari* sp. n. are heavily granulated and bilimbate whereas in *P. fallax* they are distally granulated and alimbate. The pygidium lacks pigmentation in *P. parapari*.

Prionospio parapari sp. n. is also similar to *P. komaeti* Hylleberg & Nateewathana, 1991, *P. depauperata* Imajima, 1990, and *P. oligopinnulata* Delgado-Blas, 2015, in that all three species have a prostomium that is truncated on the anterior margin, the same shaped neuropodial postchaetal lamellae on chaetiger II, and a high membranous dorsal crest on chaetiger VII that decreases in height on chaetigers VIII–IX. However, *P. parapari* sp. n. differs from the first two species in that it has rounded (rather than square or lanceolate) notopodial and neuropodial postchaetal lamellae on chaetiger I, and an oval neuropodium on chaetiger III with the dorsal edge enlarged (rather than one that is square or triangular). In addition, the branchiae of *P. parapari* sp. n. have long, naked, smooth distal tips, whereas those of *P. komaeti* and *P. depauperata* have pinnules extending to the distal end, and *P. parapari* lacks low dorsal crests on chaetigers X–XI/XIII. *Prionospio parapari* sp. n. also differs from *P. depauperata* in that it has sabre chaetae without a distal filament, the notopodial hooded hooks start on chaetigers XIX–XXXVIII rather than XLV–XLVII, and the pygidium has two long lateral lobes rather than two short lateral cirri. Furthermore, *P. parapari* sp. n. is similar to *P. oligopinnulata* in that both species show the same pygidial structure, but differs in having cirriform rather than triangular second and third branchial pairs. In addition, the low dorsal crests on chaetigers X–XIV are absent in *P. parapari* sp. n., the neuropodium on chaetiger III is oval with the dorsal edge enlarged (rather than subtriangular and ventrally pointed), and the sabre chaetae are bilimbate (rather than alimbate). *Prionospio parapari* sp. n. is similar to *P. rotunda* Delgado-Blas, 2015 in that both species have large, rounded neuropodial postchaetal lamellae on chaetiger I, cirriform second and third branchial pairs, the first branchial pair always longer than fourth pair, and the same pygidium structure. However, *P. parapari* sp. n. differs from *P. rotunda* in having a bottle-shaped prostomium that is truncated on the anterior margin (rather than a pyriform and rounded one). In addition, the low dorsal crests in *P. parapari* sp. n. are present on chaetigers VIII–IX whereas in *P. rotunda* they are absent, and the neuropodium on chaetiger III is oval with an enlarged dorsal edge (rather than rounded). The differences between this new species and the other species examined are provided in the key.

Etymology. The species is named in honor of Dr Julio Parapar, in recognition of his major contribution to the study of polychaetes from Spanish coasts.

Type locality. Ría de Ferrol and the mouth of Piedras River, Huelva, Spain.

Distribution. To date, this species has been recorded only on the Spanish Atlantic coast (Ria de Ferrol and the mouth of Piedras River, Huelva).

Key to *Prionospio* species with four branchial pairs from the Iberian coastline

1 First 3 pairs of branchiae apinnate and pair 4 with pinnules; or first pair of branchiae with pinnules and pairs 2–4 apinnate..... **2**
– First and fourth pair of branchiae pinnate and pairs 2–3 apinnate **4**
2 First 3 pairs of branchiae apinnate and pair 4 with pinnules; dorsal crest on chaetiger VII; notopodial prechaetal lamellae very large on anterior chaetigers, basally fused with notopodial postchaetal lamellae; interparapodial pouches absent; all hooded hooks bidentate..... ***P. caspersi***
– First pair of branchiae with pinnules and pairs 2–4 apinnate..... **3**
3 Second and third branchial pairs slightly expanded distally, with short, sharp tips; a low crest on chaetiger V; sabre chaetae sheathed ..... ***P. ehlersi***
– Second and third branchial pairs triangular and thick, a dorsal cord-shape on chaetiger V; sabre chaetae alimbate ..... ***P.* cf. *ehlersi***
4 Ventral crests present on chaetigers XI/XII–XV/XIX; high dorsal crests on chaetigers X–XI, and low dorsal crests on chaetigers III–IV, XII–XXII/XXX-IV; notopodial prechaetal lamellae very large on anterior chaetigers, basally fused with notopodial postchaetal lamellae ..... ***P. cristaventralis* sp. n.**
– Ventral crests absent; high dorsal crest on chaetiger VII, and low dorsal crests on chaetigers VIII–IX or absent; notopodial prechaetal lamellae moderate or low on anterior chaetigers, not basally fused with notopodial postchaetal lamellae..... **5**
5 Prostomium square; caruncle long; peristomium medium-length; second and third branchial pairs cirriform; dorsal crests on chaetigers VIII–IX; neuropodial postchaetal lamellae oval, ventrally directed on chaetiger II, and oval, dorsally directed on chaetiger III..... ***P. parapari* sp. n.**
– Prostomium bottle-shaped; caruncle short; peristomium short; second and third branchial pairs subtriangular; dorsal crests absent; neuropodial postchaetal lamellae subtriangular, ventrally pointed on chaetiger II, and subtriangular, dorsally pointed on chaetiger III..... ***P. fallax***

Acknowledgments

We would like to thank Julio Parapar and Lorenzo López Serrano for kindly providing the material from the coast of Galicia and the mouth of the Piedras River, respectively. This study was supported by the research project "Fauna Ibérica XI" (CGL2014-53332-C5-3-P) of the Ministerio de Economía y Competitividad of the Government of Spain. Andrew SY Mackie provided important comments and editing during reviewing the manuscript. We would also like to thank two anonymous referees who carefully reviewed a previous version of this manuscript. Their comments unquestionably improved the quality of this paper. Also, we thank the subject editor Chris Glasby for the careful review that resulted in a significant improvement of this final version.

References

Aguirrezabalaga F, Cebeiro A (2005) Spionidae (Annelida: Polychaeta) from the Cap Breton Canyon (Bay of Biscay, NE Atlantic) with descriptions of a new genus and three new species. Marine Biology Research 1: 267–280. https://doi.org/10.1080/17451000500262066

Amoureux L (1972) Annélides Polychètes recuillies sur les pentes du talus continental au large de la Galice (Espagne). Campagnes 1967 et 1968 de la "Thalassa". Cahiers de Biologie Marine 13: 63–89.

Amoureux L (1974) Annélides Polychètes recuillies sur les pentes du talus continental au Nord-Ouest de l'Espagne et du Portugal (Campagne 1972 de la "Thalassa"). Cuadernos de Ciencias Biológicas 3: 121–154.

Blake JA, Kudenov JD (1978) The Spionidae (Polychaeta) from southeastern Australia and adjacent areas, with a revision of the genera. Memoirs of the National Museum of Victoria 39: 171–280. https://doi.org/10.24199/j.mmv.1978.39.11

Dagli E, Çinar ME (2009) Species of the subgenera *Aquilaspio* and *Prionospio* (Polychaeta: Spionidae: *Prionospio*) from the southern coast of Turkey (Levantine Sea, eastern Mediterranean), with description of a new species and two new reports for the Mediterranean fauna. Zootaxa 2275: 1–20.

Delgado-Blas VH (2015) *Prionospio* (Polychaeta, Spionidae) from the Grand Caribbean Region, with the descriptions of five new species and a key to species recorded in the area. Zootaxa 3905: 69–90. https://doi.org/10.11646/zootaxa.3905.1.4

Desbruyères D, Guille A, Ramos JM (1972) Bionomie benthique du plateau continental de la côte catalane espagnole. Vie Milieu 23(2B): 335–336.

Dexter D (1992) Soft botton invertebrates of the Portuguese benthos. Boletim do Instituto de Investigaçao das Pescas, Lisboa 17: 61–88.

Fauvel P (1928) Annelides polychetes nouvelles du Maroc. Bulletin de la Societé Zologique de France 53: 9–13.

Foster NM (1971) Spionidae (Polychaeta) of the Gulf of Mexico and the Caribbean Sea. Studies on the Fauna of Curaçao and other Caribbean Islands 36: 1–183.

Gil JC (2011) The European Fauna of Annelida Polychaeta. PhD Thesis, Universidade de Lisboa. Lisboa, 1554 pp.

Gil J, Sardá R (1999) New records of Annelida Polychaeta for the Portuguese fauna (with comments of some already known species). Arquivos do Museu Bocage, Nova Série 3(10): 287–334.

Grube AE (1850) Die Familien der Anneliden. Archiv fur Naturgeschichte, Berlin 16: 249–364.

Hutchings PA, Rainer SF (1979) The polychaete fauna of Careel Bay, Pittwater, New South Wales, Australia. Journal of Natural History 13: 745–796. https://doi.org/10.1080/00222937900770561

Hylleberg J, Nateewathana A (1991) Polychaetes of Thailand. Spionidae (Part 1); *Prionospio* of the *steenstrupi* group with description of eight new species from the Andaman Sea. Phuket Marine Biology Center Research Bulletin 55: 1–32.

Imajima M (1990) Spionidae (Annelida, Polychaeta) from Japan IV. The genus *Prionospio (Prionospio)*. Bulletin of the National Science Museum Series A (Zoology) 16: 105–140.

Laubier L (1962) Quelques Annélides Polychètes de la Lagune de Venise. Description de *Prionospio caspersi* n. sp. Vie Milieu 13(1): 123–159.

López Jamar E, González G (1986) Infaunal macrobentyhos of Galician continental shelf off La Coruña Bay, North-west Spain. Biological Oceanography 4(2): 165–192.

Maciolek NJ (1985) A revision of the genus *Prionospio* Malmgren, with special emphasis on species from the Atlantic Ocean, and new records of species belonging to the genera *Apoprionospio* Foster and *Paraprionospio* Caullery (Polychaeta, Annelida, Spionidae). Zoological Journal of the Linnean Society 84: 325–383.https://doi.org/10.1111/j.1096-3642.1985.tb01804.x

Mackie ASY, Hartley JP (1990) *Prionospio saccifera* sp. nov. (Polychaeta: Spionidae) from Hong Kong and the Red Sea, with a redescription of *Prionospio ehlersi* Fauvel, 1928. In: Morton B (Ed.) The Marine Flora and Fauna of Hong Kong and Southern China. Proceedings of the Second International Marine Biological Workshop, Hong Kong 1986, vol. 1. Introduction and Taxonomy. Hong Kong University Press, Hong Kong, 363–375.

Malmgren AJ (1867) Annulata Polychaeta: Spetsbergiae, Groenlandiae, Islandiae et Scandinaviae. Hactenus Cognita. Kongl. Vetenskaps-Akademiens Förhandliugar 4: 127–235. [pl 2–15]

Pardal M, Caldeira AM, Marques JC (1992) Contribution to knowledge of the Polychaete fauna of Portugal. Part I. Orbiniida, Cossurida and Spionida. Ciência Biológica. Ecology and Systematics, Portugal 12(1/2): 1–25.

Quintino V, Gentil F (1987) Étude faunistique et coenotique de la faune annélidienne des lagunes d'Albufeira et Obidos (Portugal). Cahiers de Biologie Marine 28: 59–72.

Quintino V, Rodrigues AM, Gentil F (1989) Assessment os macrozoobenthis communities in the lagoon of Obidos, western coast of Portugal. Scientia Marina53(2–3): 645–654.

Ravara A, Moreira MH (2013) Polychaeta (Annelida) from the continental shelf off Aveiro (NW Portugal): Species composition and community structure. Chek List 9(3): 533–539. https://doi.org/10.15560/9.3.533

Sigvaldadóttir E (1998) Cladistic analysis and classification of *Prionospio* and related genera (Polychaeta, Spionidae). Zoologica Scripta 27: 175–187. https://doi.org/10.1111/j.1463-6409.1998.tb00435.x

Sigvaldadóttir E, Mackie ASY (1993) *Prionospio steenstrupi*, *P. fallax* and *P. dubia* (Polychaeta, Spionidae): reevaluation of identity and status. Sarsia 78: 203–219. https://doi.org/10.1080/00364827.1993.10413535

Söderström A (1920) Studien über die polychatenfamilie Spionidae. Dissertation zu Uppsala, 286 pp. [1 pl.]

Warren LM, Hutchings PA, Doyle S (1994) A revision of the genus Mediomastus Hartman, 1994 (Polychaeta: Capitellidae). Records of the Australian Museum 46: 227–256. https://doi.org/10.3853/j.0067-1975.46.1994.6

Wilson RS (1990) *Prionospio* and *Paraprionospio* (Polychaeta: Spionidae) from southern Australia. Memoirs of the Museum of Victoria 50: 243–274. https://doi.org/10.24199/j.mmv.1990.50.02

Zhou J, Li X (2009) Report of *Prionospio* complex (Annelida: Polychaeta: Spionidae) from China's waters, with description of a new species, Acta Oceanologica Sinica 28(1): 116–127.

ZooKeys 810: 19–44 (2018)
doi: 10.3897/zookeys.810.29824
http://zookeys.pensoft.net

RESEARCH ARTICLE

A peer-reviewed open-access journal
ZooKeys
Launched to accelerate biodiversity research

Enantiomorphs and taxonomy of three conchological species in flat-shelled snails *Trichocathaica* (Pulmonata, Camaenidae)

Barna Páll-Gergely[1], András Hunyadi[2], Takahiro Asami[3]

1 *Plant Protection Institute, Centre for Agricultural Research, Hungarian Academy of Sciences, Budapest, Hungary* **2** *Adria sétány 10G 2/5., Budapest 1148, Hungary* **3** *Department of Biology, Shinshu University, Matsumoto 390-8621, Japan*

Corresponding author: *Barna Páll-Gergely* (pall-gergely.barna@agrar.mta.hu)

Academic editor: *E. Gittenberger* | Received 18 September 2018 | Accepted 4 December 2018 | Published 20 December 2018

http://zoobank.org/F67F5B77-293D-49D9-97D9-3E147A5B80C0

Citation: Páll-Gergely B, Hunyadi A, Asami T (2018) Enantiomorphs and taxonomy of three conchological species in flat-shelled snails *Trichocathaica* (Pulmonata, Camaenidae). ZooKeys 810: 19–44. https://doi.org/10.3897/zookeys.810.29824

Abstract

Biomodal (flat/globular or slender/tall) shell/body shapes are associated with dichotomous (simultaneous reciprocal or non-reciprocal) modes of copulation behaviour in the fully-shelled stylommatophoran snails. In flat-shelled groups that copulate simultaneously reciprocally, no study has found an example of enantiomorphism that persists within a population. However, the original description of a flat camaenid snail, *Trichocathaica amphidroma*, noted that it is dextral- or sinistral-coiled. By examination of shell surface morphology, we found that shell specimens classified as those of this species include shells of three different morphological species. Namely, *T. amphidroma*, *Trichocathaica vestita* (Pilsbry, 1934), **comb. n.**, and *Trichocathaica macrosquamata* Páll-Gergely, **sp. n.** In each of the three species, both sinistral and dextral shells have been collected from presumably one area. Ethanol-fixed soft bodies of single dextral and sinistral individuals of *T. vestita*, which were available for the first time for interchiral comparison of genital morphology in the present genus, differed from each other in the pattern of penial microsculpture. They might represent enantiomorphs that have recently diverged in allopatry instead of enantiomorphism within a population or species. However, their shell and genital differences were not discrete enough to divide them taxonomically into two morphologically distinct species. Our results demonstrate the importance of evaluating individual variation relative to differences between incipient species in penial morphology, especially between conchologically indistinguishable enantiomorphs in the flat groups. We revise the taxonomy of the genus *Trichocathaica* including the above-mentioned new species, and *Trichocathaica puteolata* Páll-Gergely, **sp. n.**

Keywords
Chirality, enantiomorphism, Gastropoda, left-right reversal, penial morphology, Stylommatophora

Introduction

Left-right reversal of development seldom evolves in the Bilateria (Utsuno et al. 2011). Against this homochirality (directional asymmetry) rule of evolution, reversals of bilateral primary asymmetry, which visceral asymmetry represents, as well as secondary asymmetry such as coiling direction have recurrently evolved in gastropods (Okumura et al. 2008). Within gastropods, the evolution of left-right reversed species (chiral speciation) has been accelerated in terrestrial hermaphroditic groups of the Stylommatophora (Gittenberger et al. 2012). At least in pulmonates, the left-right polarity of spiral cleavage, on which the direction of whole-body asymmetry depends, is determined by a maternal effect of a single nuclear gene. Thus, the chiral phenotype, dextral (clockwise-coiled) or sinistral (counter clockwise-coiled), exhibits maternal inheritance (Okumura et al. 2008; Asami et al. 2008; Utsuno and Asami 2010; Utsuno et al. 2010; Davison et al. 2016).

In stylommatophorans, their bimodal shell shapes are associated with the dichotomous mating modes. Groups with the flat/globular shaped shell copulate simultaneously reciprocally, whereas those with the tall shape copulate non-reciprocally, although exceptional cases are present (Asami 1993; Davison and Mordan 2007). In both of the modes, copulation between the reversed mutant and wild type (interchiral copulation) is less successful than intrachiral copulation with the same morph, which results in positive frequency-dependent selection (Johnson 1982). Interchiral copulation is less difficult in the non-reciprocal mode than in the simultaneous reciprocal mode (Gittenberger 1988; Asami et al. 1998). Thus, the mutant allele for reversal could persist longer under relaxed frequency-dependent selection in populations of tall species, which could then have a larger chance for fixation for the reversal allele, than in those of flat species. This prediction has been verified with observations of more frequent evolutions of reversed species in tall groups than in flat groups (Gittenberger 1988; Asami et al. 1998). Frequency-dependent selection against the less common chiral morph is therefore playing a key role for suppression of chiral speciation at least in stylommatophorans.

However, the frequency-dependent selection also plays a reverse role for chiral speciation, particularly in flat groups, which are subject to more stringent selection than the tall groups. Positive frequency-dependent selection works for the more frequent morph and against the less frequent opposite morph. This means that a population in spatial isolation could promptly be fixed for reversal once the reversed morph exceeds 50% in phenotypic frequency, for example through random genetic drift (Ueshima and Asami 2003) or survival advantage (Hoso et al. 2007, 2010). The homozygote of the recessive reversal mutant allele initially appears from mating between the heterozygotes. Because of the maternal inheritance, this homozygote develops the dominant phenotype. For example, in cases where the dextral wild-type is dominant to the sinistral mutant phenotype, crosses between the heterozygotes first generate the homozygotes of the

sinistral allele, which develop into the dextral. These dextrals, having no mating difficulty with the dextral wild-type, generates only sinistral offspring. Thus, maternal inheritance could contribute to increase of the frequency of the reversed phenoype by drift. In the case of flat groups, population fixation for reversal in allopatry could establish premating reproductive (sexual) isolation from the other non-reversed populations, resulting in single-gene speciation (Gittenberger 1988; Orr 1991; van Batenburg and Gittenberger 1996; Ueshima and Asami 2003; Davison et al. 2005).

This stringency of frequency-dependent selection predicts that populations of flat groups are stably monomorphic for the direction of left-right asymmetry and that stably coexisting dextrals and sinistrals of flat snails are sexually isolated from each other. For example, a flat dextral camaenid ground-snail *Euhadra aomoriensis* evolved by reversal from the sinistral clade of *E. quesita*. Their shell surface morphologies have diverged since their speciation (Ueshima and Asami 2003). In accordance with the prediction, no evidence has validated chiral dimorphism (enantiomophism) that stably persists in a population of flat snails (Asami 1993; Asami et al. 1998).

However, as its name indicates, Möllendorff (1899) described a flat ground-snail *Trichocathaica amphidroma* to have clockwise- or counterclockwise-coiled shell. The other congeners, *T. foliosquama* Wu, 2001, *T. goepeliana* Yen, 1938, *T. lyonsae* (Gude, 1919) *T. lyonsae comosa* (Pilsbry, 1934) and *T. rugosobasis* (Pilsbry, 1934), are all described to be sinistral. In the Camaenidae, to which *Trichocathaica* belongs, many species perform simultaneous reciprocal mating, and no example of non-reciprocally mating has been found. Thus, most probably *Trichocathaica* snails also copulate simultaneously reciprocally. The taxonomical description of enantiomorphs as one species in this group (Möllendorff 1899) therefore poses the question, whether any morphological sign of divergence is detectable between them. Thus, the present study examined whether dextral and sinistral specimens of *T. amphidroma* exhibit differences in shell and/or genital traits of morphology.

Here we show the presence of enantiomorphs that are not distinguishable in shell surface morphology in each of three conchological species of *Trichocathaica*. We also taxonomically revise the *Trichocathaica* and describe two new species.

Materials and methods

We examined shell and/or genital morphologies of specimens of the genus *Trichocathaica* available from the public and private collections listed below. Table 1 presents locality names cited verbatim from the specimen labels in the systematic part. Figure 1 shows the localities and rivers that are identifiable exactly on the map. A total of 155 shell specimens, two of which were deposited with ethanol-fixed soft-bodies, were available for our examination in eight species, including the two new species. One of the two with the soft-bodies was dextral and the other sinistral from one of the collecting localities, Wasihekou. We dissected these bodies for comparison of their genital morphology. We counted the whorls of each adult shell according to Kerney and Cameron (1979).

Table 1. Correspondence between locality names spelled on museum labels/literature and those in the present time.

Original	Present
Fulin Ton	Unknown
Ja sz'kou	Wasigou
Liu-ting	Luding
Lu Ho	Dadu River
Lu Tin Chouw	Unknown
Maochow	Unknown
Ta Tu Ho	Dadu River
Tapa	Unknown
Tapien	Unknown
Tung	Dadu River
Wa-sae-Kou	Wasigou
Wa-sy-kou	Wasigou

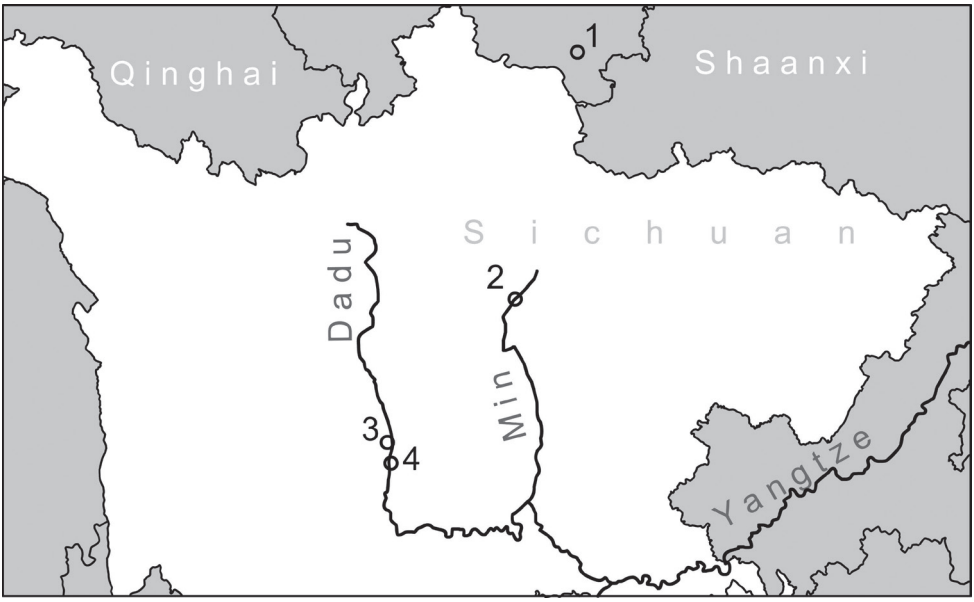

Figure 1. Map showing the exactly identifiable localities of *Trichocathaica* species **1** type locality of *Trichocathaica foliosquama* Wu, 2001 **2** Type locality of *T. lyonsae comosa* (Pilsbry, 1934) **3** Localities of *T. vestita* (2015/64 and 2015/65) **4** Localities of *T. amphidroma* (Möllendorff, 1899) (2015/67 and Wu 2001).

Abbreviations

ANSP Academy of Natural Sciences (Philadelphia, USA)
D shell diameter
H shell height
HA Collection András Hunyadi (Budapest, Hungary)
NHM The Natural History Museum (London, UK)

NHMUK When citing NHM registered specimens
PGB Collection Barna Páll-Gergely (Mosonmagyaróvár, Hungary)
SMF Senckenberg Forschungsinstitut und Naturmuseum (Frankfurt am Main, Germany)

Results

We found that all 72 specimens labelled as *Trichocathaica amphidroma* were collected from the areas of Luding and Wasigou in west Sichuan, China. Five of the nine lots included both clockwise-coiled (dextral) and counter clockwise-coiled (sinistral) specimens. In total, 39 were dextral and 33 were sinistral. However, our further examination of shell morphology revealed that they include three distinct morphotypes that differ in fine sculpture of the shell surface, especially in the size of the periostracal scales. The dextral and sinistral soft-bodies exhibited no distinct differences in the gross anatomy of the genital system. However, the patterns of microsculpture in the internal surface of the penial tube were slightly different between them.

There were 28, 5 and 29 shells corresponding to the three morphotypes. We found no example of intermediate morphology in shell traits between those morphotypes. Each of the three morphotypes was present in mixture with one of the other morphotypes in four different lots of SMF collection. This suggests that those pairs of morphotypes probably exhibit their discrete shell differences in sympatry as well. On the other hand, the differences of penial sculpture were detected between only single specimens available in each of enantiomorphs. Their shells did not differ in traits that divide the three morphotypes. For these reasons, we recognize the three morphotypes as distinct species, *T. amphidroma*, *T. macrosquamata* sp. n. and *T. vestita* (Pilsbry, 1934). We classified the dextral and sinistral individuals, the penial sculpture patterns of which were examined, in *T. vestita* and describe their penial difference. Deviation of the morph frequency from 0.5 was not statistically significant in 28 specimens of *T. amphidroma* ($P = 0.06$, $\chi^2 = 3.6$) (Table 2). In contrast, dextrals were more frequent than sinistrals in 39 specimens of *T. vestita* ($P = 0.002$, $\chi^2 = 9.3$). Between these species, sinistrals were more frequent in *T. amphidroma* ($P = 0.001$, Fisher's exact test).

Systematic part

Family Camaenidae Pilsbry, 1895

Remarks. Camaenidae and Bradybaenidae are traditionally distinguished on the basis of the absence of the dart sac and mucous glands in the former and the presence of these structures in the latter. The molecular phylogeny of Wade et al. (2007) showed that the dart sac was lost multiple times during the evolution of the Camaenidae. Camaenidae and Bradybaenidae form a single clade, and neither of them is mono-

Table 2. Numbers of enantiomophic specimens found in three morphological species.

Locality	Collecting year	*T. amphidroma*	*T. macrosquamata* sp. n.	*T. vestita*
"Liu-Ting am Tung" (Luding at Dadu River)	1884–1886	2 sinistrals	–	2 dextrals
"Thal des Tung" (Valley of Dadu River)	1884–1886	3 sinistrals	–	
Luding (2015/67)	2015	6 sinistrals	–	
"Ta Tu Ho" (Dadu River)	1930	8 sinistrals 9 dextrals	–	2 dextrals
"Wa-sae-Kou" (Wasigou)	probably 1884–1886	–	1 sinistral 1 dextral	3 dextrals
"Wa-sy-Kou am Tung" (Wasigou at Dadu River)	1884–1886	–	2 sinistrals	–
"W-Sytshuan" (West Sichuan)	1884–1886	–	1 sinistral	1 dextral
"Wasihekou" (Wasigou, 2015/64)	2015	–	–	19 dextrals
"Wasihekou" (Wasigou, 2015/65)	2015	–	–	10 sinistrals 2 dextrals
Total		19 sinistrals 9 dextrals	4 sinistrals 1 dextral	10 sinistrals 29 dextrals

phyletic. Therefore Gittenberger et al. (2012) formally treated the Bradybaenidae as a junior synonym of Camaenidae. Bouchet et al. (2017) retained the subfamily Bradybaeninae Pilsbry, 1934 under Camaenidae. This system is followed here.

Genus *Trichocathaica* Gude, 1919

Cathaica (*Trichocathaica*) Gude, 1919: 119.

Type species. *Cathaica* (*Trichocathaica*) *lyonsae* Gude, 1919, by original designation.

Distribution. All *Trichocathaica* are known from the eastern edge of the Tibetan Plateau in the Chinese Sichuan and Gansu provinces (valleys of the Dadu and Min rivers).

Remarks. Wu (2015) mentioned *Trichocathaica maoensis*, but this name has not been made available.

Enantiomorphic species

Trichocathaica amphidroma (Möllendorff, 1899)

Figure 2

Euhadra amphidroma Möllendorff, 1899: 83, plate 4, figs 2, 2a, 3.
Trichocathaica amphidroma – Yen 1939: 150, plate 15, fig. 44.
Trichocathaica amphidroma – Yen 1939: 292, figs 1–4.

Material examined. W-Sytschuan, Liu-Ting am Tung, coll. Möllendorff ex coll. Potanin, SMF 8942/1 lectotype (sinistral shell, D = 20.8 mm, H = 11.6 mm, Fig. 2A–C); same data, SMF 8938/1 paralectotype (sinistral shell); W-Sytschuan, Thal des Tung,

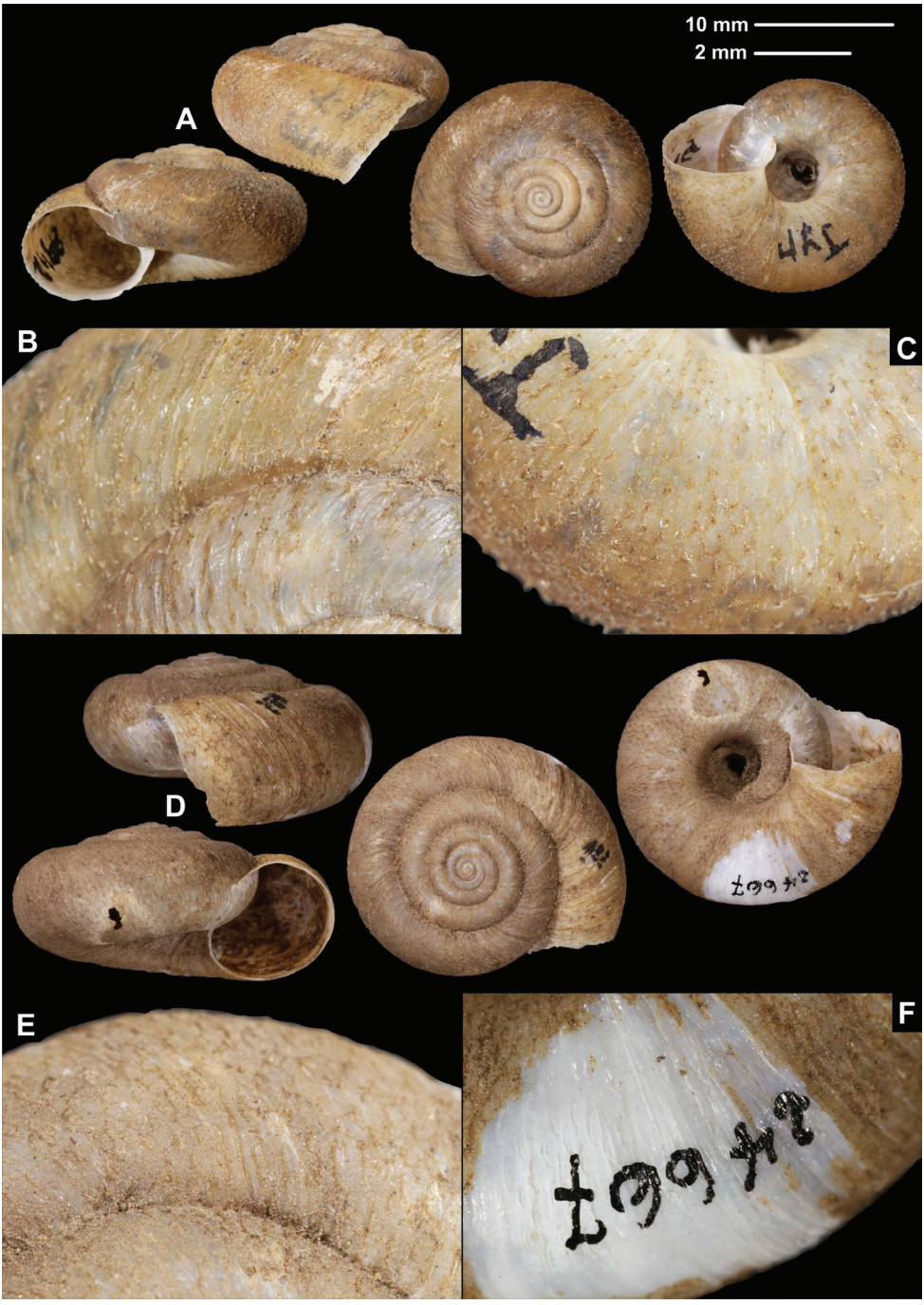

Figure 2. Shells (**A, D**), dorsal (**B, E**), and ventral (**C, F**) sculpture of *Trichocathaica amphidroma* (Möllendorff, 1899) **A–C** SMF 8942 (lectotype, D = 20.8 mm) **D–F** SMF 24667 (paralectotype, D = 23.6 mm). Scale bars: Upper scale (**A, D**) lower scale (**B, C, E, F**). All photos: B. Páll-Gergely.

coll. Möllendorff ex coll. Potanin, SMF 8937a/3 sinistral, juvenile paralectotype shells; China (Szytschuan): W-Ufer d. Lu Ho (Ta Tu Ho) zw. Tapien und Ja sz'kou, ex Krejci-Graf, 05.08.1930, SMF 24667/8 sinistral + 9 dextral shells (1 of the dextral shells is photographed: Fig. 2D–F); **2015/67** Sichuan, Ganzi Zhou, Luding Xian, Luding, rocks above bus station, approximate GPS coordinates: 29°54.451'N, 102°13.923'E, leg. Hunyadi, A., 15.06.2015, HA/6 sinistral shells.

Diagnosis. Shell sinistral or dextral, body whorl rounded, teleoconch roughly wrinkled with large, triangular periostracal folds, fold scars represented as long curved lines.

Description. Shell sinistral or dextral, spire slightly elevated, body whorl rounded, protoconch consists of 1.25–1.5 whorls, finely, irregularly wrinkled; entire shell with 5.5–5.75 whorls; teleoconch roughly, irregularly wrinkled, with large, triangular periostracal folds having long, curved (C-shaped) base; in specimens/shell parts without periostracum the base of folds visible as prominent curved lines on the surface; aperture subcircular, peristome slightly expanded, thin, sharp; inner thickening parallel to peristome weak.

Measurements (in mm). D = 20.5–25.9, H = 10.3–13.1 (n = 6).

Differential diagnosis. The fine sculpture of the teleoconch surface, namely the rough wrinkles and large triangular periostracal folds with the long base, distinguish this species form the other congeners.

Distribution. This species is known from the valley of the Dadu River near Luding. We were not able to locate Tapien on a map. Wu (2001) also reported this species from Luding County (29.9°N, 102.2°E).

Trichocathaica macrosquamata Páll-Gergely sp. n.

http://zoobank.org/C0AE35B8-C9AC-486D-AC75-FA21FF03C1BD
Figure 3

Material examined. Setschuan, Wa-sae-Kou, coll. Jaeckel ex coll. Schäfer, SMF 216281, holotype (1 sinistral shell, D = 18.8 m, H = 10.6 mm, Fig. 3D–F); same data, SMF 349504, paratype (1 dextral shell, Fig. 3A–C); China, W-Sytschuan: Wa-sy-Kou am Tung, coll. O. Möllendorff ex coll. Potanin, SMF 8941, paratypes (2 sinistral shells, paralectotypes of *amphidroma*, 1 of them is corroded without hair scars); W-Sy-tschuan, SMF 9171, paratype (1 sinistral shell, paralectotype of *amphidroma*).

Diagnosis. Shell sinistral or dextral, body whorl rounded with a very slight indication of a keel, teleoconch finely wrinkled with medium-sized scale-like periostracal folds; fold scars represented as medium-sized curved lines.

Description. Shell sinistral or dextral, spire slightly elevated, body whorl rounded with a very slight indication of a keel; protoconch consists of 1.25–1.5 whorls, finely, irregularly wrinkled; entire shell with 5.5–6 whorls; teleoconch finely, irregularly wrinkled, with medium-sized, low, dense periostracal folds having curved (C-shaped) base; scales visible to the naked eye; in specimens/shell parts without periostracum the bases

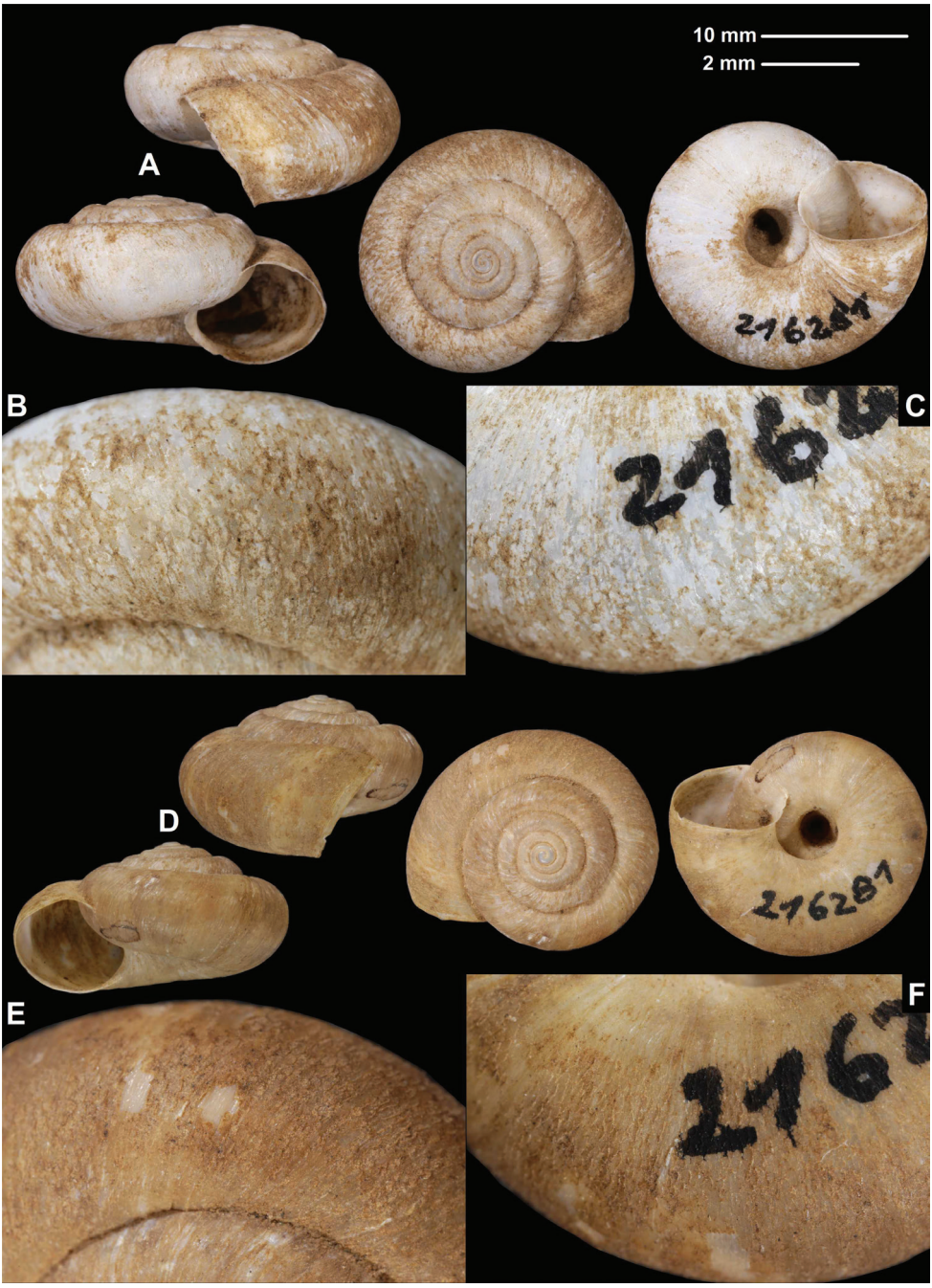

Figure 3. Shells (**A, D**), dorsal (**B, E**), and ventral (**C, F**) sculpture of *Trichocathaica macrosquamata* Páll-Gergely sp. n. **A–C** SMF 349504 (paratype, D = 21.8 mm) **D–F** SMF 216281 (holotype, D = 18.8 mm). Scale bars: Upper scale (**A, D**), lower scale (**B, C, E, F**). All photos: B. Páll-Gergely.

of folds visible as curved lines; aperture subcircular, peristome slightly expanded, thin, sharp; inner, white thickening parallel to the peristome prominent, situated in some distance from peristome edge.

Measurements (in mm). D = 18.8–23.7, H = 10.6–13 (*n* =4).

Differential diagnosis. *Trichocathaica macrosquamata* sp. n. differs from *T. vestita* by exhibiting larger periostracal folds (scales) over the entire shell surface.

Etymology. This species is named after its scales on the shell surface, which are larger than those of *T. vestita*.

Distribution. This species is known from the valley of the Dadu River at Wasigou.

Trichocathaica vestita (Pilsbry, 1934), comb. n.

Figures 4A, 5–8

Cathaica constantinae vestita Pilsbry, 1934: 15, plate 3, figs 5–7.

Types examined. Between Wenchwan and Weichow, June, 1931, ANSP 159708 (photos of the holotype were examined).

Additional material examined. 2015/64 Sichuan, Ganzi Zhou, Kangding Xian, Wasihekou, southern side of the river, along the highway, 1420 m a.s.l., 30°04.564'N 102°09.865'E, leg. A. Hunyadi, 14.06.2015, HNHM 103470 (dextral shell, Fig. 5D–F + ethanol-preserved body: Figs 6A, 7A, 8A), HA/15 dextral shells, PGB/3 dextral shells; **2015/65** China, Sichuan, Ganzi Zhou, Kangding Xian, Wasihekou 200 m towards Guzan Zhen, around the stupa, 1420 m a.s.l., 30°04.565'N, 102°10.085'E, leg. Hunyadi, A. & Szekeres, M., 14.06.2015, HNHM 103471 (1 sinistral shell, Fig. 5A–C + ethanol-preserved body: Figs 6B–C, 7B, 8B), HA/6 sinistral shells + 2 dextral shells, PGB/3 sinistral shells; W-Sytschuan, Wa-sy-Kou am Tung, coll. Möllendorff ex coll. Potanin, SMF 8940 (1 dextral shell, paralectotype of *amphidroma*); China, W-Sytschuan: Wa-sy-Kou am Tung, coll. O. Möllendorff ex coll. Potanin, SMF 349506 (1 dextral shell, paralectotype of *amphidroma*, ex SMF 8941); Sy-tschuan, rechter Ufer des Flusses Tun bei dem Torfe (?) Wa-sy-ku, coll. O. Möllendorff ex coll. Potanin 3898a, 1903, SMF 95002 (1 dextral shell, paralectotype of *amphidroma*); W-Sy-tschuan, coll. Möllendorff, SMF 349505 (1 dextral shell, paralectotype of *amphidroma*, ex SMF 9171); W-Sytschuan, Liu-Ting am Tung, coll. Möllendorff ex coll. Potanin, SMF 349503 (2 dextral shells, paralectotypes of *amphidroma*, ex SMF 8938); W-Ufer d. Lu Ho (Ta Tu Ho) zw. Tapien und Ja sz'kou, ex Krejci-Graf, 05.08.1930, SMF 349507 (2 dextral shells, ex SMF 24667).

Diagnosis. Shell sinistral or dextral, body whorl rounded to keeled, teleoconch finely wrinkled with small scale-like periostracal folds; fold scars (if visible) represented as short curved lines.

Description. Shell sinistral or dextral, spire slightly elevated; body whorl rounded (with a very slight indication of a keel) to keeled, protoconch consists of 1.25–1.5 whorls, finely, irregularly wrinkled; entire shell with 5.25–5.75 whorls; teleoconch finely, irregularly wrinkled, with small, low, dense periostracal folds having curved (C-shaped) base; scales not visible to the naked eye; in specimens/shell parts without

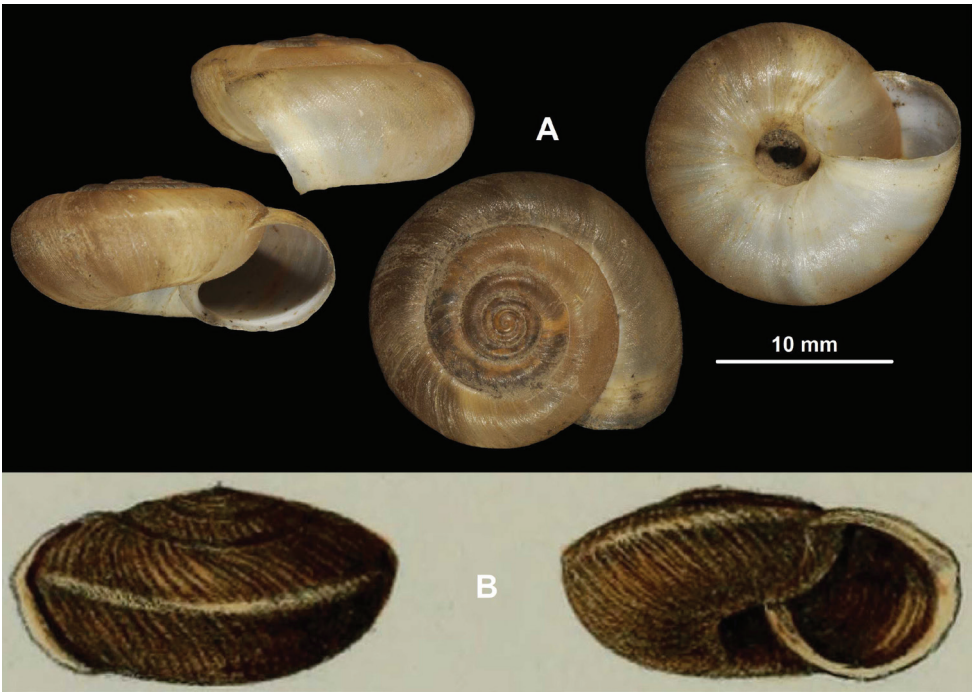

Figure 4. Shells of *Trichocathaica vestita* (Pilsbry, 1934) (holotype, ANSP 159708) (**A**) and *Helix* (*Camaena*) *constantinae* Adams, 1870 (**B**) (illustration from the original description). Scale bars: Scale refers only to **A**.

periostracum the bases of folds or sometimes not visible as small curved lines; aperture subcircular, peristome slightly expanded, thin, sharp; inner, white thickening parallel to the peristome prominent, situated in some distance from peristome edge.

Measurements (in mm). D = 21.2–23.6, H = 11.1–13.6 (*n* = 12).

Anatomy (Figs 6, 7). Genital morphology of two specimens (HNHM 103470, dextral specimen and HNHM 103471, sinistral specimen) showed that the left ommatophoral retractor crosses between penis and vagina in the sinistral specimen, and that the right retractor in the dextral specimen. Atrium short, penis with a slimmer, shorter distal, and a thicker, longer proximal portion, distal portion covered by a weak penial sheath; epiphallus much more slender than penis, approximately as long as penis; retractor muscle shorter in sinistral and longer in dextral specimen, inserts on epiphallus, close to its meeting point with penis; proximal part of penis internally with reticulated zigzag sculpture caused by the perpendicular projections of longitudinal folds (Fig. 8); dart sac well developed, with thickened, larger basal part and smaller head part; dart was only found in the dextral specimen (Fig. 7); long glandulae insert on 4–6 points on the "neck" of the dart sac (at the meeting point of the body and head of the dart sac) (Fig. 6C); vagina short in dextral and longer in sinistral specimen, stalk of bursa copulatrix long, relatively slender, bursa ovoid, diverticulum absent; spermoviduct slender, no embryos found; albumen gland crescent shaped, talon relatively large.

We found no discrete differences between the dextral and sinistral individuals in gross anatomy of the genital system or in the internal structure of the dart sac (Figs 6, 7).

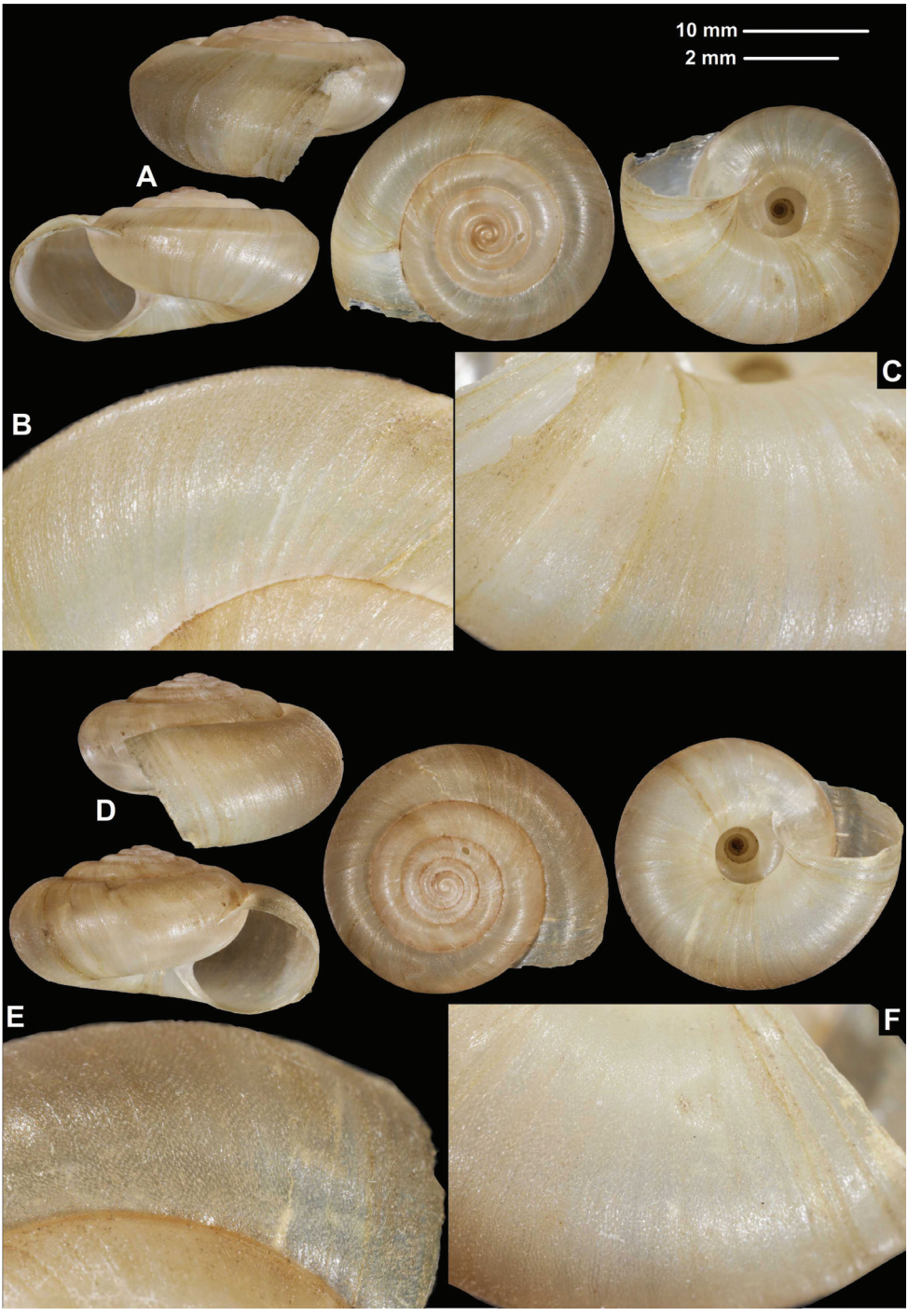

Figure 5. Shells (**A, D**), dorsal (**B, E**), and ventral (**C, F**) sculpture of *Trichocathaica vestita* **A–C** HNHM 103471 (D = 22.7 mm) **D–F** HNHM 103470 (D = 22.8 mm). Upper scale (**A, D**), lower scale (**B, C, E, F**). All photos: B. Páll-Gergely.

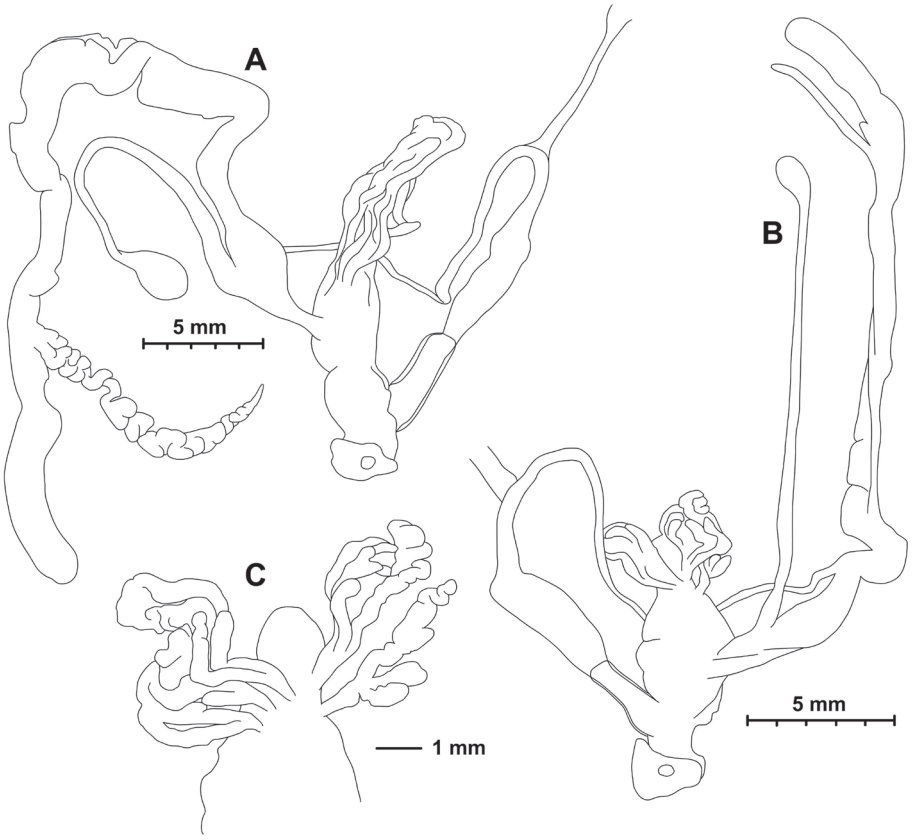

Figure 6. Genital anatomy of *Trichocathaica vestita* **A** Dextral specimen (HNHM 103470) **B, C** Sinistral specimen (HNHM 103471).

The internal surface of the penial tube exhibited complex patterns of microsculpture typical to camaenid snails (Fig. 8). In this structure, several slight differences were noticeable between these specimens of enantiomorphs. Around the area leading to the epiphallus (upper edge in Fig. 8), thin longitudinal pilasters are more tightly gathered with narrower furrows in the dextral than in the sinistral. In both of them, toward the middle of the penial tube, these pilasters become thick and sparse with wider furrows and form a reticulate pattern. Longitudinally (in the direction towards the genital orifice, the bottom in Fig. 8) under the reticulated range, zigzag crenulated pilasters are present in parallel. In these portions, structural change from the reticulate pattern to the parallel pilasters is more distinct in the dextral than in the sinistral. Smooth-bottomed furrows separate the zigzag pilasters in the dextral, whereas those furrows are not obviously present between the irregularly zigzag-shaped pilasters in the sinistral. This structure of the dextral is present in a longitudinally wider range than the sinistral. In the sinistral, instead, the irregular zigzag structure becomes weak or disappears from the longitudinal pilasters, which become thick and pronounced near the genital orifice. This longitudinal structural change is not present in the dextral. The dextral

Figure 7. Opened dart sac of sculpture of *Trichocathaica vestita* **A** Dextral specimen (HNHM 103470) **B, C** Sinistral specimen (HNHM 103471). Arrow shows dart. Scale bars: 1 mm.

instead exhibits a different pattern such that the longitudinally parallel zigzag pilasters are continuously present and merge with one another without forming major pilasters.

Differential diagnosis. *Trichocathaica vestita* differs from *T. macrosquamata* sp. n. by having the smaller periostracal folds (scales) on the entire shell surface.

Distribution. This species is known from the valley of the Dadu River at Luding and Wasigou.

Remarks. This species was described as a subspecies of *Helix* (*Camaena*) *constantinae* Adams, 1870. We had no possibility to examine that species; however, it has remarkably different shell traits, such as the strongly sculptured shell surface and a white band (see Fig. 4B). That species is probably not a *Trichocathaica*, but something entirely different, as Pilsbry (1934) already suspected. Moreover, *Trichocathaica* seems to inhabit only the mountains in Sichuan and southern Gansu, and *Helix* (*Camaena*) *constantinae* was collected in the "Ichang gorge" on the Yangtze River in Hubei Province (ca 30°55'N, 110°50'E, Adams 1870). Therefore, we handle *Trichocathaica vestita* (Pilsbry, 1934) as a species of its own right.

Pilsbry (1934) already noted in the original description that the species show an extreme variability in terms of the development of the keel. Our data also indicates that the keel morphology is variable within and between populations. In the sample of 2015/64, 15 shells had nearly rounded body whorls, two were keeled, and two were intermediate between those rounded and keeled forms. Although every shell in the sample of 2015/65 had a keel, two of them were similar to the intermediate form of the 2015/64 sample.

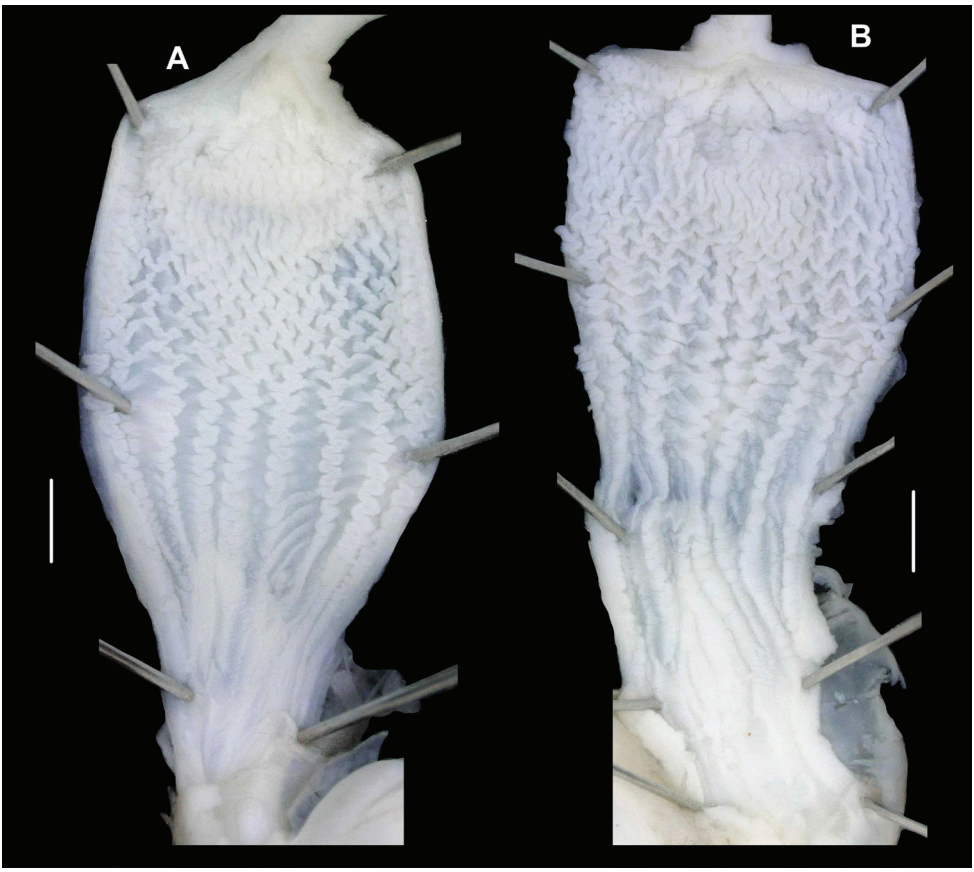

Figure 8. Penial sculpture of *Trichocathaica vestita* **A** Dextral specimen (HNHM 103470) **B, C** Sinistral specimen (HNHM 103471). Scale bars: 1 mm.

Sinistral species

***Trichocathaica foliosquama* Wu, 2001**

Trichocathaica foliosquama Wu, 2001: 294, figs 5–13.

Type locality. Lijiexiang, Zhouqu County (33.8N, 104.3E), Gansu Province.

Description (based on the original description and photos). Shell sinistral, spire slightly elevated, body whorl rounded with a very slight indication of a blunt keel; protoconch consists of 1.55–1.75 whorls, finely granulose; entire shell with 5–5.38 whorls; teleoconch roughly, irregularly wrinkled, with large scales, each scale with 2 or 3 lamellae around 1 central ridge; aperture subcircular, peristome slightly expanded, thin, sharp; inner thickening parallel to peristome situated in some distance from peristome edge.

Measurements (in mm, based on the original description). D = 17.03–18.48, H = 9.33–10.35.

Distribution. This species is known from the type locality only.

Remarks. We did not examine specimens of this species. It can be distinguished from the other species by the narrow umbilicus and the morphology of periostracal folds, described as "shell surface scaly, and each scale with 2–3 lamellae around 1 central ridge" (Wu 2001).

Trichocathaica goepeliana Yen, 1938

Figure 9

Trichocathaica goepeliana – Yen 1939: 150, plate 15, fig. 45.

Material examined. W-Sy-tschuan: Tapa, coll. Möllendorff ex Potanin 444, SMF 8939/2 (syntypes).

Diagnosis. Shell sinistral, small, body whorl keeled at the middle of body whorl, teleoconch finely wrinkled with small scales.

Description. Shell small, sinistral, spire elevated, dorsal surface domed/conical; body whorl bluntly keeled, keel situated at about mid part of body whorl; shallow subsutural furrow present on body whorl above keel; protoconch consists of 1.5 whorls, finely pitted and wrinkled; entire shell with 5.5–5.75 whorls; teleoconch finely, irregularly wrinkled, with fine, curved scales (present near suture); aperture subcircular, peristome not developed in the two available specimens.

Measurements (in mm). D = 9.5–9.6, H = 5.7–6.1 (n = 2).

Differential diagnosis. This species is smaller than the other congeners, and its keel is situated in the middle of the body whorl.

Distribution. This species is known from the type locality only. We were not able to determine the locality Tapa on the map among more than 20 similarly called localities.

Remarks. This species differs from the other congeners by its smaller shell; both the available shells are smaller than 10 mm in diameter, whereas the others have shells larger than 15 mm. Though the small scales on the shell surface suggest that this species belongs to the genus *Trichocathaica*, due to its small shell size, its generic placement needs to be verified by examination of genital morphology.

Trichocathaica lyonsae (Gude, 1919)

Remarks. This species can be distinguished from the other congeners by the long and slender hairs, which are mostly present on the side of the body whorl and the upper edge of the preceding whorls (i.e. inside the suture). We received photos of the types of the two subspecies, and therefore, their fine sculpture could not be examined.

Distribution. This species is only known from the valley of the Min River.

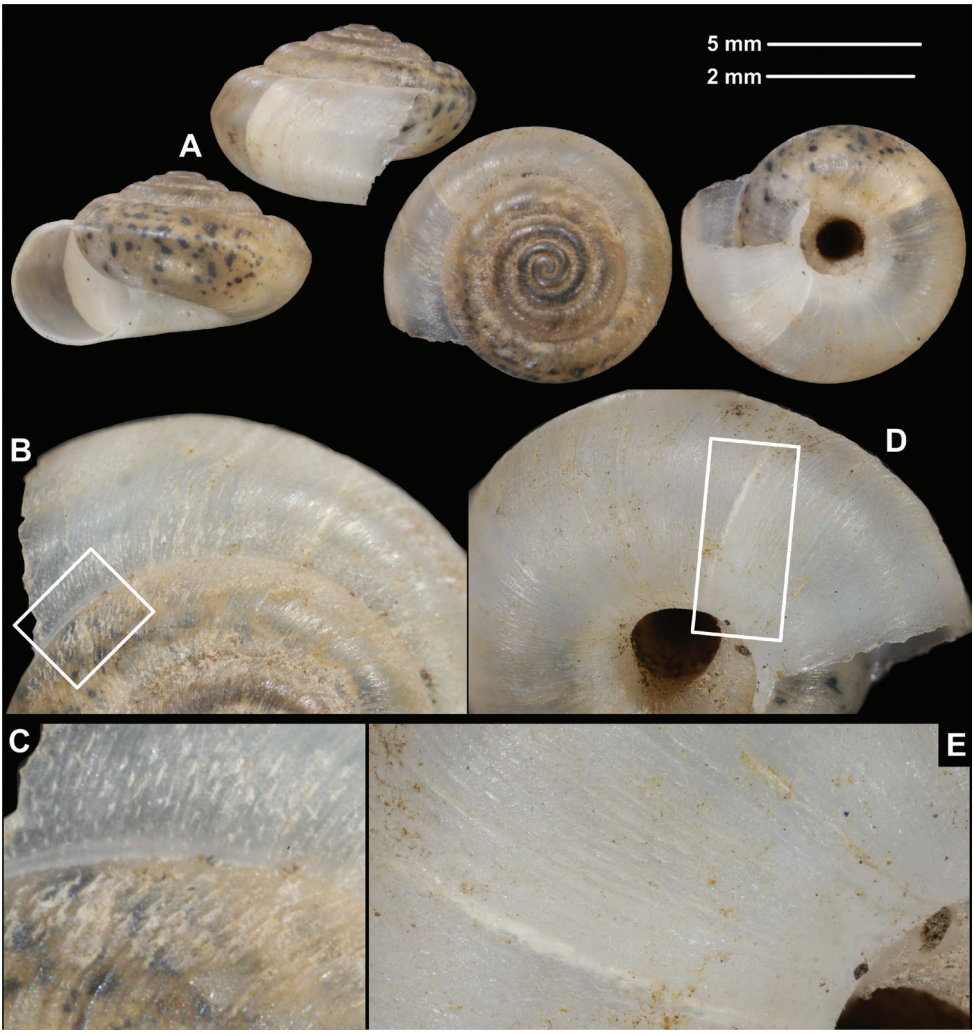

Figure 9. Lectotype of *Trichocathaica goepeliana* Yen, 1938 (SMF 8939, syntype, D = 9.6 mm). **A** Entire shell **B, C** Dorsal sculpture **D, E** Ventral sculpture **C, E** show white framed area of **B** and **D** respectively. Scale bars: Upper scale (**A**), lower scale (**B, D**) **C, E** not to scale. All photos: B. Páll-Gergely.

Trichocathaica lyonsae lyonsae (Gude, 1919)

Figure 10A–C

Cathaica (*Trichocathaica*) *lyonsae* Gude, 1919: 119 + unnumbered figure.
Trichocathaica lyonsae – Yen 1939: 150, plate 15, fig. 43.

Types examined. Min Valley, Setchuen, coll. Gude, NHMUK 1922.8.29.86 (syntype).
Type locality. "Min Valley, Setchuen".

Diagnosis. Shell sinistral, body whorl slightly shouldered, teleoconch roughly wrinkled with medium-sized scale-like periostracal folds; some folds are developed to long hairs.

Description. Shell sinistral, spire slightly elevated, dorsal side rather low conical; body whorl slightly shouldered; protoconch consists of 1.5 whorls, finely, irregularly wrinkled; entire shell with 5.5 whorls; teleoconch roughly, irregularly wrinkled, with moderately large, triangular periostracal folds; some folds on the edge of body whorl and in the suture developed to long, cylindrical hairs; in shell parts without periostracum the base of folds visible as deep scars; aperture subcircular, slightly ovoid (depressed in dorsobasal direction); upper peristome edge strongly descending (mostly visible from lateral view); peristome slightly expanded, sharp; inner thickening parallel to the peristome strong, white.

Measurements (in mm). D = 17.3, H = 8.7 (photographed syntype).

Distribution. This subspecies is known from the type locality only.

Trichocathaica lyonsae comosa (Pilsbry, 1934)

Figure 10D–E

Bradybaena (*Trichocathaica*) *lyonsae comosa* Pilsbry, 1934: 86: 11–12, plate 4, figs 4, 5.

Types examined. Wenchwan, Szechuan, China, on a dry hill slope, (W. China exp., Brooke Dolan, 24.04.1931), ANSP 159641 (holotype).

Type locality. "Wenchwan, Szechuan, on a dry hill slope"; "between Kwanhsien and Yuchi".

Measurements (in mm). D = 15.7, H = 7.0 (*n* = 1, according to the original description).

Differential diagnosis. *Trichocathaica lyonsae comosa* differs from the nominotypical subspecies by the slightly smaller shell, the less descending aperture and the flat dorsal side.

Trichocathaica puteolata Páll-Gergely, sp. n.

http://zoobank.org/C89554FE-A309-42C5-BDC5-328153FB7EF6

Figure 11A–C

Laeocathaica (*Trichocathaica*) *lyonsae* – Wenz 1960: 639, fig. 2235.

Material examined. China, Sytschuan, "Hügel bei der Fähre aus Ta Tu Ho bei %" (one side of the label), "Fulin Ton boden, Maisfelden, 31.07.1930" (other side of the label), SMF 24666a/1 (holotype, orig. Handb. Pal. 2235); same data, SMF 349516/61 shells (most of them are juveniles); same data, SMF 349514/1 paratype shell (orig. Yen, 1939: plate 15, fig. 43); China, Sytschuan, Osthang des Lu-ho (=Ta Tu-Ho), s.

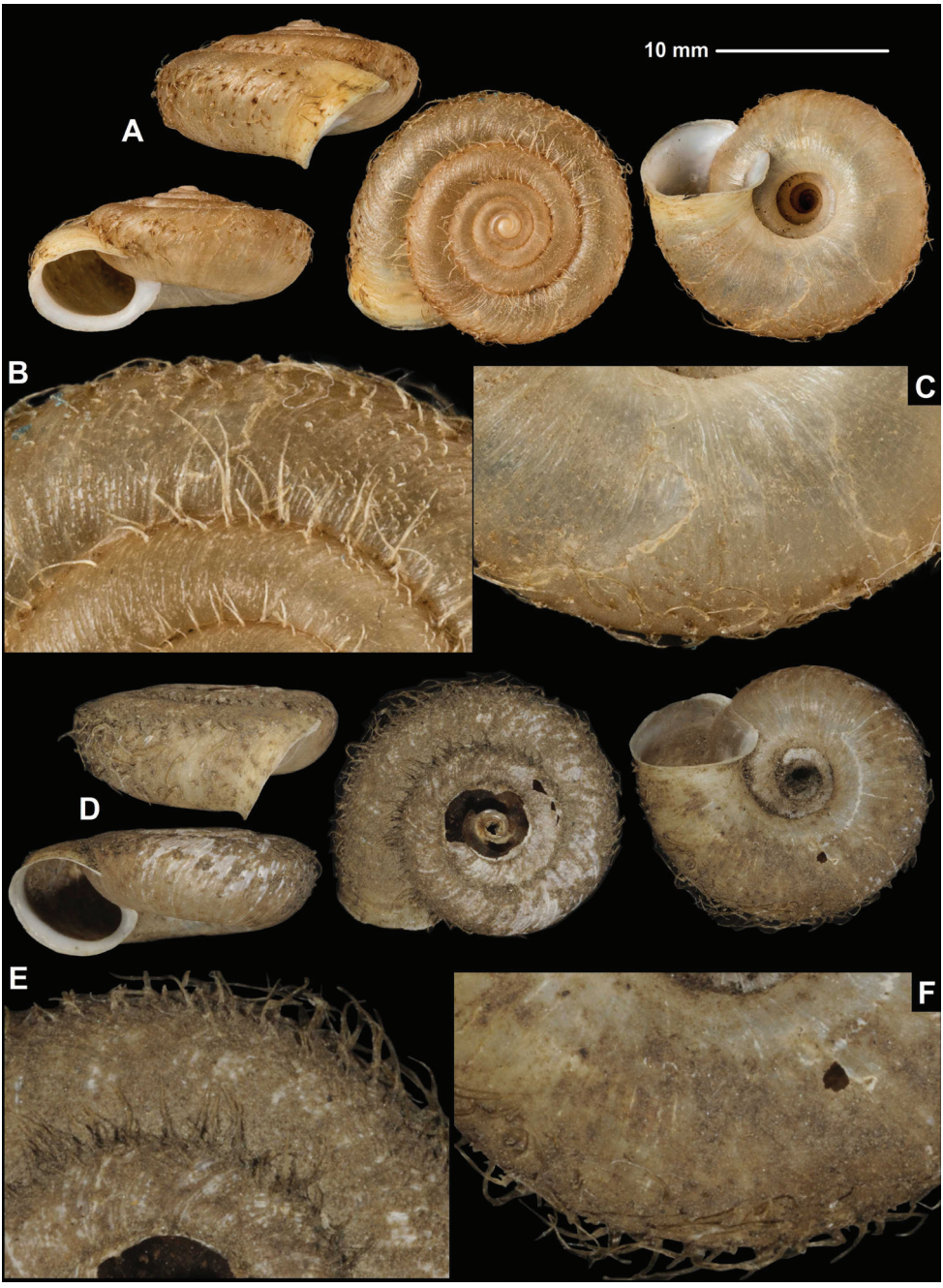

Figure 10. A–C *Trichocathaica lyonsae lyonsae* (Gude, 1919), NHMUK 1922.8.29.86 (syntype, D = 17.3 mm) **D–F** *Trichocathaica lyonsae comosa* (Pilsbry, 1934), ANSP 159641 (holotype, D = 15.7 mm). Close-up images show the dorsal (**B, E**), and the ventral (**C, F**) sculpture. Scale refers to **A, D** other figures not to scale. Photos: K. Seizova, ANSP Malacology Department (**D–F**) and H. Taylor (**A–C**).

Lu Tin Chouw (?), ex coll. K. Krejci-Graf, 04,08,1930 (1933), SMF 24665/15 (most of them are juveniles).

Diagnosis. Shell large, sinistral, body whorl keeled above mid-part of body whorl, teleoconch roughly wrinkled with moderately large, slender periostracal folds, fold scars represented as deep pits.

Description. Shell sinistral, spire very slightly elevated in most specimens (dorsal side nearly flattened), but in some shells dorsal surface domed; body whorl slightly keeled, keel situated above mid part of body whorl; protoconch consists of 1.25–1.75 whorls, finely, irregularly wrinkled; entire shell with 4.5–5.5 whorls; teleoconch roughly, irregularly wrinkled, with moderately large, slender triangular, sometimes cylindrical, hair-like periostracal folds having short, curved base; in specimens/shell parts without periostracum the base of folds visible as deep fold scars; aperture subcircular, peristome slightly expanded, thin, sharp; inner thickening parallel to the peristome weak.

Measurements (in mm). D = 15.7–22.8, H = 7.5–11.4 (*n* = 6).

Differential diagnosis. The shell of *T. rugosobasis* is similar to that of *T. puteolata* sp. n. but smaller with the narrower umbilicus, less keeled body whorl, and stronger radial sculpture.

Etymology. The Latin puteolata (= pitted) refers to the pitted surface of the shells.

Distribution. This species is known only from the valley of the Dadu River.

Remarks. All shells we examined in the SMF were labelled as *T. lyonsae*.

Trichocathaica rugosobasis (Pilsbry, 1934)

Figure 11D–F

Bradybaena (*Trichocathaica*) *rugosobasis* Pilsbry, 1934: 86: 12, plate 4, figs 6, 7.

Type examined. Wenchwan to Maochow, Szechuan, China (W. China exp., Brooke Dolan, 24.04.1931), ANSP 159636 (holotype [photos examined] + 2 paratypes [not examined]).

Type locality. "Between Wenchwan and Maochow, Szechuan, on rocks in the arid valley of the Min River, 3500–4100 ft. elevation".

Description (based on photos of the holotype). Shell sinistral, spire slightly elevated, body whorl rounded with a very slight indication of a blunt keel; protoconch consists of 1.75 whorls, probably finely, irregularly wrinkled; entire shell with 5.75 whorls; teleoconch very roughly, irregularly wrinkled, with large hair scars, periostracal elements not visible; aperture subcircular, peristome slightly expanded, thin, sharp; inner thickening parallel to peristome seemingly normally developed, situated in some distance from peristome edge.

Measurements (in mm). D = 14.3–15.0, H = 7.0–7.2 (*n* = 2, according to the original description).

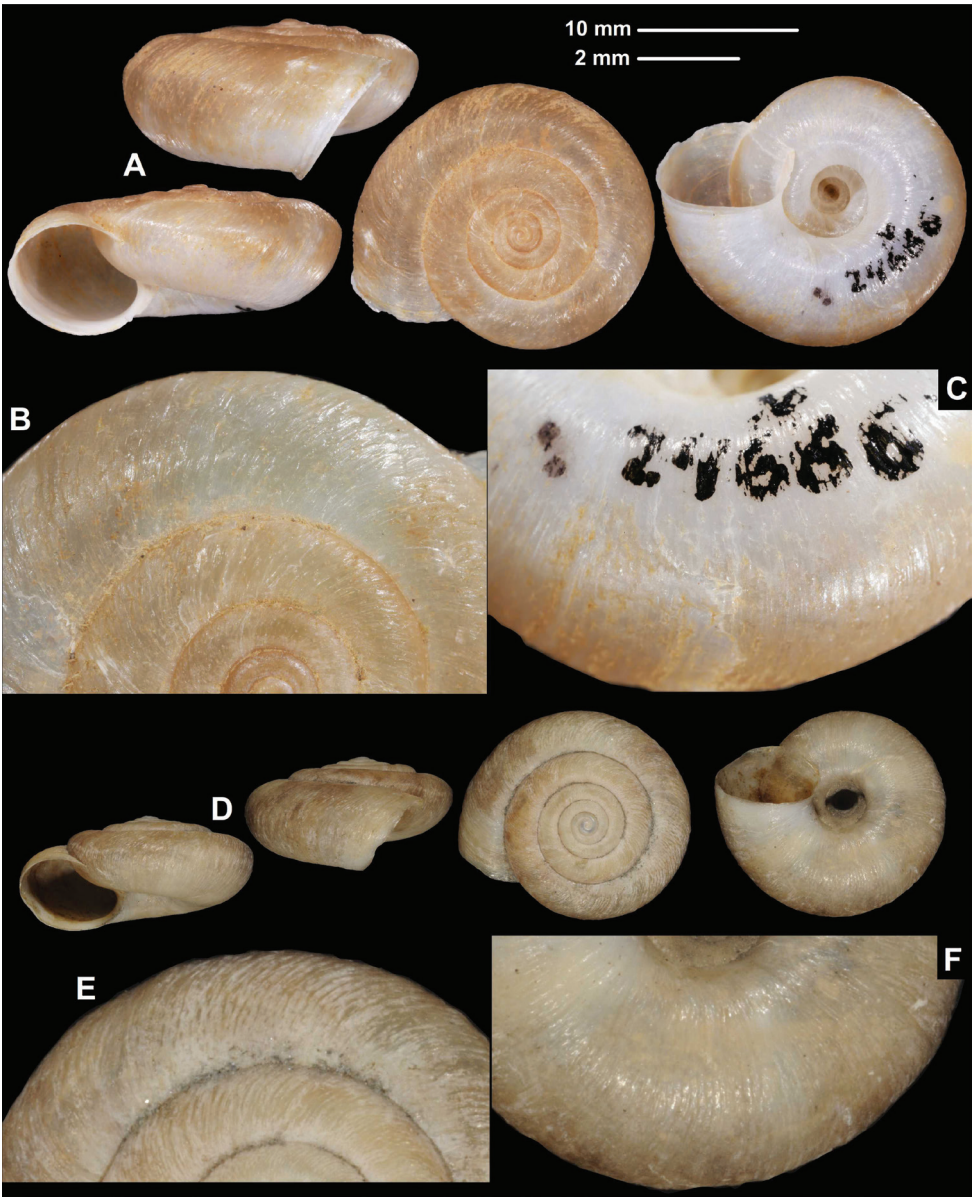

Figure 11. Shells (**A, D**), dorsal (**B, E**), and ventral (**C, F**) sculpture of *Trichocathaica* species **A–C** *Trichocathaica rugosobasis* (Pilsbry 1934), ANSP 159636 (holotype, D = 15 mm) **D–F** *Trichocathaica puteolata* Páll-Gergely sp. n., holotype (SMF 24666, D = 19.5 mm). Scale bars: Upper scale (**A, D**); lower scale (**B, C, E, F**). Photos: B. Páll-Gergely (**D–F**) and K. Seizova, ANSP Malacology Department (**A–C**).

Remarks. This species is characterized by its medium-sized shell with rough radial sculpture. The holotype is somewhat corroded, and thus, the periostracal folds could not be examined.

Figure 12. Shell (**A**), dorsal (**B**), and ventral (**C**) sculpture of *Trichocathaica* sp. (SMF 8937, D = 20.2 mm). Scale bars: Upper scale (**A**), lower scale (**B, C**). All photos by B. Páll-Gergely.

***Trichocathaica* sp.**
Figure 12

Material examined. W-Sytschuan, Thal des Tung, coll. Möllendorff ex coll. Potanin, SMF 8937/1 sinistral shell.

Measurements (in mm). D = 20.2, H = 12.0 (*n* = 1).

Remarks. The single shell specimen is not corroded and has no scales/hairs on its surface. Thus, this specimen might be of an undescribed species. However, we hesitate to describe this taxon until more specimens become available.

Discussion

The present study discovered that both dextral and sinistral individuals are frequently found in the flat-shelled stylommatophoran snail genus *Trichocathaica*. We found that three morphologically distinguishable species had been classified as *T. amphidroma*, and thus, treated as three species including *T. macrosquamata* sp. n. and *T. vestita*. We recognized them based on the traits of their shell surface morphology.

In flat-shelled stylommatophoran snail groups, which ordinarily mate simultaneously reciprocally, it is unusually frequent to find both dextral and sinistral specimens

in five out of the nine specimen lots. Observations of three cases of enantiomorphism across the three congeneric species are also extraordinary in flat snails. These numerical data rule out the possibility of transient enantiomorphism that results from stochastic appearance of the reversed morph in a simultaneously reciprocally mating population.

Transient enantiomorphism maybe recurrent, however, if snails of *Trichocathaica* employ non-reciprocal copulation by shell mounting. For example, snails of the genus *Oreohelix* of the family Oreohelicidae copulate non-reciprocally, exceptionally for flat groups (Webb 1951). It has been noted that sinistral variants are more frequently found in this group than in other genera in North America (Pilsbry 1939). In the present cases, enantiomorphs were collected in each of the three species only once in 1880s, 1930 or 2015. Thus, transient enantiomorphism in non-reciprocally mating populations might also be the case in the present genus. Our results, therefore, indicate the importance of explicit examination of their copulation mode and quantitative surveys of chiral variation in this genus.

In the Camaenidae, tree snails of the subgenus *Amphidromus* present exceptions regarding the mating mode and interchiral copulation. They are tall-shelled snails but mate simultaneously reciprocally (Sutcharit et al. 2007; Schilthuizen et al. 2007). Despite their mating mode, they frequently achieve interchiral copulation. Their populations exhibit enantiomorphism, probably because interchiral copulation occurs more frequently than expected in random mating (Schilthuizen et al. 2007). If any mechanism were similarly in effect for maintenance of enantiomorphism in the present three species, both dextrals and sinistrals would have been found commonly across the distribution range of each species. However, the dextral and sinistral specimens were present in mixture in only one of lots that included specimens of each species. Thus, the enantiomorphism in *Trichocathaica* could not be ascribed to balanced enantiomorphism which is positively maintained within populations.

The hypothesis of speciation by left-right reversal predicts morphological divergence following the completion of sexual isolation between populations of enantiomorphs. Shell traits do not necessarily diverge even between genetically isolated good species with distinct genital morphology (Kameda and Fukuda 2015). For comparison of the patterns of penial microsculpture in this study, only a single individual specimen was available for each of the enantiomorphs in *T. vestita*. Thus, there was technical limitation to demonstrate difference associated with enantiomorphs instead of individuals, especially if their populations began to diverge recently. We found that these dextral and sinistral specimens slightly differed in penial sculpture pattern, although their differences were not large enough to describe them as morphologically distinct species. Thus, our results do not rule out the possible presence of sexual isolation between these enantiomorphs. We know no study that evaluated individual variation in penial microsculpture. The present study is the first example of comparing the patterns of penial microsculpture between conchologically indistinguishable enantiomorphs that were locally frequent and repeatedly found among closely related flat species. Our results demonstrate the critical importance of further explicit examination of possible interchiral divergence in penial morphology in *Trichocathaica* as well as in the other stylommatophoran snails.

Acknowledgements

We are grateful to Sigrid Hof and Ronald Janssen (SMF) for opening access to their museum collection, to Jonathan Ablett (NHM) to search for the holotype of *T. lyonsae* and arranging for it to be photographed, to K. Seizova and H. Taylor for taking photographs, to Miklós Szekeres for help in the field, and to Chen Zheyu for help in identifying Chinese localities. We also thank to Bernhard Hausdorf and Seng Liew Thor for reviewing the manuscript. This study was supported by the MTA (Hungarian Academy of Sciences) Premium Post Doctorate Research Program to Barna Páll-Gergely.

References

Adams H (1870) Descriptions of ten new species of land and freshwater shells collected by Robert Swinhoe, Esq., in China and Formosa. Proceedings of the Zoological Society of London 1870: 377–380.

Asami T (1993) Genetic variation and evolution of coiling chirality in snail. Forma 8: 263–276.

Asami T, Ohbayashi K, Cowie RH (1998) Evolution of mirror images by sexually asymmetric mating behaviour in hermaphroditic snails. American Naturalist 152: 225–236. https://doi.org/10.1086/286163

Bouchet O, Rocroi J-P, Hausdorf B, Kaim A, Kano Y, Nützel A, Parkhaev P, Schrödl M Strong EE (2017) Revised classification, nomenclator and typification of gastropod and monoplacophoran families. Malacologia 61(1–2): 1–526. https://doi.org/10.4002/040.061.0201

Danaisawadi P, Asami T, Ota H, Sutcharit C, Panha S (2016) A snail-eating snake recognizes prey handedness. Scientific Reports 6: 23832. https://doi.org/10.1038/srep23832

Davison A, Chiba S, Barton NH, Clarke B (2005) Speciation and gene flow between snails of opposite chirality. PLOS Biology 3: e282. https://doi.org/10.1371/journal.pbio.0030282

Davison A, Mordan P (2007) A literature database on the mating behavior of stylommatophoran land snails and slugs. American Malacological Bulletin 23: 173–181. https://doi.org/10.4003/0740-2783-23.1.173

Gittenberger T (1988) Sympatric speciation in snails; a largely neglected model. Evolution 42: 826–828. https://doi.org/10.2307/2408875

Gittenberger E, Hamann TD, Asami T (2012) Chiral speciation in Terrestrial Pulmonate Snails. PLOS ONE 7(4): e34005. https://doi.org/10.1371/journal.pone.0034005

Gude GK (1919) Description of two new species and a new sub-genus of land shells from China. Proceedings of the Malacological Society of London 13: 118–119. https://doi.org/10.1093/oxfordjournals.mollus.a063696

Hoso M, Asami T, Hori M (2007) Right-handed snakes: convergent evolution of asymmetry for functional specialization. Biology Letters 3: 169–173. https://doi.org/10.1098/rsbl.2006.0600

Hoso M, Kameda Y, Wu SP, Asami T, Kato M, Hori M (2010) A speciation gene for left-right reversal in snails results in anti-predator adaptation. Nature Communications 1: 133. https://doi.org/10.1038/ncomms1133

Johnson MS (1982) Polymorphism for direction of coil in Partula suturalis: behavioural isolation and positive frequency dependent selection. Heredity 49: 145–151. https://doi.org/10.1038/hdy.1982.80

Kameda Y, Fukuda H (2015) Redefinition of *Satsuma ferruginea* (Pilsbry, 1900) (Camaenidae), with description of a new cryptic species endemic to the coasts and islands of the central Seto Inland Sea, western Japan. Venus 73: 15–40.

Kerney MP, Cameron RAD (1979) A Field Guide to the Land Snails of Britain and North-west Europe. Collins, London, 288 pp.

Möllendorff O von (1899) Binnen-Mollusken aus Westchina und Central-Asien I. Annuaire du Musée Zoologique de l'Académie Impériale des Sciences de Saint Pétersbourg 4: 46–142.

Okumura T, Utsuno H, Kuroda J, Gittenberger E, Asami T, Matsuno K (2008) The development and evolution of left-right asymmetry in invertebrates: lessons from Drosophila and snails. Developmental Dynamics 237: 3497–3515. https://doi.org/10.1002/dvdy.21788

Orr HA (1991) Is single-gene speciation possible? Evolution 45: 764–769. https://doi.org/10.1111/j.1558-5646.1991.tb04345.x

Richards PM, Morii Y, Kimura K, Hirano T, Chiba S, Davison A (2017) Single-gene speciation: mating and gene flow between mirror-image snails. Evolution Letters 1: 282–291. https://doi.org/10.1002/evl3.31

Pilsbry HA (1893–1895) Manual of Conchology, ser. 2, vol. 9. (Helicidae, vol. 7). Guide to the study of helices. Academy of Natural Sciences, Conchological Section, Philadelphia 366: 1–126.

Pilsbry HA (1934) Zoological results of the Dolan West China expedition of 1931, Part II, Mollusks. Proceedings of the Academy of Natural Science of Philadelphia 86: 5–28.

Pilsbry HA (1939) Land Mollusca of North America (north of Mexico), Vol. l, Part I. Academy of Natural Sciences of Philadelphia, Monographs, 573 pp.

Schilthuizen M, Craze, PG, Cabanban, AS, Davison A, Stone J, Gittenberger E, Scott BJ (2007) Sexual selection maintains wholebody chiral dimorphism in snails. Journal of Evolutionary Biology 20: 1941–1949. https://doi.org/10.1111/j.1420-9101.2007.01370.x

Sutcharit C, Asami T, Panha S (2007) Evolution of whole-body enantiomorphy in the tree snail genus *Amphidromus*. Journal of Evolutionary Biology 20: 661–672. https://doi.org/10.1111/j.1420-9101.2006.01246.x

Sturtevant AH (1923) Inheritance of direction of coiling in *Limnaea*. Science 58: 269–270. https://doi.org/10.1126/science.58.1501.269

Ueshima R, Asami T (2003) Single-gene speciation by left-right reversal. Nature 425: 679. https://doi.org/10.1038/425679a

Utsuno H, Asami T (2010) The maternal inheritance of racemism in the terrestrial snail Bradybaena similaris. Journal of Heredity 101: 11–19. https://doi.org/10.1093/jhered/esp058

Utsuno H, Kasem S, Fukuda H, Asami T (2010) Genetic basis of racemism and ease of interchiral mating in a clausiliid species of snails. Molluscan Research 30: 37–47.

Utsuno H, Asami T, Dooren TJMV, Gittenberger E (2011) Internal selection against the evolution of left-right reversal. Evolution 65: 2399–2411. https://doi.org/10.1111/j.1558-5646.2011.01293.x

van Batenburg FHD, Gittenberger E (1996) Ease of fixation of a change in coiling: computer experiments on chirality in snails. Heredity 76: 278–286. https://doi.org/10.1038/hdy.1996.41

Yen T-C (1939) Die Chinesischen Land-und Süßwasser-Gastropoden des Natur-Museums Senckenberg. Abhandlungen der Senckenbergischen Naturforschenden Gesellschaft, Frankfurt am Main, 234 pp.

Wade CM, Hudelot C, Davison A, Naggs F, Mordan PB (2007) Molecular phylogeny of the helicoid land snails (Pulmonata: Stylommatophora: Helicoidea), with special emphasis on the Camaenidae Journal of Molluscan Studies 73: 411–415. https://doi.org/10.1093/mollus/eym030

Webb GR (1951) Sexological notes on the landsnail *Oreohelix*. Natural History Miscellanea 78: 15.

Wu Min (2001) On new species of Chinese endemic snails of *Trichocathaica* (Gastropoda: Stylommatophora: Bradybaenidae). Acta Zootaxonomica Sinica 26(3): 292–296.

Wu, Min (2015) A Photographic Guide to Land Snails of China. Chongqing University Press, Chongqing, 211 pp.

Zilch A (1959–1960) Euthyneura. In: Wenz W (Ed.) Handbuch der Paläozoologie. Band 6, Teil 2. Gebrueder Borntraeger, Berlin, 834 pp.

ZooKeys 810: 45–89 (2018)
doi: 10.3897/zookeys.810.29253
http://zookeys.pensoft.net

RESEARCH ARTICLE

A peer-reviewed open-access journal
ZooKeys
Launched to accelerate biodiversity research

Onychocamptus Daday, 1903 from Thailand, with descriptions of two new species and two new records (Crustacea, Copepoda, Harpacticoida, Laophontidae)

Chaichat Boonyanusith[1], Thanida Saetang[2], Koraon Wongkamheng[2], Supiyanit Maiphae[2]

1 *School of Biology, Faculty of Science and Technology, Nakhon Ratchasima Rajabhat University, Nakhon Ratchasima, 30000, Thailand* **2** *Department of Zoology, Faculty of Science, Kasetsart University, Lad Yao, Chatuchak, Bangkok, 10900, Thailand*

Corresponding author: *Supiyanit Maiphae* (supiyanit.m@ku.ac.th)

Academic editor: *Danielle Defaye* | Received 24 August 2018 | Accepted 22 November 2018 | Published 20 December 2018

http://zoobank.org/5361B367-7FA8-495D-81B2-7151B77D2CB4

Citation: Boonyanusith C, Saetang T, Wongkamheng K, Maiphae S (2018) *Onychocamptus* Daday, 1903 from Thailand, with descriptions of two new species and two new records (Crustacea, Copepoda, Harpacticoida, Laophontidae). ZooKeys 810: 45–89. https://doi.org/10.3897/zookeys.810.29253

Abstract

In this paper, two new species of *Onychocamptus* Daday, 1903 are described from Thailand: *Onychocamptus satunensis* **sp. n.** and *Onychocamptus tratensis* **sp. n.** The following features mainly distinguish *O. satunensis* **sp. n.** from known species: internal sausage-like and internal rounded structures on cephalothorax and one outer seta on the male P5 exopod that is as long as the supporting segment. In contrast, the cephalothorax of *O. tratensis* **sp. n.** is smooth but has rounded integumental window-like structures, and the outer seta on the male P5 exopod is two times as long as the supporting segment. *Onychocamptus anomalus* shows the highest similarity with the two new species, but in contrast to both Thai species, it has only one seta on the exopod of the antenna. In addition, in the present study, two additional species, *O. bengalensis* and *O. vitiospinulosa*, are newly recorded in Thailand. Thus, the number of *Onychocamptus* species recorded in Thailand increases to five species. A key to all known species of this genus in the world is also proposed.

Keywords

Laophontidae, Southeast Asia, stygobiont

Introduction

The genus *Onychocamptus* comprises eight species: (1) *Onychocamptus mohammed* (Blanchard & Richard, 1891), the type species, with *O. heteropus* Daday, 1903 considered a junior synonym (Zykoff 1904: 247, Lang 1948: 520, Huys 2009: 84); (2) *O. bengalensis* (Sewell, 1934); (3) *O. besnardi* Jakobi, 1954; (4) *O. vitiospinulosa* (Shen & Tai, 1963); (5) *O. anomalus* (Ranga Reddy, 1984); (6) *O. taifensis* (Kikuchi, Dai & Itô, 1993); (7) *O. krusensterni* (Schizas & Shirley, 1994), and (8) *O. fratrisaustralis* (Gómez, 2001). Most of the species are widely distributed in various types of inland waters, from fresh to saline (Lee and Chang 2005).

In Thailand, only one species, *O. mohammed*, had been reported (Apostolov 2007). However, from a more intensive study of harpacticoids in Thailand, including both intensive sampling and detailed study of the morphological characteristics, four more species of *Onychocamptus* have been found: *O. bengalensis* and *O. vitiospinulosa* are newly recorded in Thailand, and *O. satunensis* sp. n. and *O. tratensis* sp. n. are proposed as new species. This paper presents the joint results of two different research projects, a study on the diversity of cave-dwelling copepods in Satun province and a study on the diversity of copepods in important surface water bodies throughout Thailand. This study represents the first attempt to revise our knowledge on the diversity of this genus in Thailand.

Materials and methods

Plankton samples were collected from the Samer-rach peat swamp (Trat Province) in eastern Thailand, and from the Prawattisart and Khao Thanan caves (Satun Province), Thale-Noi Lake (Pattalung Province), and Ta-pom swamp (Krabi Province) in southern Thailand (Fig. 1). A plankton net with a 60-μm mesh was used for collecting the samples, which were immediately preserved in 70% ethanol. The copepods were sorted using an Olympus SZ-40 stereo microscope, and identified specimens of *Onychocamptus* were dissected and mounted on a slide, with glycerine as the mounting medium, and sealed with nail varnish. Drawings were made from both complete and dissected specimens using a camera lucida attached to an Olympus CH-2 compound microscope. For scanning electron microscopy, the samples were dehydrated in a series of increasing ethanol concentrations: 60%, 80%, 90%, 95%, 96%, and 100%. The samples were dehydrated twice in each concentration, for 15 min each time. Then, the specimens were subjected to the critical point drying process, mounted on stubs, coated with gold, and examined with a scanning electron microscope (Quanta 450 FEI). The descriptive terminology proposed by Huys et al. (1996) and the armature formula P1-P4 proposed by Sewell (1949) (cited by Huys and Boxshall 1991) were adopted. P1–P6, swimming legs 1–6; enp-1 (2, 3), proximal (middle, distal) segment of the endopod; and exp-1 (2, 3), proximal (middle, distal) segment of the exopod. Holotype, allotype, and paratypes were deposited in the reference collection of the Princess Maha Chakri Sirindhorn National History Museum, Prince of Songkla

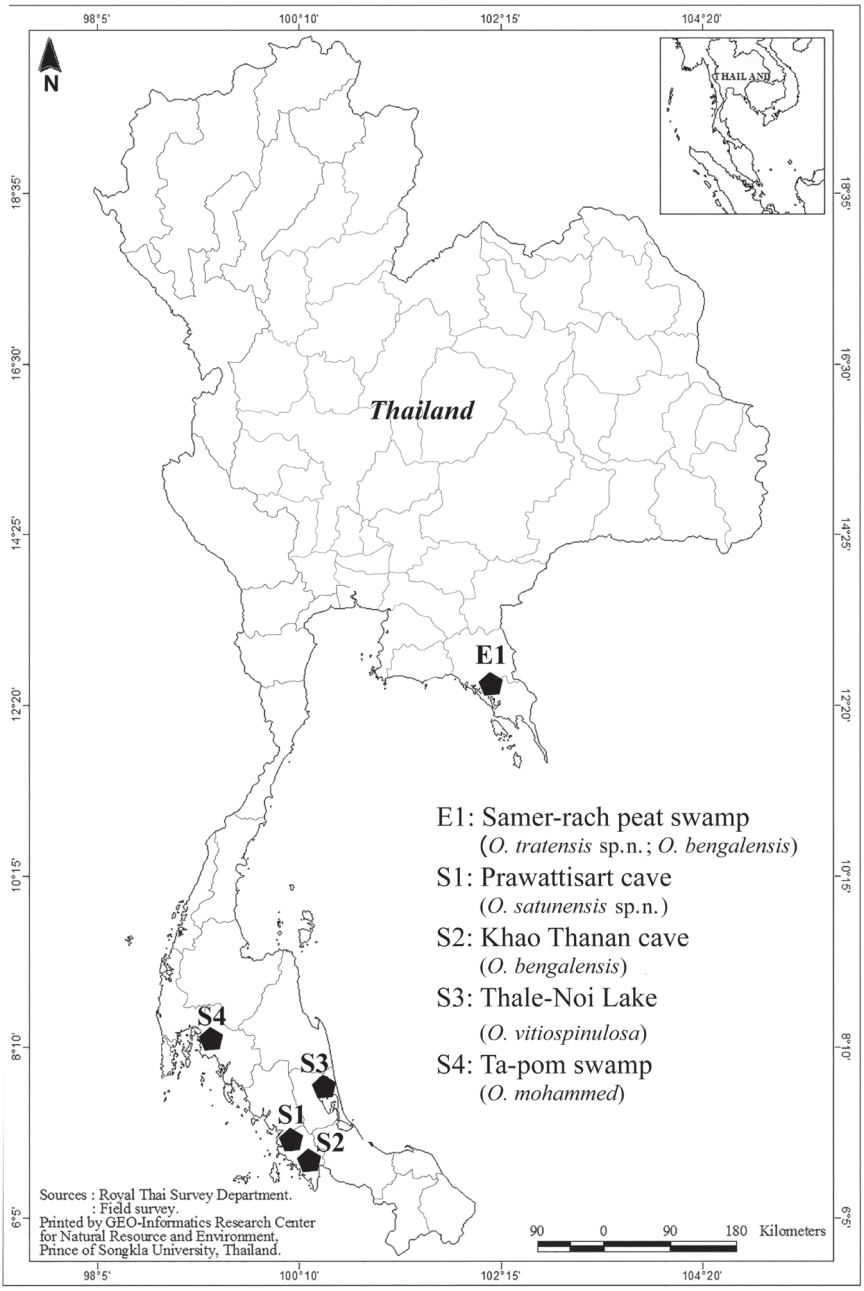

Figure 1. Sampling sites.

University, Songkhla, Thailand (**PSUNHM**). Voucher specimens were deposited in the collections of the first author (CB) and in the crustacean reference collection of the Zoological Museum, Kasetsart University (**ZMKU_CP**).

Taxonomy

Order Harpacticoida Sars, 1903
Family Laophontidae T. Scott, 1904
Genus *Onychocamptus* Daday, 1903

***Onychocamptus satunensis* sp. n.**
http://zoobank.org/F38757B6-A85E-4F7C-B4AC-520821E6C650
Figs 2–8, 23A

Material examined. Holotype. Adult female, dissected and mounted onto one slide, collected from type locality on 30 July 2015 (PSUZC-PK2002-01). **Allotype.** One adult male, dissected and mounted onto one slide, (PSUZC-PK2002-02), all collected from type locality on 20 January 2016. **Paratypes**. One undissected adult ovigerous female paratype mounted onto one slide (PSUZC-PK2002-03), and one undissected adult male paratype, mounted onto one slide (PSUZC-PK2002-04), coll. C Boonyanusith and K Wongkamheng; type locality on 30 July 2015 and 20 January 2016, respectively.

Additional material. One adult ovigerous female and one adult male, both collected from type locality on 2 April 2015 and stored in 70% ethanol, deposited in the collection of the first author (CB).

Type locality. Prawattisart cave, Muang district, Satun Province, southern Thailand, 6°42'55.82"N, 100°05'19.17"E. The cave is in an isolated, wedge-shaped, limestone hill. It is surrounded by irrigation canal and paddy fields, but there are no connections between water in and outside cave. Beyond entrance of the cave there is a long horizontal gallery, with approximately 5–10 m high and approximately 2–3 m wide. At some place there are two openings, which are large enough for entry, indicating a complex tunnel system. The collecting point is a part of a large water body inside the cave, fulfilled by approximately 10–50 cm depth of water. Water depth varies according to season, but it has never dried out. Water was turbid and flowed slowly. Water temperature was 25.5 °C, pH 7.8, conductivity 360 μS cm^{-1}, dissolved oxygen 4.9 mgL^{-1}.

Etymology. The specific name *satunensis* is derived from the name of Satun Province, where the species was collected. The name is a noun in the genitive singular, masculine.

Differential diagnosis. Laophontidae. Body gradually tapering posteriorly. Cephalothorax with internal sausage-like structure, and internal rounded structures. Posterior margin of cephalothorax and body somites (except penultimate and anal somite) with sensillum-bearing tubercles. Second and third urosomite partly fused ventrally in female, representing genital double-somite. Caudal rami approximately 2.5 times as long as wide, with one transverse inner row of spinules near insertion of dorsal seta. Caudal seta IV and V fused. Allobasis of antenna without abexopodal seta. Endopodal lobe of P5 with three, and exopod with four pinnate setae. Male P3 enp-2 with apophysis on outer distal corner, reaching tip of enp-3. Exopod of male P5 with three setae, outer seta as long as supporting segment. Male P6 reduced, with outer seta and inner bipinnate seta apically; inner seta approximately twice as long as outer one.

Description of adult female. Body (Fig. 2A). Total body length, measured from tip of rostrum to posterior margin of caudal rami, 401–445 μm (mean 419 μm, n = 3; 445 μm in holotype); preserved specimen colourless. Body covered with setules (Fig. 8E, F), cylindrical; gradually tapering posteriorly, with maximum width at posterior part of cephalothorax. Prosome approximately 1.3 times as long as urosome (including caudal rami) (Fig. 2A). Rostrum small, completely fused to cephalothorax. Cephalothorax as long as wide, approximately 0.5 times the length of prosome, just under integument with anterior internal structure comprising three parts; each of which sausage-like, and with internal rounded structures near distal margin (Figs 2A, B, 8A, B). Cephalothorax and all free thoracic somites with sensillum-bearing tubercles along posterior margin (Fig. 2A, B). Second and third urosomite fused ventrally (Fig. 2D), distinct dorsally and laterally (Fig. 2A–C), original division between sixth thoracic somite and first abdominal somite, with dorsal sensillum-bearing tubercles (Fig. 2C). Genital field ribbon-shaped, with seta representing P6 at outer distal corner (Fig. 2D). The remnant of first abdominal somite (posterior half of genital double-somite) with lateral sensillum-bearing tubercles (Fig. 2C, D). Posterior margin of genital double-somite and fourth urosomites with outer sensillum-bearing tubercles; posterior half of genital double-somite and fourth urosomite with posterior setules dorsally (Fig. 2C) and small spinules ventrally (Fig. 2D) between sensillum-bearing tubercles. Penultimate urosomite with posterior setules dorsally and laterally, with one posterior row of spinules ventrally. Anal somite as long as wide, with arch row of long spinules posterior to anal operculum (Figs 2A, C, 3A, 8D), with ventrolateral row of minute spinules near insertion of caudal rami (Fig. 2D). Anal operculum poorly developed, with minute spinules along posterior margin (Figs 2C, 3A, 8D).

Caudal rami (Figs 2C, D, 3A). Slightly convergent, 2.5 times as long as wide, with one transverse row of inner spinules near insertion of caudal seta (VII) (Figs 2C, 3A). Anterolateral accessory seta (I) minute, close to anterolateral seta (II), both subapical. Posterolateral seta (III) inserted on minute pedestal. Outer terminal seta (IV) slender, fused at base with inner terminal seta (V), the latter longest, without fracture plane, approximately 0.6 times as long as body length. Inner accessory seta (VI) slender. Dorsal seta (VII) tri-articulate, inserted at quarter of rami. Length ratio of caudal setae to ramus length, from seta I to seta VII of the holotype: 0.4 : 0.8 : 1.3 : 0.7 : 9.7 : 0.7 : 1.1.

The ovigerous female bears one oval egg sac with eight eggs, located ventrally between pair of fifth legs.

Antennule (Fig. 3B, C). Short, 5-segmented. First segment with medial and distal rows of spinules. Armature formula: I-[1], II-[8], III-[7+(1+aesthetasc)], IV-[1], V-[9+acrothek]. Aesthetasc on third segment robust, fused basally to one seta. Apical acrothek on fifth segment slender, consisting of one aesthetasc fused basally to two slender smooth seta.

Antenna (Fig. 3D). Comprising coxa, allobasis, and 1-segmented endopod and exopod. Coxa without ornamentation. Allobasis with one row of inner spinules, with 1-segmented exopod; the latter with two apical and two lateral bipinnate setae. Free endopodal segment with one strong, sharp spine, and one seta at distal third of segment; the former accompanied by several strong, short spinules; distal end with six

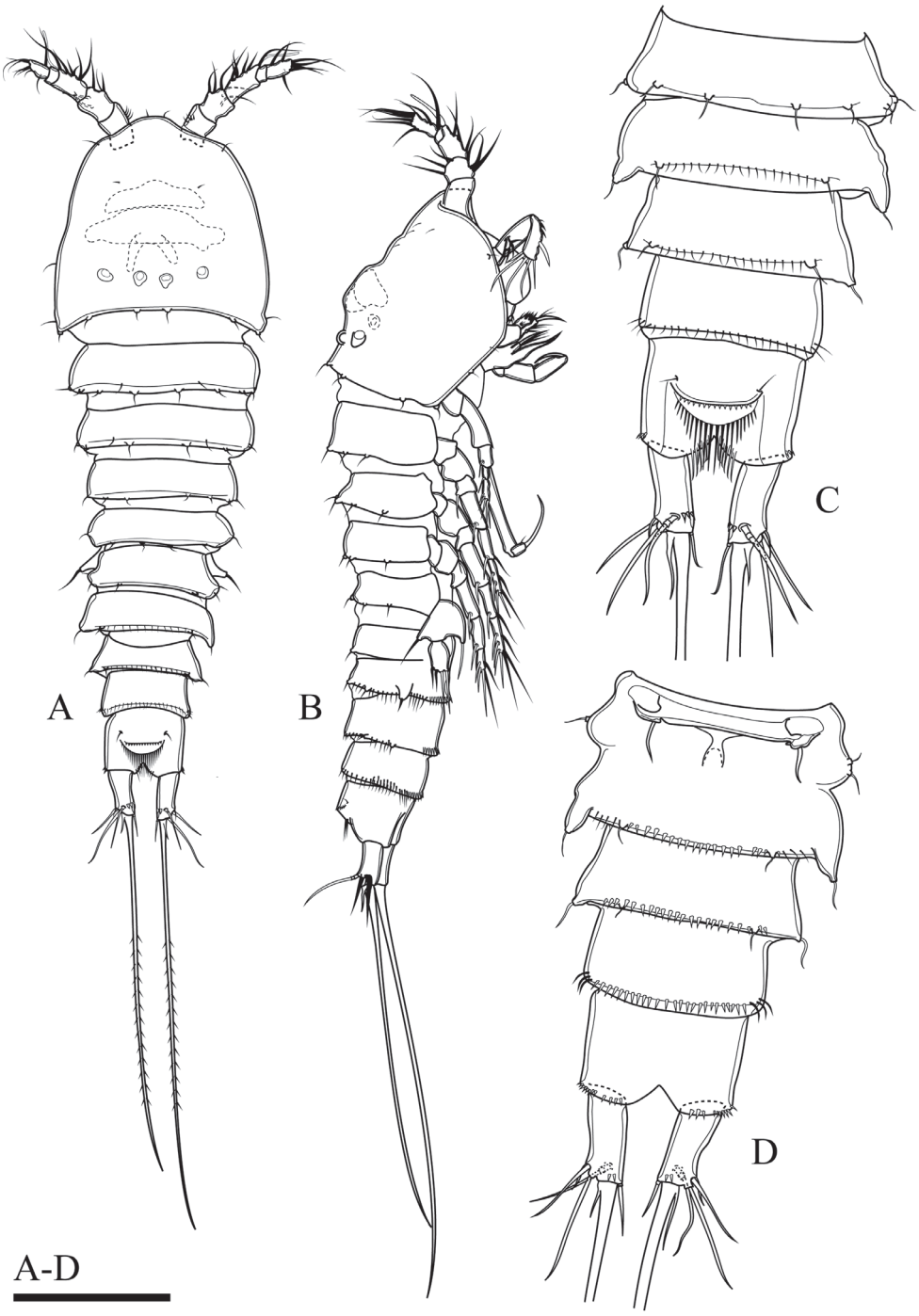

Figure 2. *Onychocamptus satunensis* sp. n., female holotype. **A** habitus, dorsal view **B** habitus, lateral view **C** urosome, dorsal view **D** urosome, ventral view. Scale bar: 0.1 mm (**A, B**), 0.05 mm (**C, D**).

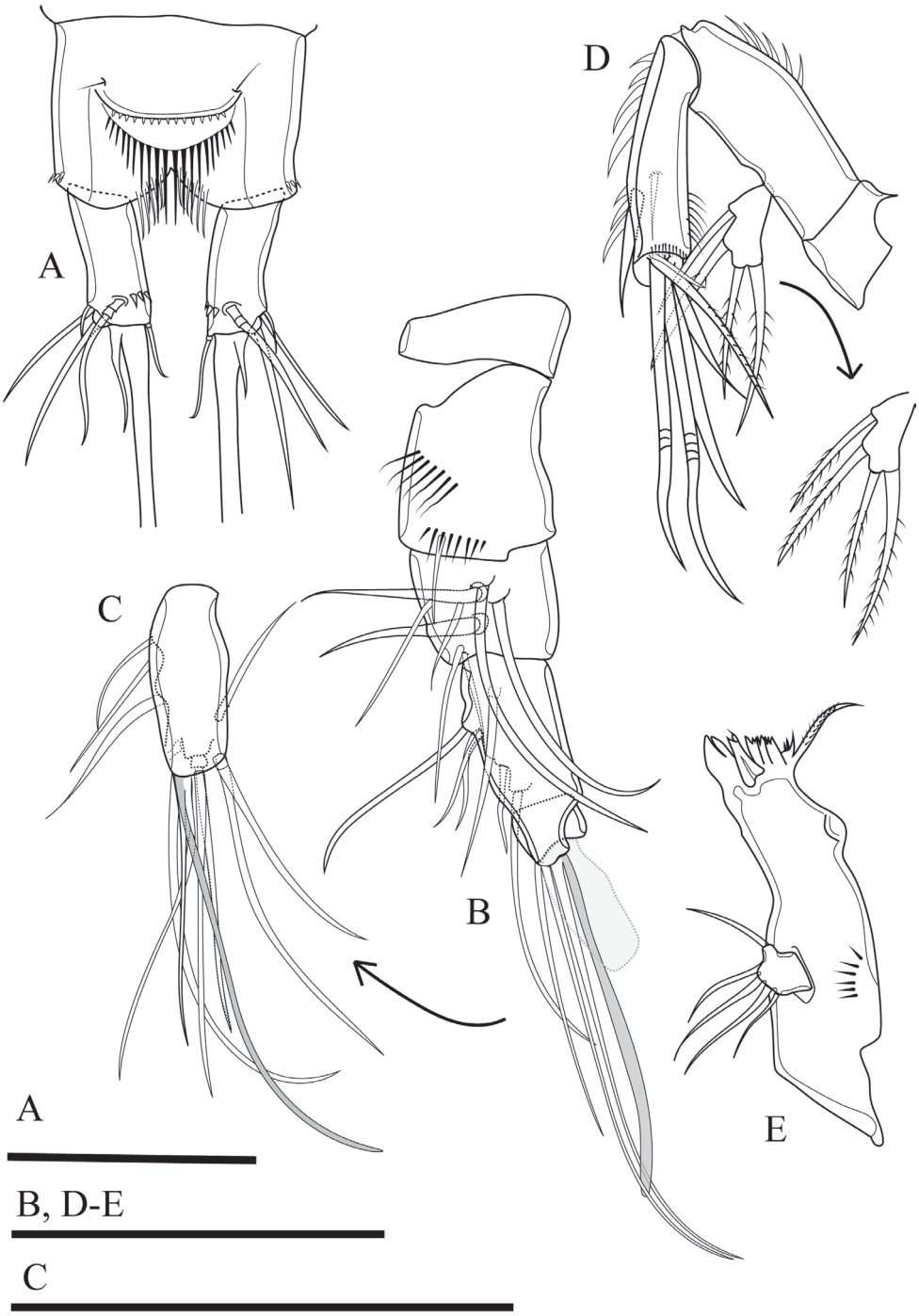

Figure 3. *Onychocamptus satunensis* sp. n., female holotype. **A** anal somite, dorsal view **B** antennule **C** ultimate segment of antennule **D** antenna **E** mandible. Scale bars: 0.05 mm.

elements: one minute seta, one slender, bipinnate seta, two geniculate setae, and two strong, smooth spines.

Mandible (Fig. 3E). Gnathobase with strong, chitinised teeth and lateral pinnate seta. Mandibular palp short, 1-segmented, with five slender setae sub-equal in length.

Maxillule (Fig. 4A). Composed of robust precoxa, coxa, basis, endopod fused to basis, and 1-segmented free exopod. Precoxal arthrite with six strong apical spines and one slender lateral seta. Coxa with cylindrical endite bearing two smooth setae, one of which robust. Basis with cylindrical endite bearing three setae, one of which robust. Endopod incorporated to basis, with three setae. Exopod free, 1-segmented, with two sub-equal apical setae.

Maxilla (Fig. 4B). Composed of syncoxa, allobasis, and 1-segmented endopod. Syncoxa with two endites; proximal endite with three apical pinnate setae, distal endite with two pinnate and one slender apical seta, outer margin with spinules. Allobasis with apical drawn out into claw, with one anterior and one posterior seta. Endopod 1-segmented, with two smooth apical setae.

Maxilliped (Fig. 4C). Subchelate, 3-segmented, comprising syncoxa, basis, and endopod. Syncoxa with one pinnate seta at inner distal corner. Basis with two transverse rows of outer spinules, one of which near base of endopod. Endopod drawn out into strong claw, with one minute seta near its base.

P1 (Fig. 4D). Coxa with longitudinal row of outer setules. Basis with one outer bipinnate spine and one inner spine near insertion of endopod, with longitudinal row of anterior spinules medially, with long setules along inner margin. Both rami 2-segmented. Exopod reaching proximal third of enp-1; exp-1 with one bipinnate outer spine, with one row of outer spinules; exp-2 with three outer spines, two apical geniculate setae, with outer spinules and inner setules. Enp-1 approximately seven times as long as wide, with outer spinules and inner setules; enp-2 with one median strong outwardly curved claw-like smooth spine and one slender inner seta, with few outer spinules.

P2 (Fig. 5A, B). Coxa with oblique row of spinules on anterior surface near outer margin, with row of spinules at distal outer corner. Basis with outer spine. Rami with 3-segmented exopod and 2-segmented endopod; endopod reaching tip of exp-2. Exp-1 with one outer bipinnate spine; exp-2 with one outer bipinnate spine and one inner plumose seta; exp-3 with three outer bipinnate spines, two apical elements (of which outer one spiniform seta with outer spinules and inner setules, inner element one plumose seta), and one inner plumose seta. All segments of exopod with row of outer spinules and inner setules. Enp-1 without armature, enp-2 with two apical and two inner plumose setae. All segments of endopod with row of outer spinules and long inner setules.

P3 (Fig. 5C). Coxa, basis, and segmentation of rami as in P2. Outer element of basis one long seta. Endopod reaching tip of exp-2. Exp-1 with one outer bipinnate spine; exp-2 with one outer bipinnate spine and one inner plumose seta; exp-3 with three outer bipinnate spines, two apical elements (of which outer one spiniform seta with outer spinules and inner setules, inner element one plumose seta), and one inner plumose seta. Ornamentation of exopod as in P2. Enp-1 without armature; enp-2 with one outer bipinnate seta, two apical, and three inner plumose setae. Outer and inner margins of segments of endopod with setules.

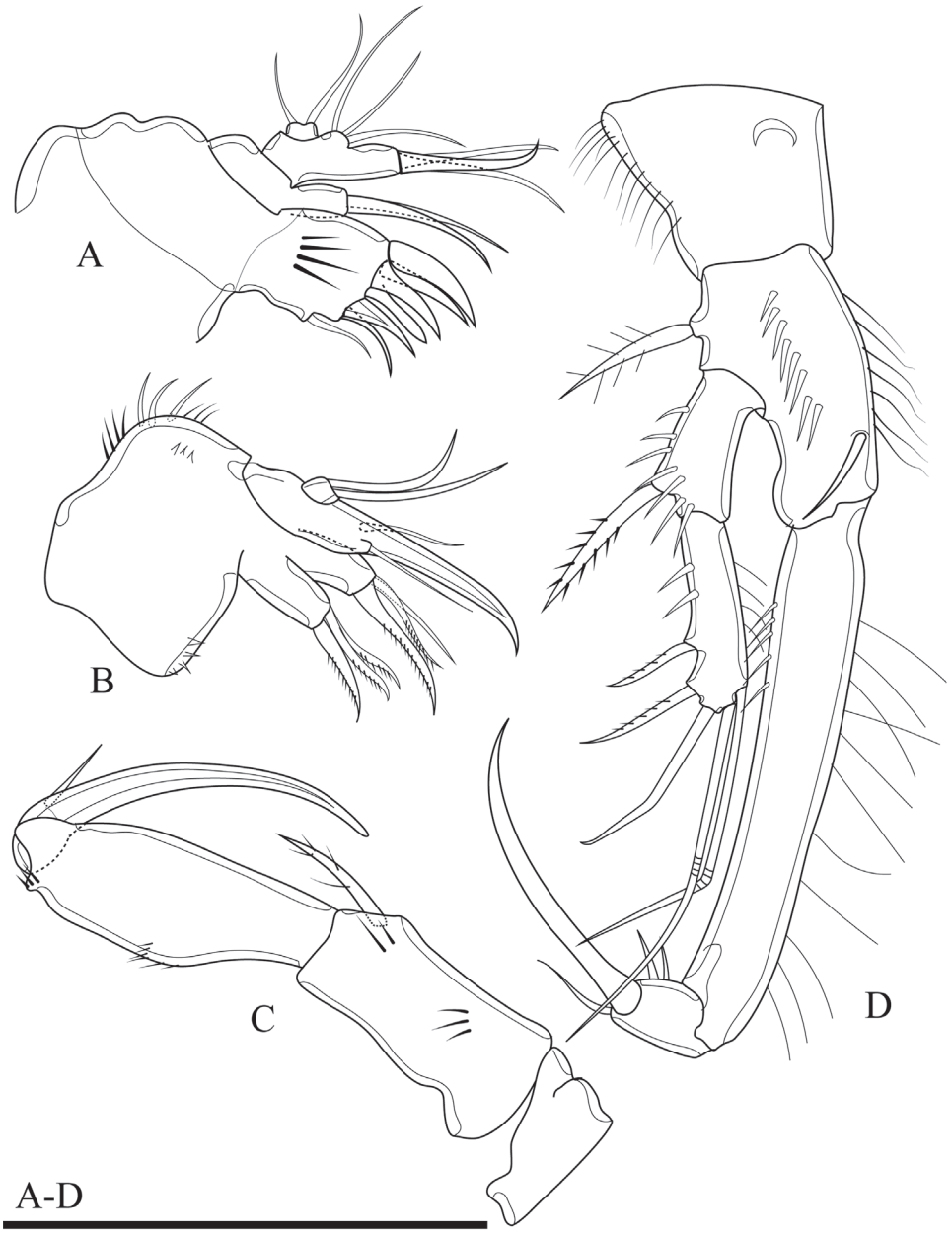

Figure 4. *Onychocamptus satunensis* sp. n., female holotype. **A** maxillule **B** maxilla **C** maxilliped **D** P1. Scale bar: 0.05 mm.

P4 (Fig. 6A). Coxa with row of outer long spinules. Basis with one slender outer seta. Rami with 3-segmented exopod and 2-segmented endopod; endopod reaching tip of exp-1. Exp-1 with one outer bipinnate spine; exp-2 with one outer bipinnate spine and one inner plumose seta; exp-3 with two outer bipinnate spines, two apical elements (of which outer one spiniform seta with outer spinules and inner setules,

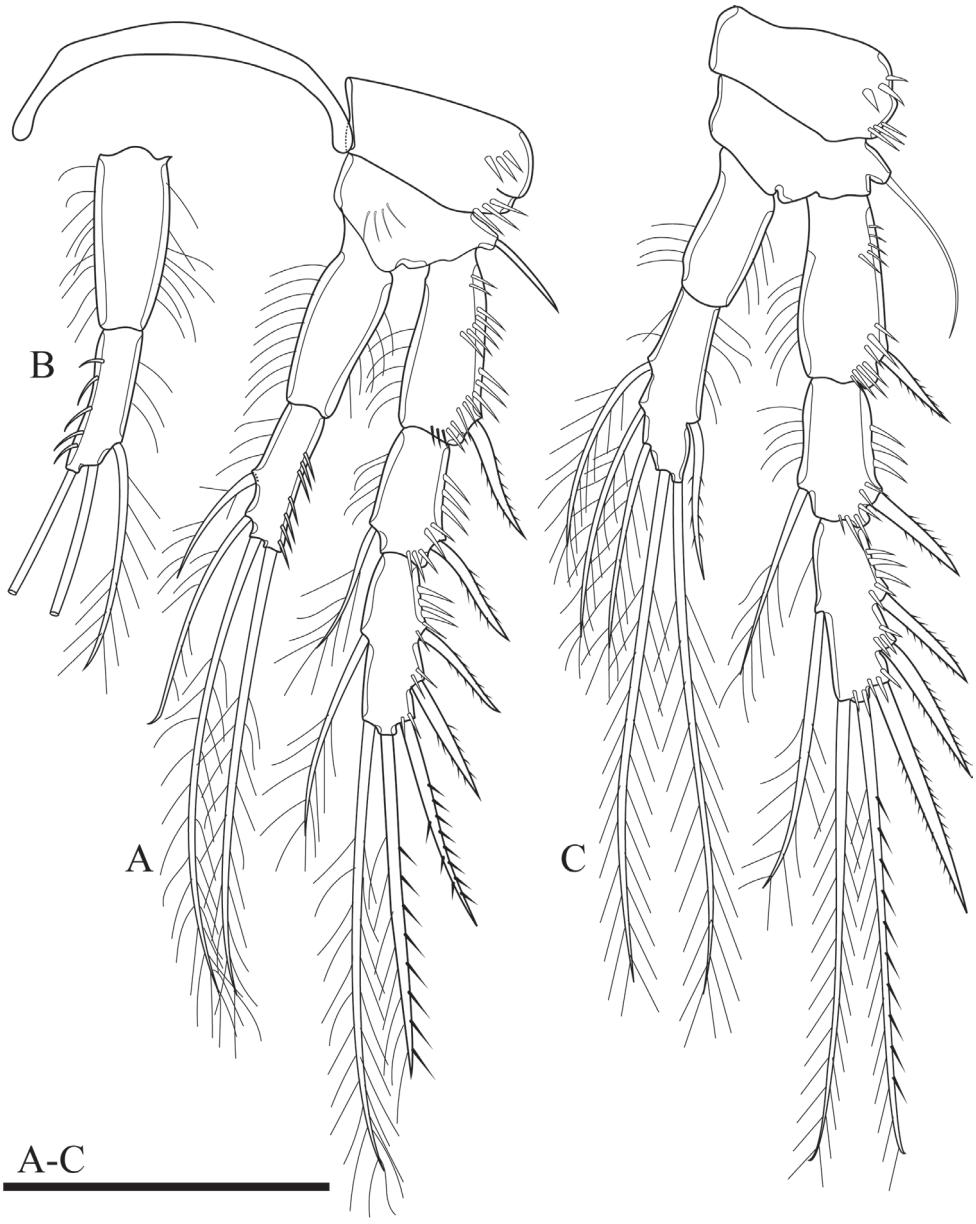

Figure 5. *Onychocamptus satunensis* sp. n., female holotype. **A** P2 **B** right P2 endopod **C** P3. Scale bars 0.05 mm.

inner element one plumose seta), and one inner plumose seta. Ornamentation of exopod as in P2 and P3. Enp-1 without armature, with long inner subdistal spinules and smaller outer spinules; enp-2 with one outer bipinnate seta, one apical plumose seta, and one inner plumose seta.

Armature formula of P1–P4 as in Table 1.

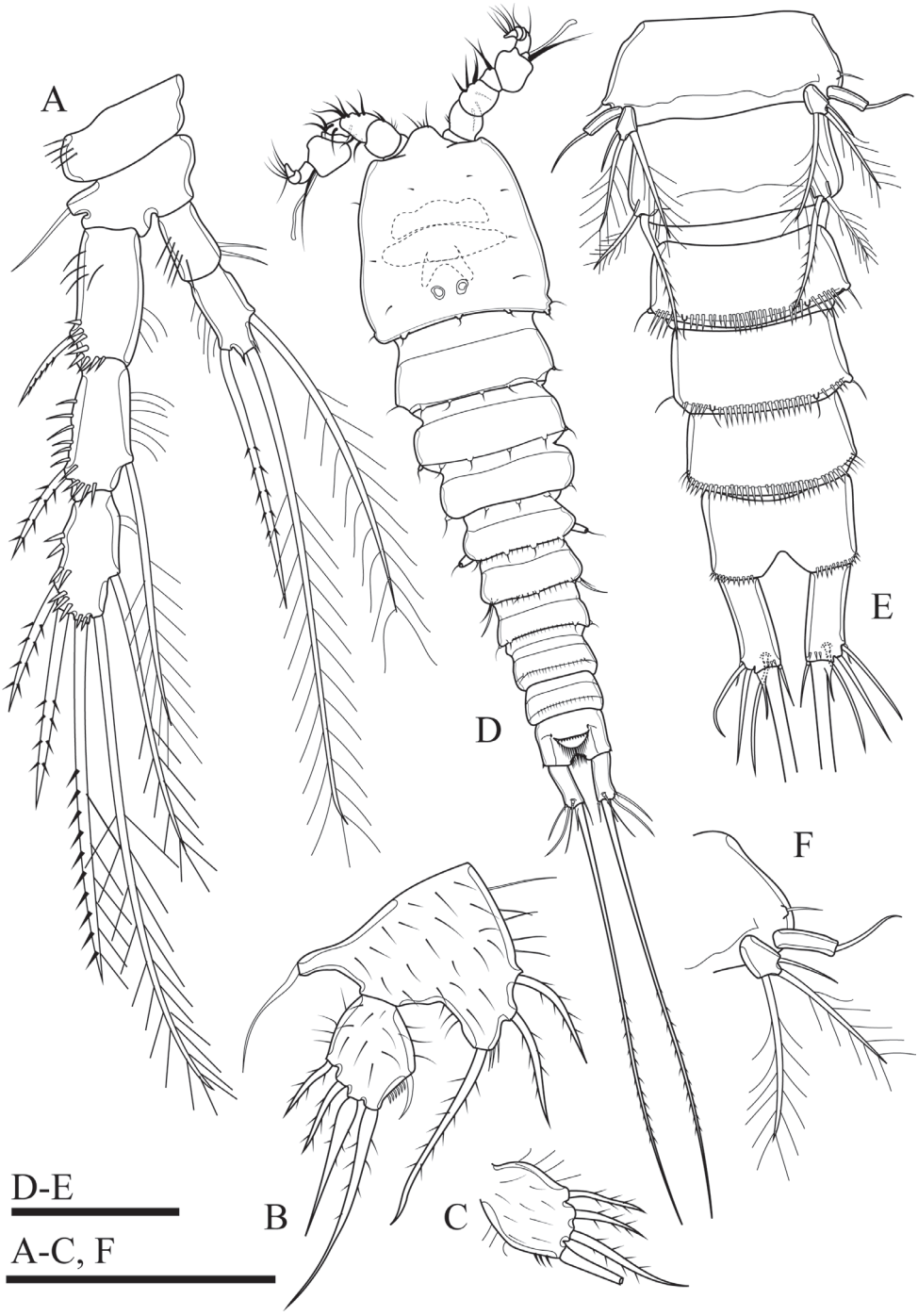

Figure 6. *Onychocamptus satunensis* sp. n., female holotype. **A** P4 **B** right P5 **C** left P5 exopod **D** *Onychocamptus satunensis* sp. n., male allotype. habitus, dorsal view **E** urosome, ventral view **F** left P5. Scale bars: 0.05 mm.

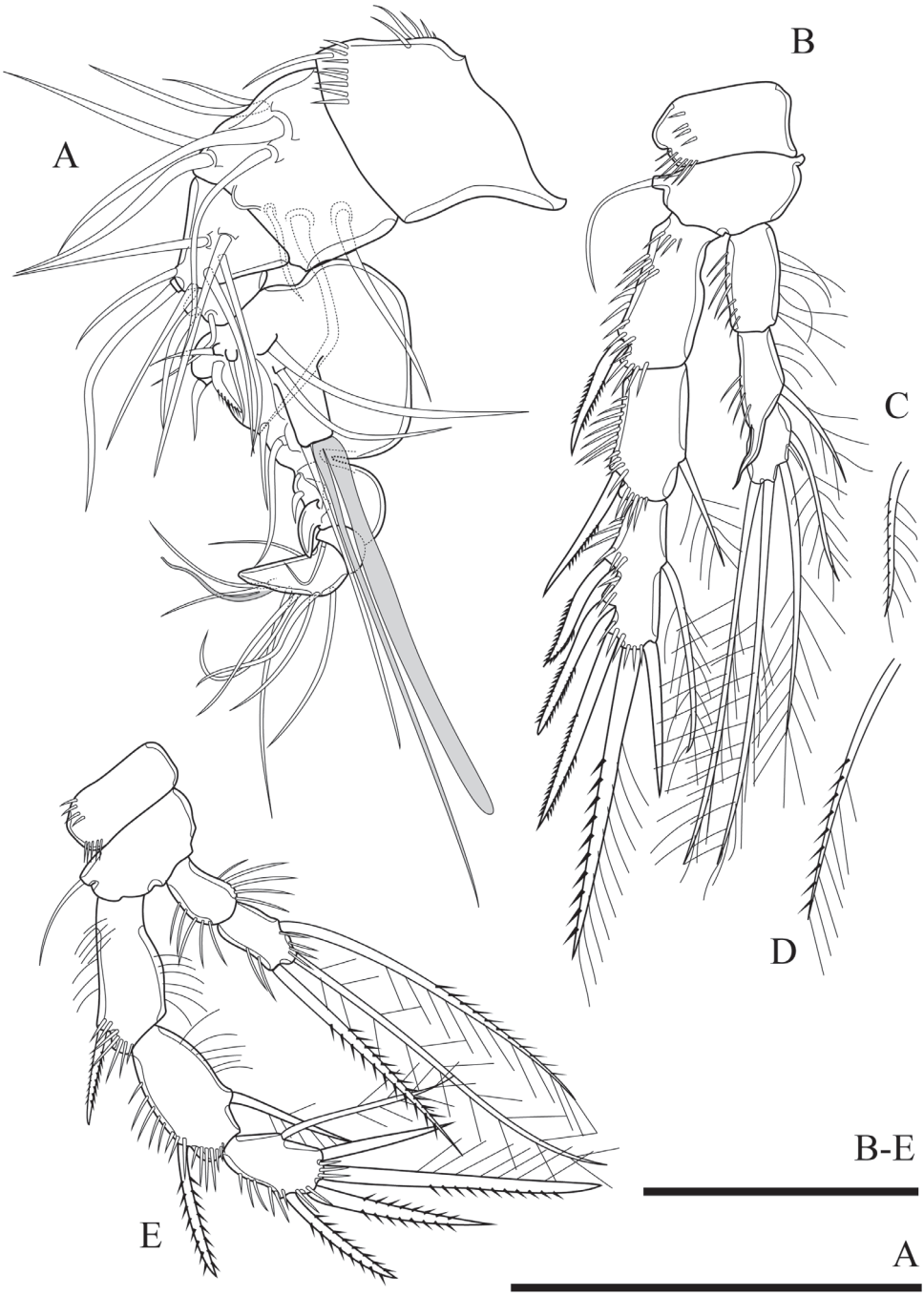

Figure 7. *Onychocamptus satunensis* sp. n., male allotype. **A** antennule **B** right P3 **C** proximal inner seta on left P3 enp-3 **D** distal inner seta on left P3 enp-3 **E** P4. Scale bars: 0.05 mm.

Table 1. Armature formula of P1–P4 of *Onychocamptus satunensis* sp. n. and *Onychocamptus tratensis* sp. n.

Swimming legs		Basis	Exopod	Endopod
P1	female	I-I	I-0; III,2,0	0-0; 0,I1,0
	male	I-I	I-0; III,2,0	0-0; 0,I1,0
P2	female	I-0	I-0; I-1; III,2,1	0-0; 0,2,2
	male	I-0	I-0; I-1; III,2,1	0-0; 0,2,2
P3	female	1-0	I-0; I-1; III,2,1	0-0; 1,2,3
	male	1-0	I-0; I-1; III,2,1	0-0; 0-1; 0,2,2
P4	female	1-0	I-0; I-1; II,2,1	0-0; 1,1,1
	male	1-0	I-0; I-1; II,2,1	0-0; 1,1,1

P5 (Figs 6B, C, 23A). Baseoendopod and exopod separated, with setules as on figures. Baseoendopod with basal seta and three pinnate setae on endopodal lobe, with spinules at base of distalmost seta. Exopod with four pinnate setae; innermost one longest.

P6 (Fig. 2D). Reduced to minute prominence at outer distal corner of genital field, with one short, slender seta.

Description of adult male. Body (Fig. 6D). Total body length, measured from tip of rostrum to posterior margin of caudal rami, 352–410 μm (mean 374 μm, n = 3; 410 μm in allotype); preserved specimen colourless. Prosome approximately 1.3 times as long as urosome (Fig 6D). Cephalothorax as long as wide, 0.5 times the length of prosome, internal sausage-like structure as in female, with two internal rounded structures. All free thoracic somites with sensillum-bearing tubercles along dorsal posterior margin, but fifth thoracic somite (first urosomite) with additional row of posterior setules dorsally (Fig. 6D). Second and third urosomite completely separated. Second urosomite with dorsal sensillum-bearing tubercles along posterior margin (Fig. 6D). Fourth urosomite without lateral protuberances, with lateral sensillum-bearing tubercles, with one posterior row of dorsal setules and ventral spinules. Ornamentation on next three urosomites as in female (Fig. 6E). Anal somite and anal operculum as in female.

Caudal rami as in female (Fig. 6D, E).

Antennule (Fig. 7A). 8-segmented, geniculate, with three segment distal to geniculation. First segment with proximal and subdistal outer spinules. Armature formula I-[1], II-[9], III-[7], IV-[2], V-[9+(1+aesthetasc)], VI-[1], VII-[1], VIII-[7+acrothek)]. Aesthetasc on fifth segment robust, fused basally to one seta. One pinnate seta on fifth segment. Apical acrothek on eighth segment small, consisting of one aesthetasc fused basally to two slender smooth seta.

Rostrum, antenna, mouthparts and P1, P2 (not shown) as in female.

P3 (Fig. 7B). General shape as in female but both rami 3-segmented. Endopod reaching tip of exp-2. Exp-3 with three outer bipinnate spines, two apical elements (of which outer one spiniform robust seta with outer spinules and inner setules, inner element one smooth spiniform seta), and one inner plumose seta. Enp-2 with inner seta and outer apophysis on outer distal corner reaching tip of enp-3, with long outer spinules and few inner setules; enp-3 with two inner and two apical plumose setae.

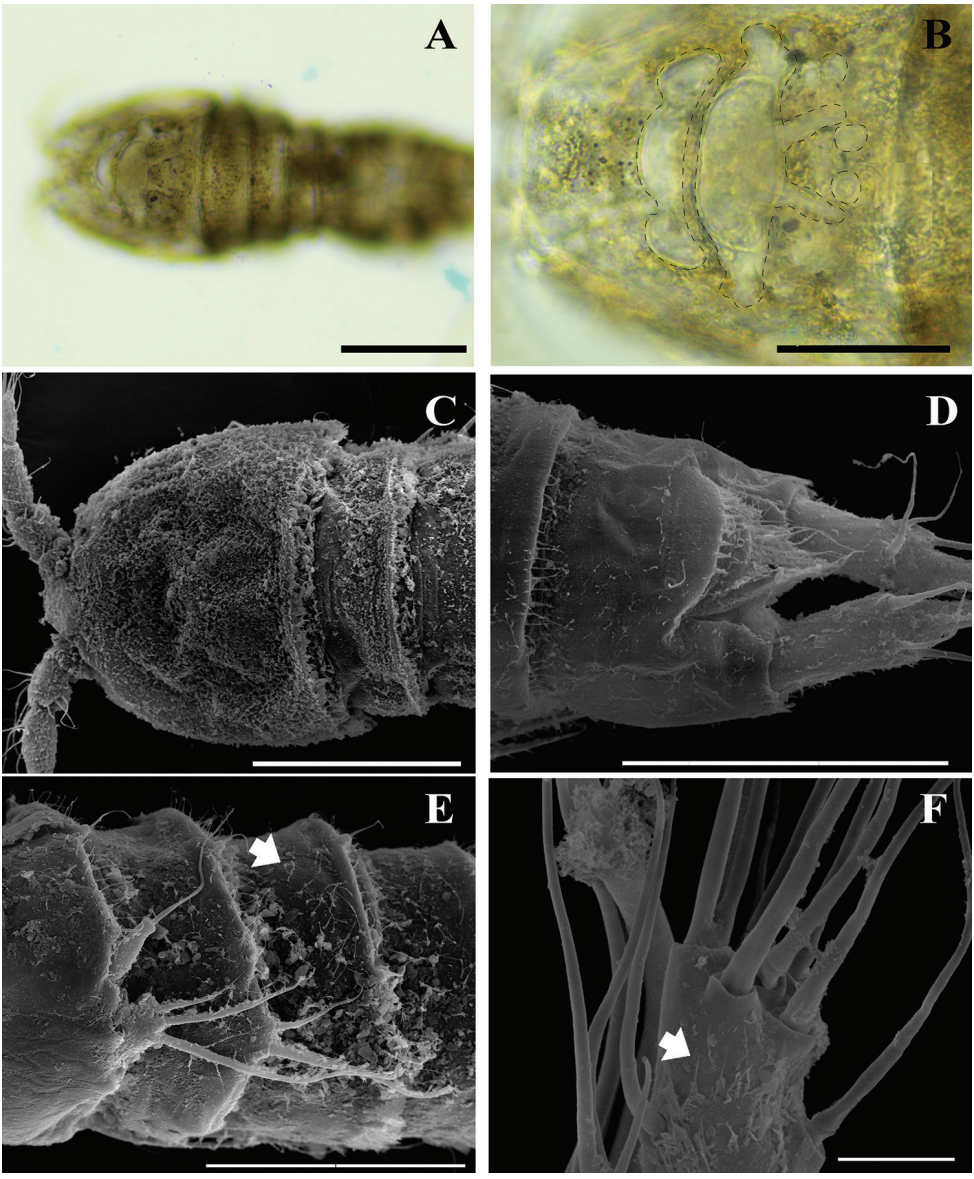

Figure 8. *Onychocamptus satunensis* sp. n., Digital photographs (**A, B**) and SEM photographs. **A–C** cephalothorax (dotted line on figure B indicates margin of internal structures) **D** anal somite and caudal rami **E** male urosome, lateral view, arrow indicates setules **F** tip of female antennule, arrow indicates setules. Scale bars: 0.1 mm (**A, C**), 0.05 mm (**B, D**), 0.005 mm (**E**), 0.02 mm (**F**).

P4 (Fig. 7E). General shape as in female but exp-3 relatively shorter and with stronger elements. Exp-3 with two outer bipinnate spines, two apical elements (of which outer one spiniform robust seta with outer spinules and inner setules, inner element one spiniform seta), and one inner plumose seta.

Armature formula of P1–P4 as in Table 1.

P5 (Fig. 6E, F). With outer basal seta arising from long setophore; without endopodal lobe. Exopod with three setae, outermost slender and slightly longer than segment, approximately 1/3 times as long as the middle seta.

P6 (Fig. 6E). Reduced to one minute rectangular protuberance, with outer plumose seta and inner bipinnate seta; inner seta approximately twice as long as outer one and reaching posterior margin of next urosomite.

Variability. The right P2 enp-2 lacks the proximalmost inner seta (Fig. 5B), and one additional small inner seta on the P5 exopod was observed (Fig. 6B) in the holotype. The P3 enp-3 of the allotype possesses two inner setae. Also, on the right ramus the setae possess outer and inner setules (Fig. 7B), but those of the left ramus possess inner spinules (Fig. 7C, D).

Onychocamptus satunensis sp. n. is the only species of *Onychocamptus* with internal sausage–like structure on cephalothorax (Figs 2A, B, 8A–C), differing from other members. *O. satunensis* sp. n. is most similar to *O. tratensis* sp. n., both species sharing the following remarkably characters: 1) absence of abexpodal seta on allobasis, 2) presence of 4 setae on exopod of antenna, 3) presence of 2 outer spines on P4 exp-3, 4) presence of 4 setae on exopod of P5 of the female, and 5) presence of 3 setae on exopod of P5 of the male. The southern Thai species (*O. satunensis* sp. n.), however, can be distinguished from the eastern one (*O. tratensis* sp. n.) by the presence of internal sausage–like structure, the presence of internal rounded structures, and the relative length of outer seta on P3 enp-2. Comparative study between two Thai new species and their congeners is provided in Table 3.

Distribution. This species is known from the type locality only.

***Onychocamptus tratensis* sp. n.**
http://zoobank.org/3C3184B8-A779-436B-87BA-B009F324F54E
Figs 9–15, 22A, 23B

Material examined. Holotype. Adult female, dissected and mounted onto two slides (PSUZC-PK2003-01–PSUZC-PK2003-02). **Allotype.** One adult male, dissected and mounted onto two slides (PSUZC-PK2003-03–PSUZC-PK2003-04). **Paratypes.** One undissected adult female, mounted onto one slide, (PSUZC-PK2003-05). One undissected adult male, mounted onto one slide, (PSUZC-PK2003-06). One adult female, dissected and mounted onto two slides, (PSUZC-PK2003-07–PSUZC-PK2003-08).

All specimens were collected by S Maiphae and T Saetang from type locality on 9 January 2017.

Additional material. Ten females and five males, all collected from type locality on 9 January 2017 and stored in 70% ethanol, deposited in crustacean reference collection, Zoological Museum, Kasetsart University (ZMKU_CP).

Type locality. Samer-rach peat swamp, Trat Province, eastern Thailand, 12°28'04.0"N, 102°21'20.6"E. Water temperature ranged between 28.83 °C, pH of 6.23, salinity 6.91 ppt, total dissolved solids 7.9 mg L^{-1}, and dissolved oxygen 4.41 mg L^{-1}.

Etymology. The specific name *tratensis* is derived from the name of Trat Province, where the species was collected. The name is a noun in the genitive singular, masculine.

Differential diagnosis. Laophontidae. Body gradually tapering posteriorly. One middle and two lateral rounded integumental window-like structures on cephalothorax. Second and third urosomite fused ventrally in female forming genital double-somite. Caudal rami cylindrical, both sides parallel, approximately 2.5 twice as long as wide, with one longitudinal row of minute spinules on inner margin near insertion of dorsal seta and horizontal row of minute spinules near insertion of inner terminal seta. Outer terminal seta (seta IV) fused at base with inner terminal seta. Allobasis of antenna without abexopodal seta. Endopodal lobe of P5 with two bipinnate and one plumose setae on inner margin and exopod of P5 with four plumose setae. Enp-2 of male P3 with apophysis on outer distal corner; apophysis reaching the tip of enp-3. Exopod of male P5 with three bipinnate setae, outer seta two times as long as supporting segment. P6 of the male reduced, with outer seta and inner bipinnate seta apically; inner seta approximately twice as long as outer one.

Description of adult female. Body. Total body length, measured from tip of rostrum to posterior margin of caudal rami, 360–450 μm (mean 400 μm, n = 14; 420 μm in holotype); preserved specimen colourless. Body covered entirely with setules, cylindrical; gradually tapering posteriorly, with maximum width at posterior part of cephalothorax. Prosome 1.3 times as long as urosome (including caudal rami) (Fig. 9A). Rostrum small, completely fused to cephalothorax. Cephalothorax as long as wide, approximately 0.5 times the length of prosome length, with one middle and two lateral rounded integumental window-like structures on cephalothorax. Cephalothorax and all free thoracic somites with sensillum-bearing tubercles along posterior margin. Second and third urosomite fused ventrally (Fig. 9C, D), distinct dorsally. Genital field ribbon-shaped, with seta representing P6 at outer distal corner (Fig. 9C). The remnant of first abdominal somite (posterior half of genital double-somite) with lateral sensillum-bearing tubercles (Fig. 9C, D). Posterior margin of genital double-somite and fourth urosomites with outer sensillum-bearing tubercles; posterior half of genital double-somite and fourth urosomite with posterior setules dorsally (Fig. 9D) and small spinules ventrally (Fig. 9C) between sensillum-bearing tubercles. The penultimate urosomite with posterior setules dorsally and laterally, with one posterior row of spinules ventrally. Anal somite approximately 0.6 times longer than wide, with arch row of long spinules posterior to anal operculum (Fig. 9D), with ventrolateral row of minute spinules near insertion of caudal rami (Fig. 9C). Anal operculum poorly developed, with minute spinules along posterior margin (Fig. 9D).

Caudal rami (Fig. 9C, D). Cylindrical, both sides parallel, 2.5 times as long as wide, with one longitudinal row of minute inner spinules near insertion of caudal seta (VII) and horizontal row of minute spinules near insertion of inner terminal seta (V). Anterolateral accessory seta (I) minute, inserted, close to anterolateral seta (II), both subapical. Posterolateral seta (III) inserted on minute pedestal. Outer terminal seta (IV) slender, fused at base with inner terminal seta (V), the letter longest, without fracture plane, approximately 0.9 times as long as body length. Inner accessory seta (VI) slender. Dorsal seta (VII) tri-articulate, inserted at quarter of rami. Length ratio

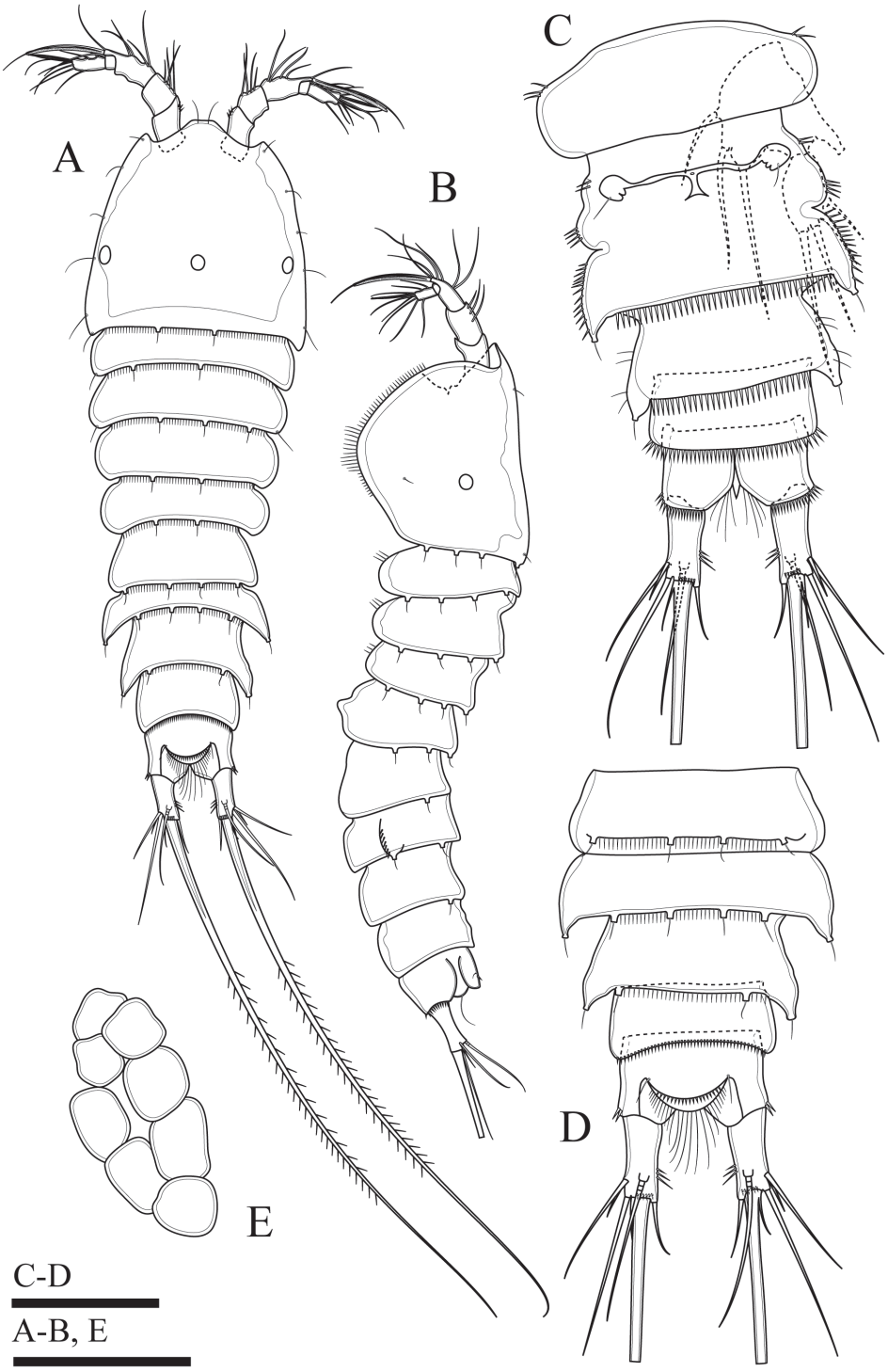

Figure 9. *Onychocamptus tratensis* sp. n., female holotype. **A** habitus, dorsal view **B** habitus, lateral view **C** urosome, ventral view **D** urosome, dorsal view **E** egg sac. Scale bars: 0.1 mm (**A, B, E**), 0.05 mm (**C, D**).

of caudal setae to ramus length, from seta I to seta VII of holotype: 0.5 : 1.7 : 2.5 : 0.7 : 13.3 : 0.7 : 2.0.

Egg sac (Fig. 9E). Ovigerous female with two egg sacs ventrally between pair of P5, each with eight eggs.

Antennule (Fig. 10A). Short, 5-segmented, large aesthetasc on third segment and small aesthetasc on fifth segment. Surface of all segments smooth, except for medial and distal rows of small spinules on first segment. Armature formula I-[1], II-[7+(1+aesthetasc)], III-[8+aesthetasc], IV-[1], V-[9+acrothek]. Aesthetasc on third segment fuse basally to one smooth seta. Apical acrothek consists of one aesthetasc fused basally to two slender smooth setae. Only seta on first segment bipinnate, all other setae smooth.

Antenna (Figs 10B, 22A). Comprising coxa, allobasis, 1-segmented endopod, and exopod. Coxa without ornamentation. Allobasis with one row of inner spinules, with 1-segmented exopod; the latter with two apical and two lateral bipinnate setae. Free endopod with two strong sharp spines accompanied by several strong, short spinules along outer margin, distal end with five elements; one slender seta, two geniculate setae, and two strong spines.

Mandible (Fig. 11A). Gnathobase with strong, chitinised teeth and dorsal pinnate seta along cutting edge. Mandibular palp short, 1-segmented, with five slender setae sub-equal in length.

Maxillule (Fig. 11B). Composed of robust precoxa, coxa, basis, endopod fused to basis, and 1-segmented free exopod. Precoxal arthrite with six strong apical spines, with lateral spine. Coxa with cylindrical endite bearing two smooth setae. Basis with cylindrical endite bearing three setae. Endopod incorporated to basis, with three setae. Exopod free, 1-segmented, with two sub-equal apical setae.

Maxilla (Fig. 11C). Composed of syncoxa, allobasis, and 1-segmented endopod. Syncoxa with two endites; each endite with two apical pinnate setae, outer margin with spinules. Allobasis with apical drawn out into claw, with one anterior and one posterior seta. Endopod 1-segmented, with two smooth apical setae.

Maxilliped (Fig. 11D). Subchelate, 3-segmented, comprising syncoxa, basis, and endopod. Syncoxa with one pinnate seta at outer distal corner. Basis with two transverse rows of outer spinules, one of which near base of endopod. Endopod drawn out into strong naked claw, with one small seta near base.

P1 (Fig. 12A). Intercoxal sclerite naked. Precoxa small and triangular, with one row of spinules at distal margin (not shown). Coxa with one row of long outer spinules. Basis with one outer bipinnate spine and one inner plumose seta near insertion of endopod, with longitudinal row of anterior spinules medially, with long setules along inner margin. Both rami 2-segmented. Exopod reaching proximal third of enp-1; exp-1 with one bipinnate outer spine, with one row of outer spinules; exp-2 with three outer smooth spines and two apical geniculate setae, with row of outer spinules and inner setules. Enp-1 approximately 4.4 times as long as wide, with one row of outer and inner setules; enp-2 with one median strong outwardly curved claw-like smooth spine and one slender inner seta, with few outer spinules.

P2 (Fig. 12B). Intercoxal sclerite and precoxa as in P1. Coxa with two oblique parallel rows of long outer spinules (one on anterior and others on posterior surface), with

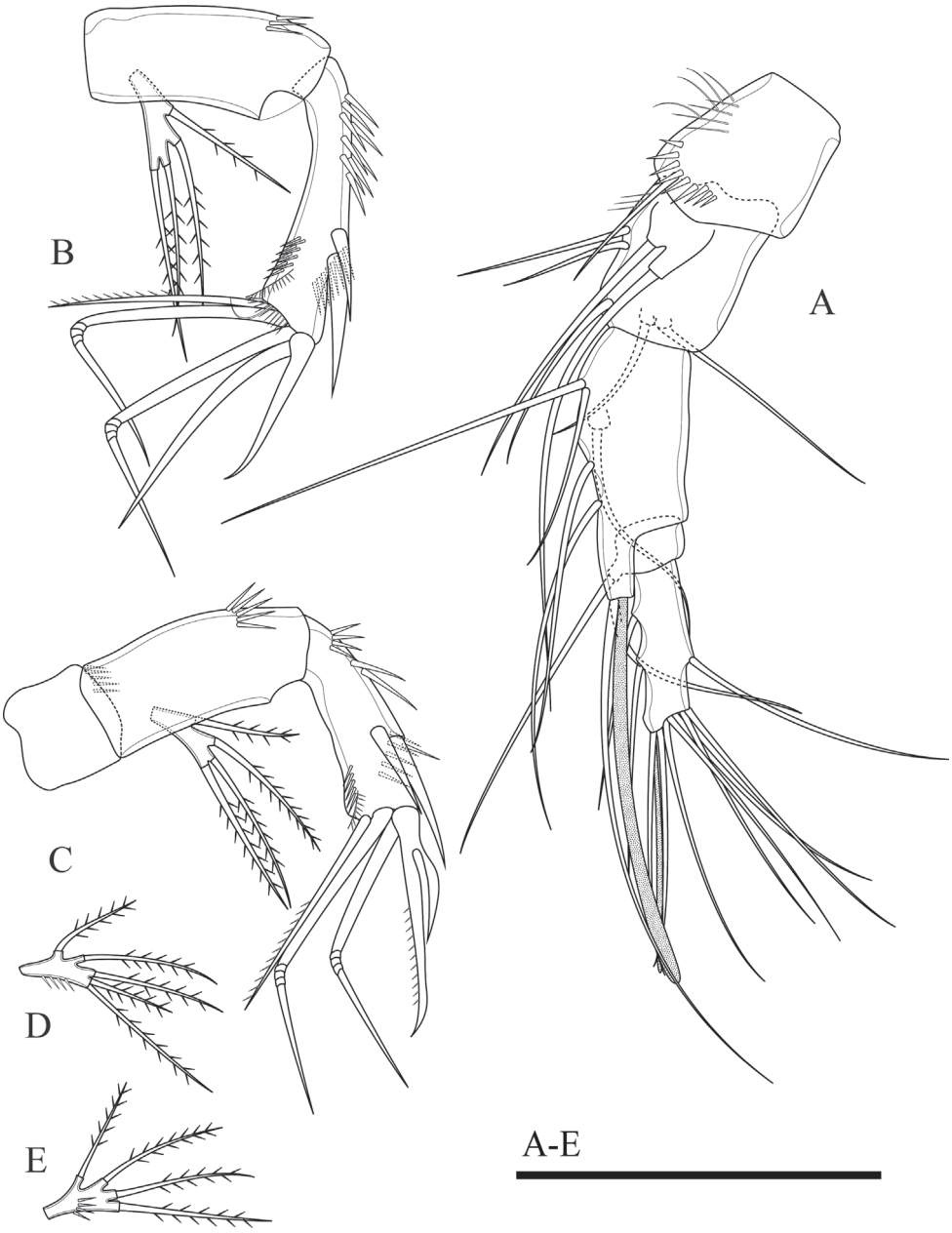

Figure 10. *Onychocamptus tratensis* sp. n., female holotype. **A** antennule **B, C** antenna **D, E** *Onychocamptus tratensis* sp. n., male allotype **D, E** exopod of antenna. Scale bar: 0.05 mm.

one row of spinules at distal margin, and few spinules at inner margin. Basis with outer bipinnate spine, with spinules at base of spine, with one row of long spinules between exopod and endopod, and with one row of inner setules. Rami with 3-segmented exopod and 2-segmented endopod; endopod reaching tip of exp-2. Exp-1 with one

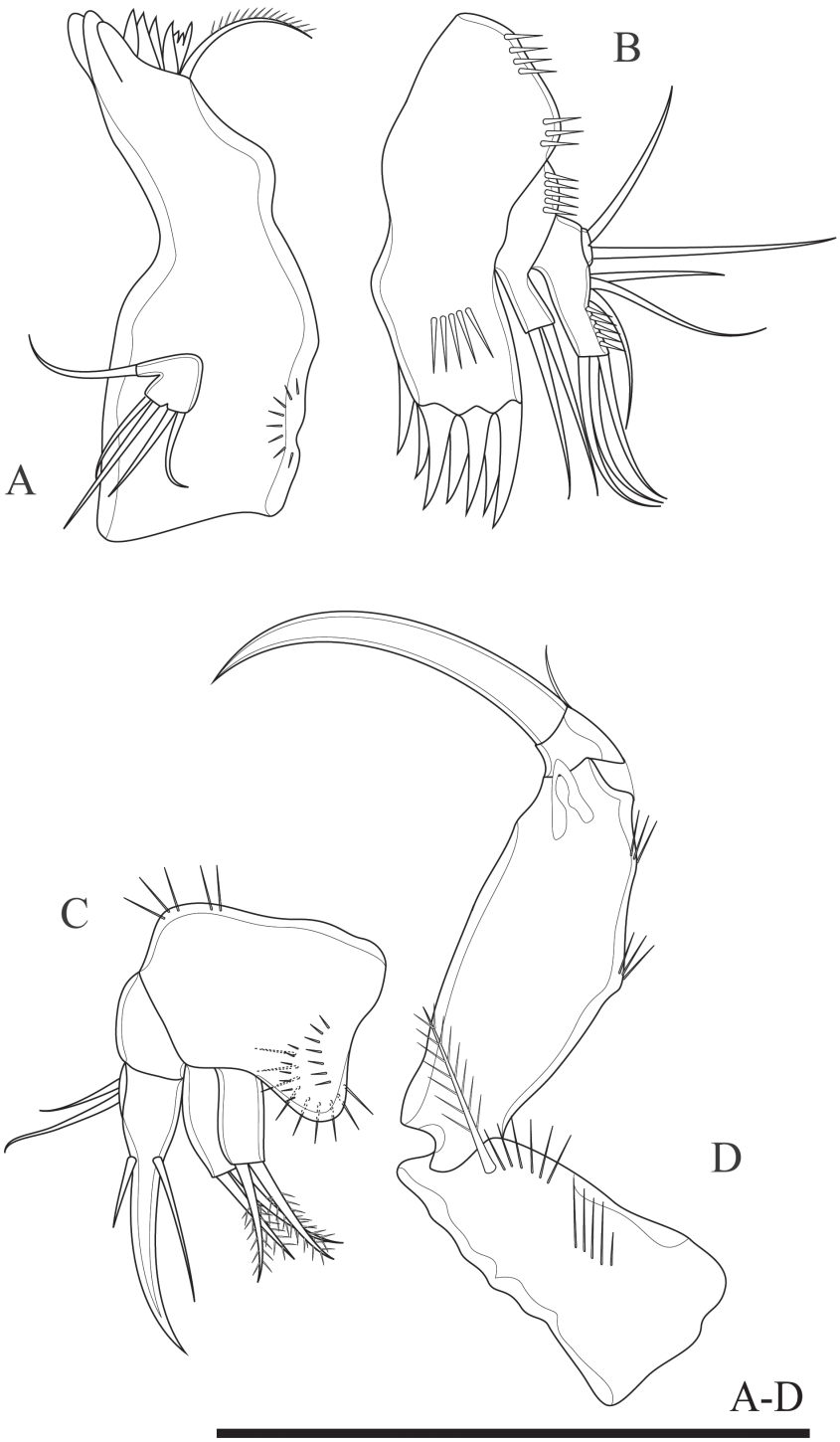

Figure 11. *Onychocamptus tratensis* sp. n., female holotype. **A** mandible **B** maxillule **C** maxilla **D** maxilliped. Scale bar: 0.05 mm.

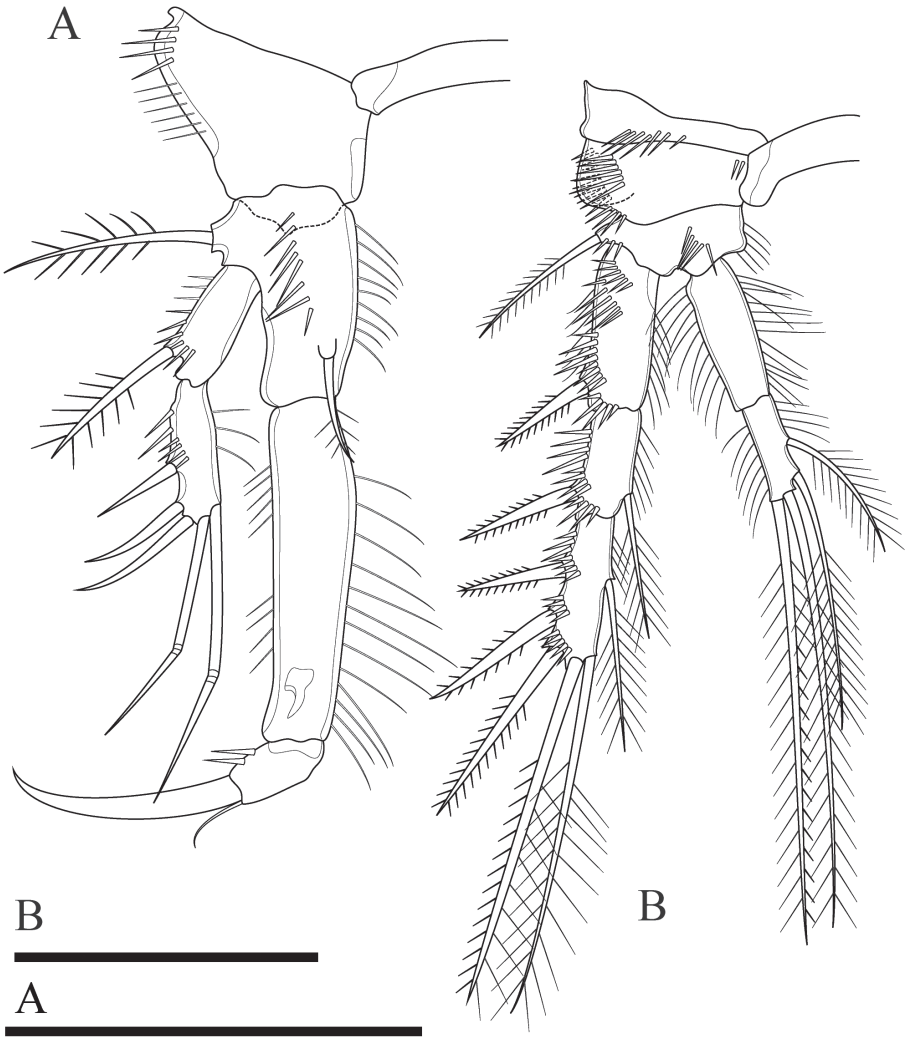

Figure 12. *Onychocamptus tratensis* sp. n., female holotype. **A** P1 **B** P2. Scale bars: 0.05 mm.

outer bipinnate spine; exp-2 with one outer bipinnate spine and one inner plumose seta; exp-3 with three outer bipinnate spines, two apical elements (of which outer one spiniform seta with outer spinules and inner setules, inner element one plumose seta), and one inner plumose seta. All segments of exopod with several rows of strong outer spinules and inner setules, and only exp-1 with one row of outer setules. Enp-1 without armature, enp-2 with two apical and two inner plumose setae. All segments of endopod with one row of long outer and inner setules.

P3 (Fig. 13A). Intercoxal sclerite and precoxa as in P1. Coxa with two parallel rows of long spinules along outer margin (one on anterior and other on posterior surface). Basis

with one smooth outer seta; with spinules at base of seta and one row of inner setules. Segmentation of rami as in P2, endopod reaching to middle segment of exp-2. Exp-1 with one outer bipinnate spine; exp-2 with one outer bipinnate spine and one inner plumose seta; exp-3 with three outer bipinnate spines, two apical elements (of which outer one spiniform seta with outer spinules and inner setules, inner element one plumose seta), and one inner plumose seta. All segments of exopod with several rows of strong outer spinules and one row of inner setules, and exp-1 and exp-2 with one row of outer setules. Enp-1 without armature, enp-2 with one outer bipinnate seta, two apical, and three inner plumose setae. Outer and inner of all segments of endopod with long setules.

P4 (Fig. 13B). Intercoxal sclerite and precoxa (not shown) as in P1. Coxa with one row of setules and several outer spinules. Basis with one smooth outer seta; with spinules at base of seta and one row of inner setules. Rami with 3-segmented exopod and 2-segmented endopod, endopod smaller than exopod. Exp-1 with one outer bipinnate spine; exp-2 with one outer bipinnate spine and one inner plumose seta; exp-3 with two outer bipinnate spines, two apical elements (of which outer one bipinnate spine, inner element one plumose seta), and one inner plumose seta. All segments of exopod with several rows of strong outer spinules and with fewer inner setules. Enp-1 without armature, enp-2 with one outer seta with plumose proximally and bipinnate distally, one apical plumose seta, and one inner plumose seta. Outer and inner of all segments of endopod with setules.

Armature formula of P1–P4 as in Table 1.

P5 (Figs 13C, 23B). Baseoendopod and exopod separated with setules as figured. Baseoendopod with basal seta and three inner setae on endopodal lobe; one proximal bipinnate seta, one middle bipinnate seta and one apical plumose seta, with one row of spinules at base of each seta, as well as with one distal row of spinules between distal seta of baseoendopod and exopod. Exopod with four plumose setae, with row of inner and outer setules, and with spinules at base of innermost seta.

Description of adult male. Body (Fig. 14A, B). Total body length, measured from tip of rostrum to posterior margin of caudal rami, 340–360 μm (mean 350 μm, n = 3; 350 μm in paratype); preserved specimen colourless. Prosome approximately 1.5 times as long as urosome. Cephalothorax as long as wide, 0.5 times the length of prosome. All free thoracic somites with sensillum-bearing tubercles along posterior margin, but fifth thoracic somite (first urosomite) with additional row of posterior setules dorsally. Second and third urosomite completely separated. Second urosomite with dorsal sensillum-bearing tubercles along posterior margin. Fourth urosomite without lateral protuberances, with one posterior row of dorsal setules and ventral spinules. Ornamentation on next three urosomites as in female. Anal somite approximately 0.5 times longer than wide. Anal operculum as in female.

Caudal rami (Fig. 14A, B). As in female.

Antennule (Fig. 14C). 8-segmented, large aesthetasc on fifth segment and small aesthetasc on eighth segment. First segment with proxim al setules and subdistal outer

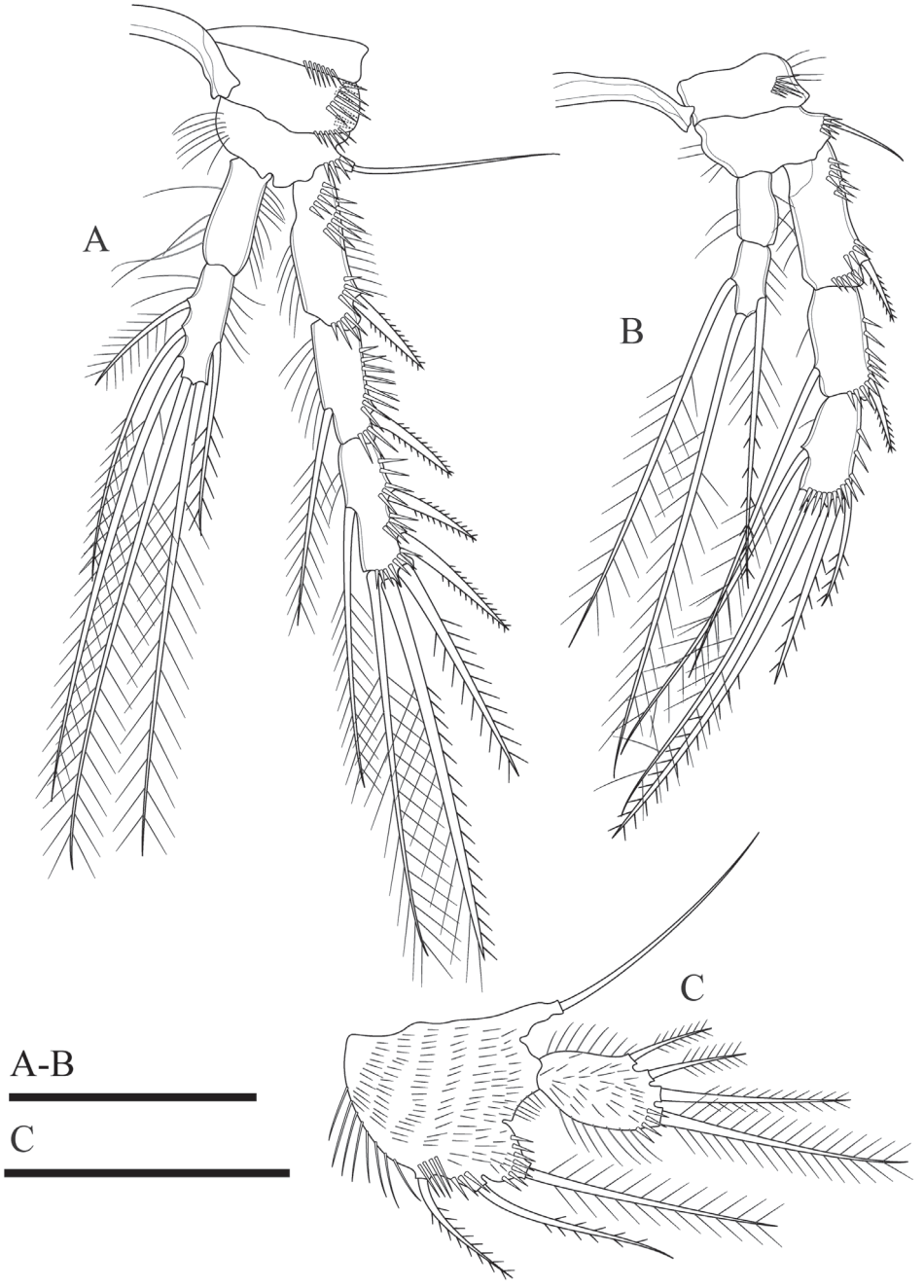

Figure 13. *Onychocamptus tratensis* sp. n., female holotype. **A** P3 **B** P4 **C** P5. Scale bars: 0.05 mm.

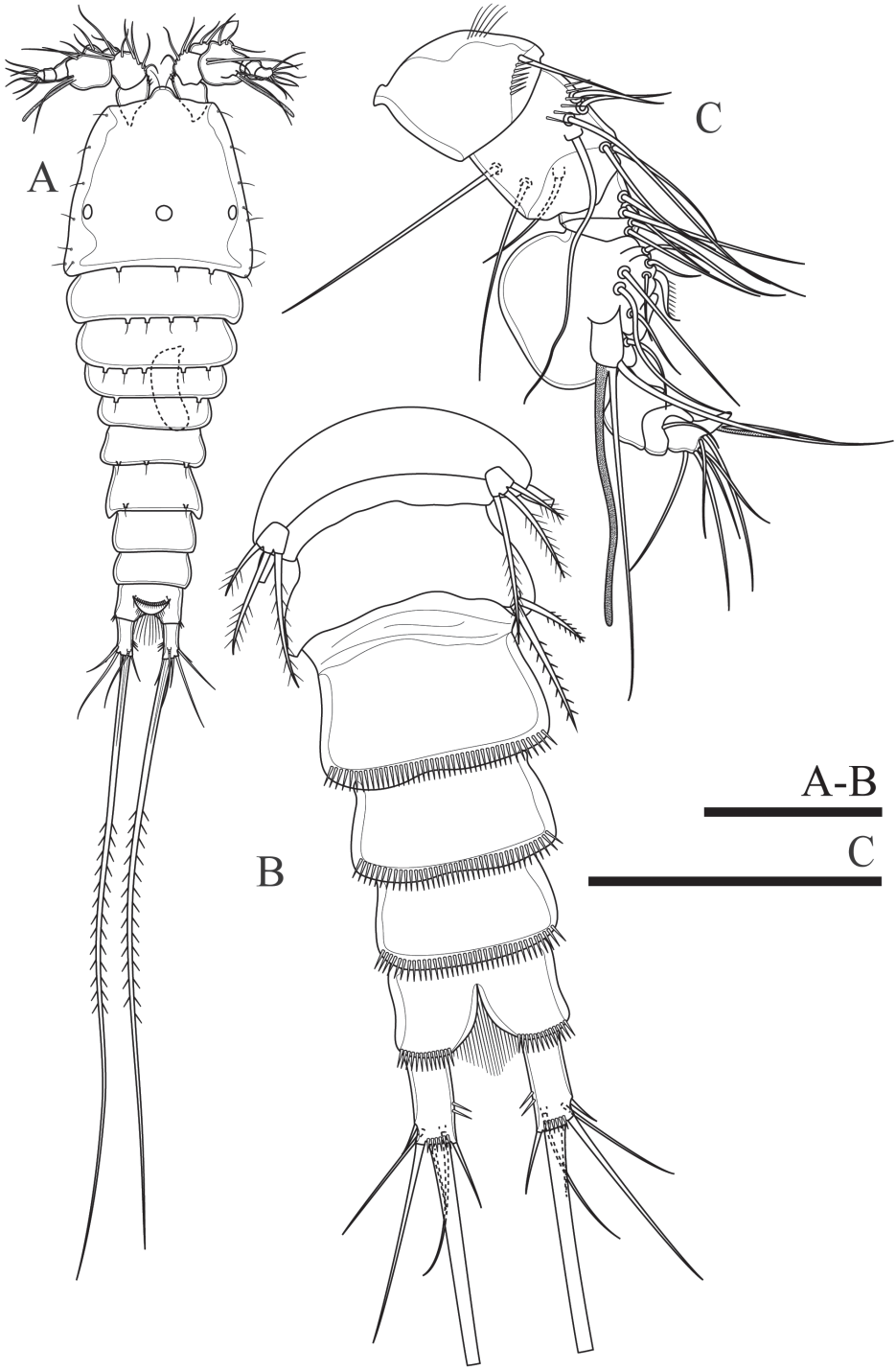

Figure 14. *Onychocamptus tratensis* sp. n., male allotype. **A** habitus, dorsal view **B** urosome, ventral view **C** antennule. Scale bars: 0.1 mm (**A**), 0.05 mm (**B, C**).

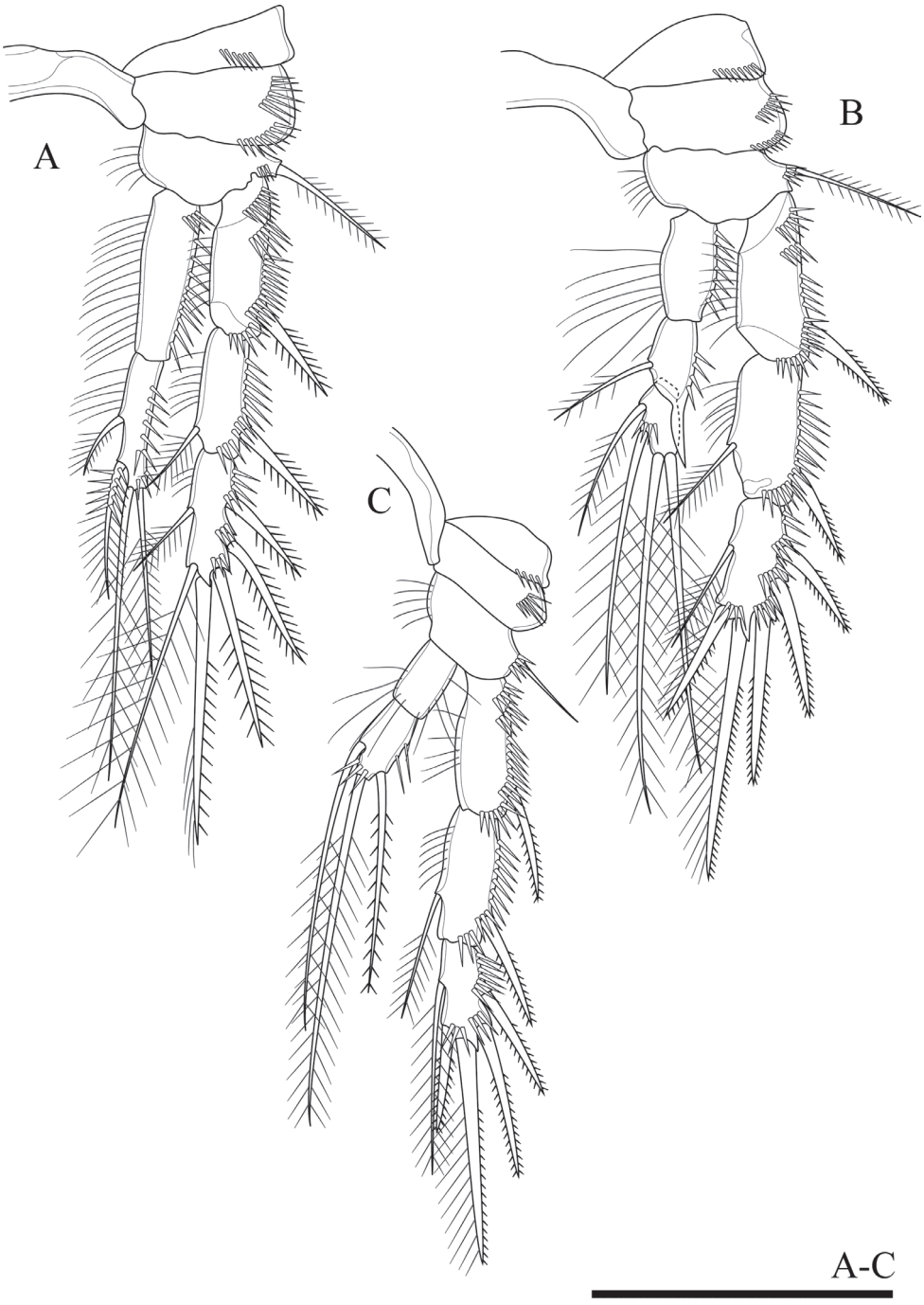

Figure 15. *Onychocamptus tratensis* sp. n., male allotype. **A** P2 **B** P3 **C** P4. Scale bar: 0.05 mm.

spinules, second segment with one row of outer spinules, other segments smooth. Armature formula I-[1], II-[9], III-[3], IV-[2], V-[9+(1+aesthetasc)], VI-[0], VII-[1], VIII-[7+acrothek]. Aesthetasc on fifth segment robust. Apical acrothek consists of one aesthetasc fused basally with two slender smooth setae.

Rostrum, antenna (coxa, allobasis, and endopod), mouthparts, and P1 as in female.

P2 (Fig. 15A). Intercoxal sclerite naked. Precoxa small and triangular, with one row of spinules at distal margin. Coxa with two rows of outer spinules. Basis with one outer bipinnate seta, with spinules at base of spine, and with one row of inner setules. Rami with 3-segmented exopod and 2-segmented endopod, endopod reaching to middle of exp-3. Armature and all ornamentation of endopod as in female. Enp-1 without armature, enp-2 with two apical plumose setae and two inner plumose setae. All segments of endopod with one row of outer spinules and one row of inner setules.

P3 (Fig. 15B). Intercoxal sclerite and precoxa as in P2. Coxa with two rows of outer spinules. Basis with one outer plumose seta; with spinules at base of seta and one row of inner setules. Both rami 3-segmented, endopod reaching to middle of exp-2. Exp-1 with one outer bipinnate spine; exp-2 with one outer bipinnate spine and one inner plumose seta, inner seta much shorter than in female; exp-3 with three outer bipinnate spines, two apical elements (both spiniform seta with outer spinules and inner setules), and one inner plumose seta, inner seta much shorter than in female. All segments of exopod with several rows of strong outer spinules and one row of inner setules except exp-3. Enp-1 without armature, enp-2 with outer distal apophysis exceeding the tip of enp-3, one inner plumose seta, and with one row of outer spinules and fewer inner setules; enp-3 with two inner plumose setae and two apical plumose setae, and with one row of spinules at base of outer seta.

P4 (Fig. 15C). Intercoxal sclerite and precoxa as in P2. Coxa with one row of spinules along outer margin. Basis with one smooth seta on outer distal corner; ornamented with spinules at base of seta and one row of setules along inner margin. Rami with 3-segmented exopod and 2-segmented endopod. Exp-1 with one outer bipinnate spine; exp-2 with one outer bipinnate spine and one inner plumose seta, inner seta much shorter than in female; exp-3 with two outer bipinnate spines, two apical elements (of which outer one spiniform seta with outer spinules and inner setules, inner element one spiniform seta), and one inner plumose seta. Endopod reaching tip of exp-1; enp-1 without armature; enp-2 with one outer bipinnate seta, one apical plumose seta, and one inner plumose seta. All segments of exopod with several rows of strong spinules along outer margin, and with one row of setules along inner margin except exp-3. Armature and all ornamentation of endopod as in female, but presence of one row of spinules at base of apical seta.

Armature formula of P1–P4 as in Table 1.

P5 (Fig. 14B). With outer basal seta arising from long setophore; without endopodal lobe. Exopod with three plumose setae, outermost shortest, 2.5 times as long as segment, approximately 0.5 times as long as the middle seta.

P6 (Fig. 14B). Reduced to one minute rectangular protuberance, with one outer and one inner bipinnate seta; inner seta approximately twice as long as outer one and reaching posterior margin of next urosomite.

Variability. In male, variability was observed in the exopod of antenna, four specimens with four setae and one specimen with five setae (Fig. 10D, E). In female antenna, two strong spines of distal end of endopod not fused in six specimens and fused in only one specimen (Fig. 10C).

Distribution. This species is known from the type locality only. It was found in two months, January and September 2017.

***Onychocamptus bengalensis* (Sewell, 1934)**
Figs 16–18, 22B, 23C

Laophonte bengalensis Sewell, 1934: 98, fig 10a–k.
Onychocamptus bengalensis: Lang 1948: 1409, abb. 571.9, 1420, abb. 578.2; Hamond 1973: 406, figs 42–65; Song and Chang 1995: 72, 75, fig 6; Lee and Chang 2005: 40, fig. 5.

Material examined. Two females and two males from Khao Thanan cave, Satun Province, southern Thailand, 07°03'43.2"N, 99°41'42.7"E; coll. C Boonyanusith and K Wongkamhaeng; 12 December 2014. One female from Samer-rach peat swamp, Trat Province, eastern Thailand, 12°28'04.0"N 102°21'20.6"E.; coll. S Maiphae and T Saetang; 25 May 2017.

Differential diagnosis. Laophontidae. Caudal rami more than four times as long as wide in female and approximately three times as long as wide in male. Female P5 exopod and baseoendopod fused, endopodal lobe and exopod with three setae each. P4 exp-3 with three outer spines.

Redescription of adult female. Female (Fig. 16A). Total body length measured from tip of rostrum to posterior margin of caudal rami, 530–550 μm (mean 536 μm, n = 3); preserved specimen colourless. Body covered with setules, cylindrical, gradually tapering posteriorly, with maximum width at posterior part of cephalothorax. Prosome 1.6 times as long as urosome. Rostrum small, completely fused to cephalothorax, with pair of apical sensilla. Cephalothorax as long as wide, approximately 0.5 times the length of prosome (Fig. 16A). Cephalothorax and all free thoracic somites with less developed posterior sensillum-bearing tubercles (Fig. 16A, B). Second and third urosomite fused ventrally forming genital double-somite, with dorsal and lateral remnant of original division (Fig. 16C). Posterior half of genital double-somite and subsequent somites with lateral sensillum-bearing tubercles. Other characters on urosomite as in *O. tratensis* sp. n.

Caudal rami (Fig. 16C, D). Cylindrical, parallel, 4.3 times as long as wide, with seven setae of different lengths. Anterolateral accessory seta (I) minute, inserted close to anterolateral seta (II) at distal third of rami. Posterolateral seta (III) inserted on minute protuberance. Outer terminal seta (IV) slender, fused at base to inner terminal seta (V), the latter longest, without fracture plane, approximately 0.6 times as long as body length. Inner accessory seta (VI) slender. Dorsal seta (VII) tria-rticulate, inserted at quarter of ramus. Length ratio of caudal setae to ramus length from seta I to seta VII: 0.2 : 0.5 : 0.8 : 1.1 : 9.7 : 0.3 : 0.8.

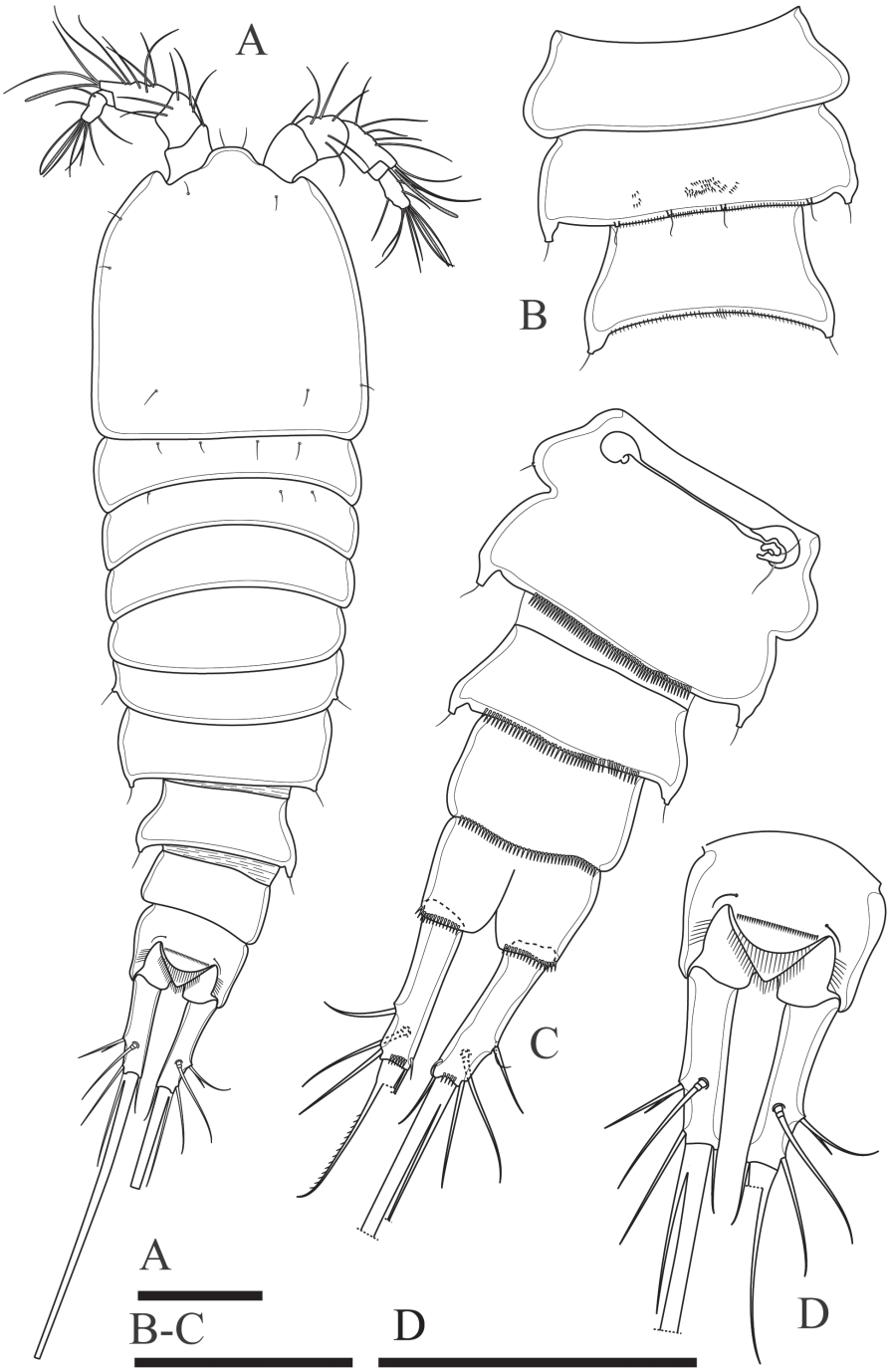

Figure 16. *Onychocamptus bengalensis*, female. **A** habitus, dorsal view **B** urosome, ventral view **C** genital double-somite and fourth urosomite, dorsal view **D** anal somite and caudal rami, dorsal view. Scale bars: 0.1 mm (**A**), 0.05 mm (**B–D**).

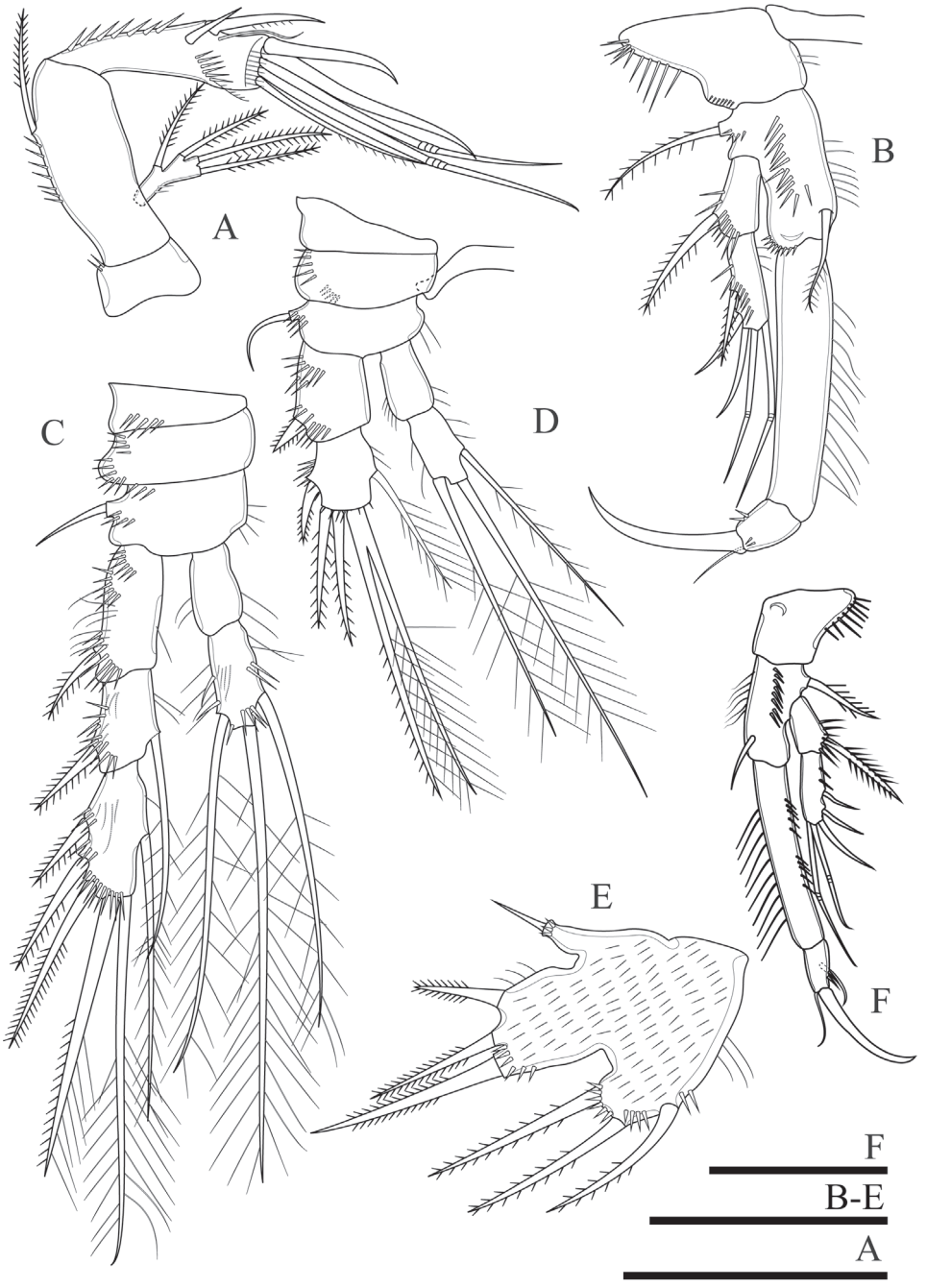

Figure 17. *Onychocamptus bengalensis*, female. **A** antenna **B** P1 **C, D** P4 **E** P5 **F** male P1. Scale bars: 0.05 mm.

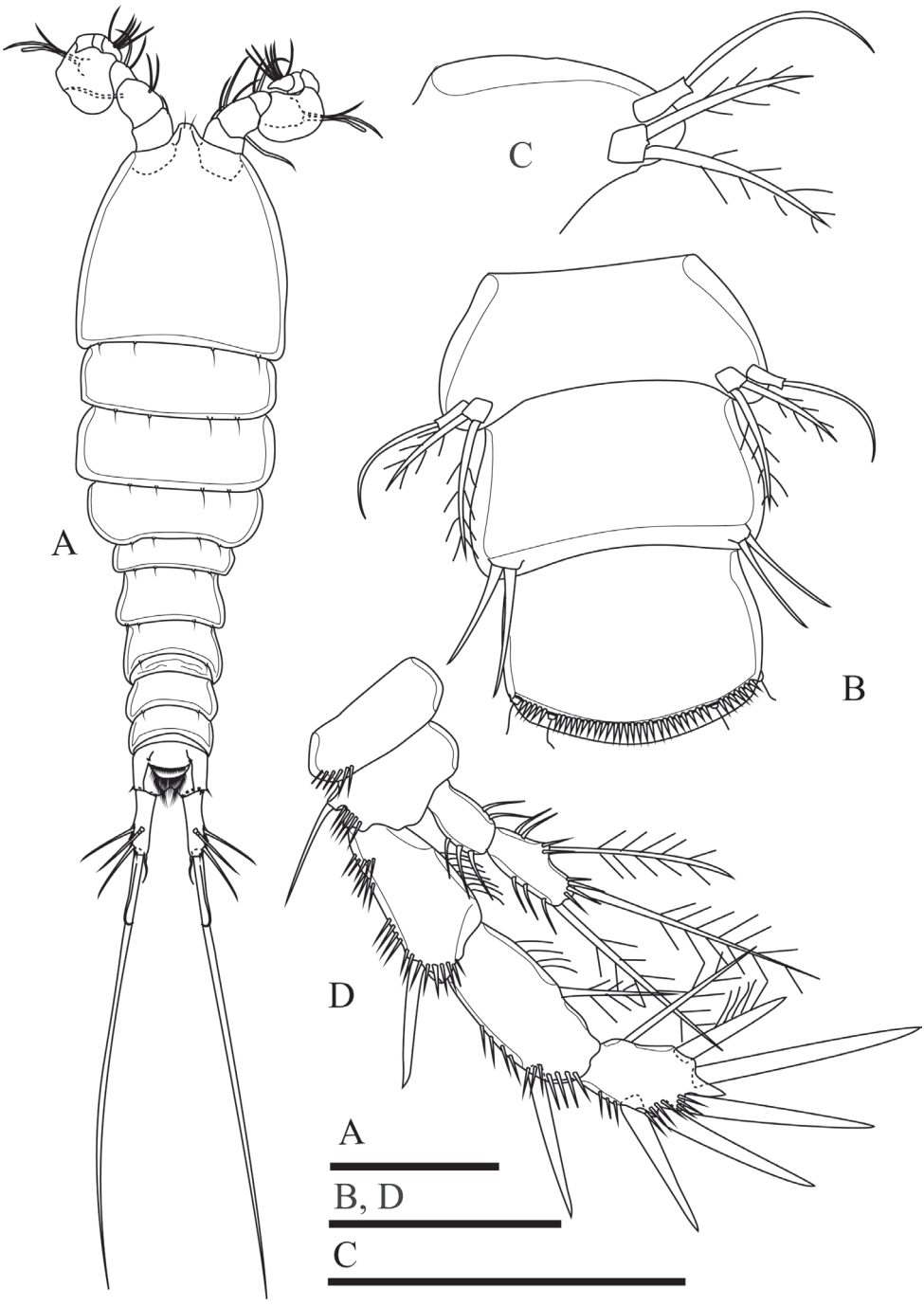

Figure 18. *Onychocamptus bengalensis*, male. **A** habitus, dorsal view **B** urosome, ventral view **C** left P5 **D** P4. Scale bars: 0.1 mm (**A**), 0.05 mm (**B–D**).

Table 2. Armature formula of P1–P4 of *Onychocamptus bengalensis*, *O.vitiospinulosa*, and *O. mohammed*.

Swimming legs		Basis	Exopod	Endopod
P1	female	I-1	I-0; III,2,0	0-0; 0,I1,0
	male	I-1	I-0; III,2,0	0-0; 0,I1,0
P2	female	I-0	I-0; I-1; III,I1,1	0-0; 0,2,2
	male	I-0	I-0; I-1; III,I1,1	0-0; 0,2,2
P3	female	1-0	I-0; I-1; III,I1,1	0-0; 1,2,3
	male	1-0	I-0; I-1; III,II,1	0-0; 0-1; 0,2,2
P4	female	1-0	I-0; I-1; III,2,1	0-0; 1,1,1
	male	1-0	I-0; I-1; III,2,1	0-0; 1,1,1

Antennule and mouthparts as in *O. satunensis* sp. n. and *O. tratensis* sp. n., except for allobasis of antenna with one bipinnate abexopodal seta (Figs 17A, 22B).

P1 (Fig. 17B), P2, P3 and P4 (Fig. 17C) as in *O. satunensis* sp. n. and *O. tratensis* sp. n., except for P4 exp-3 with three outer spines. Armature formula of P1–P4 as in Table 2.

P5 (Figs 17E, 23C). Baseoendopod and exopod fused; exopod rectangular. Baseoendopod with basal seta, endopodal lobe with three pinnate setae and with row of spinules at base of each seta. Exopod with three bipinnate setae, innermost longest and with spinules at its base.

P6 (Fig. 16C). Reduced to minute prominence at outer distal corner of genital field, with short slender seta.

Redescription of adult male. Body (Fig. 18A). Total body length, measured from tip of rostrum to posterior margin of caudal rami, 450–470 μm (n = 2); habitus smaller than female; preserved specimen colourless. Prosome approximately 1.1 times as long as urosome. Cephalothorax as long as wide, 0.5 times as long as prosome. Other characters as in *O. satunensis* sp. n. and *O. tratensis* sp. n.

Caudal rami (Fig. 18A). slightly divergent, three times as long as wide; length ratio of caudal setae to ramus length from seta I to seta VII : 0.3 : 0.7 : 1.2 : 1.5 : 7.6 : 0.4 : 1.2.

Antennule, antenna, mouthparts, P1, P2, P3 as in *O. satunensis* sp. n. and *O. tratensis* sp. n., except for P4 exp-3 with three robust outer spines (Fig. 18D).

Armature formula of P1–P4 as in Table 2.

P5 (Fig. 18C). Baseoendopod absent. Exopod with two setae, inner approximately 1.4 times as long as outer.

P6 (Fig. 18B). Reduced to minute, rectangular protuberance with two setae apically; inner seta approximately 1.5 times as long as outer one.

Variability. In male, one additional seta on left P1 enp-2 (Fig. 17F). In female, left P4 with 2-segmented, two apical elements of exp-2 fused (Fig. 17D).

Onychocamptus bengalensis is characterised by the relatively long caudal ramus and fusion of exopod and baseoendopod of P5 in the female. The length:width ratio of caudal ramus in female is variable (three times as long as wide in Lang (1948) and Song and Chang (1995), 3.8–4.0 times as long as wide in Lee and Chang (2005), and six times as long as wide in Hamond (1973)). The length:width ratio of the caudal ramus shown in Hamond (1973), is however, approximately 4.5 (Song and Chang 1995). The length:width ratio of the caudal ramus of the Thai specimens is 4.3. Other

characters observed from the Thai specimens match well Hamond's (1973) redescription, except for the basis of P3 and P4 with one row of setules along inner margin, and posterior margin of anal operculum with one row of spinules in the Thai material. The ornamentation of anal operculum is similar to that of the Korean specimens from the estuary of Ssangcheon Stream (Lee and Chang 2005), but it differs from the Australian specimens by lacking ornamentation at posterior margin (Hamond 1973).

Distribution. This species has been recorded from Calcutta (India) (Sewell 1934), brackish lagoons in northern coastal suburbs of Sydney (Australia) (Hamond 1973), crab burrows in a mud flat a little apart from shore line in Chindo Island (Korea) (Song and Chang 1995), and from Ssangcheon Stream (Korea) (Lee and Chang 2005).

In this study, we found the species in i) Samer-rach peat swamp, Trat Province, eastern Thailand; water temperature, 27.65 °C; pH, 5.38; salinity, 6.06 ppt; conductivity, 11285.2 μS cm^{-1}; total dissolved solids, 6982 mg L^{-1}; dissolved oxygen, 3.86 mg L^{-1}, ii) Khao Thanan cave, Satun Province, southern Thailand; this is a limestone cave which normally dries out during the dry season (April); water pH, 8.85; dissolved oxygen, 2.7 mg L^{-1}; conductivity, 2.1 μS cm^{-1}; salinity varies seasonally because of the effect from the sea nearby.

Onychocamptus vitiospinulosa (Shen & Tai, 1963)

Figs 19, 20, 22C, 23D

Laophonte vitiospinulosa Shen & Tai, 1963: 423, figs 42–46.
Onychocamptus mahammed vitiospinulosa: Lang 1965: 447.
Onychocamptus vitiospinulosa: Tai and Song 1979: 264, figs 147–148; Ishida 1990: 46, plate 4; Ishida and Kikuchi 2000: 34, fig 57; Lee and Chang 2005: 32, figs 1–3.

Material examined. Seven females and four males from Thale-Noi Lake, Pattalung Province, southern Thailand, 07°46'30.47"N, 100°9'31.68"E; coll. S Maiphae and T Saetang; 23 October 2013.

Differential diagnosis. Laophontidae. Caudal rami more than 2.3 times as long as wide in female and approximately 1.8 times as long as wide in male. P4 exp-3 with three outer spines. Female P5 exopod and baseoendopod separated, with three bipinnate spiniform setae on exopod and two on baseoendopod. Exopod of P5 male with two bipinnate spiniform setae.

Description of adult female. Body (Fig. 19A). Total body length, measured from tip of rostrum to posterior margin of caudal rami, 400–460 μm (mean 423 μm, n = 7); body cylindrical, gradually tapering posteriorly. Prosome 1.5 times as long as urosome. Rostrum small, completely fused to cephalothorax, and with pair of apical sensilla. All free thoracic somites with sensillum-bearing tubercles along posterior margin. Second and third urosomite fused ventrally forming the genital double-somite, remnant of division dorsally and laterally; penultimate urosomite with row of spinules dorsally and laterally.

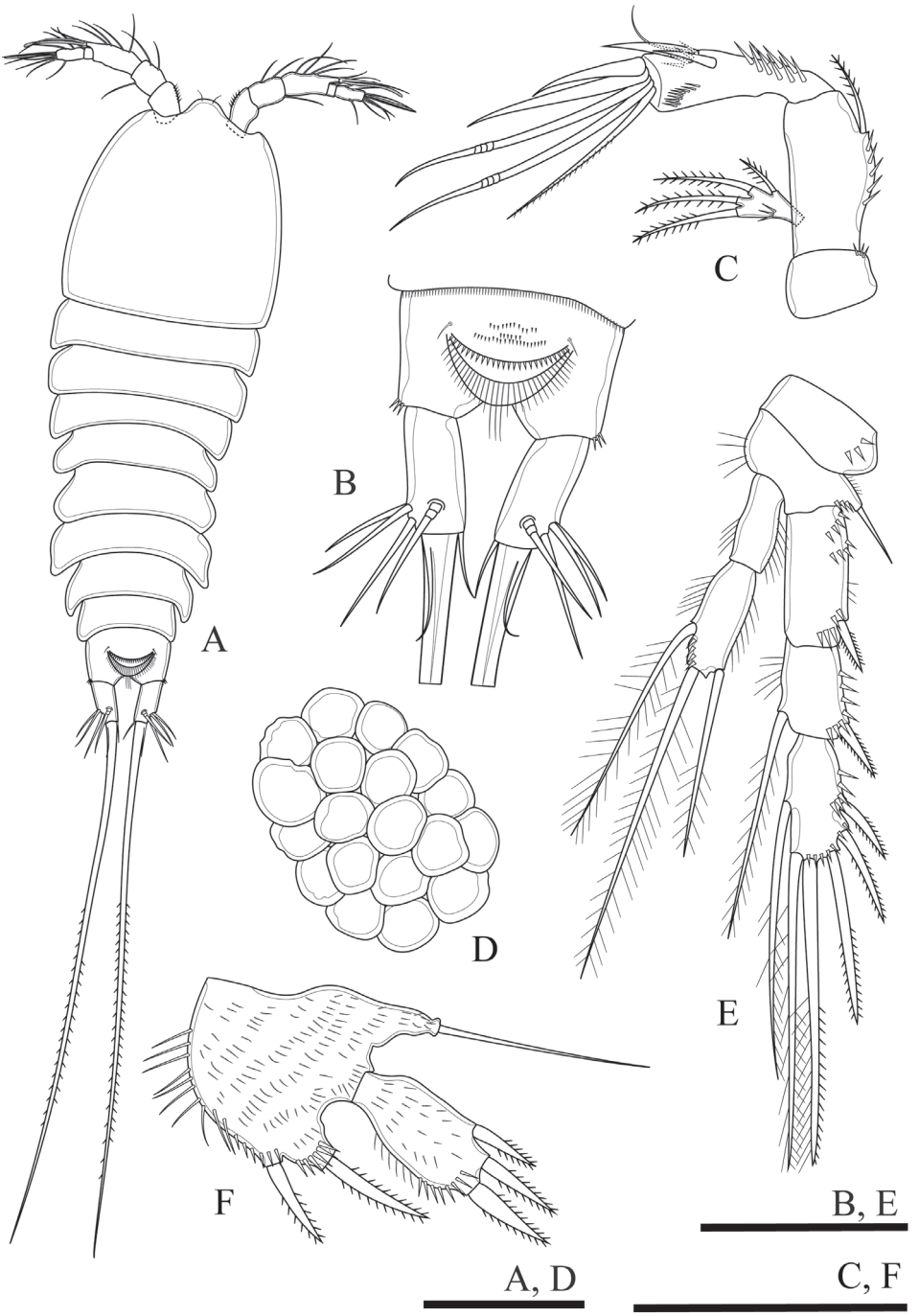

Figure 19. *Onychocamptus vitiospinulosa*, female. **A** habitus, dorsal view **B** anal somite and caudal rami, dorsal view **C** antenna **D** egg sac **E** P4 **F** P5. Scale bars: 0.1 mm (**A, D**), 0.05 mm (**B, C, E, F**).

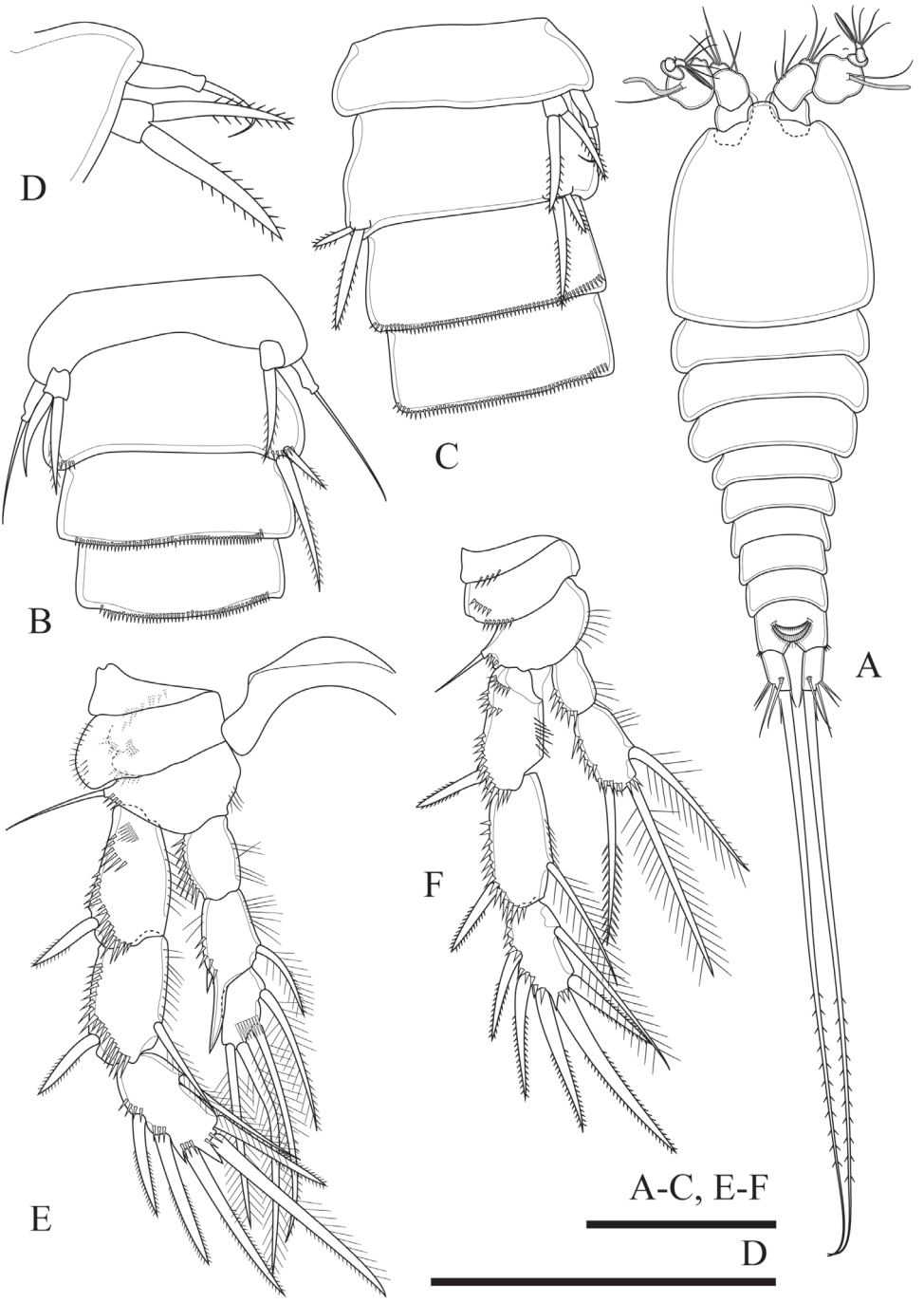

Figure 20. *Onychocamptus vitiospinulosa*, male. **A** habitus, dorsal view **B, C** urosome, ventral view **D** left P5 **E** P3 **F** P4. Scale bars: 0.1 mm (**A**), 0.05 mm (**B–F**).

Anal somite approximately 0.6 times as long as wide, with two rows of spinules; anal operculum poorly developed, with minute spinules along posterior border (Fig. 19B).

Caudal rami (Fig. 19B). Cylindrical, slightly convergent, 2.3 times as long as wide, with seven setae of different lengths. Position of caudal setae as in previous species. Length ratio of caudal setae to ramus length from seta I to seta VII: 0.7 : 0.9 : 1.0 : 0.7 : 11.1 : 0.4 : 1.0.

Egg sac (Fig. 19D). Ovigerous female with one rounded egg sac ventrally between pair of fifth legs, with nineteen eggs.

Antennule and mouthparts as those of previous described species, but allobasis of antenna with one bipinnate abexopodal seta (Figs 19C, 22C).

P1, P2, P3 and P4 (Fig. 19E) as those of previous species, except P4 exp-3 with three outer spines.

Armature formula of P1–P4 as in Table 2.

P5 (Figs 19F, 23D). Baseoendopod and exopod separated, covered with surface setules; baseoendopod with outer basal seta, endopodal lobe with two bipinnate spiniform setae, with one row of spinules at base of each seta; exopod with three bipinnate spiniform setae, with spinules at base of innermost seta only.

P6. Reduced to minute, rectangular protuberance, with one naked seta.

Description of adult male. Body (Fig. 20A). Total body length, measured from tip of rostrum to posterior margin of caudal rami, 320–360 μm (mean 349 μm, n = 4); body cylindrical, gradually tapering posteriorly. Prosome 1.4 times as long as urosome. Rostrum small, completely fused to cephalothorax, with pair of apical sensilla. Anal somite approximately 0.8 times as long as wide, anal operculum poorly developed.

Caudal rami (Fig. 20A). As in female.

Antennule, antenna, mouthparts, P1, P2, P3 (Fig. 20E), P4 (Fig. 20F) as in *O. satunensis* sp. n. and *O. tratensis* sp. n., except P4 exp-3 with three robust, outer spines.

Armature formula of P1–P4 as in Table 2.

P5 (Fig. 20D, 23D). Baseoendopod absent. Exopod with two bipinnate spiniform setae, outer seta not reaching beyond second urosomite.

P6 (Fig. 20C). Represented by two bipinnate spiniform setae, inner approximately twice as long as outer, and inner seta reaching beyond distal margin of third urosomite.

Variability. Thai specimens agree with Shen and Tai (1979), however the inner seta of the male P6 comes beyond the distal margin of four urosomite and the outer seta is approximately 1/3 as long as the inner seta in one specimen of our samples (Fig. 20B).

Distribution. This species has been recorded from the delta of the Pearl River (Kwangtung Province, south China) (Shen and Tai 1963), from a stream in Okinawa and Ishigaki Island (Japan) (Ishida 1990) and from Hangetsu Lake (Shiribeshi Province, Japan) (Ishida and Kikuchi 2000), and from reed marshes of the lower reaches of Gonyangcheon Stream and Sopocheon Stream (Jindo Island, Korea) (Lee and Chang 2005).

In this study, we found this species only in Thale-Noi Lake, Pattalung Province (southern Thailand) in June, August, and October 2013. Water temperature ranged between 28.3–31.6 °C, pH of 5.22–7.83, salinity 0.1–1.2 ppt, conductivity 209.5–2385 μS cm^{-1}, transparency 0.05–1.35 m, depth 0.35–1.65 m, chlorophyll a 0.27–37.53, and dissolved oxygen 2.89–5.76 mg L^{-1}.

***Onychocamptus mohammed* (Blanchard & Richard, 1891)**
Fig. 21, 22D, 23E

Laophonte mohammed Blanchard & Richard, 1891: 526, pl VI, figs 1–15; Daday 1906: Taf. 16, figs 9–16; Shen and Tai 1962: 397, figs 20–32: Tai and Song 1979: 261, figs 145–146.
Onychocamptus heteropus Daday, 1903: 157–161, figs18–24.
Laophonte calamorum Willey, 1923: 305, figs 2–4.
Onychocamptus mohammed: Lang 1948: 1417, abb. 576; Ishida and Kikuchi 2000: 34, fig 56; Lee and Chang 2005: 39–40, figs 4, 5a, b.

Material examined. Four females from Ta-pom swamp, Krabi Province, southern Thailand, 08°12'50.19"N 98°46'41.24"E, coll. S Maiphae and T Saetang, on 8 December 2016.

Diagnosis. Laophontidae. Caudal rami more than 2.2 times as long as wide in female. P4 exp-3 with three outer spines. Baseoendopod and exopod separated, each with three bipinnate spiniform setae.

Description of the adult female. Body (Fig. 21A). Total body length, measured from tip of rostrum to posterior margin of caudal rami, 410–480 μm (mean 440.50 μm, n = 4); body cylindrical, gradually tapering posteriorly. Prosome 1.3 times as long as urosome. Rostrum small, completely fused to cephalothorax, with pair of apical sensilla. All free thoracic somites with sensillum-bearing tubercles along posterior margin. Second and third urosomite fused ventrally forming genital double-somite; remnant of division dorsally and laterally. Anal somite approximately 0.7 times as long as wide. Anal operculum poorly developed, with minute spinules along upper posterior border.

Caudal rami (Fig. 21B). Cylindrical, parallel, 2.2 times as long as wide, with seven setae of different lengths. Position of caudal setae as in previous species. Inner terminal seta (V) approximately 0.7 times as long as body length. Length ratio of caudal setae to ramus length, from seta I to seta VII : 0.4 : 0.6 : 0.9 : 0.8 : 8.5 : 0.4 : 1.0.

Egg sac (Fig. 21E). Ovigerous female with one oval egg sac with eight eggs ventrally between fifth pair of legs.

Antennule and mouthparts as in previous species, but allobasis of antenna with one bipinnate abexopodal seta (Fig. 22D).

P1, P2, P3 and P4 (Fig. 21C) as in *O. satunensis* sp. n. and *O. tratensis* sp. n. except P4 exp-3 with three robust, outer spines.

Armature formula of P1–P4 as in Table 2.

P5 (Figs 21D, 23E). Baseoendopod and exopod separated; both rami densely covered with setules; baseoendopod with outer basal seta, endopodal lobe with three inner bipinnate spiniform setae, with one row of spinules at base of each seta; exopod with three bipinnate spiniform setae, with spinules at base of innermost seta only.

P6. Reduced to minute, rectangular protuberance, with one naked seta.

Variability. The length of the baseoendopodal setae of the female P5 is variable. The original description shows the lateral most seta as the longest (Blanchard and Richard 1891). This seta is also the longest in specimens from Japan (Ishida and Kikuchi 2000). However, the middle seta is the longest in specimens from China and Korea

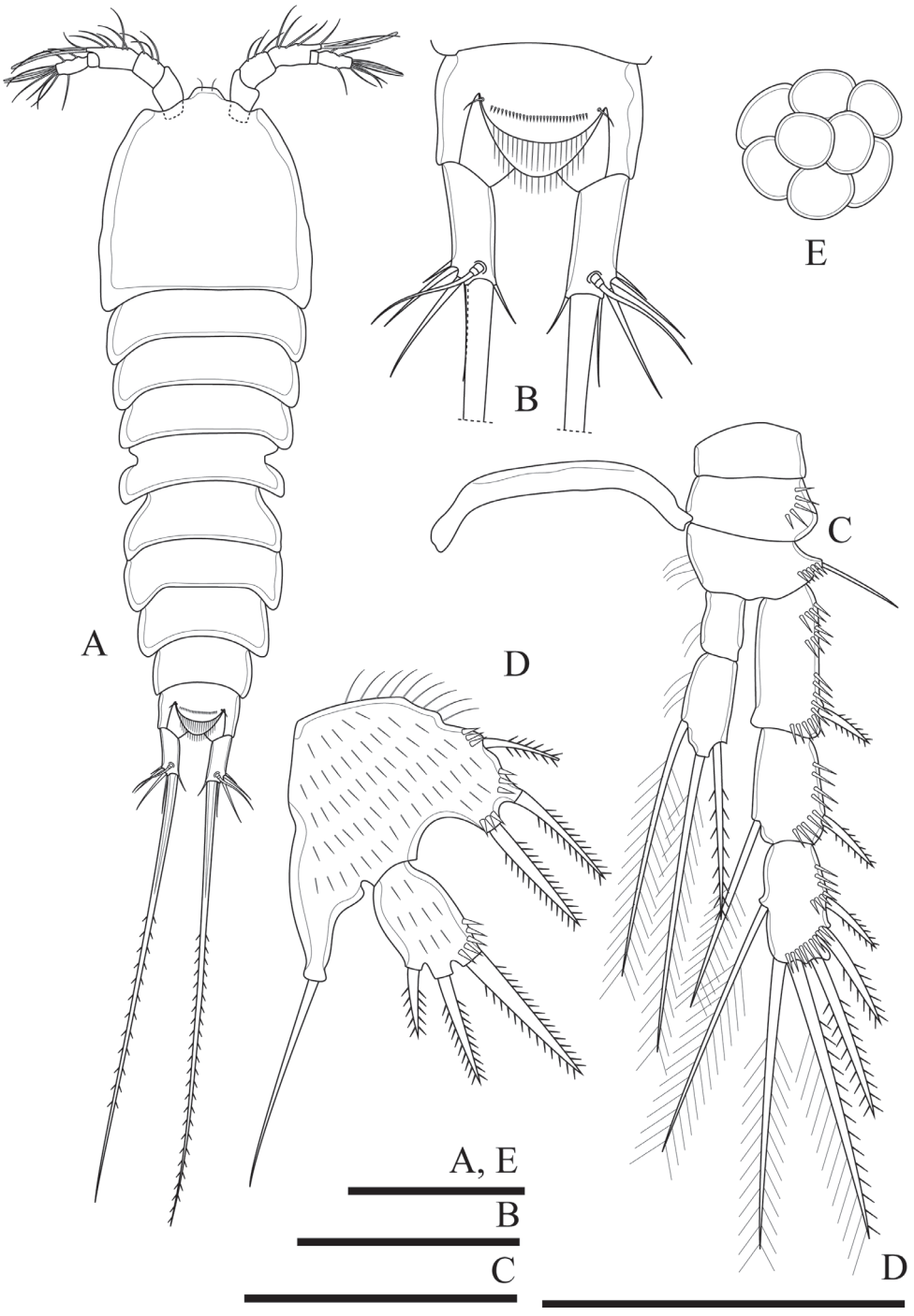

Figure 21. *Onychocamptus mohammed*, female. **A** habitus, dorsal view **B** anal somite and caudal rami, dorsal view **C** P4 **D** P5 **E** egg sac. Scale bars: 0.1 mm (**A, E**), 0.05 mm (**B–D**).

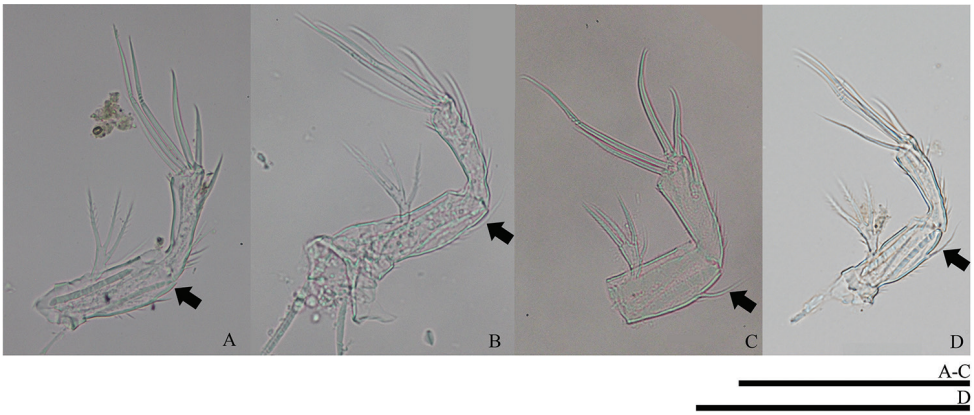

Figure 22. Allobasis of female antenna (digital photographs). **A** *O. tratensis* **B** *O. bengalensis* **C** *O. vitiospinulosa* **D** *O. mohammed*. Scale bars: 0.1 mm.

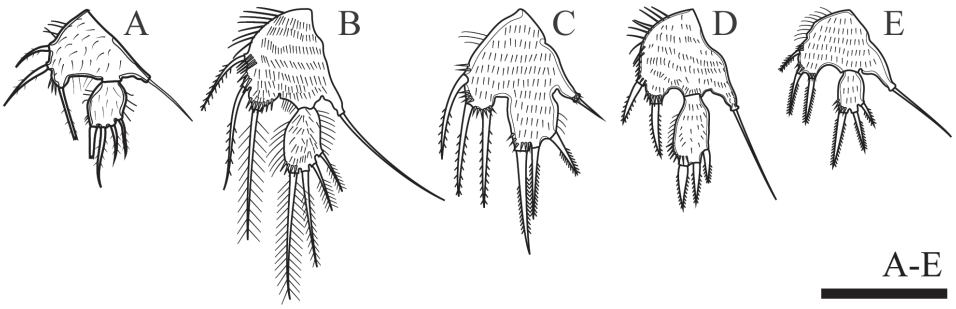

Figure 23. P5 of female. **A** *O. satunensis* **B** *O. tratensis* **C** *O. bengalensis* **D** *O. vitiospinulosa* **E** *O. mohammed*. Scale bar: 0.05 mm.

(Shen 1962, Lee and Chang 2005), and the lateral most seta is equal to the middle seta in the Thai specimens.

Distribution. This species has been found in many localities such as Wu-Li Lake (Kiangsu Province, China) (Shen and Tai 1962), in Harutori Lake (Kushiro, Japan) (Ishida and Kikuchi 2000), in Daecheong Lake and Yedang Reservior (Korea) (Lee and Chang 2005), in Vietnam (Ho and Tran 2007), and in central Thailand (Daday 1906, Watiroyram et al. 2015).

In the present study, we found the species in Ta-pom swamp (southern Thailand, Krabi Province) in December 2016, water temperature was 26.27 °C, pH 6.74, salinity 0.27 ppt, conductivity 571 μS cm^{-1}, and dissolved oxygen 4.32 mg L^{-1}.

Key to the females of *Onychocamptus* worldwide

1 Exopod of P5 with four setae **2**
– Exopod of P5 with three setae **4**

2 Exopod of antenna with one seta .....***O. anomalus*** **(Ranga Reddy, 1984)**
– Exopod of antenna with four setae.....**3**
3 Cephalothorax with internal sausage-like structure .....***O. satunensis*** **sp. n.**
– Cephalothorax without internal sausage-like structure ..... ***O. tratensis*** **sp. n.**
4 P4 exp-3 without inner seta ..... ***O. besnardi*** **Jakobi, 1954**
– P4 exp-3 with inner seta **5**
5 Exopod of P5 fused to baseoendopod ..... ***O. bengalensis*** **(Sewell, 1934)**
– Exopod and baseoendopod of P5 completely separated.....**6**
6 Baseoendopodal lobe with two setae ... ***O. vitiospinulosa*** **(Shen & Tai, 1963)**
– Baseoendopodal lobe with three setae 7
7 Antenna without abexpodal seta on allobasis .....
.....***O. taifensis*** **Kikuchi, Daiand & Itô, 1993**
– Antenna with abexpodal seta on allobasis.....**8**
8 P4 exp-3 with two outer spines.....**9**
– P4 exp-3 with three outer spines...***O. mohammed*** **(Blanchard & Richard, 1891)**
9 Caudal rami 2.8 times as long as wide, genital field with rows of spinules near P6..... ***O. krusensterni*** **Schizas & Shirley, 1994**
– Caudal rami twice as long as wide, genital field without rows of spinules near P6.....***O. fratrisaustralis*** **Gómez, 2001**

Key to the males of *Onychocamptus* (the male of *O. fratrisaustralis* Gómez, 2001 remains unknown and has not been included here) worldwide

1 Exopod of P5 with three setae.....**2**
– Exopod of P5 with two setae.....**4**
2 Exopod of antenna with one seta .....***O. anomalus*** **(Ranga Reddy, 1984)**
– Exopod of antenna with four setae.....**3**
3 Cephalothorax with internal sausage-like structure .....***O. satunensis*** **sp. n.**
– Cephalothorax without internal sausage-like structure ..... ***O. tratensis*** **sp. n.**
4 P4 exp-3 without inner seta ..... ***O. besnardi*** **Jakobi, 1954**
– P4 exp-3 with inner seta **5**
5 Caudal rami more than four times as long as wide...***O. bengalensis*** **(Sewell, 1934)**
– Caudal rami less than or approximately three times as long as wide **6**
6 Antenna without abexpodal seta on allobasis .....
.....***O. taifensis*** **Kikuchi, Daiand & Itô, 1993**
– Antenna with abexpodal seta on allobasis.....**7**
7 P4 exp-3 with two outer spines.... ***O. krusensterni*** **Schizas & Shirley, 1994**
– P4 exp-3 with three outer spines.....**8**
8 Inner seta on P6 approximately or less than twice as long as outer seta.....
..... ***O. mohammed*** **(Blanchard & Richard, 1891)**
– Inner seta on P6 approximately or more than 2.5 times as long as outer seta
..... ***O. vitiospinulosa*** **(Shen & Tai, 1963)**

Discussion

The two new species identified in this study can confidently be assigned to the genus *Onychocamptus* based on the combination of characteristics mentioned by Huys and Lee (2000) and Lee and Huys (1999): (1) female antennule with five segments, (2) male antennule with up to three segments distal to the geniculation, (3) caudal ramus with strongly developed seta V, (4) mandibular palp uniramous, (5) maxilliped with one seta on the syncoxa, (6) P1 with two-segmented exopod, (7) enp-1 of P1 without inner seta, (8) endopodal lobe of P5 with three setae, (9) inner distal element of P3 and P4 exp-3 showing sexual dimorphism (setiform in females, but spiniform in males) and (10) male P3 enp-2 with one inner seta. Based on the retention of the ancestral inner seta on P3 enp-2 of the male and geographical distribution, Lee and Huys (1999) suggested that *Onychocamptus* belongs to an ancient lineage which probably diverged from the stem group of the family Laophontidae.

When compared to the representatives of *Onychocamptus*, the two new species share the highest similarity with the Indian species *O. anomalus*, and the following features were common to all species: absence of the abexopodal seta on antenna, P4 exp-3 with only two outer spines, and four and three setae on the exopod of P5 of the female and the male respectively (Table 3). This suggests a close phylogenetic relationship among Thai and Indian species, as these three species are different from all other members of the genus with regard to several characteristics. For example, *O. taifensis* lacks the abexopodal seta of antenna (Kikuchi et al. 1993), the outer spine on P4 exp-3 is reduced in *O. krusensterni* (Schizas and Shirley 1994), and both *O. taifensis* and *O. krusensterni* have three and two setae on the P5 exopod of the female and the male, respectively. A detailed comparison of the characteristics and geographical distribution of the ten species is provided in Table 3. Three groups which comprise the most closely related species are evident: the American species group (*O. fratrisaustralis*, *O. krusensterni*, and *O. besnardi*), the South Asian species group (*O. anomalus*, *O. satunensis* sp. n, and *O. tratensis* sp. n.), and the group containing the remaining species. The American species group is characterised by reduction of the spine on P4 exp-3 and the presence of the abexopodal seta. The South Asian species group is characterized by the presence of one additional seta on the P5 exopod and the absence of one abexopodal seta. The remaining species show retention of three spines on P4 exp-3.

With the description of the two new species and new records of the two species from Thailand, the number of *Onychocamptus* species recorded in Thailand has now increased from one to five. Sampling of cave-dwelling copepods in this country has revealed a large number of new species of the genera *Elaphoidella, Bryocyclops, Fierscyclops*, and *Thermocyclops* (Boonyanusith et al. 2013, Brancelj et al. 2010, Karanovic et al. 2017, Watiroyram 2018, Watiroyram and Brancelj 2016, Watiroyram et al. 2012, 2015a, b), and a new genus, *Siamcyclops*, from west Thailand (Boonyanusith et al. 2018). Most of the samples were collected from a single cave.

Based on previous studies on cave-dwelling copepods in more than twenty caves in other regions of the country (Boonyanusith 2013; Watiroyram 2012) and nine caves in Satun and Songkhla province by the first and the third authors, it seems

Table 3. Comparison of characters of female and male of genus *Onychocamptus*.

	O. anomalus	*O. bengalensis*	*O. besnardi*	*O. fratrisaustralis*	*O. krusensterni*	*O. mohammed*	*O.taifensis*	*O. vitiospinulosa*	***O. satunensis* sp. n.**	***O. tratensis* sp. n.**
Ornamentation on cephalothorax	smooth	smooth	smooth	smooth	smooth	smooth	smooth	smooth	**internal sausage-like structure, and internal rounded structures**	**1 middle and 2 lateral rounded integumental window-like structures**
Exp of antenna (setae)	1, reduced	4, well developed	4, well developed	4, well developed	4, well developed	4, well developed	4, well developed	4, well developed	4, well developed	4, well developed
Lateral seta on exp of antenna	complete absent	pinnate spinulose seta	NA	pinnate spinulose seta	pinnate spinulose, seta	NA	bare, slender, short seta	bare, slender, short seta	pinnate spinulose, seta	pinnate spinulose seta
Abexopodal seta of antenna	absent	present	present	present	present	present	absent	present	absent	absent
P2 enp-2 (inner setae)	2	2	2	2	2	2	1	2	2	2
P4 exp-3 (outer spines)	2	3	2	2	2	3	3	3	2	2
P4 exp-3 (inner seta)	present	present	absent	present	present	present	present	present	present	present
Female P5 exp and beseoendopod	separated	fused	separated*	separated	separated	separated	separated	separated	separated	separated
Setae on female P5 exp:enp	4:3	3:3	3:3	3:3	3:3	3:3	3:3	3:2	4:3	4:3
Setae on male P5 exp	3	2	2	NA	2	2	2	2	3	3
Male P5, outer seta of exp	A	C	NA	NA	C	C	B	B	**D**	**E**
CR (L:W ratio)	2.7	3.0–6.0	2	2.2–3.0	2.0–3.0	2.4–3	1.8–2.0	1.8–2.2	2.5	2.2
Seta of male P6	a	d	NA	NA	c	c	e	b	a	a
Segment of male antennule	6	6–7	?	NA	6–7	7	7	7–8	8	8
Distribution	India	India, Japan, Korea, Australia	Brazil, Micronesia, NW Mexico	NW Mexico	Alaska	Cosmo-politan	China and Korea	Korea	Thailand	Thailand
Ecology	Lake	Estuary	With marine algae	Estuary	Lagoon, 1 m	Cave, FW	Lake	Inland water	Cave	Peatswamp

Note: **?** = doubtful. **NA** = not available. * = separated, noted in written description but fused in figure (Jakobi 1954: 197-198, 211, pl.VI, Figs 1–15). A = long; outer seta 4 times as long as supporting segment; outer and middle setae sub-equal; B = seta not reaching beyond second urosomite, sub-equal in length; C = reaching beyond second urosomite, sub-equal in length; D = short, outer seta as long as supporting segment, 1/3 as long as the middle seta; E = outer seta 2 times as long as supporting segment, 1/2 as long as the middle seta. **Male P6**, length of seta of male P6, a = inner seta long, reaching beyond distal margin of Ab1; outer seta 1/2 times as long as inner seta length; b = inner seta long extending beyond third urosomite; outer seta 1/4-1/2 as long as inner seta; c = inner seta long reaching beyond third urosomite; outer seta 3/4 times as long as inner seta; d = inner seta long, reaching beyond third urosomite; outer and inner seta sub-equal in length; e = inner and outer seta relatively.

that *O. satunensis* sp. n. was encountered only in its type locality. The occurrence of *O. satunensis* in caves is interesting, as all the other species were only recorded from surface water habitats near the coast of all continents (Table 3). Morphological comparison of all swimming legs clearly showed a low degree of differentiation. This

finding indicates the relatively recent speciation of this representative of the genus. Watiroyram et al. (2017) suggested that penetration into groundwater during the Quaternary glaciation might have resulted in the speciation of several cave-dwelling copepods in this country. This might explain why a lesser number of species have been found in Holarctic countries. This may also be the reason why the distribution of several *Onychocamptus* species is, in general, fragmentary, most species are found in a narrow distribution range (Table 3): *O. fratrisaustralis* and *O. krusensterni* from North America, *O. besnardi* from Central and South America, *O. anomalus* from South Asia, *O. satunensis* sp. n. and *O. tratensis* sp. n. from Southeast Asia, and *O. taifensis* and *O. vitiospinulosa* from East Asia along the Western coast of the North Pacific Ocean. In our case, *O. satunensis* sp. n. is very morphologically similar to *O. tratensis* sp. n., and this is indicative of their very close phylogenetic relationship. We assumed that a *O. tratensis*-like common ancestor was distributed in both ancient East and South of Thailand during the connection of the East and South of Thailand by landmass at 120 m above sea level in the late Pleistocene (Voris 2000), and that a population of common ancestors might have penetrated the caves before the rising of the sea level up to 5 m above the previous sea level in the Miocene separated them from each other.

Acknowledgments

This research was financial supported by the Office of the Higher Education Commission, Thailand (2558A13562002), Center of Excellence on Biodiversity (BDC), Office of Higher Education Commission (BDC-PG2-161004) and Kasetsart University Research and Development Institute (KURDI), Kasetsart University.

References

Apostolov A (2007) Notes sur les harpacticoïdes cavernicoles (Crustacea: Copepoda) de Vietnam du nord. Historia naturalis bulgarica 18: 65–73.

Blanchard R, Richard J (1891) Faune des lacs salés d' Algérie. Mémoires de la Societe zoologique de France 4: 512–535. https://biodiversitylibrary.org/page/10114729

Boonyanusith C (2013) Species diversity and distribution of copepods in caves in western part of Thailand. Ph.D. Thesis, Khon Kaen University, Khon Kaen, 232 pp.

Boonyanusith C, Brancelj A, Sanoamuang L (2013) First representatives of the genus *Fierscyclops* Karanovic, 2004 (Copepoda, Cyclopidae) from South East Asia. Journal of Limnology 72(Supplement 2): 275–289. https://doi.org/10.4081/jlimnol.2013.s2.e13

Boonyanusith C, Sanoamuang L, Brancelj A (2018) A new genus and two new species of cave-dwelling cyclopoids (Crustacea, Copepoda) from the epikarst zone of Thailand and up-to-date keys to genera and subgenera of the *Bryocyclops* and *Microcyclops* groups. European Journal of Taxonomy 431: 1–30. https://doi.org/10.5852/ejt.2018.431

Daday EV (1903) Die Schwarmbildung pelagischer Thiere. Zoologischer Anzeiger 18: 168–172.

Daday EV (1906) Untersuchungen über die Copepodenfauna von Hinterindien, Sumatra und Java, nebst einem Beitrag zur Copepodenkenntnis der Hawaii-Inseln. Zoologische Jahrbucher (Systematik) 24: 175–206. http://www.zobodat.at/pdf/Zoologische-Jahrbuecher-Syst_24_0175-0206.pdf

Gómez S (2001) A new species of *Onychocamptus* Daday, 1903 (Copepoda: Harpacticoida: Laophontidae) from northwestern Mexico. Proceedings of the Biological Society of Washington 114: 262–274.

Hamond R (1973) The harpacticoid copepods (Crustacea) of the saline lakes in southeast Australia, with special reference to the Laophontidae. Records of Australian Museum 28: 393–420. https://doi.org/10.3853/j.0067-1975.28.1973.406

Ho TH, Tran DL (2007) To add six new species freshwater crustaceans (Cyclopoida, Harpacticoida-Copepoda) to the fauna of inland freshwater zooplankton of Vietnam. Tạp chí Sinh học 29: 9–16. https://doi.org/10.15625/0866-7160/v29n2.5367

Huys R (2009) Unresolved cases of type fixation, synonymy and homonymy in harpacticoid copepod nomenclature (Crustacea: Copepoda). Zootaxa 2183: 1–99.

Huys R, Boxshall GA (1991) Copepod evolution. The Ray Society, London, 468 pp.

Huys R, Gee JM, Moore CG, Hamond R (1996) Marine and brackish water harpacticoid copepods. Part 1. In: Kermack DM, Barnes RSK, Crothers JH (Eds) Synopses of the British Fauna (New series) No. 51. The Linnean Society of London and The Estuarine and Coastal Sciences Association, London, 1–352.

Huys R, Lee W (2000) Basal resolution of laophontid phylogeny and the paraphyly of *Esola* Edwards. Bulletin of the Natural History Museum 66: 49–107.

Ishida T (1990) Copepods in the Mountain waters of Kyushu, Tsushima and Ryukyu Islands, southwestern Japan. Sci. Rep. Hokkaido Salmon Hatcher 44: 39–51.

Ishida T, Kikuchi Y (2000) Illustrated fauna of the freshwater harpacticoid copepods of Japan. Bulletin of the Biogeographical Society of Japan 55: 7–94. https://www.cabdirect.org/cabdirect/abstract/20013037939.

Jakobi H (1954) Especies novas de Harpacticoida (Copepoda-Crustacea) encontrados em algas marinhas do litoral Paraná-Santa Catarina. Boletim do Institute Oceanografico, Sao Paulo 5: 189–221. http://www.scielo.br/pdf/bioce/v5n1-2/v5n1-2a08.pdf.

Karanovic T, Koomput K, Sanoamuang L (2017) Two new *Thermocyclops* species (Copepoda, Cyclopoida) from Thailand, with notes on the genus phylogeny inferred from 18S and ITS sequences. Zoologischer Anzeiger – A Journal of Comparative Zoology 269: 26–47. https://doi.org/10.1016/j.jcz.2017.07.003

Kikuchi Y, Dai AY, Itô T (1993) Three species of harpacticoids (Crustacea, Copepoda) from Lake Tai-Hu, eastern China. Publications of the Itako Hydrobiological Station 6: 17–25.

Lang K (1948) Monographie der Harpacticiden. Lund, Håkan Ohlssons Boktryckeri, Vol. 2, Stockholm, 1682 pp.

Lang K (1965) Copepoda Harpacticoida from the Californian Pacific coast. Kungliga Svenska vetenskapsakademiens handlingar 10: 1–566.

Lee JM, Chang CY (2005) Harpacticoid copepods of genus *Onychocamptus* (Laophontidae) from Korea. The Korean Journal of Systematic Zoology 21: 31–43. http://www.koreascience.or.kr/search/articlepdf_ocean.jsp?admNo=DMBRBT_2005_v21n1_31

Lee W, Huys R (1999) *Bathylaophonte* gen. nov. from deep-sea hydrothermal vents and the polyphyly of *Paronychocamptus* (Copepoda: Harpacticoida). Cahiers de Biologie Marine 40: 293–328. http://www.vliz.be/en/imis?refid=66854

Ranga Reddy Y (1984) *Ameira confluens* n. sp. and *Paronychocamptus anomalus* n. sp. (Copepoda, Harpacticoida) from Lake Kolleru, South India. Crustaceana 46: 95–103. https://doi.org/10.1163/156854084X00090

Schizas NV, Shirley TC (1994) *Onychocamptus krusensterni* (Copepoda, Harpacticoida, Laophontidae) – a new species from Krusenstern Lagoon, Alaska. Crustaceana 66: 227–239. https://doi.org/10.1163/156854094X00710

Sewell RBS (1934). A study of the fauna of the salt lakes, Calcutta. Records of the Indian Museum, 36:45–121. http://faunaofindia.nic.in/PDFVolumes/records/036/01/0045-0121.pdf

Shen CJ, Tai AY (1962) The Copepoda of the Wu-Li Lake, Wu-Sih, Kiangsu Province. III. Harpacticoida. Acta Zoologica Sinica 14: 393–410.

Shen CJ, Tai AY (1963) On five new species, a new subgenus and a new genus of freshwater Copepoda (Harpacticoida) from the delta of Pearl River, South China. Acta Zoologica Sinica 15: 417–431.

Song SJ, Chang CY (1995). Marine harpacticoid copepods of Chindo Island, Korea. The Korean Journal of Systematic Zoology 11: 65–77. http://www.koreascience.or.kr/search/articlepdf_ocean.jsp?admNo=DMBRBT_1995_v11n1_65

Tai AY, Song YZ (1979) Harpacticoida. In: Shen CJ, Fauna Editorial Committee (Eds) Freshwater Copepoda. Fauna Sinica, Crustacea. Science Press, Beijing, 164–300.

Voris HK (2000) Maps of Pleistocene sea levels in Southeast Asia: shorelines, river systems and time durations. Journal of Biogeography 27: 1153–1167. https://doi.org/10.1046/j.1365-2699.2000.00489.x

Watiroyram S (2012) Species diversity and distribution of freshwater Copepoda in caves in northern Thailand. Ph.D. Thesis, Khon Kaen University, Khon Kaen, 187 pp.

Watiroyram S (2018) Two new species of the genus *Bryocyclops* Kiefer, 1927 (Copepoda: Cyclopoida: Cyclopidae) from southern Thailand. Raffles Bulletin of Zoology 66: 149–169.

Watiroyram S, Brancelj A (2016) A new species of the genus *Elaphoidella* Chappuis (Copepoda, Harpacticoida) from a cave in the south of Thailand. Crustaceana 89: 459–476. https://doi.org/10.1163/15685403-00003536

Watiroyram S, Brancelj A, Sanoamuang L (2012) A new *Bryocyclops* Kiefer (Crustacea: Copepoda: Cyclopoida) from karstic caves in Thailand. Raffles Bulletin of Zoology 60: 11–21. https://archive.org/stream/raffles-bulletin-zoology-60-011-021#page/n0

Watiroyram S, Brancelj A, Sanoamuang L (2015a) A new cave-dwelling copepod from northeastern Thailand (Cyclopoida: Cyclopidae). Raffles Bulletin of Zoology 63: 426–437.

Watiroyram S, Brancelj A, Sanoamuang L (2015b) Two new stygobiotic species of *Elaphoidella* (Crustacea: Copepoda: Harpacticoida) with comments on geographical distribution and ecology of harpacticoids from caves in Thailand. Zootaxa 3919: 81–99. https://doi.org/10.11646/zootaxa.3919.1.4

Wells JBJ (2007) An annotated checklist and keys to the species of Copepoda Harpacticoida (Crustacea). Zootaxa 1568: 1–872. http://www.mapress.com/zootaxa/2007f/z01568p872f.pdf

Willey A (1923) Notes on the distribution of free-living Copepoda in Canadian waters. Contributions to Canadian Biology (new series) 1: 303–334. https://doi.org/10.1139/f29-033

Zykoff WP (1904) Bemerkung über *Laophonte mohammed* Rich. Zoologischer Anzeiger 28: 246–249. https://www.zobodat.at/pdf/ZoologischerAnzeiger_28_0246-0249.pdf

ZooKeys 810: 91–111 (2018)
doi: 10.3897/zookeys.810.30726
http://zookeys.pensoft.net

RESEARCH ARTICLE

A peer-reviewed open-access journal
ZooKeys
Launched to accelerate biodiversity research

The freshwater crabs of Macau, with the description of a new species of *Nanhaipotamon* Bott, 1968 and the redescription of *Nanhaipotamon wupingense* Cheng, Yang, Zhong & Li, 2003 (Crustacea, Decapoda, Potamidae)

Chao Huang[1,2,3], Kai Chin Wong[4], Shane T. Ahyong[1,2]

1 *Palaeontology, Geobiology and Earth Archives Research Centre, School of Biological, Earth and Environmental Sciences, University of New South Wales, Kensington, NSW 2052, Australia* **2** *Australian Museum, 1 William St, Sydney NSW 2010, Australia* **3** *School of Life Sciences, Sun Yat-sen University, Guangzhou 510275, China* **4** *Macao Civic and Municipal Affairs Bureau, Macao SAR, China*

Corresponding author: *Shane T. Ahyong* (shane.ahyong@austmus.gov.au)

Academic editor: *S. De Grave* | Received 21 October 2018 | Accepted 26 November 2018 | Published 20 December 2018

http://zoobank.org/2A23FBC5-0BFD-4665-8FDB-12CF86E8FCC3

Citation: Huang C, Wong KC, Ahyong ST (2018) The freshwater crabs of Macau, with the description of a new species of *Nanhaipotamon* Bott, 1968 and the redescription of *Nanhaipotamon wupingense* Cheng, Yang, Zhong & Li, 2003 (Crustacea, Decapoda, Potamidae). ZooKeys 810: 91–111. https://doi.org/10.3897/zookeys.810.30726

Abstract

Four species of freshwater crabs from three genera and two families (*Cantopotamon hengqinense* Huang, Ahyong & Shih, 2017, *Nanhaipotamon guangdongense* Dai, 1997, *Nanhaipotamon macau* **sp. n.**, and *Somanniathelphusa zanklon* Ng & Dudgeon, 1992) are documented from Macau for the first time. One new species, *Nanhaipotamon macau* **sp. n.**, is described. The large flap on the male first gonopod terminal segment sets it apart from all other known congeners except *N. wupingense* Cheng, Yang, Zhong & Li, 2003, from Fujian. Characters of the carapace, male first gonopod and size, however, clearly differentiate these two species. Preliminary genetic studies also suggest that the two are not closely related. A neotype is designated for *N. wupingense*. The taxonomic status of *Nanhaipotamon guangdongense* is also discussed. Notes on the general biology and conservation status of these crabs are also included.

Keywords

Freshwater crabs, Gecarcinucidae, Macau, new species, Potamidae, systematics

Introduction

Best known as the gambling capital of the world, Macau (also known as Macao) has a total land area of only 30.8 km^2 but a population of more than 650,000 people, making it one of the most densely populated regions in the world (Government of Macao Special Administrative Region Statistics and Census Service). Macau historically consists of the Macau Peninsula (bordered by Zhuhai to the north) and two islands: Taipa and Coloane. The two islands are now joined by Cotai, an area created by land reclamation in 2005.

The freshwater crabs of Macau have not been scientifically documented to the best of our knowledge. General wetland faunal surveys from 2007 onwards have found freshwater crabs in Coloane resulting in a small collection kept in the Macao Civic and Municipal Affairs Bureau. Upon examination, it was found that these freshwater crab specimens contained three species, *Cantopotamon hengqinense* Huang, Ahyong & Shih, 2017, *Somanniathelphusa zanklon* Ng & Dudgeon, 1992, and a new species of *Nanhaipotamon* Bott, 1968. This has led to more extensive surveys in 2018, covering 14 survey points (two in Taipa and 12 in Coloane; Fig. 1) focused exclusively on freshwater crabs. Three species of potamid crabs, *Cantopotamon hengqinense* Huang, Ahyong & Shih, 2017, *Nanhaipotamon guangdongense* Dai, 1997, and *Nanhaipotamon macau* sp. n. and one species of gecarcinucid crab, *Somanniathelphusa zanklon* Ng & Dudgeon, 1992, were found. *Nanhaipotamon macau* sp. n. is very similar to the poorly known, *N. wupingense* Cheng, Yang, Zhong & Li, 2003, from Fujian Province. Unfortunately, the identity of *N. wupingense* is ambiguous because the type account is inadequate and the type material lost, requiring a neotype designation.

Materials and methods

Specimens were collected by hand and preserved in 75% ethanol from 2007 onwards from South China. They are deposited in the Sun Yat-sen Museum of Biology, Sun Yat-sen University, Guangzhou, China (**SYSBM**); the Australian Museum, Sydney, Australia (**AM**); the Zoological Reference Collection of the Lee Kong Chian Natural History Museum, National University of Singapore, Singapore (**ZRC**); and the Macao Civic and Municipal Affairs Bureau (**IACM**). Measurements, in millimetres, are of the carapace width and length, respectively. Other abbreviations are as follows:

G1 male first gonopod;
G2 male second gonopod;
CW carapace width.

The terminology used primarily follows that of Dai (1999) and Davie et al. (2015). The Kimura 2-parameter (K2P) COI sequence distances (Kimura 1980) were calculated using MEGA6 (Tamura et al. 2013). H-T Shih kindly provided the COI sequence data of various species of *Nanhaipotamon* for use in this study (GenBank accession nos. MK226142-MK226145).

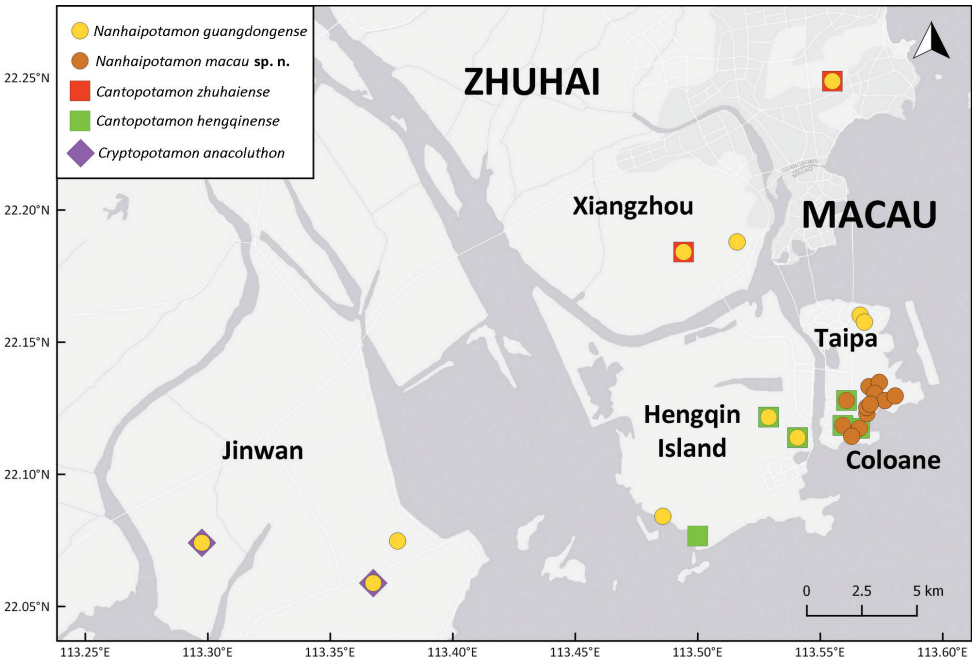

Figure 1. Localities of the sampling sites in and around Macau.

Taxonomy

Family Potamidae Ortmann, 1896
Subfamily Potamiscinae Bott, 1970
Genus *Cantopotamon* Huang, Ahyong & Shih, 2017

***Cantopotamon hengqinense* Huang, Ahyong & Shih, 2017**
Fig. 2C

Cantopotamon hengqinense Huang, Ahyong & Shih, 2017: 9, fig. 5.

Type material. Holotype: SYSBM 001558, male (19.9 × 16.0 mm), Dahengqin Mountain (22.11N, 113.50E), Hengqin Island, Zhuhai City, Guangdong, China, small hillstream, under rocks, coll. C. Huang, February 2016. Paratypes: SYSBM 001559, 1 female (13.0 × 10.6 mm), same data as holotype. SYSBM 001560–001561, 2 males (15.5 × 12.4 mm, 13.2 × 10.7 mm), same data as holotype.

Other material examined. China: IACM, 2 males (20.5 × 16.5 mm, 19.5 × 16.5 mm), Coloane (22.12N, 113.56E), Macau, small hillstream, under rocks, coll. K.C. Wong, November 2009. SYSBM 001640, 1 male (17.5 × 13.6 mm), Dahengqin Mountain, Hengqin Island, Zhuhai City, Guangdong, small hillstream, under rocks, coll. C. Huang, August 2017. SYSBM 001641–1644, 4 females (20.5 × 16.0 mm, 15.1 × 11.8 mm, 14.1 × 10.8 mm, 12.3 × 10.0 mm), same as SYSBM 001640. ZRC, 1 male (19.7 × 15.4 mm), Coloane, Macau, small hillstream, under rocks, coll.

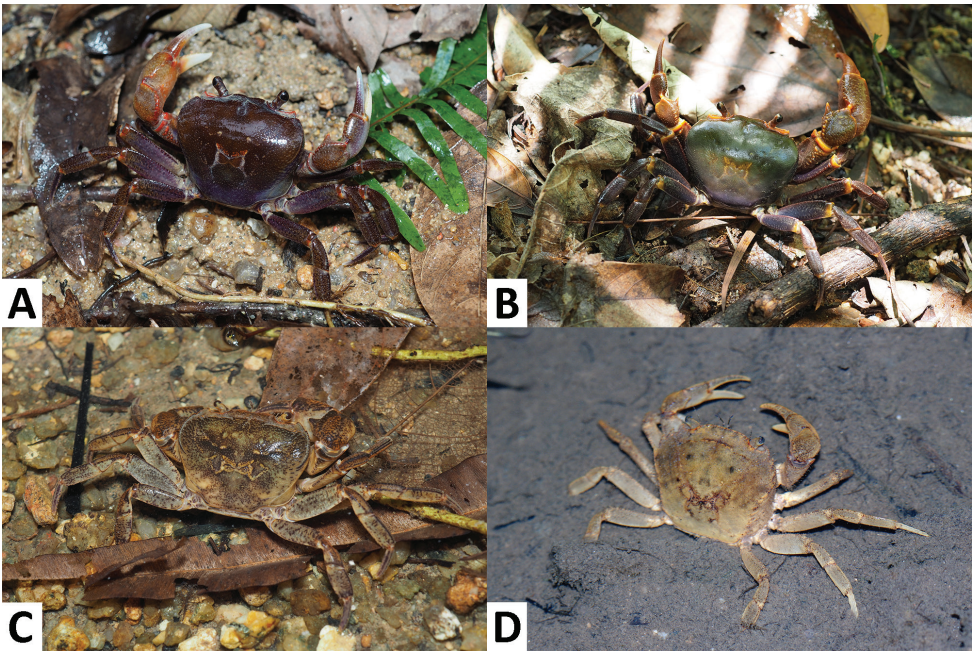

Figure 2. The freshwater crabs of Macau, colour in life. *Nanhaipotamon macau* sp. n., male (29.0 × 24.2 mm), SYSBM 001654 (**A**); *Nanhaipotamon guangdongense* Dai, 1997, male (35.9 × 28.8 mm), SYSBM 001645 (**B**); *Cantopotamon hengqinense* Huang, Ahyong & Shih, 2017, male, specimen not collected (**C**); *Somanniathelphusa zanklon* Ng & Dudgeon, 1992, photographed in Zhuhai, specimen not collected (**D**).

C. Huang, January 2018. ZRC, female (16.7 × 13.2 mm), same data as above. AM P101300, male (19.0 × 15.4 mm), Coloane, Macau, small hillstream, under rocks, coll. C. Huang, February 2018.

Distribution. Hengqin Island, Zhuhai, Guangdong; Coloane, Macau.

Conservation status. *Cantopotamon hengqinense* was previously only known from three hill streams in Dahengqin Mountain in Hengqin Island. This study found it to be present in another three hill streams in the neighbouring southwest corner of Coloane, Macau, which extends its extent of occurrence to 34.6 km^2 (excluding sea area), area of occupancy to 11.7 km^2 and number of locations to two. The populations in Hengqin and Macau are currently isolated from each other by a narrow strip of sea. Unlike the Hengqin population, whose habitat is threatened by urban development (Huang et al. 2017), the Macau population does not face serious imminent threat as all localities at which it was found are not currently open to development. Specimens from Macau are morphologically indistinguishable from those found in Hengqin Island. *Cantopotamon hengqinense* has not been found in Xiangzhou, Zhuhai to the north and Sanzao Island to the west despite considerable survey efforts during 2011–2018. In fact, no species of *Cantopotamon* are known from Sanzao Island, where instead *Cryptopotamon anacoluthon* (Kemp, 1918) is abundant. Given that the extent of occurrence and area

of occupancy of *C. hengqinense* is much lower than 5, 000 km^2 and 5000 km^2, respectively, with fewer than five known locations and projected decline in habitat quality in Hengqin, the suggested corresponding conservation status of this species under IUCN Red List criteria remains as indicated by Huang et al. (2017), as Endangered B2(a)(b).

Genus *Nanhaipotamon* Bott, 1968

Nanhaipotamon macau sp. n.

http://zoobank.org/550E7796-5748-4522-9825-C2A6EDB3BD8B
Figs 2A, 3–5, 6A–C

Type material. Holotype: SYSBM 001649, male (37.4 × 30.9 mm), Coloane (22.12N, 113.56E), Macau, China, forest floor, coll. K.C. Wong, July 2010. Paratypes: SYSBM 001650, female (31.3 × 25.5 mm), Coloane, Macau, China, mud burrow adjacent to small hill stream, coll. C. Huang, February 2018. SYSBM 001651, male (36.6 × 29.3 mm), same data as above. IACM, 2 males (36.5 × 31.1 mm, 34.6 × 28.5 mm), Coloane, Macau, forest floor, coll. J. Z. Huang, July 2009. AM P101301, male (27.7 × 22.9 mm), same data as above. ZRC, male (22.3 × 19.0 mm) Coloane, Macau, China, under rock in small hillstream, coll. C. Huang, January 2018.

Other material examined. Macau: SYSBM 001652-55, 4 males (35.3 × 28.8 mm, 32.1 × 26.5 mm, 29.0 × 24.2 mm, 28.9 × 24.1 mm), Coloane, in burrows adjacent to small hill stream, coll. C. Huang, February 2018.

Diagnosis. Carapace broader than long, regions indistinct, dorsal surface convex, anterolateral region weakly rugose (Figs 3A, 4B); postorbital cristae sharp, laterally expanded, almost fused with epibranchial teeth and epigastric cristae (Figs 3A, 4B); external orbital angle sharply triangular, outer margin gently convex to almost straight, separated from anterolateral margin by conspicuous gap (Figs 3A, B, 4B); sub-orbital regions covered by sparse low granules, pterygostomial regions covered with short rows of a few rounded granules; sub-hepatic regions covered with lined striae (Fig. 3B); maxilliped III exopod reaching to proximal one-third of merus with short flagellum (Fig. 5A); female vulva ovate, medium-sized, positioned closely to one another (Fig. 4D); male pleon triangular, lateral margins almost straight (Fig. 3C); G1 slender, subterminal segment tapering distally, terminal segment large, distally expanded, distal margin laminar, apex blunt, directed outward (Figs 5C–E, 6A–C). G2 basal segment subovate (Fig. 5B).

Description. Carapace broader than long, width about 1.2 × length (n = 6); regions indistinct, dorsal surface convex; surface generally smooth, pitted, anterolateral region weakly rugose (Figs 3A, 4B). Front deflexed, margin ridged in dorsal view (Figs 3A, 4B). Epigastric cristae low, separated by narrow gap (Figs 3A, 4B). Postorbital cristae sharp, laterally expanded, almost fused with epibranchial teeth and epigastric cristae (Figs 3A, 4B). Branchial regions slightly swollen (Figs 3A, B, 4B). Cervical groove shallow (Figs 3A, 4B). Mesogastric region slightly convex (Figs 3A, 4B). External orbital

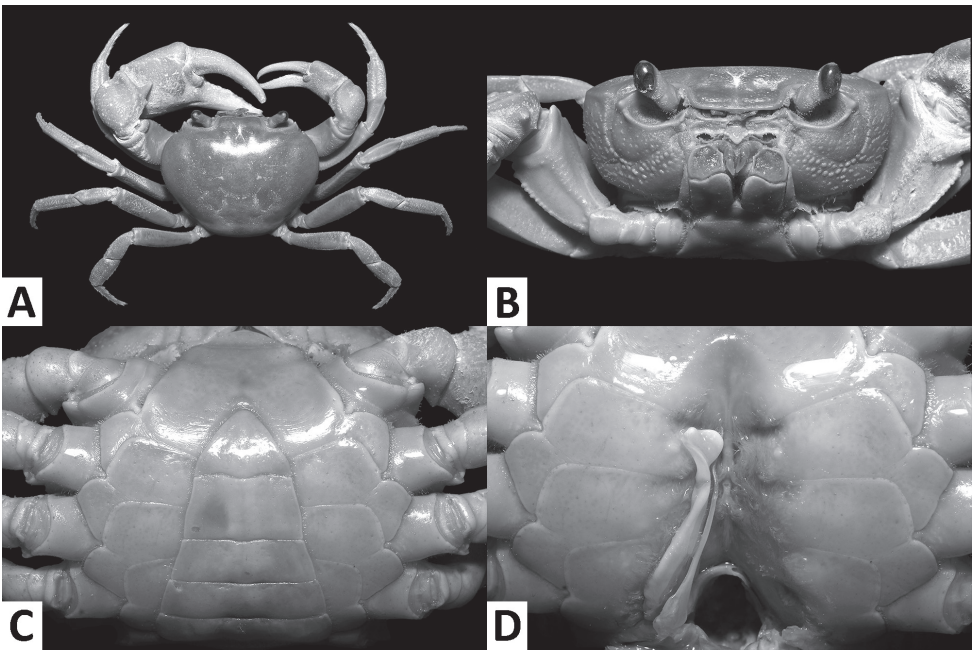

Figure 3. *Nanhaipotamon macau* sp. n., male holotype (37.4 × 30.9 mm), SYSBM 001649 Dorsal habitus (**A**); cephalothorax, anterior view (**B**); anterior thoracic sternum and pleon, ventral view (**C**); sternopleonal cavity with right G1 *in situ* (left G1 removed), ventral view (**D**).

angle sharply triangular, outer margin gently convex to almost straight, separated from anterolateral margin by conspicuous gap (Figs 3A, B, 4B). Epibranchial tooth small, granular, indistinct (Figs 3A, B, 4B). Anterolateral margin cristate, lined with 20–23 granules, less distinct in some larger specimens; bent inward posteriorly (Figs 3A, 4B). Posterolateral surface with low, oblique striae, converging towards posterior carapace margin (Figs 3A, 4B). Orbits large; supraorbital, infraorbital margins cristate (Fig. 3B). Sub-orbital regions covered by sparse low granules, pterygostomial regions covered with short rows of a few rounded granules; sub-hepatic regions covered with lined striae (Fig. 3B). Epistome posterior margin narrow; median lobe broadly triangular, lateral margins slightly sinuous (Fig. 3B).

Maxilliped III merus about as wide as long; ischium width about 0.7 × length; merus subtrapezoidal, with median depression; ischium subtrapezoidal, with distinct median sulcus, mesial margin rounded. Exopod reaching to proximal one-third of merus; flagellum short (Fig. 5A).

Chelipeds (pereiopod I) unequal (Figs 3A, 5F–I); less inflated in females (Figs 4B, 5H, I). Merus trigonal in cross section; margins crenulated, dorsal-outer surface granulated. Carpus with sharp spine at inner-distal angle, spinule at base (Figs 3A, 4B). Major cheliped palm length about 1.2–1.4 × height in males (n = 5), 1.3 × in female (n = 1); dactylus 0.9–1.0 × palm length in males (n = 5), 0.9 × in female (n = 1) (Fig. 5G, I). Palm surface pitted, dorsal-outer surface granulated in larger

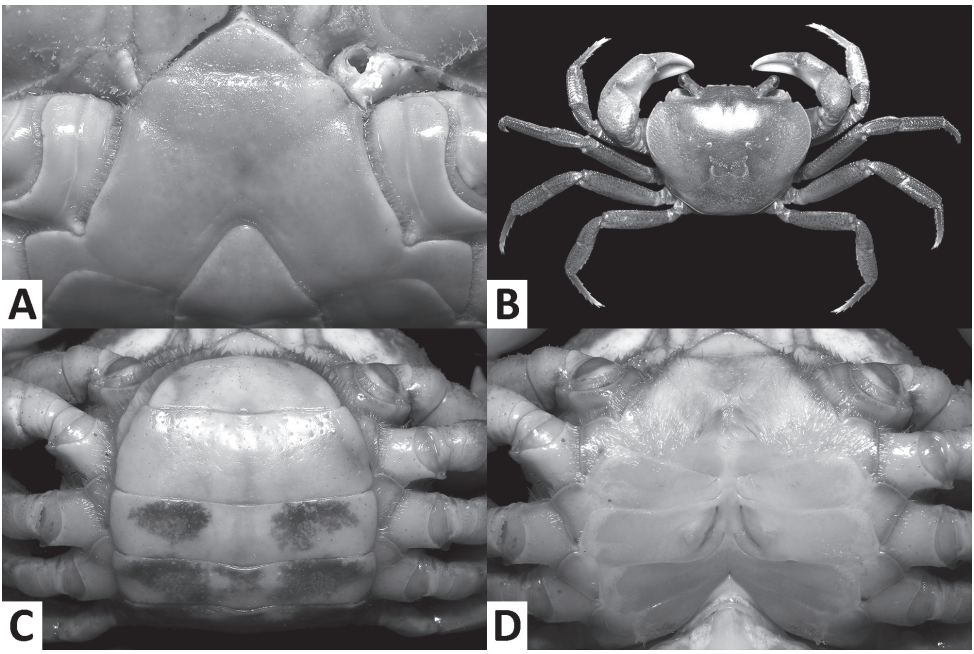

Figure 4. *Nanhaipotamon macau* sp. n., male holotype (37.4 × 30.9 mm), SYSBM 001649 (**A**); female paratype (31.3 × 25.5 mm), SYSBM 001650 (**B–D**). Anterior thoracic sternum (**A**); dorsal habitus (**B**); pleon, ventral view (**C**); vulvae, ventral view (**D**).

males (Fig. 5G). Dactylus as long as pollex (Fig. 5F–I). Occlusal margin of fingers with irregular blunt teeth; slight gape when closed (Fig. 5F–I).

Ambulatory legs (pereiopods II–V) slender, setae short, very sparse (Figs 3A, 4B). Pereiopod III merus 0.6–0.7 × carapace length in males (n = 5), 0.6 × carapace length in female (n = 1) (Figs 3A, 4B). Pereiopods V propodus 2.1–2.2 × as long as broad in males (n = 5), 2.1 × as long as broad in female (n = 1), shorter than dactylus (Figs 3A, 4B).

Male thoracic sternum generally smooth; sternites I–IV narrow, width about 1.5 × length; sternites I, II forming triangular structure; sternites II, III fused, but demarcated by shallow transverse sulcus; sternites III, IV fused, demarcation inconspicuous (Fig. 4A). Male sterno-pleonal cavity reaching anteriorly beyond level of posterior articular condyle of cheliped coxa (Fig. 4A); deep median longitudinal groove between sternites VII, VIII (Fig. 3D). Male pleonal locking tubercle positioned at mid-length of sternite V (Fig. 3D). Female vulva ovate, medium-sized, not reaching the sutures of sternites V/VI or VI/VII, positioned closely to one another (Fig. 4D).

Male pleon triangular; somites III–VI progressively narrower, lateral margins almost straight; somite VI width 1.8–2.1 × length (n = 6); telson width 1.3–1.4 × length (n = 6); apex rounded (Fig. 3C). Female pleon broadly ovate (Fig. 4C).

G1 slender; in-situ, tip of terminal segment exceeding pleonal locking tubercle, almost reaching suture between thoracic sternites IV/V (Fig. 3D); subterminal segment length about 3.1 × length of terminal segment; subterminal segment tapering distally;

terminal segment large, distally expanded, distal margin laminar, slightly sinuous to V-shaped, apex blunt, directed outward, orientation perpendicular to oblique to main axis of G1 (Figs 5C–E, 6A–C). G2 subterminal segment about 1.9 × length of flagelliform distal segment; exopod absent (Fig. 5B).

Etymology. This species is named after the type locality, Macau; used as a noun in apposition.

Colour in life. Variable, carapace and ambulatory legs dark brown to purple; chelipeds a combination of brown, orange and white (Fig. 2A).

Habitat. *Nanhaipotamon macau* sp. n. is a typical semi-terrestrial species that burrows in wet soil in the bank adjacent to hill streams. It was sympatric with *Cantopotamon hengqinense* at three localities (22.117N, 113.566E; 22.118N, 113.559E; 22.128N, 113.561E).

Distribution. Coloane, Macau.

Remarks. As with many other species of *Nanhaipotamon*, *N. macau* sp. n. shows intraspecific variation in G1 morphology. In the terminal segment, the curves of the inner-distal and distal margins vary (Fig. 5C–E). The general shape and large size of the terminal segment, however, readily separates *N. macau* from other congeners in the Pearl River Delta Region, such as *N. guangdongense* Dai, 1997 (Fig. 7).

Nanhaipotamon wupingense Cheng, Yang, Zhong & Li, 2003, from Fujian Province, is the only other known congener that also possesses such a large terminal segment. Based on the redscription of *N. wupingense* below, *N. macau* sp. n. differs by its larger maximum size (CW to 37.4 mm vs 27.5 mm in *N. wupingense*; Cheng et al. 2003); more inflated and less rugose branchial regions (compare Figs 3A, B, 8A, B); pterygostomial region granules larger, less numerous (compare Figs 3B, 8B); the G1 tip usually points laterally and the convex anterior margin next to the tip is often lower (Figs 5C–E, 6A–C) (tip points anterolaterally with higher adjacent convex margin, Fig. 6D; Cheng et al. 2003: fig. 7); G1 subterminal segment length about 3.0–3.2 × length of terminal segment in *N. macau* sp. n. (Figs 5C–E, 6A) (2.7 in the neotype of *N. wupingense*, see below, Fig. 6D). In keeping with their wide geographic separation, sequences of the COI barcoding region between *N. macau* sp. n. (SYSBM 001654; GenBank accession number MK226142) and *N. wupingense* (GenBank accession number: AB470511.1), courtesy of Hsi-Te Shih, shows a high (13.51%) Kimura 2-parameter (K2P) distance, corroborating their separate species status.

Conservation status. *Nanhaipotamon macau* sp. n. has an extremely restricted distribution with an extent of occurrence of only 5.3 km^2 (excluding sea area) and an area of occupancy of around 3 km^2. However, all 12 hill streams at which *N. macau* sp. n. was found are not currently open to urban development (one of these, Ka-Ho Reservoir Freshwater Wetland, is a protected area) and they seem to be locally abundant. We are unaware of any commercial harvesting of these crabs for human consumption or the aquarium trade. As such, no imminent threats to this species are apparent and it cannot be assigned to any level of threat according the IUCN Red List criteria. However, we emphasize the fragility of this species due to its highly restricted distribution; the habitat integrity of the hills of Coloane is paramount to this species' survival.

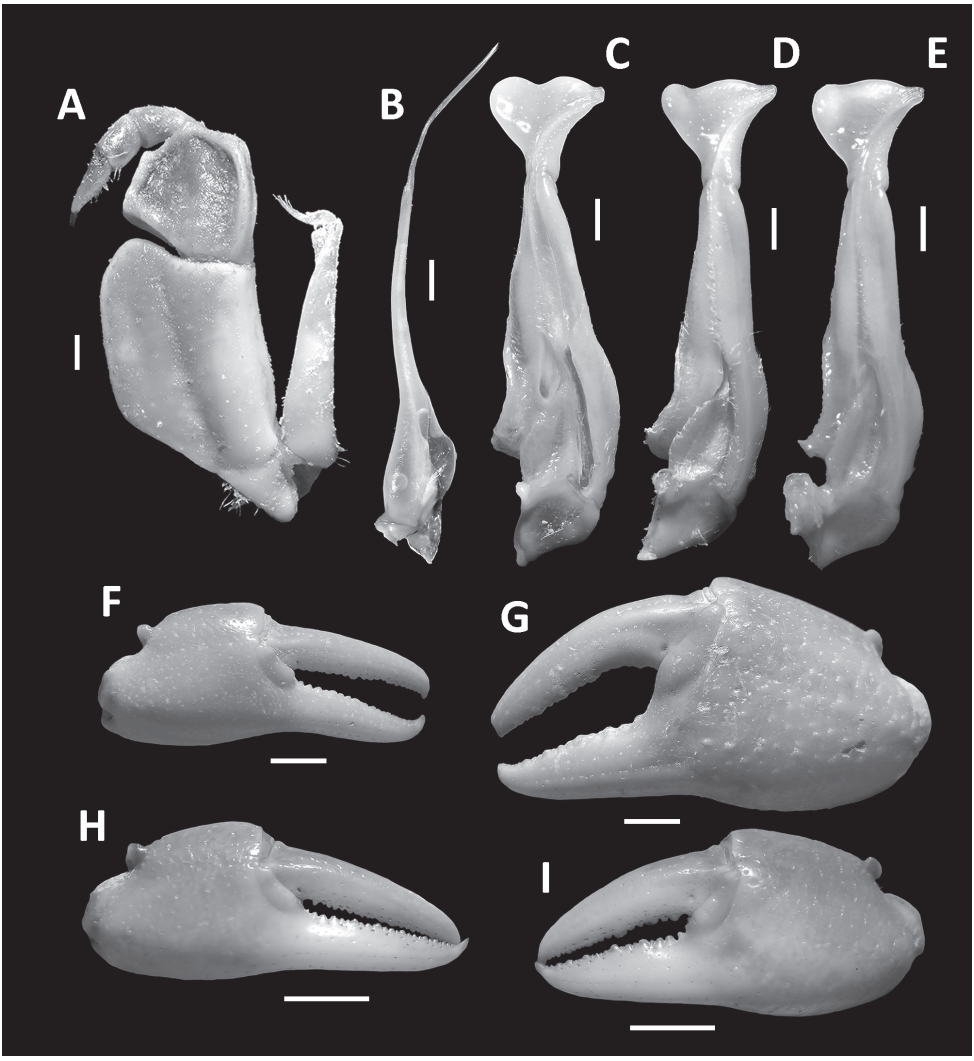

Figure 5. *Nanhaipotamon macau* sp. n., male holotype (37.4 × 30.9 mm), SYSBM 001649 (**A–C, F, G**); male paratype (36.6 × 29.3 mm), SYSBM 001651 (**D**); male (35.3 × 28.8 mm), SYSBM 001652 (**E**); female paratype (31.3 × 25.5 mm), SYSBM 001650 (**H–I**). Left maxilliped 3 (**A**); left G2, ventral view (**B**); left G1, ventral view (**C–E**); minor cheliped (**F, H**); major cheliped (**G, I**). Scale bars: 1.0 mm (**A–E**); 5.0 mm (**F–I**).

Nanhaipotamon guangdongense Dai, 1997

Figs 2B, 6G, 7

Nanhaipotamon guangdongense Dai, 1997: 229, fig. 9; Dai 1999: 121, pl. 8(1), fig. 60; Huang et al. 2012: 57, fig. 1A, 60; fig. 4, 61; fig. 5A–C.

Type material. Holotype: AS-CB 05141, male (33.2 × 26.4 mm), Guangdong Province, China, gift from Sun Yat-Sen Medical College, no date [photographs examined].

Other material examined. SYSU 001001, male (38.5 × 30.0 mm), Xiangzhou (22.25N, 113.57E), Zhuhai City, Guangdong, blue, mud hole next to small hillstream, coll. C. Huang, May 2012. SYSBM 001003, 1 male (36.2 × 28.4 mm), Xiangzhou, Zhuhai City, Guangdong, mud hole next to small hill stream, coll. C. Huang, February 2011. SYSBM 001004, 1 male (30.5 × 24.3 mm), Xiangzhou, Zhuhai City, Guangdong, mud hole next to small hill stream, coll. C. Huang, August 2012. SYSBM 001177, 1 male (35.4 × 29.4 mm), Xiangzhou, Zhuhai City, Guangdong, mud hole next to small hill stream, coll. C. Huang, May 2013. SYSBM 001178, 1 female, (35.9 × 29.4 mm), same data as above. SYSU 001758–001760, 3 males (40.1 × 32.7 mm, 36.0 × 29.8 mm, 30.2 × 25.1 mm), Xiangzhou, Zhuhai City, Guangdong, blue, mud hole next to small hillstream, coll. C. Huang, September 2018. SYSU 001761–001764, 4 males (42.1 × 33.5 mm, 40.5 × 32.4 mm, 38.1 × 32.0 mm, 32.5 × 27.0 mm), Xiangzhou, Zhuhai City, Guangdong, mud hole next to small hill stream, coll. C. Huang, September 2018. SYSBM 001141–001143, 3 males (38.4 × 31.5 mm, 40.8 × 32.2 mm, 36.7 × 29.4 mm), Gujing (22.36N, 113.12E), Jiangmen City, Guangdong, coll. local, August 2013. IACM, 2 males (39.5 × 31.5 mm, 25.2 × 21.1 mm), Taipa (22.16N, 113.58E), Macau, mud hole next to small hill stream, coll. K.C. Wong, March 2018. SYSBM 001645–001646, 2 males (35.9 × 28.8 mm, 30.9 × 24.8 mm), Taipa, Macau, mud hole next to small hill stream, coll. C. Huang, June 2018. SYSBM 001656, 1 male (45.5 × 37.0 mm), Dahengqin mountain (22.11N, 113.50E), Hengqin Island, Zhuhai City, Guangdong, in small hill stream pool, coll. C. Huang, August 2017. SYSBM 001672, 1 male (22.4 × 18.5 mm), Jinwan (22.08N, 113.35E), Zhuhai City, Guangdong, mud hole next to small hill stream, coll. C. Huang, June 2018. SYSBM 001673–001674, 2 females (31.7 × 25.7 mm, 25.9 × 20.8 mm), same data as above. SYSBM 001017–001019, 3 males (33.4 × 26.5 mm, 29.2 × 23.6 mm, 27.6 × 21.7 mm), Doumen (22.19N, 113.29E), Zhuhai City, Guangdong, coll. local, April 2013. SYSBM 001657–001658, 2 males (36.9 × 30.4 mm, 23.0 × 19.5 mm), Jinzhong Reservoir (22.48N, 113.38E), Zhongshan City, Guangdong, mud hole next to small hill stream, coll. C. Huang, January 2018. SYSBM 001659, 1 female (23.6 × 19.8), same data as above. SYSBM 001016, 1 male (40.5 × 33.1 mm), Qi'ao Island (22.43N, 113.66E), Zhuhai City, Guangdong, mud hole next to small hill stream, coll. C. Huang, May 2011. SYSBM 001023, 1 female (40.5 × 33.1 mm), same data as above. SYSBM 001750, 1 male (39.6 × 32.5 mm), Gudou Mountain (22.22N, 112.97E), Jiangmen City, Guangdong, coll. local, July 2018. SYSBM 001751, 1 male (35.1 × 26.0 mm), Xinhui (22.52N, 113.08E), Jiangmen City, Guangdong, coll. local, July 2018.

Colour in life. Highly variable, even within the same population. Carapace and ambulatory legs dark brown to purple; chelipeds a combination of brown, orange and white (Fig. 2B). Blue variants are sometimes seen.

Distribution. Guangdong: Zhuhai, Zhongshan, Jiangmen; Macau: Taipa.

Remarks. *Nanhaipotamon guangdongense* has been found at only one locality in Macau (Tai Tam Hill, Taipa). One specimen (SYSBM 001646) has exopods on the G2 on both sides, the first such report for a freshwater crab (Fig. 6G). The G2 exopod is

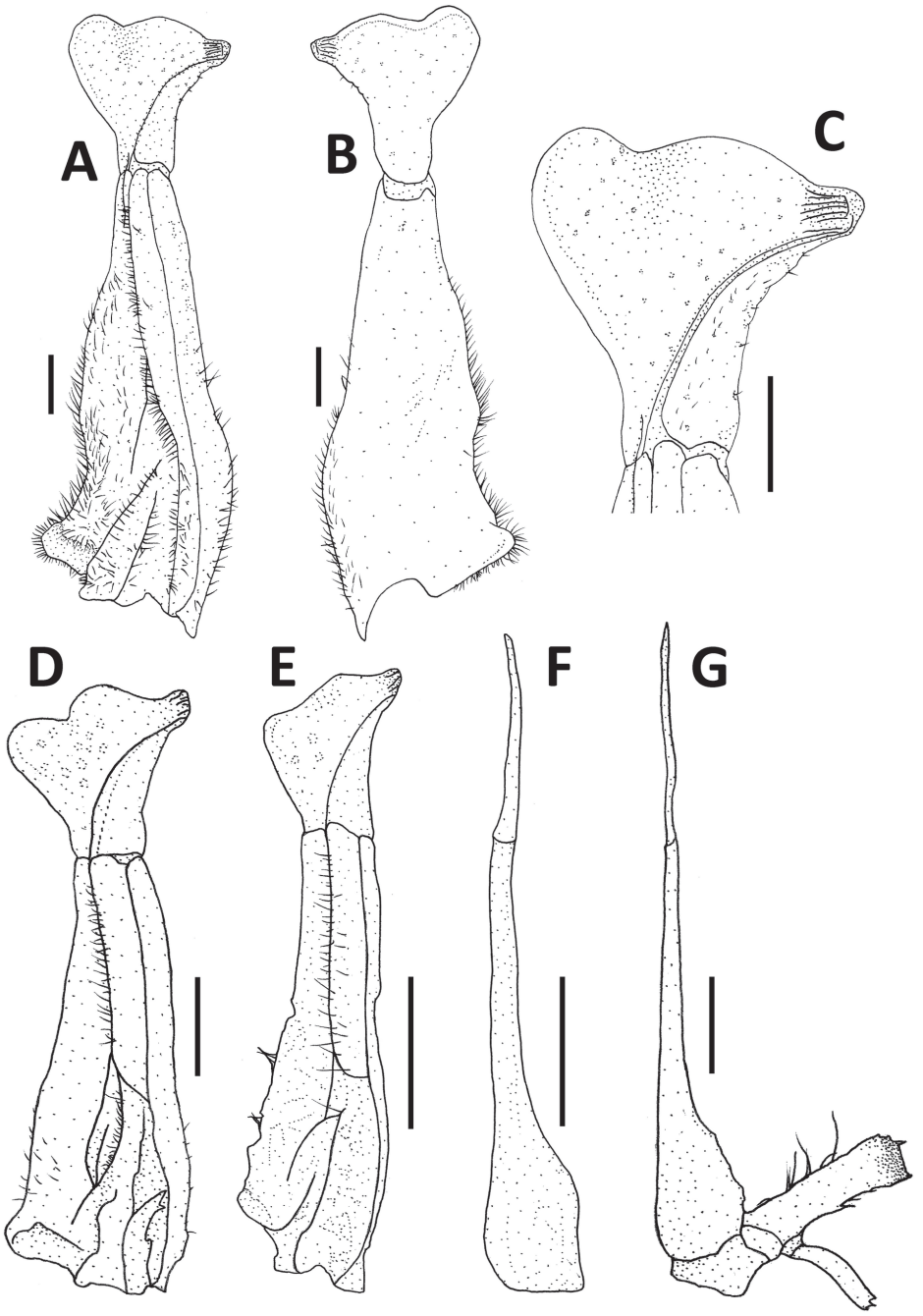

Figure 6. *Nanhaipotamon macau* sp. n., male holotype (37.4 × 30.9 mm), SYSBM 001649 (**A–C**); *Nanhaipotamon wupingense* Cheng, Yang, Zhong & Li, 2003, male neotype (22.4 × 18.3 mm), JX 050563 (**D–F**); *Nanhaipotamon guangdongense* Dai, 1997, male, (30.9 × 24.8 mm), SYSBM 001646 (**G**). Left G1, ventral view (**A, D, E**); left G1, dorsal view (**B**); Left G1 terminal segment, ventral view (**C**); Left G2, ventral view (**F, G**). Scale bar: 1.0 mm.

likely the result of a developmental abnormality and is an extremely rare occurrence (Gordon, 1963). The majority of brachyurans lack the male G2 exopod although it is being increasingly recognized as a normal feature among many pinnotherid crabs (Ahyong et al. 2012; Ng and Ho 2016).

Little was previously known about *N. guangdongense* as it was described from a single specimen without a precise locality. Attempts to sequence the DNA of *N. guangdongense* were unsuccessful, probably because of formalin fixation, compounding the problem of its identification (Shih et al. 2011). Huang et al. (2012) reported *N. guangdongense* from Zhuhai. Small differences in the G1 morphology, however, suggest the holotype of *N. guangdongense* was probably collected from another locality (Peter Ng pers. comm.). More recent collection efforts in Guangdong have found this species at multiple locations in Zhuhai, Zhongshan, and Jiangmen. Specimens from Gujing, Jiangmen (Fig. 7A–C) most closely resemble the holotype in G1 morphology suggesting that the holotype was probably collected from that area.

Normal and blue coloured *Nanhaipotamon* were sympatric at a locality in Xiangzhou, Zhuhai. *Nanhaipotamon zhuhaiense* Huang, Huang & Ng, 2012 was described based on only three blue specimens that had a distinctive G1 that pointed laterally and not anterolaterally as seen in the normal coloured comparative specimens. More recent collections from Xiangzhou, Zhuhai, however, have found a normal coloured specimen that has a laterally pointing G1 (Fig. 7E) and also a blue specimen that has an anterolaterally pointing G1 (Fig. 7F). Therefore, the colouration of the crab does not always correspond to a particular gonopod morphology. Specimens of intermediate G1 morphology have also been collected, while one uncollected female specimen was observed to be of intermediate colour. Furthermore, the COI K2P distances between the blue specimens SYSBM 001001 (GenBank no: MK226143), SYSBM001249 (GenBank no: MK226144) and the normal coloured specimen SYSBM 001015 (GenBank no: MK226145) are 1.23% and 0.77% respectively, which is of intraspecific level among closely related congeners. This new evidence strongly suggests that the normal and blue coloured crabs are different colour phases of the same species, but the G1 morphological differences between different specimens remains to be further studied. This seems to be a similar case to that of *N. hepingense* Dai, 1977, and *N. pinghense* Dai, 1977 (see Shih et al. 2011; Huang et al. 2012). Given that we are unable to confidently separate *N. zhuhaiense* from *N. guangdongense*, we regard them as probably conspecific, but refrain from making formal taxonomic changes until further detailed comparisons can be completed.

The G1 of specimens of *N. guangdongense* from different localities varies (Fig. 7). It is becoming increasingly evident that intraspecific variation of gonopodal morphology in some species of *Nanhaipotamon* is wider than previously recognized, while external differences are often hard to detect between species, making the taxonomy of this genus problematic (Figs 5C–E, 7; Huang et al., 2012: fig. 5; unpublished data). Clearly, there is need for a revision of this genus. To avoid compounding the problem in the future, we strongly recommend that new species of *Nanhaipotamon* should only be described when a large series of specimens is available to account for intraspecific variation.

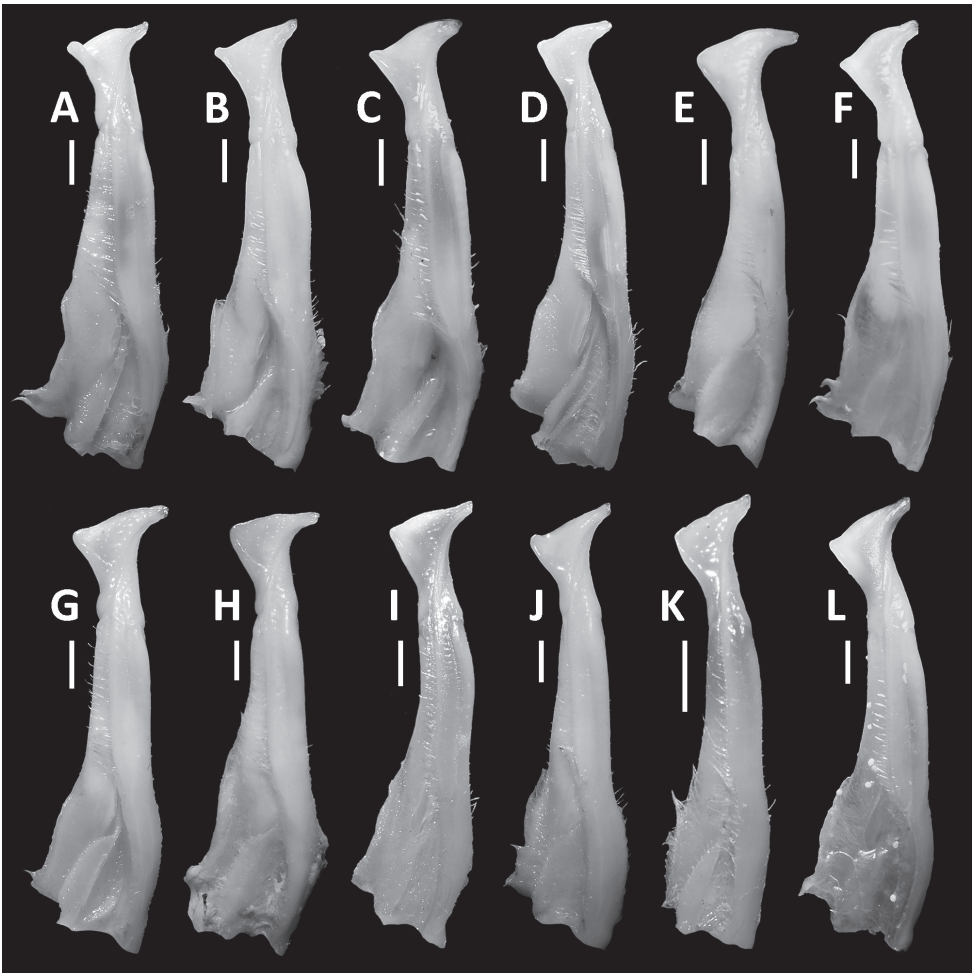

Figure 7. Comparison of G1 of *Nanhaipotamon guangdongense* Dai, 1997, from different localities. Male (38.4 × 31.5 mm), SYSBM 001141, Gujing, Jiangmen (**A**); male (40.8 × 32.2 mm), SYSBM 001142, Gujing, Jiangmen (**B**); male (36.7 × 29.4 mm), SYSBM 001143, Gujing, Jiangmen (**C**); male (35.4 × 29.4 mm), SYSBM 001177, Xiangzhou, Zhuhai (**D**); male (32.5 × 27.0 mm), SYSBM 001764, Xiangzhou, Zhuhai (**E**); male (40.1 × 32.7 mm), SYSBM 001758, Xiangzhou, Zhuhai (**F**); male (35.9 × 28.8 mm), SYSBM 001645, Coloane, Macau (**G**); male (45.5 × 37.0 mm), SYSBM 001656, Hengqin Island, Zhuhai (**H**); male (22.4 × 18.5 mm), SYSBM 001672, Jinwan, Zhuhai (**I**); male (33.4 × 26.5 mm), SYSBM 001017, Doumen, Zhuhai (**J**); male (36.9 × 30.4 mm), SYSBM 001657, Jinzhong Reservoir, Zhongshan (**K**); male (40.5 × 33.1 mm), SYSBM 001016, Qi'ao Island, Zhuhai (**L**). Scale bars: 1.0 mm.

Conservation status. *Nanhaipotamon guangdongense* was previously assessed as Data Deficient, being known from one unspecified location in Guangdong (Cumberlidge 2008). This species is sometimes collected for food and for the pet trade, though we are uncertain as to the extent. Nevertheless, this species has been found in many locations with a wider range than previously thought, having an extent of occurrence of around 2,400 km^2 (excluding sea area) and an area of occupancy of around 1,600

km^2. As such, we suggest the conservation status of this species under IUCN criteria would be more appropriate as Least Concern (LC). Nevertheless, *N. guangdongense* is quite rare in Macau, being found in only one location in the Ecological Pond of Grand Taipa, and thus may warrant local conservation attention.

Nanhaipotamon wupingense Cheng, Yang, Zhong & Li, 2003

Figs 6D–F, 8

Nanhaipotamon wupingense Cheng, Yang, Zhong & Li, 2003: 678, figs 1–8.

Type material. Neotype: JX 050563, male (22.4 × 18.3 mm), Xiaba (24.89N, 116.05E), Wuping county, Longyan City, Fujian Province, China, coll. X. M. Zhou, May 2007.

Other material examined. JX 050564, JX 050566, JX 050568–050569, 4 males (16.2 × 13.2 mm, 15.5 × 12.6 mm, 13.0 × 10.9 mm, 14.0 × 11.5 mm), same data as neotype. JX 050565, JX 050567, JX 050570–050576, 9 females (16.1 × 13.2 mm, 13.0 × 10.5 mm, 25.3 × 20.8 mm, 23.4 × 19.5 mm, 24.9 × 20.3 mm, 21.6 × 17.6 mm, 16.9 × 13.7 mm, 14.8 × 11.7 mm, 15.2 × 12.4 mm), same data as neotype.

Description. Carapace broader than long, width about 1.2 × length (n = 14); regions indistinct, dorsal surface convex; surface generally smooth, pitted, anterolateral region slightly rugose (Fig. 8A). Front deflexed, margin ridged in dorsal view (Fig. 8A). Epigastric cristae low, separated by narrow gap (Fig. 8A). Postorbital cristae sharp, laterally expanded, almost confluent with epibranchial teeth and epigastric cristae (Fig. 8A). Branchial regions slightly swollen (Fig. 8A, B). Cervical groove shallow (Fig. 8A). Mesogastric region slightly convex (Fig. 8A). External orbital angle sharply triangular, outer margin gently convex, separated from anterolateral margin by conspicuous gap (Fig. 8A, B). Epibranchial tooth small, granular, indistinct (Fig. 8A, B). Anterolateral margin cristate, lined with 17–20 granules, less distinct in some larger specimens; curved inward posteriorly (Fig. 8A). Posterolateral surface with low, oblique striae, converging towards posterior carapace margin (Fig. 8A). Orbits large; supraorbital, infraorbital margins cristate (Fig. 8B). Sub-orbital, pterygostomial and sub-hepatic regions covered with numerous rounded granules (Fig. 8B). Epistome posterior margin narrow; median lobe broadly triangular, lateral margins slightly sinuous (Fig. 8B).

Maxilliped III merus about as wide as long; ischium width about 0.7 × length; merus subtrapezoidal, with median depression; ischium subtrapezoidal, with distinct median sulcus, mesial margin rounded. Exopod reaching to proximal one-third of merus; flagellum short.

Chelipeds (pereiopod I) unequal (Fig. 8A); less inflated in females. Merus trigonal in cross section; margins crenulated, dorsal-outer surface granulated (Fig. 8A). Carpus with sharp spine at inner-distal angle, spinule at base (Fig. 8A). Major cheliped palm length about 1.3 × height (n = 1) in males, 1.3–1.4 × height (n = 4) in females; dactylus about 1.0 × palm length (n = 1) in males, 1.0–1.1 × palm length (n = 4) in females.

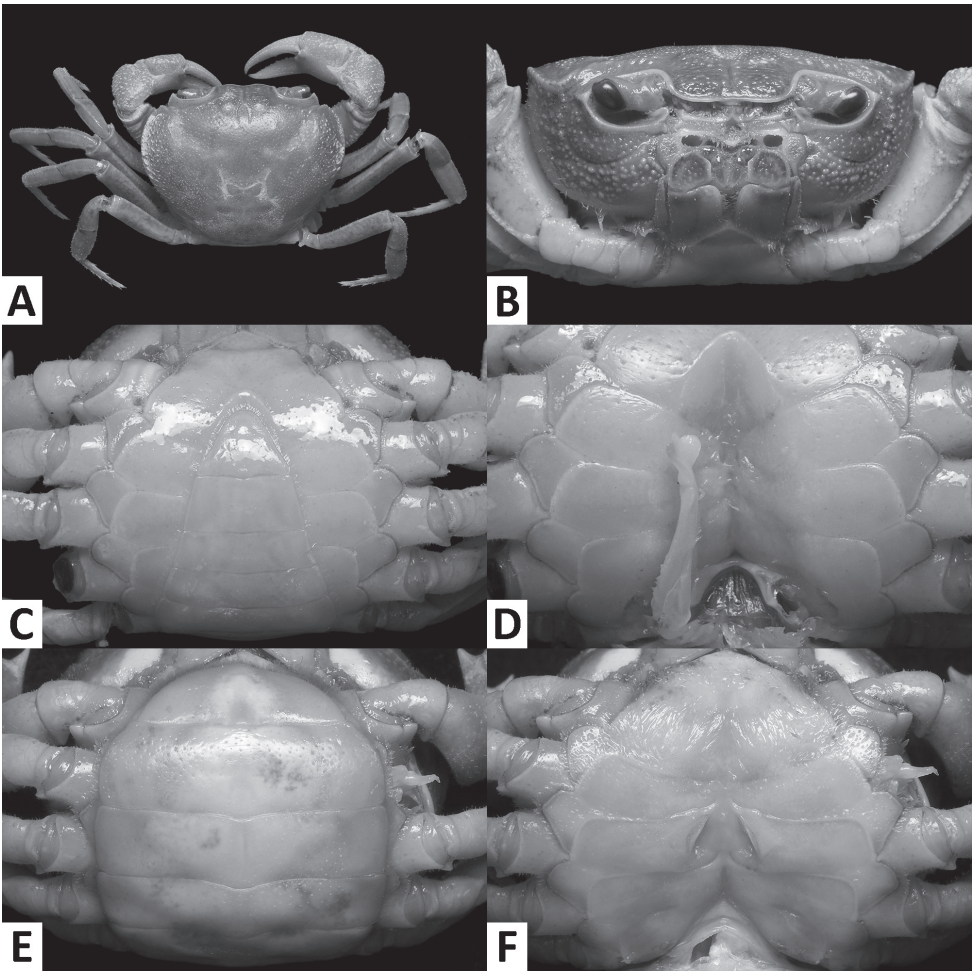

Figure 8. *Nanhaipotamon wupingense* Cheng, Yang, Zhong & Li, 2003, male neotype (22.4 × 18.3 mm), JX 050563 (**A–D**); female (25.3 × 20.8 mm), JX 050570 (**E–F**). Dorsal habitus (**A**); cephalothorax, anterior view (**B**); anterior thoracic sternum and pleon, ventral view (**C**); sterno-pleonal cavity with right G1 *in situ* (left G1 removed), ventral view (**D**); pleon, ventral view (**E**); vulvae, ventral view (**F**).

Palm surface pitted. Dactylus as long as pollex (Cheng et al. 2003: fig. 1). Occlusal margin of fingers with irregular blunt teeth; slight gape when closed.

Ambulatory legs (pereiopods II–V) slender, setae short, very sparse (Fig. 8A). Pereiopod III merus 0.6 × carapace length (n = 3) in males, 0.6–0.7 × carapace length (n = 7) in females (Fig. 8A). Pereiopods V propodus 2.3–2.4 × as long as broad in males (n = 3), 2.3–2.4 × as long as broad in females (n = 5), shorter than dactylus (Fig. 8A).

Male thoracic sternum generally smooth; anterior thoracic sternum (sternites I–IV) narrow, width about 1.5 × length; sternites I, II forming triangular structure; demarcation between sternites II, III complete; sternites III, IV fused with vestigial median suture (Fig. 8C). Male sterno-pleonal cavity reaching anteriorly beyond level

of posterior articular condyle of cheliped coxa (Fig. 8C); deep median longitudinal groove between sternites VII, VIII (Fig. 8D). Male pleonal locking tubercle positioned at mid-length of sternite V (Fig. 8D). Female vulva ovate, not reaching the sutures of sternites V/VI or VI/VII, positioned closely to one another (Fig. 8F).

Male pleon triangular, lateral margins almost straight; somites III–VI progressively narrower; somite VI width 2.1–2.2 × length (n=2); telson width 1.2–1.3 × length (n=2); apex rounded (Fig. 8C). Female pleon broadly ovate (Fig. 8E).

G1 slender; in-situ, tip of terminal segment exceeding pleonal locking tubercle, reaching suture between thoracic sternites IV/V (Fig. 8D, G1 not flat against the body); subterminal segment length about 2.7 × length of terminal segment; subterminal segment tapering posteriorly; terminal segment large, distally expanded, anterior margin laminar, convex anterior margin next to the tip high, tip blunt (Fig. 6D, E). G2 subterminal segment about 2.1 × length of flagelliform distal segment; exopod absent (6F).

Distribution. Currently only known from Xiaba, Wuping County, Longyan City, Fujian.

Remarks. The original description of *Nanhaipotamon wupingense* is brief and minimally illustrated (Cheng et al. 2003), neither describing nor figuring details of the carapace physiognomy and pterygostomial ornamentation, which are diagnostic differences between *N. wupingense* and *N. macau* sp. n. Although the gonopods of *N. wupingense* were described and figured, and were distinctive at the time of original description, they are similar to that to the newly discovered *N. macau* sp. n. As such the type account of *N. wupingense* could apply equally to *N. macau* sp. n. Unfortunately, the type material of *N. wupingense* is now lost: according to the first author of *N. wupingense*, the type material of *N. wupingense*, which was originally deposited in Fujian Research Institute of Parasite Disease, Fuzhou, Fujian Province, was lost during relocation (YZ Cheng, pers. comm.). Therefore, in order to fix the identity of *N. wupingense* and allow adequate characterization of both species, we hereby designate a neotype for *N. wupingense* in accordance to ICZN (1999: art. 75.3). The neotype of *N. wupingense* (male, 22.4 × 18.3 mm, JX 050563) and other examined specimens of the species were collected from the original type locality. The neotype G1 corresponds well to that originally described and figured for *N. wupingense*, although we note some minor differences in morphometrics compared to the original type description (Cheng et al. 2003). The G1 subterminal/terminal segment length ratio of *N. wupingense* is 3.0 according to Cheng et al. (2003), but, we measure the ratio at 2.7 in the neotype (Fig. 6D) and 2.6 based on the illustration of the G1 of the holotype (Cheng et al. 2003: fig. 7). The G2 subterminal/terminal segment length ratio of *N. wupingense* is inconsistently recorded in Cheng et al. (2003): 1.8 in the Chinese description, erroneously as 2.7 in the English abstract, and 2.0 if based on the figure of the holotype G2 (Cheng et. al. 2003: fig. 6). This ratio could not be measured for the neotype as the G2 terminal segment broke off inside the G1 during dissection, although the ratio in JX 050564, a sub-adult, is 2.2 (Fig. 6F). The G1 is not fully developed in this specimen (Fig. 6E).

Family Gecarcinucidae Rathbun, 1904
Genus *Somanniathelphusa* Bott, 1968

***Somanniathelphusa zanklon* Ng & Dudgeon, 1992**
Figs 2D, 9

Somanniathelphusa zanklon Ng & Dudgeon, 1992: figs 11–13.
Parathelphusa sinensis: Doflein 1902: 662.
Parathelphusa (*Parathelphusa*) *sinensis*: Gee 1925: 159; Wu 1934: 339.
Somanniathelphusa sinensis sinensis: Bott 1968b: 409, figs 11, 12, 30; Bott 1970a: 338; Bott 1970b: 111, pl. 20, figs 42–44; Ng, 1988: 105.
Somanniathelphusa sinensis: Dai 1999: 67, fig. 29, pl. 2.

Material examined. SYSBM 101001, 1 male (27.2 × 23.1 mm), Nanping (22.19N, 113.5E), Zhuhai City, Guangdong, reservoir, coll. C. Huang, April 2015. SYSBM 101002–101003, 2 males (38.8 × 31.9 mm, 30.4 × 25.6 mm), Jinding (22.38N, 113.54E), Zhuhai City, Guangdong, coll. local, May 2014. SYSBM 101004–101005, 2 males (42.0 × 33.5 mm, 34.2 × 28.1 mm), Sun Yat-sen University (23.10N, 113.30E), Guangzhou City, Guangdong, fish pond, coll. C. Huang, June 2013. SYSBM 101006, 1 female (37.1 × 29.5 mm), same data as above. SYSBM 101007, 1 male (30.6 × 24.5 mm), Coloane (22.12N, 113.56E), Macau, reservoir, coll. K.C. Wong, July 2008. SYSBM 101008, 1 male (28.2 × 22.5 mm), Coloane, Macau, reservoir, coll. K.C. Wong, July 2009. IACM, 1 male (24.2 × 19.8 mm), Coloane, Macau, reservoir, coll. K.C. Wong, February 2013. SYSBM 101009–101010, 2 males (19.5 × 16.8 mm, 19.2 × 16.4 mm), Shenzhen City (22.6N, 114.0E), Guangdong, coll. local, August 2015. SYSBM 101011, 1 female (19.6 × 16.4 mm), same data as above. SYSBM 101015–101016, 2 males (35.7 × 28.4 mm, 37.2 × 29.9 mm), Sihui City (23.12N, 113.56E), Guangdong, coll. local, August 2013. SYSBM 101017, 1 female (31.6 × 25.9 mm), same data as above. SYSBM 101018–101020, 3 males (38.2 × 30.8 mm, 35.4 × 28.1 mm, 28.3 × 21.3 mm), Renhua, Shaoguan City, Guangdong, coll. local, August 2013. SYSBM 101021, 1 male (31.5 × 26.6 mm), Lianhua Mountain, Shanwei City, Guangdong, coll. local, October 2013. SYSBM 101022, 1 female (27.3 × 23.2 mm), same data as above. SYSBM 101030, 1 male (39.4 × 33.0 mm), Heyuan City, Guangdong, coll. Z.C. Zhou, January 2014. SYSBM 101031, 1 female (32.4 × 27.3 mm), same data as above. SYSBM 101032–101035, 4 males (35.0 × 28.3 mm, 32.7 × 26.9 mm, 30.8 × 25.0 mm, 25.9 × 21.7 mm), Raoping, Chaozhou City, Guangdong, coll. Z.C. Zhou, January 2014. SYSBM 101036, 1 female (24.6 × 20.8 mm), same data as above. SYSBM 101037–101040, 4 males (26.3 × 20.4 mm, 30.9 × 25.8 mm, 26.6 × 23.0 mm, 27.0 × 22.5 mm), Wenzhou City, Zhejiang, coll. local, October 2013. SYSBM 101041, 1 female (29.8 × 24.6 mm), same data as above.

Colour in life. Generally brown overall; larger individuals may have dark markings near the cardiac region (Fig. 2D).

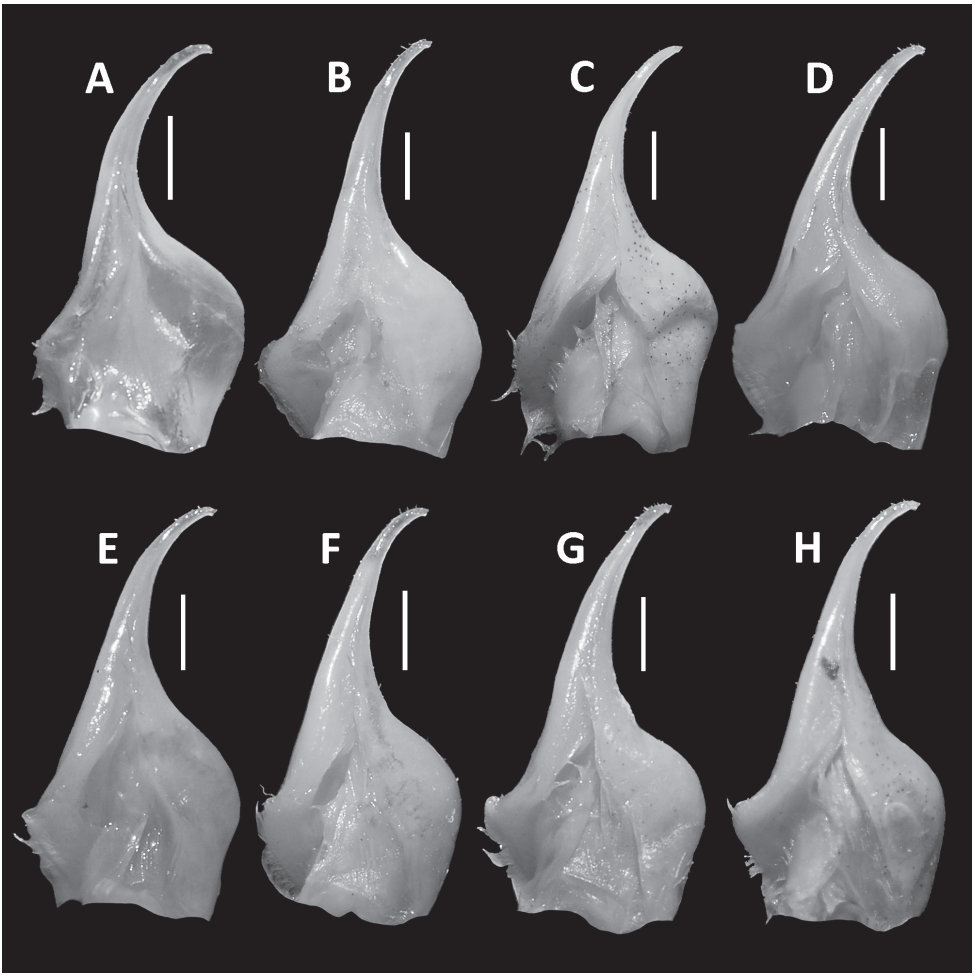

Figure 9. Comparison of G1 of *Somanniathelphusa zanklon* Ng & Dudgeon, 1992, from different localities. Male (30.6 × 24.5 mm), SYSBM 101007, Coloane, Macau (**A**); male (38.8 × 31.9 mm), SYSBM 101002, Jinding, Zhuhai City, Guangdong (**B**); male (42.0 × 33.5 mm), SYSBM 101004, Sun Yat-sen University, Guangzhou City, Guangdong (**C**); male (35.7 × 28.4 mm), SYSBM 101015, Sihui City, Guangdong (**D**); male (28.3 × 21.3 mm), SYSBM 101020, Renhua, Shaoguan City, Guangdong (**E**); male (31.5 × 26.6 mm), SYSBM 101021, Lianhua Mountain, Shanwei City, Guangdong (**F**); male (35.0 × 28.3 mm), SYSBM 101032, Raoping, Chaozhou City, Guangdong (**G**); male (26.3 × 20.4 mm), SYSBM 101037, Wenzhou City, Zhejiang (**H**). Scale bars: 1.0 mm.

Distribution. Coloane, Macau; Guangdong: Guangzhou City, Shenzhen City, Zhuhai City, Sihui City, Shaoguan City, Shanwei City, Heyuan City, Chaozhou City; Zhejiang: Wenzhou City.

Remarks. Ng and Dudgeon (1992) showed former records of *Somanniathelphusa sinensis* (H. Milne Edwards, 1853) from southern China (Bott 1968, 1970; Dai 1999) to represent a new species, *S. zanklon.* Shih et al. (2007) included *S. zanklon* from Hong Kong and Guangdong (Dongguan City and Nanhai City) and showed that specimens

of *Somanniathelphusa* from eastern Guangdong, Fujian and west-central Taiwan were all very closely related genetically, probably even conspecific. Specimens examined here from different localities were all very similar morphologically (Fig. 9), with those from Zhejiang Province having a slightly longer G1 distal part (Fig. 9H), though the overall shape is very much like the others. We tentatively treat all of these as the same species pending a full revision. Interestingly, Dai (1999) also reported the genus from Zhejiang, but none of the species of *Somanniathelphusa* in her monograph lists Zhejiang among its localities. The Chinese *Somanniathelphusa* are particularly problematic as many species look identical externally and were described based on minute differences that we find difficult to detect. Furthermore, being lowland species, they are readily dispersed by floods and are commonly found in aquaculture ponds where their newly hatched crablings are easily translocated. Preliminary genetic evidence suggests that the species diversity of *Somanniathelphusa* may have been overestimated (Shih et al. 2007).

Conservation status. *Somanniathelphusa zanklon* is currently assessed as Endangered (Esser and Cumberlidge 2008) as it was known from fewer than five locations in Hong Kong with a extant of occurrence less than 5,000 km^2, with degrading habitat quality. Our study, however, finds this species to have a widespread occurrence in south-east China with an area of occupancy estimated at over 120,000 km^2. Though habitat quality in some of these locations is declining, this resilient lowland species seems to be able to thrive in most water bodies that are not heavily polluted. As such, we find that *S. zanklon* does not satisfy any IUCN Red List threat categories and thus we suggest Least Concern would be a more appropriate determination at present. In Macau, all known occurrences of *S. zanklon* are from Hac-Sa Reservoir, Coloane, although it most likely also occurs in other water bodies in Coloane. There was an unconfirmed sighting of *S. zanklon* in Taipa a few years ago by the second author, though more recent surveys have failed to locate any specimens. There are three large water bodies on the Macau peninsula, of which only one reservoir on the east, next to Parque Municipal do Monte da Guia, which sources freshwater from the mainland, is suitable for lowland freshwater crabs. Although we did not survey this reservoir, it very likely also holds *S. zanklon* as this species was found in one of its water source reservoirs in Zhuhai. The other two water bodies, Sai Van Lake and Nam Van Lake, were once bays that have mostly been artificially closed off by landfill and currently hold sea water.

Acknowledgements

This project was partly funded by the PANGEA research centre student grants program (UNSW) to the first author. Special thanks are expressed to XM Zhou, JX Zou, and their students (Nanchang University) for assisting the first author in examining specimens at Nanchang University, and to ZC Zhou for his donations of several *Somanniathelphusa* specimens. We would also like to acknowledge H-T Shih for providing genetic sequences for use in this study, and to Tohru Naruse, Savel R. Daniels and the editors for greatly improving the manuscript.

References

Ahyong ST, Komai T, Watanabe T (2012) First *Viridotheres* Manning, 1996, from Japan, with a key to the species (Decapoda, Brachyura, Pinnotheridae). Studies in Malacostraca: a homage to Masatsune Takeda. Crustaceana Monographs 17: 35–47. https://doi.org/10.1163/9789004202894_003

Bott R (1968a) Potamiden aus Süd-Asien (Crustacea, Decapoda). Senckenbergiana biologica 49: 119–130.

Bott R (1968b) Parathelphusiden aus Hinterindien (Crustacea, Decapoda, Parathelphusidae). Senckenbergiana biologica 49: 403–422.

Bott R (1970a) Betrachtungen iiber entwicklungsgeschichte der Siisswasserkrabben nach der Sammlung des Naturhistorischen Museums in Genf/Schweiz. Revue Suisse (Zoologie) 77: 327–344. https://doi.org/10.5962/bhl.part.75900

Bott R (1970b) Dis Siisswasserkrabben von Europa, Asien, Australien und ihre Stammesgeschichte. Eine Revision der Potamoidea und Parathelphusoidea (Crustacea, Decapoda). Abhandlungen Senckenbergischen Naturforschenden Gesellschaft 526: 1–338.

Cheng YZ, Yang WC, Zhong YH, Li L (2003) A new species of the genus *Nanhaipotamon* (Decapoda: Potamid). Journal of Xiamen University (Natural Science) 42: 676–678.

Cumberlidge N (2008) *Nanhaipotamon guangdongense*. The IUCN Red List of Threatened Species 2008: e.T135072A4066344.

Dai AY (1997) A revision of freshwater crabs of the genus *Nanhaipotamon* Bott, 1968 from China (Crustacea: Decapoda: Brachyura: Potamidae). Raffles Bulletin of Zoology 45(2): 209–235.

Dai AY (1999) Fauna Sinica: Arthropoda Crustacea Malacostraca Decapoda Parathelphusidae Potamidae, Science Press, Beijing, 501 pp.

Davie PJ, Guinot D, Ng PKL (2015) Systematics and classification of Brachyura. In: Castro P, Davie PJF, Guinot D, Schram FR, Von Vaupel Klein JC (Eds) Treatise on zoology – anatomy, taxonomy, biology. The Crustacea 9C–I: 1049–1130. https://doi.org/10.1163/9789004190832_021

Doflein F (1902) Ostasiatische Dekapoden. Abhandlungen k. bayerischen Akademie Wissenschaft (2)21: 613–670. https://doi.org/10.1163/9789004190832_021

Esser L, Cumberlidge N (2008) *Somanniathelphusa zanklon*. The IUCN Red List of Threatened Species 2008: e.T134062A3888493.

Gee NG (1925) Tentative list of Chinese decapod Crustacea, including those represented in the collections of the United States National Museum (marked with an *) with localities at which collected. Lignan Agricultural Review 3: 156–166.

Gordon I (1963) An anomalous adult male spider crab with five pairs of pleopods. Crustaceana 5: 151–154. https://doi.org/10.1163/156854063X00426

Government of Macao Special Administrative Region Statistics and Census Service (2018) https://www.dsec.gov.mo/Statistic.aspx?NodeGuid=7bb8808e-8fd3-4d6b-904a-34fe4b302883

Huang C, Huang JR, Ng PKL (2012) A new species of *Nanhaipotamon* Bott, 1968 (Crustacea: Decapoda: Brachyura: Potamidae) from Zhuhai, Guangdong Province, China. Zootaxa 3588: 55–63.

Huang C, Shih HT, Ahyong ST (2017) *Cantopotamon* a new genus of freshwater crabs from Guangdong, China, with descriptions of four new species (Crustacea: Decapoda: Brachyura: Potamidae). Zoological Studies 56: 41. https://doi.org/10.6620/ZS.2017.56–41.

Kemp S (1918) Zoological results of a tour in the Far East. Decapod and stomatopod Crustacea. Memoirs of the Asiatic Society of Bengal 6(5): 221–297.

Kimura M (1980) A simple method for estimating evolutionary rates of base substitutions through comparative studies of nucleotide sequences. Journal of Molecular Evolution 16: 111–120. https://doi.org/10.1007/BF01731581

Milne Edwards H (1853) Observations sur les affinites zoologiques et la classification naturelle des Crustaces. Memoire sur la famille des Ocypodiens. Annales de Sciences Naturelle, Zoologie (3)20: 163–228.

Ng PKL, Dudgeon D (1992) The Potmidae and Parathelphusidae (Crustacea: Decapoda: Brachyura) of Hong Kong. Invertebrate Systematics 6(3): 741–768. https://doi.org/10.1071/IT9920741

Ng PKL, Ho PH (2016) *Orthotheres baoyu*, a new species of pea crab (Crustacea: Brachyura: Pinnotheridae) associated with abalones from Tungsha Island, Taiwan; with notes on the genus. Raffles Bulletin of Zoology 64: 229–241. https://doi.org/10.11646/zootaxa.4433.1.13

Shen CJ (1940) Four new species of Brachyura from Chinese seas. Journal of the Hong Kong Fisheries Research Station 1: 255–62.

Shih HT, Chen GX, Wang LM (2005) A new species of freshwater crab (Decapoda: Brachyura: Potamidae) from Dongyin Island, Matsu, Taiwan, defined by morphological and molecular characters, with notes on its biogeography. Journal of Natural History 39(31): 2901–2911. https://doi.org/10.1080/00222930500214010

Shih HT, Fang SH, Ng PK (2007) Phylogeny of the freshwater crab genus *Somanniathelphusa* Bott, (Decapoda: Parathelphusidae) from Taiwan and the coastal regions of China, with notes on their biogeography. Invertebrate Systematics 21(1): 29–37. https://doi.org/10.1071/is06007

Shih HT, Zhou XM, Chen GX, Chien IC, Ng PKL (2011) Recent vicariant and dispersal events affecting the phylogeny and biogeography of East Asian freshwater crab genus *Nanhaipotamon* (Decapoda: Potamidae). Molecular Phylogenetics and Evolution 58(3): 427–438. https://doi.org/10.1016/j.ympev.2010.11.013

Tamura K, Stecher G, Peterson D, Filipski A, Kumar S (2013) MEGA6: Molecular Evolutionary Genetics Analysis Version 6.0. Molecular Biology and Evolution 30: 2725–2729. https://doi.org/10.1093/molbev/mst197

ZooKeys 810: 113–126 (2018)
doi: 10.3897/zookeys.810.28457
http://zookeys.pensoft.net

RESEARCH ARTICLE

A peer-reviewed open-access journal
ZooKeys
Launched to accelerate biodiversity research

The economically important thrips from Malaysia, with a key to species (Thysanoptera, Thripinae)

Yong Foo Ng[1], J Saiful Zaimi[2]

1 *Centre for Insect Systematics (CIS), Universiti Kebangsaan Malaysia, 43600 Bangi, Selangor, Malaysia*
2 *Malaysian Agricultural Research and Development Institute, MARDI Cameron Highlands 39007 Tanah Rata, Pahang, Malaysia*

Corresponding author: *Yong Foo Ng* (ng_yf@ukm.edu.my)

Academic editor: *L. Mound* | Received 18 July 2018 | Accepted 10 October 2018 | Published 20 December 2018

http://zoobank.org/F6CF8990-E9F2-4B6D-B3D7-D6D34498BEEC

Citation: Ng YF, Zaimi JS (2018) The economically important thrips from Malaysia, with a key to species (Thysanoptera, Thripinae). ZooKeys 810: 113–126. https://doi.org/10.3897/zookeys.810.28457

Abstract

An illustrated key is provided to the economically important Thripinae (Thysanoptera) of Malaysia, together with a checklist and information on hosts and distributions. Information about the diversity and pest status for these Thripinae is provided, together with the prominent character states that are useful for recognising each species.

Keywords

Economically important, Malaysia, Thripinae, thrips, Thysanoptera

Introduction

Of the 6200 thrips species worldwide (ThripsWiki 2018), most of the economically important pest species are members of the subfamily Thripinae. Notorious for their broad range of hosts, members of this subfamily are small, pale to dark brown in colour, and often occur in large populations. The common injuries are fruit scarring and flower decolouration, which directly lowers the aesthetic value and market price of crops. Moreover, crops infested by thrips may be banned from importation into countries with strict biological quarantine procedures, such as USA, Australia, Japan, and European countries. Other indirect damages include the reduction of crop yields due to foliage and flower dropping caused by the insect's feeding activities. Several species

of Thripinae are also the only known vectors of important plant tospoviruses (Moritz et al. 2003), such as the Tomato Spotted Wilt Virus (TSWV), Impatiens Necrotic Spot Virus (INSV), and other tospoviruses as reported by Rotenberg et al. (2015). Members of Thripinae can be identified only with certainty after careful mounting onto microscope slides. Partly due to a lack of trained workers and quick identification keys, the pest management practices for these minute insects in Malaysian agriculture and horticulture industry have been impeded, compared to temperate countries where thrips are generally better studied. For instance, although commonly occurring in a wide range of ornamental flowers and vegetable crops, there has been no identification key to the range of species found on crops in Malaysia. This paper introduces the economically important pest species of the subfamily Thripinae recorded from Malaysia, together with an illustrated key to these common pests. A list of host plants and distributions for each species are also included, and information on morphology and biology is also explained wherever possible. A key to the 65 genera of Thripinae recorded from South East Asia was provided by Mound and Ng (2009), and a key to the 23 species of the genus *Thrips* recorded from Peninsular Malaysia was provided by Mound and Azidah (2009).

Material and methods

The specimens studied were obtained by field sampling in Malaysia. Methods used for collecting were by hand-searching and beating. Samples collected were processed onto permanent microscopic slides in Canada Balsam, after maceration in 5% NaOH and dehydration through a series of alcohols of 70%, 80%, 90% and absolute. These slides were then dried at 45 °C on a slide warmer, before being transferred into an oven for at least one month. All studied slides are deposited in the Centre for Insects Systematics (**CISUKM**), Universiti Kebangsaan Malaysia. Identifications and diagnoses were carried out with a differential interference contrast (DIC) microscope (Olympus BX41) as indicated in the photomicrographs that accompany the key provided here.

Results

Key to the economically important thrips from malaysia

1 Abdominal tergites with numerous rows of microtrichia (at least on the lateral third) (Fig. 10); antennae with 8 segments; body length usually about 1mm or shorter..... ***Scirtothrips dorsalis***
– Abdominal tergites without numerous rows of microtrichia (Figs 8, 9); antennae with 7 or 8 segments (Fig. 7); body length usually more than 1 mm.....**2**
2 Abdominal tergites VI–VIII with a pair of ctenidia laterally (Figs 8, 9) **3**
– Abdominal tergites VI–VII without a pair of ctenidia laterally **10**
3 Ocellar setae pair I present (Figs 1, 4, 5); Pronotal anterior margin with 1 or 2 pairs of long setae.....**4**

– Ocellar setae pair I absent (Figs 2, 3); Pronotal anterior margin without any pairs of long setae **6**

4 Tergite VIII of female without a posteromarginal comb of microtrichia; head with ocellar setae pair III close together and arising within ocellar triangle (Fig. 5) .... ***Frankliniella schultzei***

– Tergite VIII of female with posteromarginal comb of microtrichia; ocellar setae pair III arising just outside anterior margins of ocellar triangle (Fig. 4)..... **5**

5 Metanotum with a pair of campaniform sensilla (Fig. 17); postocular setae pair IV about as long as distance between hind ocelli ..... ***Frankliniella occidentalis***

– Metanotum without a pair of campaniform sensilla; postocular setae IV short, not longer than distance between hind ocelli (Fig. 4) ..... ***Frankliniella intonsa***

6 Abdominal tergites with triangular lobes of craspedum on posterior margin (Fig. 8); prosternal basantra with several setae (Fig. 13)..... ***Microcephalothrips abdominalis***

– Abdominal tergites without craspedum (cf. Fig. 9); prosternal basantra never with setae ... **7**

7 Ocellar setae II longer than setae III; postocular setae setae I and III usually long . ..... ***Stenchaetothrips biformis***

– Ocellar setae II longer than setae III; postocular setae setae I and III usually short ... **8**

8 Metanotal median setae arising far the behind anterior margin (Fig. 16); abdominal sternites IV–VI without discal setae (Fig. 12) ..... ***Thrips palmi***

– Metanotal median setae arising at anterior margin (cf. Fig. 17); abdominal sternites IV–VI with discal setae (Fig. 11) **9**

9 Postocular setae II stout, more than 0.5 as long as the distance between the bases of setae I and II (Fig. 2); forewing clavus apical setae usually as long as or longer than subapical (Fig. 19)..... ***Thrips hawaiiensis***

– Postocular setae II small, less than 0.5 as long as the distance between the bases of setae I and II (Fig. 3); forewing clavus apical setae usually shorter than subapical (Fig. 18) ..... ***Thrips florum***

10 Ocellar setae I absent; abdominal tergite VIII posterior margin with microtrichial comb present medially (Fig. 24) **11**

– Ocellar setae I present; abdominal tergite VIII posterior margin with or without microtrichial comb present medially (Fig. 24, 25) **12**

11 Pronotum without prominent postero-angular setae (Fig. 21); metafurcal spinula weak or absent (Fig. 14) ..... ***Dichromothrips corbetti***

– Pronotum with one pair of long postero-angular setae (Fig. 20); metafurcal spinula well developed (Fig. 15) ..... ***Dichromothrips smithi***

12 Abdominal tergite VIII posterior margin with microtrichial comb present medially (cf Fig. 24) ..... ***Ceratothripoides brunneus***

– Abdominal tergite VIII posterior margin without microtrichial comb medially (Fig. 25) **13**

13 Abdominal sternite VII posteromarginal setae arising in a row along posterior margin (Fig. 23); basal half antennal segments IV and V yellow (Fig. 6)..... ..... ***Megalurothips typicus***

– Abdominal sternite VII posteromarginal median setae arise in front of posterior margin (Fig. 22); antennal segments IV and V entirely brown (Fig. 7) .. ***Megalurothips usitatus***

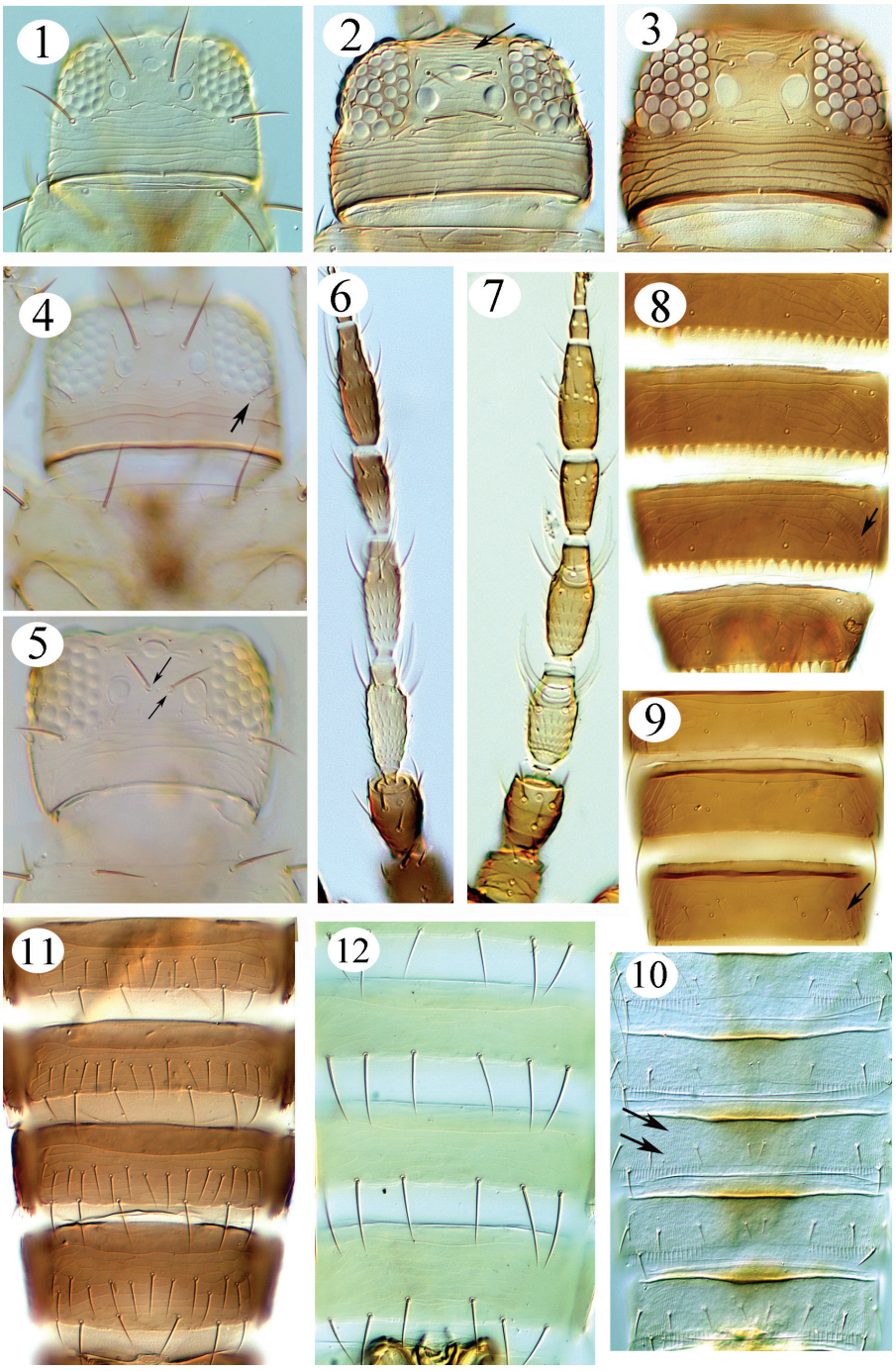

Figures 1–12. Head: **1** *Frankliniella occidentalis*, **2** *Thrips hawaiiensis*, **3** *Thrips florum*, **4** *Frankliniella intonsa*, **5** *Frankliniella schultzei*. Antenna: **6** *Megalurothips usitatus*, **7** *Megalurothrips typicus*. Abdominal tergite: **8** *Microcephalothrips abdominalis*, **9** *Thrips hawaiiensis*, **10** *Scirtothrips dorsalis*. Abdominal sternite: **11** *Thrips hawaiiensis*, **12** *Thrips palmi*.

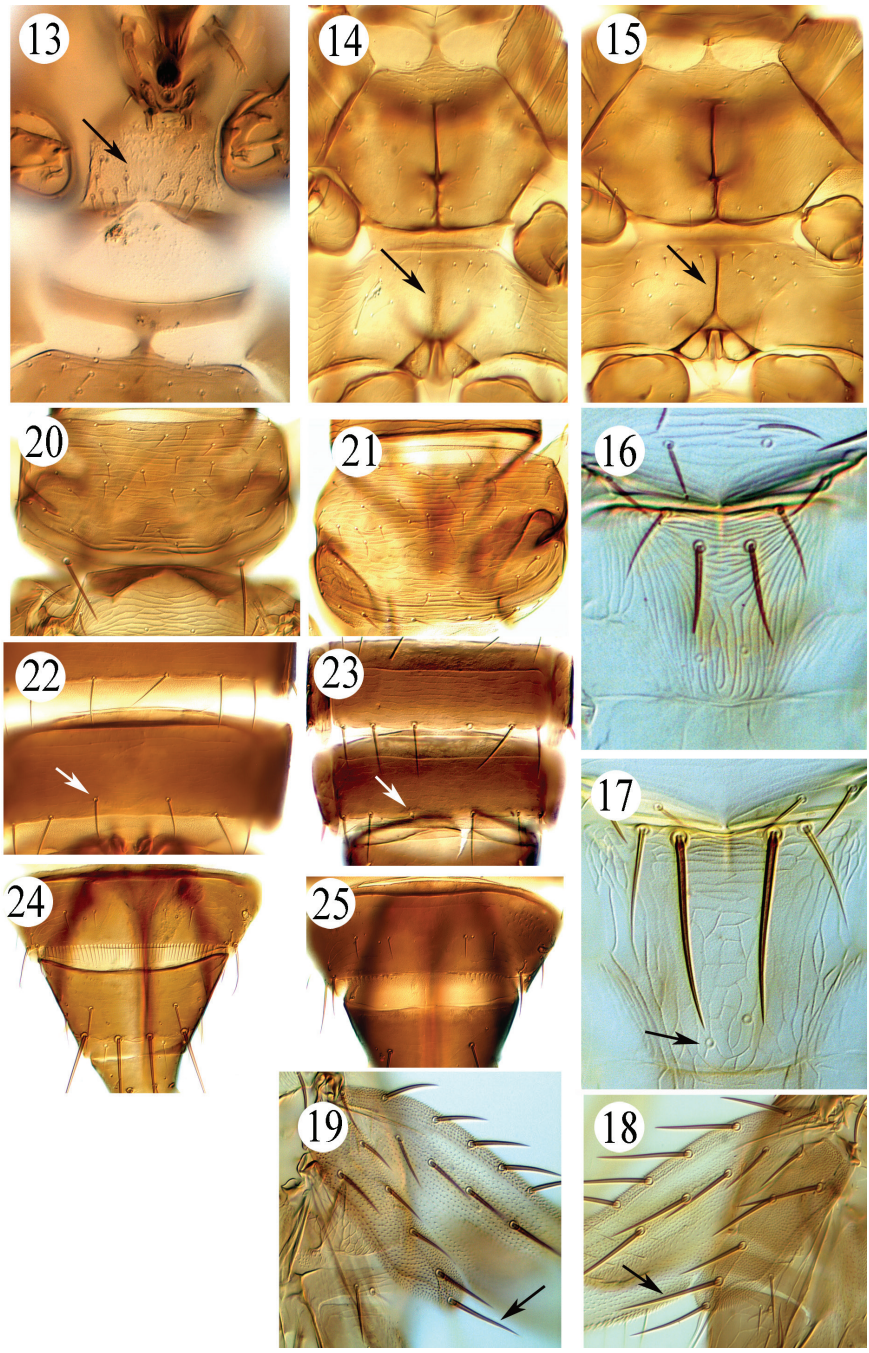

Figures 13–25. Prosternal basantra: **13** *Microcephalothrips abdominalis*. Meso- and Metasternum: **14** *Dichromothrips corbetti,* **15** *Dichromothrips smithi.* Metanotum: **16** *Thrips palmi*, **17** *Frankliniella occidentalis.* Forewing clavus: **18** *Thrips florum,* **19** *Thrips hawaiiensis.* Pronotum: **20** *Dichromothrips smithi,* **21** *Dichromothrips corbetti.* Abdominal sternite VII: **22** *Megalurothips usitatus,* **23** *Megalurothips typicus.* Abdominal tergite VIII: **24** *Dichromothrips corbetti*, **25** *Megalurothips typicus.*

Ceratothripoides brunneus Bagnall

Five species are recognized in this genus, all from the Old World (Mound and Nickle 2009), but only *C. brunneus* has been found in Malaysia. A closely related species, *C. claratris*, has been reported as a pest (Murai 2000) and vector of tospoviruses on tomatoes in Thailand (Halaweh and Poehling 2009). This species was not detected in our collections, nor was it reported during earlier surveys (Mound and Azidah 2009). The species *C. brunneus* is from Africa, but has been found recently in Peninsular Malaysia on a range of different plant species (Table 1).

Recognition: *Ceratothripoides brunneus* is a large brown species; body largely brown except fore tibiae and antennal segment III paler brown, forewing uniformly brown; abdominal segment VIII posterior margin with complete comb of microtrichia; mesonotum and metanotum without pair of campaniform sensilla; male abdominal sternites III–VII with many small pore plates; male abdominal tergite IX without drepanae. This species is similar in structure to the species of *Megalurothrips*, *Pezothrips*, *Odontothrips,* and *Odonthripiella*, and these share many characteristics including a pair of dorso-apical setae on the first antennal segment. In this paper, this species and the legume-flower thrips (*Megalurothrips*) are distinguished based on the microtrichial comb on abdominal tergite VIII. Recognition of *Ceratothripoides* is easy if males are available, because the sternites have numerous pore plates (Mound and Nickle 2009).

Dichromothrips corbetti (Priesner)

Species of the genus *Dichromothrips* are usually found on orchids. In Peninsular Malaysia, only two species have been recorded so far, although three further species are recorded from western Malaysia - *D. borneensis*, *D. nigricornis* and *D. major*. The species *D. corbetti* originated from the Oriental Region but is now introduced worldwide via cultivated orchids. It was described from *Vanda joaquim* in Kuala Lumpur (Mound 1976), but is known from a wide range of Orchidaceae including *Dendrobium* spp., *Arundina* spp., *Cattelya* spp., and *Vanda* spp. from various localities in lowland Malaysia (Table 1).

Recognition: Large and dark brown species, forewing base paler, tarsi and tibial apex yellow; antennal segments brown, segment III and IV with apices elongate. Pronotum without long posteroangular setae, and metafurcal spinula diffuse or weakly defined. These characters are useful in distinguishing the species from the other members of the genus.

Dichromothrips smithi (Zimmermann)

The original material of this species is apparently lost (Mound 1976), and the species is recognized based on female specimens from Taiwan identified by H. Priesner. Recently, it has been reported as an invasive species in US on bamboo orchids (*Arundina* spp.) from Malaysia, Thailand and Taiwan (Department of Agriculture and Plant In-

Table 1. List of economically important thrips, their host plants and distribution in Malaysia.

No.	Thrips species	Host plant		Distribution
		Family	**Species**	
1.	*Ceratothripoides brunneus*	Acanthaceae	*Strobilanthes crispus*	Pahang, Johor, Penang
		Apocynaceae	*Allamanda oenotheraefolia*	
		Lamiaceae	*Orthosiphon aristatus*	
		Rubiaceae	*Ixora* sp.	
		Verbenaceae	*Stachytarpheta mutabilis*	
2.	*Dichromothrips corbetti*	Orchidaceae	*Aracnis* sp.	Penang, Sarawak
			Arundina graminifolia	
			Cattelya spp.	
			Dendrobium spp.	
			Phalaenopsis spp.	
			Vanda spp.	
3.	*Dichromothrips smithi*	Orchidaceae	*Arundina graminifolia*	Pahang, Sarawak
4.	*Frankliniella intonsa**	Alliaceae	*Apapanthus campanulatus*	Cameron Highlands, Pahang
		Asteraceae	*Dahlia* sp.	
		Balsaminaceae	*Impatiens* sp. var. *wallerana*	
			Impatiens balsamina	
		Caryophyllaceae	*Gypsophila* sp.	
		Fabaceae	*Vigna sinensis var. sesquipedalis*	
		Iridaceae	*Gladiolus* sp.	
		Orchidaceae	*Arundina graminifolia*	
		Plantaginaceae	*Antirrhiinum* sp.	
		Rosaceae	*Fragraria ananassa*	
			Rosa sp.	
		Solanaceae	*Solanum melongena*	
		Verbenaceae	*Verbena* sp.	
5.	*Frankliniella occidentalis**	Alliaceae	*Agapanthus campanulatus*	Penang, Cameron Highlands
		Asteraceae	*Chrysanthemum morifolium*	
			Gerbera sp.	
			Tagetes sp.	
			Tanacetum parthenium	
		Iridaceae	*Gladiolus* sp.	
		Lamiaceae	*Salvia farinacea*	
		Plantaginaceae	*Antirrhinum* sp.	
		Rosaceae	*Rosa* sp.	
6.	*Frankliniella schultzei**	Euphorbiaceae	*Jatropha integerrima*	Melaka
		Nyctaginaceae	*Bougainvillea* sp.	
		Plumbaginaceae	*Plumbago auriculata*	
7.	*Megalurothrips usitatus*	Fabaceae	*Vigna sinensis*	Perak, Penang, Pahang, Selangor
		Fabaceae	*Erythrina fusca*	
		Malpighiaceae	*Tristellateia australasiae*	
8.	*Megalurothrips typicus*	Fabaceae	*Canavalia rosea*	Perak, Penang
		Moraceae	*Artocarpus champeden*	
		Passifloraceae	*Turnera ulmifolia*	
9.	*Microcephalothrips abdominalis*	Acanthaceae	*Pseuderanthemum carruthersii var. reticulatum*	Johor, Penang, Pahang
		Asteraceae	*Chrysanthemum indicum*	
			Cosmos sp.	
			Cosmos caudatus	
			Sphagneticola trilobata	

No.	Thrips species	Host plant		Distribution
		Family	Species	
	Microcephalothrips abdominalis	Asteraceae	*Tagetes patula*	Johor, Penang, Pahang
			Tridax procumbens	
		Heliconiaceae	*Heliconia* sp.	
		Orchidaceae	*Oncidium* sp.	
		Verbenaceae	*Clerodendrum paniculatum*	
10.	*Scirtothrips dorsalis**	Anacardiaceae	*Mangifera* sp.	Penang, Perak, Kedah, Terengganu, Melaka, Selangor
		Fabaceae	*Caesalpinia pulcherrima*	
		Fabaceae	*Cassia fistula*	
			Pithecellobium jiringa	
		Fabaceae	*Peliophorum pterocarpum*	
		Myrtaceae	*Psidium guajava*	
		Rosaceae	*Rosa alba*	
		Solanaceae	*Capsicum annuum*	
			Solanum torvum	
11.	*Thrips hawaiiensis*	Anacardiaceae	*Mangifera* sp.	Selangor, Pahang, Terengganu, Melaka
		Amaryllidaceae	*Hymenocallis speciosa*	
		Araceae	*Zantedeschia aethiopica*	
		Arecaceae	*Areca catechu*	
			Dahlia sp.	
		Asteraceae	*Aster dumosus*	
		Euphorbiaceae	*Jatropha integerrima*	
		Leguminosae	*Caesalpinia pulcherrima*	
		Myrtaceae	*Psidium guajava*	
		Nyctaginaceae	*Bougainvillea* sp.	
		Orchidaceae	*Arundina graminifolia*	
		Plantaginaceae	*Antirrhunum* sp.	
		Rosaceae	*Fragraria ananassa*	
			Prunus perisica	
			Rosa sp.	
		Verbenaceae	*Clerodendrum paniculatum*	
12.	*Thrips florum*	Apocynaceae	*Plumeria rubra*	Kedah, Penang
		Verbenaceae	*Clerodendrum paniculatum*	
			Lantana camara	
13.	*Thrips palmi**	Apocynaceae	*Allamanda oenotheraefolia*	Selangor, Pahang, Melaka
			Plumeria rubra	
		Asteraceae	*Chrysanthenum* sp.	
			Cosmos sulphurous	
			Sphagneticola trilobata	
			Tagetes sp.	
			Tagetes patula	
		Lamiaceae	*Salvia farinaceae*	
		Nyctaginaceae	*Bougainvillea* sp.	
		Orchidaceae	*Aracnis* sp.	
			Arundina graminifolia	
			Dendrobium spp.	
			Vanda spp.	
		Plumbaginaceae	*Plumbago auriculata*	
		Solanaceae	*Solanum torvum*	

*- Vector of Tospovirus (Mound 1996; Mound 2002; Rotenberg et al. 2015).

dustry Division 2010), and as a pest of orchids in Korea (Lee et al. 2002). There are specimens in the CSIRO collection, Canberra, Australia labelled as being associated with damage to Vanilla plants in India. In Malaysia, this species has been taken only from *Arundina graminifolia* (Bamboo orchid) from Pahang and Sarawak with its distribution restricted to highlands.

Recognition: This large, dark brown species is similar in body colour to *D. corbetti*. It is distinguished by the fore wing with the subapical area paler, the pronotum with long posteroangular setae, and the metafurcal spinula well developed.

Frankliniella intonsa Trybom

This species is known as the European Flower Thrips, due to its wide distribution in Europe, but it causes less damage to horticulture than *F. occidentalis*. Both species share many morphological characteristics, but *F. intonsa* can be recognized by the shorter postocular setae, and the absence of paired campaniform sensilla on the metanotum. Both species also seem to share similar habitats, such that they have been recorded in Peninsular Malaysia only from highlands, but from a wide range of flowers in various plant families, including Plantaginaceae, Alliaceae, Verbenaceae, Orchidaceae, and Asteraceae.

Recognition: Body colour brown, tibiae and tarsi yellow; antennal segments III and IV yellow; forewing pale with dark setae. All species of *Frankliniella* have the forewing first and second veins with complete setal rows, the head with ocellar setae pair I present, and the pronotum with four pairs of long major setae. Tergite VIII posterior margin with comb of microtrichia in females but not in males.

Frankliniella occidentalis (Pergande)

This species is known as the Western Flower Thrips, and although originally from the South Western states of the USA it is now found worldwide (Moritz et al. 2001). *Frankliniella* is the largest genus in the family Thripidae, with 230 species mostly from Central and South America. *F. occidentalis* has been collected commonly in the Cameron Highlands on many different flower hosts, including roses, orchids, daisy, and chrysanthemum. However, two specimens were collected from *Gerbera* sp. at Penang Butterfly Farm. The species is an important vector of Tomato Spotted Wilt Virus (TSWV) and Impatiens Necrotic Spot Virus (INSV). However, there are very few or perhaps no records of these viruses being transmitted among Malaysian crops.

Recognition: Body length about 1.5 mm (female), male is smaller about 1.0 mm in length. Body colour varies from yellow to brown, abdomen sometimes shaded medially in specimens from Malaysia, forewing pale yellow, femora and tibiae yellow; antennal segments III, IV and V basal half pale, segments II and VI–VIII dark brown. Pronotum anterior margin with two pairs of long setae, metanotal campaniform sensilla present. Tergite VIII posterior margin with comb of microtrichia in females but not in males.

Frankliniella schultzei (Trybom)

This species is widespread in tropical and sub-tropical countries. It is commonly collected in the lowlands of Peninsular Malaysia, breeding on flowers and leaves of many host plants. It has been sampled from flowers of *Bougainvillea* sp., *Jatropha integerrima*, and *Plumbago auriculata*. *Frankliniella schultzei* is an important vector of Tomato Spotted Wilt Virus (TSWV), although occasionally, it is a useful predator of mites on cotton (Milne and Walter 1997).

Recognition: This species apparently exists as two very different colour forms, with the body either brown or yellow. According Gikonyo et al. (2017) from the field surveys in Kenya indicate that the two colour forms of *F. schultzei* could be different species, of which, both showed distinct host preferences, lack of interbreeding and molecular differences. In general, *F. schultzei* is distinguished by the lack of ctenidia on abdominal tergite V, the position of ocellar setae pair III between the posterior ocelli, and the absence from the posterior margin of tergite VIII of a comb of microtrichia.

Megalurothrips usitatus Bagnall

This is the most common and widespread species of the genus in the Oriental area. It breeds in legume flowers and is an important pest on bean crops through feeding in the flowers in south China (Tang et al. 2015).

Recognition: Body colour brown; fore tibiae, apices of mid and hind tibiae yellow; antennal segment III slightly yellow, segment IV and V brown; antennal segments III and IV with apical constriction, segment VI unusually elongate; abdominal sternite VII posteromarginal setae S1 situated in front of posterior margin

Megalurothips typicus Bagnall

There are 13 species currently listed in *Megalurothrips*, but these are difficult to identify due to variation both within and between species. Correct identification of species in this genus requires morphological study and comparison of both sexes. In Peninsular Malaysia, only three species are reported: *M. typicus*, *M. mucunae*, and *M. usitatus*, and the latter species is the one most commonly collected on crops in both highlands and lowlands. Adults of *M. typicus* have been taken from Moraceae, Passifloraceae and Fabaceae, but with no reliable record of the host on which it breeds.

Recognition: This species is similar to *M. sjostedti*, the only species in this genus from Africa, but the colour of the forewing and antennae are different (Palmer 1987). *Megalurothrips typicus* is easy to distinguish from the other oriental *Megalurothrips* species, because all three pairs of posteromarginal setae on abdominal sternite VII arise at the posterior margin.

Microcephalothrips abdominalis (Crawford)

This sunflower thrips is widespread worldwide, and is the only species in the genus *Microcephalothrips*. In Peninsular Malaysia, adults of this species have been collected largely from the plant family Asteraceae from *Tagetes patula*, *Cosmos caudatus*, *Chrysanthemum indicum*, *Tridax procumbens*, and *Sphagneticola trilobata*. Other plant families from which adults have been taken include Heliconiaceae, Orchidaceae, and Acanthaceae.

Recognition: Body largely brown except fore tibiae, tarsi, and antennal segment III slightly paler. Based on morphology, it is related to the *Thrips* genus-group, because of the presence of a pair of ctenidia on abdominal segments V–VIII, but no other member of this group has setae on the prosternum (Figure 13). The triangular lobed craspedum on the abdominal tergites is very distinctive character of this species. Pronotum without any long setae, surface smooth without any fine transverse lines. Forewing usually curved and vein setae small.

Scirtothrips dorsalis Hood

This species is widespread from Pakistan to Japan, Taiwan, and northern Australia (Hoddle and Mound 2003), and is now introduced to the Caribbean area and Florida. *S. dorsalis* is known as a vector of Tospovirus, the species often becomes a pest of many different crops including vegetables and cut-flowers in Southeast Asia. It was also found infesting young leaves of 'Berembang' tree (*Sonneratia caseolaris*) in UKM's green house. This mangrove tree is the host to firefly, *Pteroptyx tener* from Peninsular Malaysia.

Recognition: This is amongst the smallest of species in the subfamily Thripinae, with the body of both sexes usually less than 1mm. Body yellow, with all femora, tibiae, and tarsi yellow; antennal segment I pale, segment II variable pale or slightly shaded, segments III–VIII brown; forewings pale yellow to light brown, with apex paler. Abdominal tergites and sternites IV–VII with median brown marking. An identification key to the species of this genus is available in Ng et al. (2014).

Stenchaetothrips biformis (Bagnall)

This Oriental rice thrips breeds on grasses including paddy, on which crop it is a pest in Philippines and Thailand. However, such infestation has not been reported in Malaysia. This thrips usually lives in moist places like in paddy field and grasses by the pond site.

Recognition: Body uniformly brown; antennal segments I–II dark, II paler at apex, III pale, IV slightly shaded, V–VII dark; all tibiae and tarsi pale; fore wing uniformly shaded. Metanotum with closely spaced striations, campaniform sensilla absent, median setae arising behind the anterior margin but varying in position. Meso- and metafurca each without a spinula. Male abdominal sternites III–VII with a transverse pore plate.

Thrips florum Schmutz

Identification of this species from its close relative, *T. hawaiiensis*, is not easy, and a third related species, *T. razanii*, was described recently from Peninsular Malaysia (Ng et al. 2010). For correct identification of these species it is essential that specimens are well-mounted onto slides. *Thrips florum* has not been reported as a severe pest in Malaysia's agriculture sector, but it has been collected from a wide range of flowers.

Recognition: Body colour brown; antennae brown except segment III yellow; legs yellow; forewing brown pale at base. Ocellar setae III arising outside ocellar triangle; postocular seta II much shorter than setae I and III. Mesonotum without sculpture lines near campaniform sensilla; metanotum with many lines at the anterior and laterally. Forewing clavus apical seta usually shorter than subapical seta. This species is very similar to both *T. hawaiiensis* and *T. razanii*, and comparisons are given in Ng et al. (2010). More discussion is available in Palmer (1999).

Thrips hawaiiensis (Morgan)

This is the most common and abundant species of the genus *Thrips* in Peninsular Malaysia, and is found on a wide range of cultivated plants in various families including Asteraceae, Apocynaceae, and Fabaceae. It is considered the pollinator of oil palm trees, but is reported as a pest of roses in Georgia, citrus in India, coffee and mangoes in Thailand, and banana in Australia (Palmer 1999).

Recognition: Body colour brown or bicoloured with head and pronotum paler than brown abdomen. Antennal segment III yellow, segments IV and V usually brown or paler at base; legs yellow; forewing paler at base. More discussion about the variation of this species is available in Palmer (1999) and Ng et al. (2010). A key to the species of *Thrips* genus from Peninsular Malaysia was published by Mound and Azidah (2009).

Thrips palmi Karny

This species is a common pest in Malaysia and also many other Southeast Asian countries. It is a vector of plant tospovisuses, but it can also cause severe feeding damage to the leaves of crops such as eggplant and capsicum (Tan et al. 2016).

Recognition: Body colour pale yellow; antennae 7-segmented, segments I and II pale yellow, other segments light brown. The species is easy to distinguish from most *Thrips* species because of the complete posteromarginal comb on abdominal tergite VIII and the lack of discal setae on abdominal sternites. In Malaysia, the species has been taken from crops including *Capsicum*, *Cucumis* and *Solanum* (Mound & Azidah, 2009), as well as species of Rubiaceae.

Acknowledgements

We would like to thank Dr. Laurence Mound for editing and suggestions that improved this manuscript. A special thank also to the reviewers for their invaluable comments. The study of Malaysian thrips (Thysanoptera) is funded by the Ministry of Science, Technology and Innovation (MOSTI) via research grant 06-01-02-SF0540 and Malaysia Toray Science Foundation via research grant STGL-002-2008.

References

Department of Agriculture and Plant Industry Division, The State of Hawaii (2010) Report to the Twenty-Fifth Legislature Regular Session of 2010: Report On the Fight Against Invasive Species for the Period of July 1, 2007 – June 30, 2008 & July 1, 2008 – June 30, 2009.

Halaweh N, Poehling H-M (2009) Inheritance of vector competence by the thrips *Ceratothripoides claratris* (Shumsher) (Thysanoptera: Thripidae). Journal of Applied Entomology 133: 386–393. https://doi.org/10.1111/j.1439-0418.2008.01357.x

Hoddle MS, Mound LA (2003) The genus *Scirtothrips* in Australia (Insecta, Thysanoptera, Thripidae) Zootaxa 268:1–40. https://doi.org/10.11646/zootaxa.268.1.1

Gikonyo MW, Niassy S, Moritz GB, Khamis FM, Magiri E, Subramanian S (2017) Resolving the taxonomic status of *Frankliniella schultzei* (Thysanoptera: Thripidae) colour forms in Kenya – a morphological-, biological-, molecular- and ecological-based approach. International Journal of Tropical Insect Science 37(2): 57–70. https://doi.org/10.1017/S1742758416000126

Lee GS, Ahn KS, Woo KS (2002) New record of *Dichromothrips smithi* (Zirmemann) (Thysanoptera: Thripidae) injurious to Orchidaceae in Korea. Journal Asia-Pacific Entomology 5(2): 155–160. https://doi.org/10.1016/S1226-8615(08)60146-6

Tang LD, Yan KL, Fu BL, Wu JH, Kui L, Lu YY (2015) The life table parameters of *Megalurothrips usitatus* (Thysanoptera: Thripidae) on four leguminous crops. The Florida Entomologist 98(2): 620–625. https://doi.org/10.1653/024.098.0235

Ministry of Agriculture and Agro-based Industry Malaysia (MOA) 2008: Annual Report: Ministry of Agriculture and Agro-based Industry Malaysia.

Milne M, Walter GH (1997) The significance of prey in the diet of the phytophagous thrips, *Frankliniella schultzei*. Ecological Entomology 22: 74–81. https://doi.org/10.1046/j.1365-2311.1997.00034.x

Moritz G, Kumm S, Mound LA (2003) Tospovirus transmission depends on thrips ontogeny. Virus Research 100: 143–149. https://doi.org/10.1016/j.virusres.2003.12.022

Mound LA, Ng YF (2009) An illustrated key to the genera of Thripinae (Thysanoptera) from South East Asia. Zootaxa 2265: 27–47.

Mound LA, David AN (2009) The Old-World genus Ceratothripoides (Thysanoptera: Thripidae) with a new genus for related New-World species. Zootaxa 2230: 57–63.

Mound LA, Azidah AA (2009) Species of the genus *Thrips* (Thysanoptera) from Peninsular Malaysia, with a checklist of recorded Thripidae Zootaxa 2023: 55–68.

Mound LA (2002) So many thrips-so few tospoviruses? In: Marullo R, Mound LA (Eds) Thrips and Tospoviruses. Proceedings of the 7th. International Symposium on Thysanoptera. Australian National Insect Collection, Canberra, 15–18.

Mound LA (1996) The thysanoptera vector species of tospoviruses. Acta Horticulturae 431: 298–309. https://doi.org/10.17660/ActaHortic.1996.431.26

Mound LA (1976) Thysanoptera of the genus *Dichromothrips* on Old World Orchidacea. Biological Journal of the Linnean Society 8: 245–265. https://doi.org/10.1111/j.1095-8312.1976.tb00248.x

Murai T (2000) Damage to tomato by *Ceratothripoides claratris* (Shumsher) (Thysanoptera: Thripidae) in central Thailand and a note on its parasitoid, *Goetheana shakespearei* Girault (Hymenoptera: Eulophidae). Applied Entomology and Zoology 35:505–507. https://doi.org/10.1303/aez.2000.505

Ng YF, Eow LX, Mound LA (2010) A new species of genus *Thrips* (Thysanoptera, Thripinae) from flowers in Peninsular Malaysia. Zootaxa 2638: 65–68.

Ng YF, Mound LA, Azidah AA (2014) The genus *Scirtothrips* (Thysanoptera: Thripidae) in Malaysia, with four new Species and comments on *Biltothrips*, a related genus. Zootaxa 3856(2): 253–266. https://doi.org/10.11646/zootaxa.3856.2.6

Palmer JM (1987) *Megalurothrips* in the flowers of tropical legumes: a morphometric study. In: Holman J, Pelikan J, Dixon AFG, Weismann L (Eds) Population structure, genetics and taxonomy of aphids and *Thysanoptera*. SPB Academic Publishing, The Hague, 480–495.

Palmer JM (1992) *Thrips* from Pakistan to the Pacific: a review. Bulletin of the British Museum of Natural History (Entomology) 61: 1–76.

Rotenberg D, Jacobson AL, Schneweis DJ, Whitfield AE (2015) Thrips transmission of tospoviruses. Current Opinion in Virology 15: 80–89. https://doi.org/10.1016/j.coviro.2015.08.003

Tan JL, Ooi PAC, Khoo G (2016) Thrips on eggplant, chilli and bell pepper in Cameron Highlands, Malaysia. Serangga 21(1): 71–85.

ThripsWiki (2018) ThripsWiki – providing information on the World's thrips. Available from: http://thrips.info/wiki/Main_Page [Accessed 13.vii.2018]

ZooKeys 810: 127–138 (2018)
doi: 10.3897/zookeys.810.28887
http://zookeys.pensoft.net

SHORT COMMUNICATION

A peer-reviewed open-access journal
ZooKeys
Launched to accelerate biodiversity research

Evidence of cryptic species in the blenniid *Cirripectes alboapicalis* species complex, with zoogeographic implications for the South Pacific

Erwan Delrieu-Trottin[1], Libby Liggins[2,3], Thomas Trnski[3], Jeffrey T. Williams[4], Valentina Neglia[1], Cristian Rapu-Edmunds[5], Serge Planes[6,7], Pablo Saenz-Agudelo[1]

1 *Instituto de Ciencias Ambientales y Evolutivas, Universidad Austral de Chile, Valdivia, Chile* **2** *Institute of Natural and Mathematical Sciences, Massey University, Auckland, New Zealand* **3** *Auckland War Memorial Museum, Tāmaki Paenga Hira, Auckland, New Zealand* **4** *Division of Fishes, Department of Vertebrate Zoology, National Museum of Natural History, Smithsonian Institution, Suitland, MD USA* **5** *Mike Rapu Diving Center, Caleta Hanga Roa O'tai, Isla de Pascua, Chile* **6** *PSL Research University: EPHE-UPVD-CNRS, USR 3278 CRIOBE, Université de Perpignan, Perpignan Cedex, France* **7** *Laboratoire d'Excellence "CORAIL", Papetoai, Moorea, French Polynesia*

Corresponding author: *Erwan Delrieu-Trottin* (erwan.delrieu.trottin@gmail.com)

Academic editor: *D. Morgan* | Received 5 August 2018 | Accepted 9 October 2018 | Published 20 December 2018

http://zoobank.org/E4E66F6A-17C2-4A91-B528-BD940A50045B

Citation: Delrieu-Trottin E, Liggins L, Trnski T, Williams JT, Neglia V, Rapu-Edmunds C, Planes S, Saenz-Agudelo P (2018) Evidence of cryptic species in the blenniid *Cirripectes alboapicalis* species complex, with zoogeographic implications for the South Pacific. ZooKeys 810: 127–138. https://doi.org/10.3897/zookeys.810.28887

Abstract

Rapa Nui, commonly known as Easter Island (Chile), is one of the most isolated tropical islands of the Pacific Ocean. The island location of Rapa Nui makes it the easternmost point of the geographic ranges for many western Pacific fish species that are restricted to the subtropical islands south of 20°S latitude. The blenniid fish species *Cirripectes alboapicalis* has been thought to have one of the most extensive geographic distribution ranges among these southern subtropical fish species, extending from the southern Great Barrier Reef to Rapa Nui. A phylogenetic analysis was conducted to determine the taxonomic status of the species. The results provide genetic evidence that suggests that this formerly South Pacific-wide species comprises at least three cryptic species with allopatric geographic distributions. The analyses reveal the geographic distributions of these clades and their genetic relationships with each other, and with other species within the genus *Cirripectes*. The processes that culminated in the current geographic distribution of this species complex and the zoogeographic implications of this finding for the South Pacific region are discussed.

Keywords
Austral Islands, Blenniidae, cryptic species, cytochrome oxidase I, Easter Island, endemism, French Polynesia, Gambier Islands, Kermadec Islands, mtDNA, Phylogeny, Rangitāhua, Rapa Nui

Introduction

The Indo-Malay-Philippines Archipelago is the hotspot of species richness for reef fishes in the Indo-Pacific region (Carpenter and Springer 2005), a richness that tends to decline with distance from this hotspot (Bellwood and Wainwright 2002; Connolly et al. 2003; Allen 2008; Briggs 2009). Accordingly, the high latitude and remote island of Rapa Nui (Easter Island, Chile), located on the eastern border of the South Pacific region, hosts one of the lowest levels of species richness reported for coral reef fishes, with only 139 shore fish species (Randall 1976; Randall and Cea 2011; Friedlander et al. 2013). The isolation of Rapa Nui has also resulted in a high proportion of endemic species (almost 22 %) (Randall and Cea 2011). The location of Rapa Nui (south of 20°S latitude) makes it the easternmost point of the geographic ranges for many subtropical Pacific fish species. These species are often either narrow-range endemics restricted to only a couple of subtropical islands of the south Pacific (e.g., *Itycirrhitus wilhelmi* found only around Rapa Nui and Pitcairn Islands), or they may be widespread and occur at most of the subtropical islands south of 20°S latitude from the southern Great Barrier Reef to Rapa Nui (e.g., *Anampses femininus*). However, understanding the contribution of other South Pacific locations, and Rapa Nui's own isolation, to its fish species richness and endemism is not easily answered through examination of species ranges alone. Phylogenetic analysis can provide complementary information regarding the evolutionary history of species that, together with their geographic distribution, can shed light on the origin and distribution of regional species richness.

The blenniid fish species *Cirripectes alboapicalis* (Ogilby 1899) has apparently one of the most extensive geographic distributional ranges among the southern subtropical fish species, extending from the southern Great Barrier Reef (type locality at Lord Howe Island) eastwards to Rapa Nui (Williams 1988). The taxonomic history of the Rapa Nui population of this species has not been straightforward; the first specimens collected were described as a subspecies (*Cirripectes variolosus patuki* (De Buen 1963)) and later elevated to the species level by Springer (1970). Williams (1988), co-author of the present study, placed the Rapa Nui endemic *C. patuki* in the synonymy of *C. alboapicalis* in his revision of the genus *Cirripectes*. The development of analytical techniques in molecular biology provides a new tool to explore taxonomic diversification and the geographic distributions of lineages at the population level and among closely-related species (Avise 2000). Given the unusually broad distribution of this subtropical species of blenny, the high level of reef fish endemism at Rapa Nui, and the taxonomic history of this species, phylogenetic analyses were conducted to evaluate the taxonomy of *C. alboapicalis* and understand the processes that shaped its geographic distribution.

Material and methods

Specimen collection. Recent expeditions enabled collection of *Cirripectes* cf. *alboapicalis* specimens from Rangitāhua-Kermadec Islands (LL and TT in 2015), Gambier Islands (EDT, JTW, SP in 2010), Austral Islands (EDT, JTW, SP in 2013), and Rapa Nui (EDT, VN, ECG, CRE, PSA in 2016 and 2018), while additional expeditions to the Marquesas Islands (EDT, JTW, SP) and Manuae-Scilly (JTW, SP in 2014) allowed us to collect comparative tissue samples, resulting in a total of 43 specimens of *Cirripectes* spp. for this analysis (Table 1). A variety of collecting techniques were used (Hawai'ian slings, rotenone, clove oil and hand nets). Tissues were preserved in 96% EtOH at ambient temperature.

Molecular analyses. To conduct our genetic analysis, whole genomic DNA was extracted from fin clips preserved in 96% EtOH. DNA extraction was performed using GeneJet Genomic DNA purification kit (Thermo Fisher Scientific) or the DNeasy Blood & Tissue Kit (Qiagen), according to manufacturer's protocols. A fragment of the mitochondrial gene coding for cytochrome C oxidase subunit I (COI) was amplified with the primers designed by Ward et al. (2005). PCR amplifications and sequencing were performed following the protocol of Williams et al. (2012). A 650 base-pair fragment was sequenced from each of the 43 specimens of *Cirripectes* spp. and compared with COI sequences of congeners obtained from GenBank and BOLD, with a representative of the Labrisomidae used as the outgroup (Table 1). The closest relatives of *C. alboapicalis* based on morphology are two species with very restricted distributions: *Cirripectes obscurus* (Borodin 1927), a Hawai'ian endemic species; and *Cirripectes viriosus* (Williams 1988), endemic to the Batan Islands of Philippines (northernmost islands of the Philippines) (Figure 1). We included *C. obscurus* in our study, as we collected a single specimen that was morphologically consistent with this species in the Australs; unfortunately no tissues were available from *C. viriosus* for this study. All sequences are deposited in GenBank (Table 1) and metadata uploaded to the Genomics Obervatory Metadatabase (GeOMe) (Deck et al. 2017).

Two tree-building methods were used to construct branching diagrams. First a Neighbor-joining (NJ) analysis based on the Kimura 2-parameter (K2P) model of sequence evolution (Kimura 1980) was conducted using the software package MEGA 6 (Tamura et al. 2013). Confidence in topology was evaluated by a bootstrap analysis with 1000 replicates (Felsenstein 1985). Second, a Maximum Likelihood (ML) analysis was performed using IQ-TREE (Minh et al. 2013, Nguyen et al. 2015) using the IQTREE Web Server (http://iqtree.cibiv.univie.ac.at). The best model of evolution for each partition was informed with ModelFinder (Kalyaanamoorthy et al. 2017) implemented in IQ-TREE prior to the construction of the ML tree. To assess branch support, the IQ-TREE analysis used the ultrafast bootstrap approximation (UFboot) with 1000 replicates (Minh et al. 2013) and the SH-like approximate likelihood ratio test (SH-aLRT) also with 1000 bootstrap replicates (Guindon et al. 2010). To visualize the relationships between haplotypes of *Cirripectes alboapicalis* and *C. obscurus* among the different sampling localities, a haplotype network was constructed using the haplonet

Table 1. Specimens collected for this study.

Species	Geographic locality	Voucher number	GenBank number
Cirripectes "patuki"	Rapa Nui	RN1	MH932003
	Rapa Nui	RN2	MH932004
	Rapa Nui	RN3	MH932005
	Rapa Nui	RN4	MH932006
	Rapa Nui	RN5	MH932007
Cirripectes sp. n.	Austral Islands	AUST-400	MH707846
	Austral Islands	AUST-549	MH707848
	Gambier Islands	GAM-511	MH707849
	Gambier Islands	GAM-508	MH707847
	Austral Islands	AUST-550	MH707850
	Austral Islands	AUST-546	MH707855
Cirripectes "alboapicalis"	Kermadec Islands	Kermadecs447	MH932008
	Kermadec Islands	Kermadecs448	MH932009
Cirripectes fuscoguttatus	Austral Islands	AUST-157	MH707851
	Austral Islands	AUST-397	MH707852
	Austral Islands	AUST-156	MH707853
Cirripectes jenningsi	Austral Islands	AUST-547	MH707854
Cirripectes quagga	Austral Islands	AUST-165	MH707856
	Scilly Island	SCIL-193	MH707857
	Austral Islands	AUST-403	MH707859
	Austral Islands	AUST-536	MH707861
	Gambier Islands	GAM-099	MH707863
	Gambier Islands	GAM-110	MH707858
	Gambier Islands	GAM-109	MH707864
	Austral Islands	AUST-402	MH707865
	Austral Islands	AUST-537	MH707860
	Austral Islands	AUST-168	MH707862
Cirripectes variolosus	Austral Islands	AUST-052	MH707867
	Gambier Islands	GAM-144	MH707873
	Austral Islands	AUST-164	MH707881
	Gambier Islands	GAM-143	MH707869
	Gambier Islands	GAM-145	MH707879
	Gambier Islands	GAM-794	MH707876
	Gambier Islands	GAM-737	MH707874
	Gambier Islands	GAM-793	MH707877
	Austral Islands	AUST-162	MH707870
	Austral Islands	AUST-163	MH707880
	Scilly Island	SCIL-194	MH707875
	Scilly Island	SCIL-252	MH707866
	Austral Islands	AUST-056	MH707868
	Marquesas Islands	MARQ-071	MH707872
	Marquesas Islands	MARQ-074	MH707871
	Marquesas Islands	MARQ-073	MH707878

function of the package "pegas" (Paradis 2010) in the R statistical environment (R Core Team 2017). Finally, estimates of Net Evolutionary Divergence (NET) between the different groups of sequences observed were computed using the software package MEGA 6 (Tamura et al. 2013) and were conducted using the K2P model (Kimura 1980).

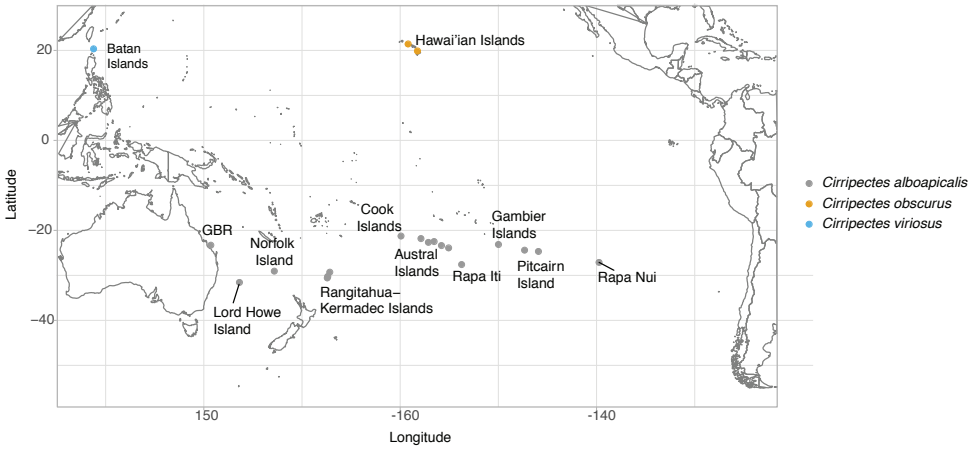

Figure 1. Geographic distribution of *Cirripectes alboapicalis*, *Cirripectes obscurus,* and *Cirripectes viriosus*

Results and discussion

Molecular data were examined for 11 of the 23 valid species of the genus *Cirripectes* and included *C. obscurus*, one of the two hypothesized closest relatives of *C. alboapicalis* (based on color and morphological characters). Both the NJ and the ML analyses resulted in identical tree topologies and reveal three well-supported and highly divergent clades among the *C. alboapicalis* specimens. Clade 1 is composed of specimens from Rangitāhua-Kermadec Islands, Clade 2 of specimens from the Australs and Gambier Islands, while specimens from Rapa Nui form Clade 3 (Figure 2). The Clade 2 (Australs - Gambier) appears more closely related to the sister species *Cirripectes obscurus* than to the two other *C. alboapicalis* clades (Rangitāhua clade and Rapa Nui clade). The results from the haplotype network corroborate our phylogenetic results, as *C. alboapicalis* haplotypes form three highly divergent haplogroups. A single haplotype (from two specimens) is found in Rangitāhua and is separated by 23 mutations from a second haplogroup comprising sequences from Rapa Nui. A third haplogroup is found in the Gambier and Austral Islands and is separated by 86 mutations from the Rapa Nui haplogroup. Interestingly, the sister species, *C. obscurus*, is positioned between Clades 2 and 3 (Figure 3). Net divergence estimates ranged from 3.7 % (Clade 1–Clade 3) to 9.2 % (Clade 1–Clade 2) among the three *C. alboapicalis* clades. In contrast, net divergence between the three *C. alboapicalis* clades and *C. obscurus* ranged from 7.4 % to 7.9%. *C. alboapicalis* is thus composed of three lineages that are on different evolutionary trajectories.

Our molecular analysis reveals the existence of at least three cryptic species within the single species previously referred to as *Cirripectes alboapicalis*. In recent years, molecular studies have been combined with morphological methods and these integrated studies have led to the discovery of many new species (e.g., Baldwin et al. 2011; Delrieu-Trottin et al. 2014; and Williams and Viviani 2016). Our results provide strong justification for a detailed morphological analysis to identify diagnostic morphological

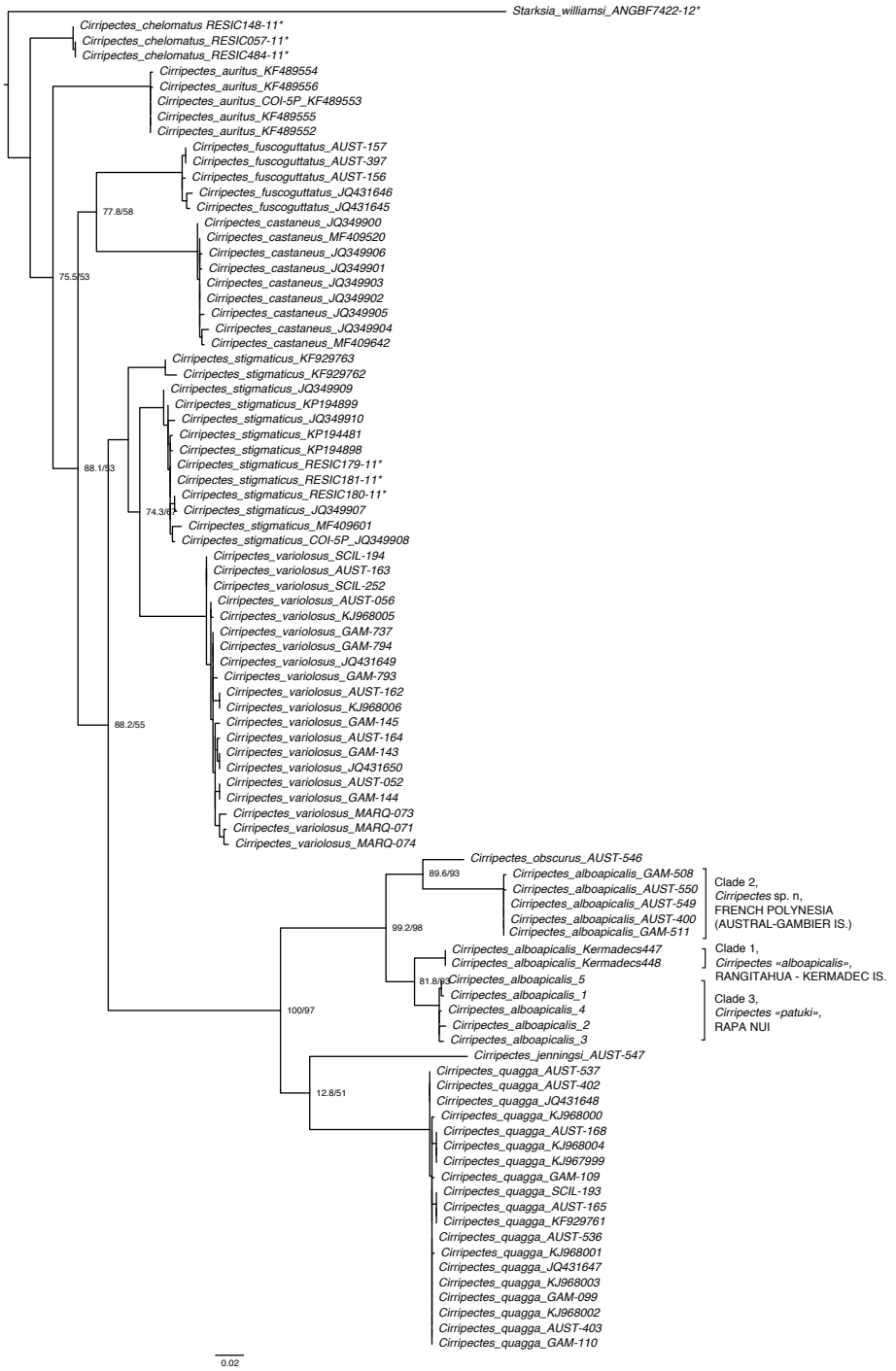

Figure 2. Maximum Likelihood tree for COI sequences with sequences representative of the maximum number of species retrieved from GenBank and BOLD. GenBank numbers are reported while BOLD numbers are denoted with an asterisk (*). Nodes show UFboot and SH-aLRT.

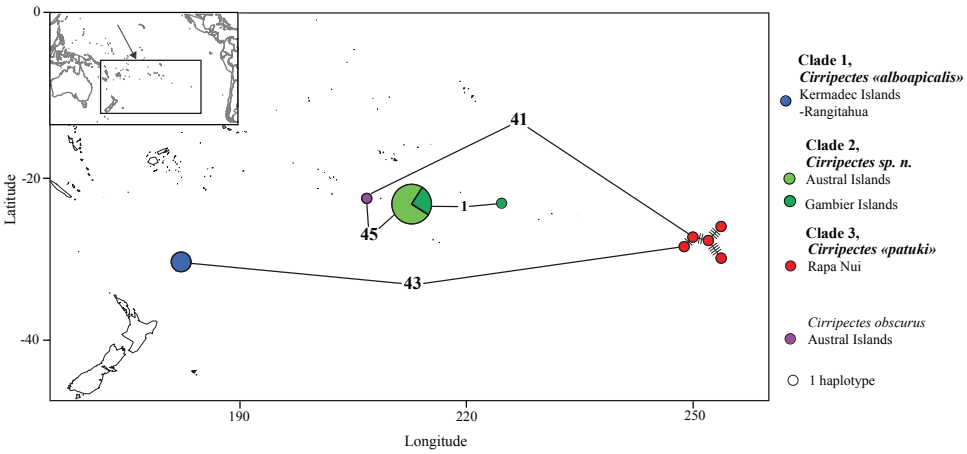

Figure 3. Haplotype network for the *Cirripectes alboapicalis* complex. COI sequences for *Cirripectes alboapicalis* from Austral Islands (Maria and Rurutu), Gambier Islands, Rangitāhua-Kermadec Islands (Raoul Island) and Rapa Nui. Sequence for *C. obscurus* from Austral Islands. Each circle corresponds to a unique sequence (i.e., haplotype); size of the circle indicates the frequency of the haplotype.

characters that may distinguish the genetically divergent species within *C. alboapicalis*. Williams (1998) did not have the advantage of being able to directly compare specimens of each lineage and might easily have overlooked subtle morphological characters that might now support a morphological diagnosis of each species in addition to the genetic differentiation. A thorough morphological analysis is needed to compare the voucher specimens from each genetic lineage and to examine fresh coloration to find distinguishing characters for the three species (Figure 4).

Given that the holotype of *C. alboapicalis* is from Lord Howe Island, the species name *alboapicalis* might be retained for Clade 1 as Rangitāhua is nearest to Lord Howe Island, unless further genetic investigation suggests that Rangitāhua also harbors a distinct lineage of *C. alboapicalis.* A new name will be needed for the specimens from the Australs and Gambier Islands (Clade 2) through a formal description, while the species name *patuki* should be elevated from synonymy and attributed to the Rapa Nui population (Clade 3) provided that morphological, coloration, or other diagnostic genetic characters are found. However, such a formal species description is beyond the scope of the current study.

Results of the present study have implications for the historical zoogeography of *Cirripectes* and the historical biogeography of the region. The discovery of a specimen morphologically consistent with *C. obscurus* in the Austral Islands suggests that this species is also present in the South Pacific, outside of the Hawai'ian Islands. Although there are no publicly available COI sequences for the Hawai'ian *C. obscurus* in GenBank or BOLD, a search in the BOLD database using the identification tool (searching both public and private projects; Ratnasingham and Hebert 2007) estimated that our COI sequence for the *C. obscurus* from the Austral Islands was 99.84 % similar to sequences from three Hawai'ian *Cirripectes* larvae. Corroborating this notion that

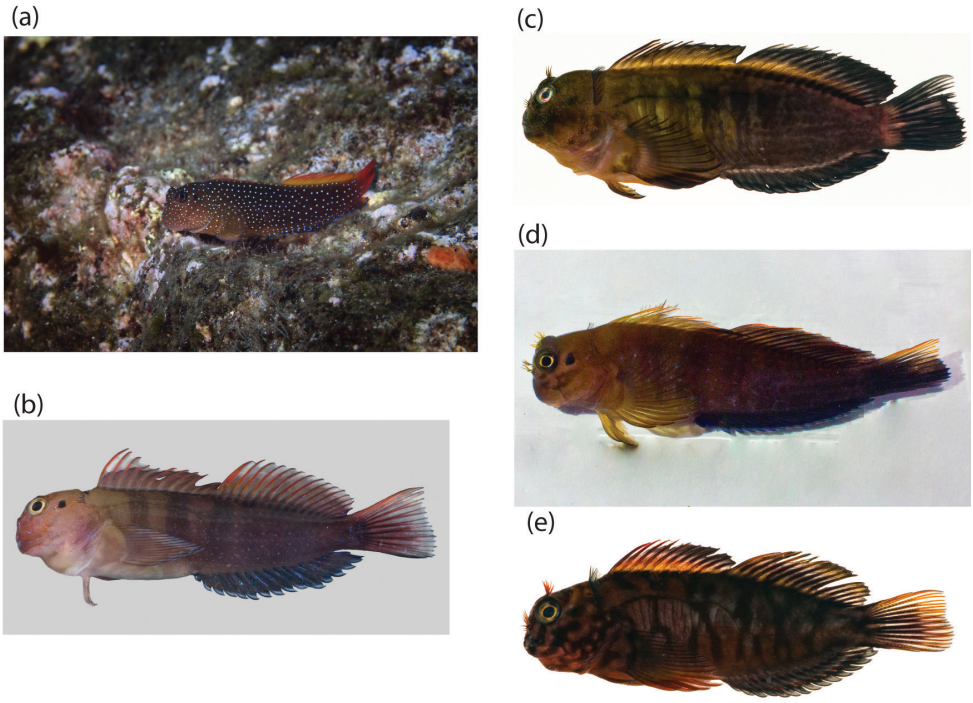

Figure 4. Pictures of specimens from the three genetic clades of this study; **a** live colors (photograph by Richard Robinson (www.depth.co.nz)) and **b** freshly dead colors (photograph by Carl Struthers Museum of New Zealand Te Papa Tongarewa) of Clade 1 from Rangitāhua - Kermadec Islands **c** Clade 2, French Polynesia from Austral - Gambier Islands (photographs by Jeffrey T. Williams) **d** Clade 3 Rapa Nui (photograph by Erwan Delrieu-Trottin); and **e** *Cirripectes obscurus* (photograph by Jeffrey T. Williams).

C. obscurus may not be a Hawai'ian endemic, but has an antitropical distribution (as defined by Hubbs (1952) and Randall (1981)), Williams (1988) also identified a potential *C. obscurus* specimen in the Cook Islands. Nonetheless, the rarity of such *C. obscurus* specimens in our collections from the South Pacific raises questions about the size of this southern population.

The full extent of the geographic distribution of the three clades identified in the blenniid *Cirripectes alboapicalis* species complex is unclear, as genetic samples from several locations across the range of this species complex are presently not available (e.g., Rapa Iti, Pitcairn Islands, Norfolk Island), and more importantly none from the type locality, Lord Howe Island. Nonetheless, the geographic distribution of the clades may follow general biogeographic patterns observed in other South Pacific species possessing a Rapa Nui population. Randall and Cea (2011) describe 17 southern subtropical fish species present in Rapa Nui including *C. alboapicalis*. Of these species, the muraenid *Gymnothorax porphyreus* has the broadest distribution, from the southern Great Barrier Reef (GBR) to South of Chile, while an additional six species have continuous ranges between the southern GBR and Rapa Nui (Table 2). The remaining 10 species have either a very restricted distribution (e.g., *Itycirrhitus wilhelmi*,

Table 2. List of subtropical reef fish species that are present in Rapa Nui, and their geographic distribution (following Randall and Cea 2011). From east to west - NSW: New South Wales, S.GBR: Southern Great Barrier Reef, LH: Lord Howe Island, Nor: Norfolk Island, NC: New Caledonia, N.NZ: Northern New Zealand, R-K: Rangitāhua-Kermadec Islands, A: Austral Islands, G: Gambier Islands, Rapa: Rapa Iti, Pit.: Pitcairn, RN: Rapa Nui, JFer: Juan Fernandez, SanF: San Felix (Desventuradas Islands), Chile. Total: the total number of locations where the species is present. The three colors for *Cirripectes alboapicalis* denote the different genetic clades (see Figure 3), and grey in this row indicates the locations where the clade affinities are unknown.

Species	NSW	S. GBR	LH	Nor	NC	N. NZ	R-K	A	G	RI	Pit	RN	JFer	SanF	Chile	Total
Cirripectes alboapicalis	1	1	1	1			1	1	1	1	1	1				10
Gymnothorax porphyreus			1	1	1	1	1			1		1	1	1	1	10
Anampses femininus	1	1	1		1			1	1	1	1	1				9
Bodianus unimaculatus	1	1	1	1		1	1			1		1				8
Enchelycore ramosa	1		1	1		1	1			1		1				7
Trachypoma macracanthus	1		1	1		1	1									5
Centropyge hotumatua								1		1	1	1				4
Aseraggodes bahamondei			1	1			1					1				4
Priolepis psygmophilia							1			1		1				3
Gymnothorax nasuta										1	1	1				3
Itycirrhitus wilhelmi											1	1				2
Goniistius plessisi											1	1				2
Chrysiptera rapanui							1					1				2
Bathystethus orientale										1		1				2

Goniistius plessisi, *Centropyge hotumatua*) or disjunct distributions with populations in both Rangitāhua-Kermadec and Rapa Nui regions (e.g., *Aseraggodes bahamondei*, *Priolepis psygmophilia*, *Chrysiptera rapanui*, see Table 2). This distribution pattern is identified as the Pitcairn-Kermadec "Province" by Rehder (1980) and includes Rapa Nui, Pitcairn, Rapa Iti, and the Rangitāhua-Kermadec Islands. Interestingly, our results suggest that the Rangitāhua-Kermadec and the Rapa Nui clades are closely related. The closest relatives of several Rapa Nui endemic species are endemic species of Rangitāhua (e.g., *Acanthistius fuscus* and *A. cinctus*, *Girella nebulosa* and *G. fimbriata*). It is thus highly likely that both the Kermadec and the Rapa Nui clades have very restricted distributions and emerged via an allopatric process following a chance colonization.

Acknowledgements

We thank Rebeca Tepano, Nina, Taveke Olivares Rapu, Liza Garrido Toleado (SERNAPESCA), Ludovic Tuki (Mesa del Mar), and the people of the Rapa Nui Island for their kind and generous support. Collections from Rangitāhua-Kermadec Islands were made possible by the *RV Braveheart* crew (Stoney Creek Shipping Company Ltd.), with support from the Auckland Museum Institute, Massey University, the Pew Charitable Trusts, and in collaboration with Natural History New Zealand. We are grateful for the support of Rangitāhua mana moana, the Māori iwi Ngāti Kuri and Te

Aupōuri and fieldwork help from J. David Aguirre, Phil Ross, and Sam McCormack. We thank Tea Frogier and Pierre Mery for their support of the Coralspot project at the Gambier Archipelago. The Coralspot expedition was funded by the "Contrat de projet Etat-Polynésie", by the ANR "IMODEL" and the French Ministry for Environment, Sustainable Development and Transport (MEDDTL). The Austral Islands expedition was part of the Global Reef Expedition and the work presented here is based in part on specimens collected in the Austral Islands made possible due to the support of the Khaled bin Sultan Living Oceans Foundation. We are grateful to Pierre Sasal, Tom Cribb, René Galzin and Michel Kulbicki, for their field assistance in the Gambier and the Austral Islands, along with the crew of the *Claymore II* and of the *Golden Shadow*. E. Delrieu-Trottin was supported by FONDECYT Postdoctorado fellowship N°3160692 and P. Saenz- Agudelo by the FONDECYT Iniciación fellowship N°11140121. L. Liggins was supported by a Rutherford Foundation Postdoctoral Fellowship. The authors declare no conflict of interest. All applicable institutional guidelines for the care and use of animals were followed. Specimens were collected in Rapa Nui under permit No. 1042, March, 21th 2018 obtained from the Chilean Subsecretary of Fishing, and No. 13270/24/162/Vrs., March, 29th 2018 obtained from Armada de Chile; Servicio Hidrografico y Oceanografico. Specimens were collected in Kermadec Islands under Authorization number: 47976-MAR from the New Zealand Department of Conservation. The Universidad Austral de Chile Ethical Care Committee and Biosecurity Protocol approved our use and handling of animals. Finally, we thank M. Erdmann for constructive comments on an earlier version of the manuscript.

References

Allen GR (2008) Conservation hotspots of biodiversity and endemism for Indo-Pacific coral reef fishes. Aquatic Conservation: Marine and Freshwater Ecosystems 18: 541–556. https://doi.org/10.1002/aqc.880

Avise JC (2000) Phylogeography: The History and Formation of Species. Harvard University Press.

Baldwin CC, Castillo CI, Weigt LA, Victor BC (2011) Seven new species within western Atlantic *Starksia atlantica*, *S. lepicoelia*, and *S. sluiteri* (Teleostei, Labrisomidae), with comments on congruence of DNA barcodes and species. ZooKeys: 79: 21–72. https://doi.org/10.3897/zookeys.79.1045

Bellwood DR, Wainwright PC (2002) The History and Biogeography of Fishes on Coral Reefs. In: Sale PS (Ed.) Coral Reef Fishes: dynamic and diversity in a complex ecosystem. Elsevier, San Diego, 5–32. https://doi.org/10.1016/B978-012615185-5/50003-7

Borodin NA (1927) A new blenny from the Hawaiian Islands. American Museum Novitates 281: 1–2.

Briggs JC (2009) Diversity, endemism and evolution in the Coral Triangle. Journal of Biogeography 36: 2008–2010. https://doi.org/10.1111/j.1365-2699.2009.02146.x

De Buen F (1963) Los peces de la Isla de Pascua. Bol de la Soc de Biol de Concepcion 35: 3–80.

Carpenter KE, Springer VG (2005) The center of the center of marine shore fish biodiversity: The Philippine Islands. Environmental Biology of Fishes 72: 467–480. https://doi.org/10.1007/s10641-004-3154-4

Connolly SR, Bellwood DR, Hughes TP (2003) Indo-pacific biodiversity of coral reefs: Deviations from a mid-domain model. Ecology 84: 2178–2190. https://doi.org/10.1890/02-0254

Deck J, Gaither MR, Ewing R, Bird CE, Davies N, Meyer C, Riginos C, Toonen RJ, Crandall ED (2017) The Genomic Observatories Metadatabase (GeOMe): A new repository for field and sampling event metadata associated with genetic samples. PLoS Biology. https://doi.org/10.1371/journal.pbio.2002925

Delrieu-Trottin E, Williams JT, Planes S (2014) *Macropharyngodon pakoko*, a new species of wrasse (Teleostei: Labridae) endemic to the Marquesas Islands, French polynesia. Zootaxa 3857: 433–443. https://doi.org/10.11646/zootaxa.3857.3.6

Felsenstein J (1985) Phylogenies and the Comparative Method. The American Naturalist 125: 1–15. https://doi.org/10.1086/284325

Friedlander AM, Ballesteros E, Beets J, Berkenpas E, Gaymer CF, Gorny M, Sala E (2013) Effects of isolation and fishing on the marine ecosystems of Easter Island and Salas y Gómez, Chile. Aquatic Conservation: Marine and Freshwater Ecosystems 23: 515–531. https://doi.org/10.1002/aqc.2333

Guindon S, Dufayard J-F, Lefort V, Anisimova M, Hordijk W, Gascuel O (2010) New algorithms and methods to estimate maximum-likelihood phylogenies: assessing the performance of PhyML 3.0. Systematic biology 59: 307–321. https://doi.org/10.1093/sysbio/syq010

Hubbs CL (1952) Antitropical distribution of fishes and other organisms. Symposium on problems of bipolarity and of pantemperate faunas. Proceedings of the Seventh Pacific Science Congress (Pacific Science Association) 3: 324–329.

Kalyaanamoorthy S, Minh BQ, Wong TKF, von Haeseler A, Jermiin LS (2017) ModelFinder: fast model selection for accurate phylogenetic estimates. Nature Methods 14: 587–589. https://doi.org/10.1038/nmeth.4285

Kimura M (1980) A simple method for estimating evolutionary rates of base substitutions through comparative studies of nucleotide sequences. Journal of Molecular Evolution 16: 111–120. https://doi.org/10.1007/BF01731581

Minh BQ, Nguyen MAT, von Haeseler A (2013) Ultrafast approximation for phylogenetic bootstrap. Molecular Biology and Evolution 30: 1188–1195. https://doi.org/10.1093/molbev/mst024

Nguyen LT, Schmidt HA, von Haeseler A, Minh BQ (2015) IQ-TREE: A fast and effective stochastic algorithm for estimating maximum-likelihood phylogenies. Molecular Biology and Evolution 32: 268–274. https://doi.org/10.1093/molbev/msu300

Ogilby JD (1899) Additions to the fauna of Lord Howe Island. Proceedings of the Linnean Society of New South Wales 23: 730–745.

Paradis E (2010) pegas: an R package for population genetics with an integrated-modular approach. Bioinformatics 26: 419–420. https://doi.org/10.1093/bioinformatics/btp696

R Core Team (2017) R: A Language and Environment for Statistical Computing. R Foundation for Statistical Computing, Vienna, Austria. http://www.R-project.org/

Randall JE (1976) The endemic shore fishes of the Hawaiian Islands, Lord Howe Island and Easter Island. Colloque Commerson, 1973. ORSTOM Travaux et Documents 47: 49–73. http://horizon.documentation.ird.fr/exl-doc/pleins_textes/pleins_textes_5/pt5/travaux_d/29300.pdf

Randall JE (1981) Examples of antitropical and antiequatorial distribution of Indo-West-Pacific fishes. Pacific Science 35: 197–209.

Randall JE, Cea A (2011) Shore Fishes of Easter Island. University of Hawai'i Press, 164 pp. http://books.google.com/books?hl=en&lr=&id=iXtCTSRTcb8C&pgis=1

Ratnasingham S, Hebert PDN (2007) BOLD: The Barcode of Life Data System (www.barcodinglife.org). Molecular Ecology Notes 7: 355–364. https://doi.org/10.1111/j.1471-8286.2007.01678.x

Rehder HA (1980) The marine mollusks of Easter Island (Isla de Pascua) and Sala y Gómez. Smithsonian Contributions to Zoology 289: 1–176. https://doi.org/10.5479/si.00810282.289

Tamura K, Stecher G, Peterson D, Filipski A, Kumar S (2013) MEGA6: molecular evolutionary genetics analysis version 6.0. Molecular Biology and Evolution 30: 2725–2729. https://doi.org/10.1093/molbev/mst197

Ward RD, Zemlak TS, Innes BH, Last PR, Hebert PDN (2005) DNA barcoding Australia's fish species. Philosophical Transactions of the Royal Society B: Biological Sciences 360: 1847–1857. https://doi.org/10.1098/rstb.2005.1716

Williams JT (1988) Revision and phylogenetic relationships of the blenniid fish genus *Cirripectes*. Bernice Pauahi Bishop Museum, 78 pp.

Williams JT, Delrieu-Trottin E, Planes S (2012) A new species of Indo-Pacific fish, *Canthigaster criobe*, with comments on other *Canthigaster* (Tetraodontiformes: Tetraodontidae) at the Gambier Archipelago. Zootaxa 3523: 80–88.

Williams JT, Viviani J (2016) *Pseudogramma polyacantha* complex (Serranidae, tribe Grammistini): DNA barcoding results lead to the discovery of three cryptic species, including two new species from French Polynesia. Zootaxa 4111: 246–260. https://doi.org/10.11646/zootaxa.4111.3.3

ZooKeys 810: 139–151 (2018)
doi: 10.3897/zookeys.139.25602
http://zookeys.pensoft.net

RESEARCH ARTICLE

A peer-reviewed open-access journal
ZooKeys
Launched to accelerate biodiversity research

Genetic signatures of polymorphic microsatellite loci in the Ambiguous silver pomfret, *Pampus argenteus* (Teleostei, Stromateidae)

Yuan Li[1], Long-Shan Lin[1], Tian-Xiang Gao[2,3]

1 *Third Institute of Oceanography, State Oceanic Administration, Xiamen, Fujian 361005, China* **2** *Zhejiang Provincial Key Laboratory for Technology Research on Sustainable Utilization of Marine Fishery Resources, Zhoushan, Zhejiang 316021, China* **3** *National Engineering Research Center for Marine Aquaculture, Zhejiang Ocean University, Zhoushan, Zhejiang 316022, China*

Corresponding author: *Tian-Xiang Gao* (gaotianxiang0611@163.com)

Academic editor: *Sven Kullander* | Received 7 April 2018 | Accepted 2 December 2018 | Published 20 December 2018

http://zoobank.org/43F1B8BC-F6F7-4751-8EC4-F07B72B9257B

Citation: Li Y, Lin L-S, Gao T-X (2018) Genetic signatures of polymorphic microsatellite loci in the Ambiguous silver pomfret, *Pampus argenteus* (Teleostei, Stromateidae). ZooKeys 810: 139–151. https://doi.org/10.3897/zookeys.810.25602

Abstract

Pampus argenteus is a broadly exploited pelagic fish species, commonly misidentified as *Pampus echinogaster*. Genetic variation and population structure in *Pampus argenteus* was studied based on seven microsatellite loci. The observed high average allele number, heterozygosity values, and polymorphism information content of *P. argenteus* suggested high genetic diversity. No population genetic differentiation was detected based on the results of pairwise F_{st}, three-dimensional factorial correspondence analysis (3D-FCA) and STRUCTURE analysis, which implied continuous gene flow. Wilcoxon signed rank tests did not indicate significant heterozygosity excess, and recent genetic bottleneck events were not detected. Coupled with previous mitochondrial DNA results, the findings presented here indicate that high gene flow characterizes the current phylogeographic pattern of the species.

Keywords

Genetic diversity, genetic structure, microsatellite DNA, population genetics

Introduction

Species of the genus *Pampus* Bonaparte, 1834, are mainly distributed in the Indo-West Pacific Ocean and have a rich landing yield in Kuwait, Iran, India, Malaysia, Thailand, China, Korea and Japan (Jia et al. 2004; Divya et al. 2017). Among these species, *P. argenteus* (Euphrasén, 1788) is a broadly exploited pelagic species that has a high economic value because of its highly appreciated taste. Although all species of *Pampus* are important economical species, the morphological similarity among species of *Pampus* has resulted in considerable confusion in species-level identification. *Pampus argenteus* is the most widely distributed species of the genus, and it is usually identified as *P. echinogaster* (Basilewsky, 1855) because of the morphological similarities (Li et al. 2013, 2017a). This is mainly a consequence of the absence of critical diagnostic morphological characteristics in the description by Euphrasén (1788), based on only one specimen. Li et al. (2013) collected samples of *P. argenteus* from Kuwait, Pakistan, and China and provided updated and improved morphological diagnosis and DNA barcode data. Li et al. (2017a) proposed diagnostic characteristics of *P. echinogaster*, which is significantly different from *P. argenteus*. Therefore, we speculate that *P. argenteus* is a warm-water species that is widely distributed south of the Taiwan Strait and across Indonesia to the Persian Gulf (Yamada et al. 2009; Li et al. 2013). *Pampus punctatissimus* (Temminck & Schlegel, 1845) was regarded as a synonym of *P. argenteus* by some ichthyologists (Bleeker 1852; Haedrich 1984), while a few researchers recognized differences between these species and provided a redescription of *P. punctatissimus* with a detailed morphological comparison with *P. argenteus* (Liu and Li 1998; Yamada et al. 2009; Nakabo 2013).

Pampus argenteus is a multiple batch spawner with indeterminate fecundity, and spawning starts in mid-May and continues until early October. Transformation from the larval to juvenile stage occurs at 40 days after hatching (Almatar et al. 2000). The eggs, larvae, and adults of this species are all pelagic. Although numerous investigations have been performed on *P. argenteus* (Meng et al. 2012; Peng et al. 2010a, 2010b; Zhao et al. 2010, 2011; Wu et al. 2012), many reports could actually be for *P. echinogaster*. Studies on *P. argenteus* mainly focus on its biology (Kuronuma and Abe 1972), reproductive development (Almatar et al. 2004), and resource investigations (Morgan 1985; Pillai and Menon 2000; Narges et al. 2011; Hashemi et al. 2012; Siyal et al. 2013). To date, few population genetic analyses have been conducted with reliable species identification for this species. Although some reports have described *P. argenteus* from the Atlantic-eastern Pacific (Fowler 1938; Davis and Wheeler 1985; Dulčić et al. 2004; Piper 2010; Sami et al. 2014), far from its center of distribution (the western Pacific and Indian Oceans), such identifications should be analyzed further.

Microsatellites (simple sequence repeats, SSRs) are tandemly repeated motifs of 1–6 bases characterized by a high degree of length polymorphism (Zane et al. 2002), and they are sensitive indicators of population genetic structure (Cheng et al. 2015; Song et al. 2016; Stepien et al. 2017). In previous studies, we evaluated the phylogeographical structure of *P. argenteus* by mitochondrial DNA markers, and two lineages were obtained (Li et al. 2017b). To further examine the genetic variation and population structure of *P. argenteus*, seven microsatellite loci were employed in this study, and

we aim to infer the relative role of biological characteristics and environmental factors involved in shaping the contemporary population genetic structure of this species by combining the results of mitochondrial DNA.

Materials and methods

Sample collection

A total of 119 specimens of *P. argenteus* was collected from the coastal waters of Kuwait, Pakistan, and China from 2010 until 2014 (Figure 1, Table 1). All individuals were identified based on morphological characteristics according to Yamada et al. (2009) and Li et al. (2013), and dorsal muscle tissue was excised and preserved in 95% alcohol.

DNA extraction, amplification and sequencing

Genomic DNA was isolated from muscle tissue by proteinase *K* digestion and extracted using the DNeasy Blood and Tissue Kit (Qiagen, Valencia, CA, USA). Seven microsatellite loci developed by Yang et al. (2006) were used in this study (Table 1). Tailed PCR was used to produce fluorescently labeled DNA fragments (Boutin-Ganache et al. 2001). M13R was added to the 5' end of one primer in each pair. An M13 reverse primer that is fluorescently labeled (FAM, HEX, and TAMRA) was included in the PCR, resulting in a labeled product for detection. All loci were conducted separately in a 25 μL reaction mixture containing 17.25 μL of ultrapure water, 2.5 μL of 10×PCR buffer (including $MgCl_2$), 2 μL of dNTPs, 1 μL of fluorescently labeled M13R primer and locus specific primer without tail, 1 μL of locus specific primer with M13 reverse tail, 0.25 μL of Taq polymerase, and 1 μL of genomic DNA (10 ng). All loci were initially screened using the following PCR protocol: 5 min at 94 °C; 35 cycles of 45 s at 94 °C, 45 s at 50–58 °C, and 45 s at 72 °C; and a final step of 15 min at 72 °C. The reactions were then exposed to 72 °C for 45 min and held at 4 °C until further analysis. PCR products were diluted 20 fold with ultrapure Milli-Q water before being further diluted (1 in 5) in formamide containing the LIZ-500 size standard. The samples were separated by capillary gel-electrophoresis on an ABI 3730xl automated sequencer (Applied Biosystems). To score the consistency of microsatellite fragments, nearly 20% of PCR products were restored for replication (Williams et al. 2015). Microsatellite loci genotyping from six populations were determined in GENEMARKER version 2.2.0 software (SoftGenetics, State College, PA, USA).

Data analysis

The number of alleles (N_A), observed heterozygosity (H_O) and expected heterozygosity (H_E) were estimated using POPGENE 1.32 (Yeh et al. 1999). The polymorphism information content (PIC) was calculated using the Microsoft Excel Microsatellite Toolkit

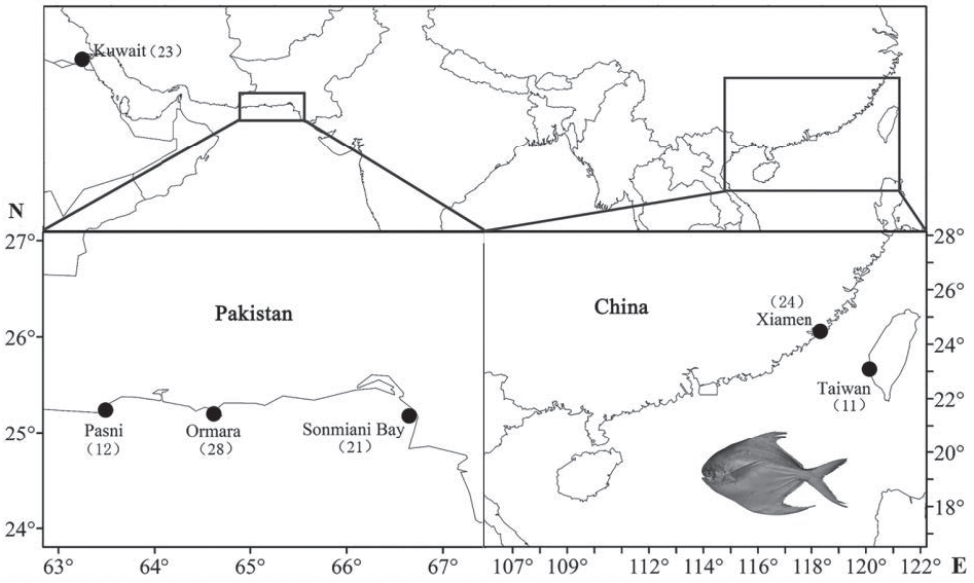

Figure 1. Locations (black circle) for sample collection of *P. argenteus.*

(Botstein et al. 1980; Raymond and Rousset 1995). GENEPOP 3.4 was used to test deviations from the Hardy–Weinberg equilibrium (HWE) and the linkage disequilibrium of each locus (Raymond and Rousset 1995). The presence of null alleles and potential scoring errors were addressed using MICRO-CHECKER 2.2.3 (Van Oosterhout et al. 2004).

FSTAT 2.9.3 (Goudent 2001) was used to calculate the allelic richness (R_S) value and assess the F_{st} values. The 3D-FCA (three-dimensional factorial correspondence analysis) was performed in Genetix version 4.05 (Belkir et al. 2004) by making no a priori assumptions about the population groupings. The $(\delta\mu)^2$ genetic distance was obtained by POPULATIONS 1.2 (Lespinet et al. 2002), and the UPGMA tree was drawn by Treeview (Page 1996).

The possibility of a cryptic population structure of *P. argenteus* was checked using STRUCTURE (Pritchard et al. 2000). Population groups were simulated from K=1 to 6, with each K run 10 independent times. Possible mixed ancestry and correlated allele frequencies were assumed, and 1,000,000 Markov chain Monte Carlo (MCMC) steps were used, with the first 100,000 steps discarded as burn-in. To estimate the most likely number of clusters (K), an *ad hoc* approach (Pritchard et al. 2000) was performed by obtaining the mean posterior probability of the data ΔK and analyzing the dataset for K=2, where the value did not increase, peak or plateau, as expected (Li and Liu 2018).

The Bottleneck 1.2.02 program (Piry et al. 1999) was implemented to detect evidence of recent bottleneck events under three mutation models, the infinite allele model (IAM), stepwise mutation model (SMM) and two-phase mutation model (TPM), where 95% single-step mutations and 5% multiple steps mutations with 1000 simulation iterations were set as recommended (Zeng et al. 2012). We also provide a graphical descriptor of the shape about the allele frequency distribution (mode-shift indicator) that differentiates bottlenecked and stable populations (Luikart et al. 1998).

Table 1. Summary statistics for the variability seven polymorphic microsatellite loci in six *P. argenteus* populations.

Location	Number of individuals	Date	Locus								Average
			Parameters	Par 03	Par 08	Par 20	Par 05	Par 12	Par 18	Par 17	
Sonmiani Bay (SO)	21	2010.12	A	19	12	10	10	15	10	13	12.71
			R_S	13.360	10.000	6.041	5.478	9.412	5.634	10.618	8.649
			H_O	0.429	0.750	0.810	0.476	0.600	0.600	0.789	0.636
			H_E	0.948	0.923	0.855	0.837	0.917	0.844	0.930	0.893
			PIC	0.920	0.892	0.815	0.798	0.885	0.800	0.898	0.858
Ormara (OR)	28	2010.12	A	18	15	12	15	16	15	16	15.29
			R_S	11.130	7.396	8.522	10.453	10.721	7.649	10.962	9.548
			H_O	0.333	0.679	0.786	0.857	0.889	0.464	0.778	0.684
			H_E	0.927	0.881	0.899	0.921	0.924	0.885	0.926	0.909
			PIC	0.904	0.852	0.872	0.897	0.899	0.856	0.902	0.883
Pasni (PS)	12	2010.12	A	11	9	8	10	14	9	13	10.57
			R_S	9.000	5.647	5.647	6.400	12.522	6.698	8.471	7.769
			H_O	0.250	0.667	1.000	0.750	0.833	0.333	0.667	0.643
			H_E	0.928	0.859	0.859	0.880	0.960	0.888	0.920	0.899
			PIC	0.879	0.805	0.800	0.828	0.914	0.833	0.871	0.847
Kuwait (KW)	23	2011.09	A	20	10	11	13	14	15	13	13.71
			R_S	13.444	3.421	6.782	6.541	9.584	8.015	8.015	7.972
			H_O	0.727	0.455	0.957	0.636	0.773	0.478	0.565	0.656
			H_E	0.947	0.724	0.871	0.867	0.916	0.895	0.895	0.874
			PIC	0.921	0.685	0.838	0.834	0.887	0.864	0.864	0.842
Taiwan (TW)	11	2012.09	A	14	10	7	11	8	9	11	10.00
			R_S	12.500	5.500	4.172	9.680	7.118	7.333	7.118	7.632
			H_O	0.500	0.727	0.636	0.727	0.455	0.545	0.545	0.591
			H_E	0.968	0.857	0.797	0.939	0.900	0.905	0.900	0.895
			PIC	0.914	0.798	0.732	0.887	0.843	0.848	0.845	0.838
Xiamen (XM)	24	2014.04	A	20	16	13	11	16	11	15	14.57
			R_S	15.781	11.755	8.229	6.227	8.417	5.409	9.600	9.345
			H_O	0.417	0.875	0.750	0.708	0.682	0.667	0.708	0.687
			H_E	0.957	0.934	0.897	0.857	0.902	0.832	0.915	0.899
			PIC	0.933	0.909	0.868	0.820	0.872	0.793	0.887	0.869

Abbreviations: A: allelic number, R_S: allelic richness, H_O: observed heterozygosity, H_E: expected heterozygosity, PIC: polymorphism information content.

Results

A total of 150 alleles were detected by seven microsatellite loci for six populations, with a range of 14 (Par 20) to 31 (Par 03) (Table 1). The N_A, *Ho*, H_E, and PIC of *P. argenteus* are shown in Table 1. All the PIC values were greater than 0.5, which suggested the high genetic diversity of this species (PIC>0.5) (Table 1). Two microsatellite loci (Par 03 and Par 05) showed deviations from the Hardy-Weinberg equilibrium in all six populations, and null alleles for these loci were also detected for these two loci. Linkage disequilibrium was not detected between pairs of loci for all populations.

The values of pairwise F_{st} showed low genetic differentiation among *P. argenteus* populations ranging from 0.001 to 0.026. Most *P*-values were not significant after sequential Bonferroni procedures except those between Kuwait (KW) and the other populations (Xiamen and Sonmiani Bay) (Table 2). The $(\delta\mu)^2$ genetic distance was obtained according to the allele frequency by POPULATION software, and the UPGMA tree was constructed by this method (Table 2). The topology of the UP-

Table 2. Pairwise F_{st} (below diagonal) and $(\delta\mu)^2$ genetic distance (above diagonal) among *P. argenteus* populations.

	SO	OR	PS	KW	TW	XM
SO		1.873	1.026	1.267	1.974	0.815
OR	0.005		1.617	1.064	1.530	2.487
PS	0.002	-0.002		0.909	0.505	0.463
KW	0.026 *	0.019	0.018		1.301	1.980
TW	-0.003	0.003	0.001	0.029		1.029
XM	0.004	0.006	0.001	0.022 *	0.010	

*indicate $P<0.05$. Abbreviations: SO: Sonmiani Bay, OR: Ormara, PS: Pasni, KW: Kuwait, TW: Taiwan, XM: Xiamen.

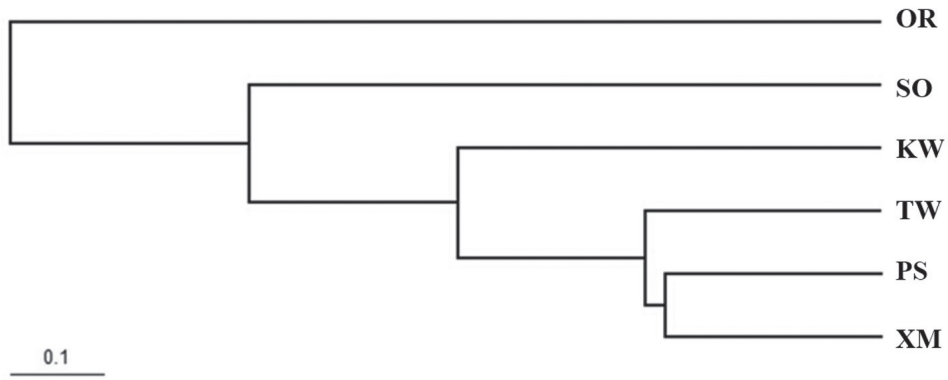

Figure 2. The UPGMA tree based on $(\delta\mu)^2$ genetic distance of six *P. argenteus* populations. Abbreviations: SO: Sonmiani Bay, OR: Ormara, PS: Pasni, KW: Kuwait, TW: Taiwan, XM: Xiamen.

GMA tree showed that *P. argenteus* populations from China, Pakistan and Kuwait coastal waters clustered together and did not relate to their geographical distributions (Figure 2).

According to the results of the 3D-FCA, the first, second and third principal components can explain 25.91%, 23.08%, and 17.92% of the overall variation, respectively (Figure 3). Individuals from population Kuwait (KW) and Taiwan (TW) showed a rather distant genetic relationship with the other four populations.

The Bayesian cluster analysis showed that the model with K=2 resulted in the highest ΔK value (Figure 4). A total of 70.8% of the sampled individuals from KW were assigned to the second cluster, while five others exhibited lower assignment probabilities to the second cluster (43.2–58.1%). Obvious differences of proportion in the two inferred clusters were not detected in the five other populations (Table 3).

The population demography analysis showed no significant heterozygosity excess observed under all three mutation models by the Wilcoxon sign-rank test ($P>0.05$), which suggested that *P. argenteus* should be in mutation-drift equilibrium (Table 4). Additionally, a normal L-shaped allele frequency distribution ('mode-shift' indicator) was detected for all six populations, suggesting population stability.

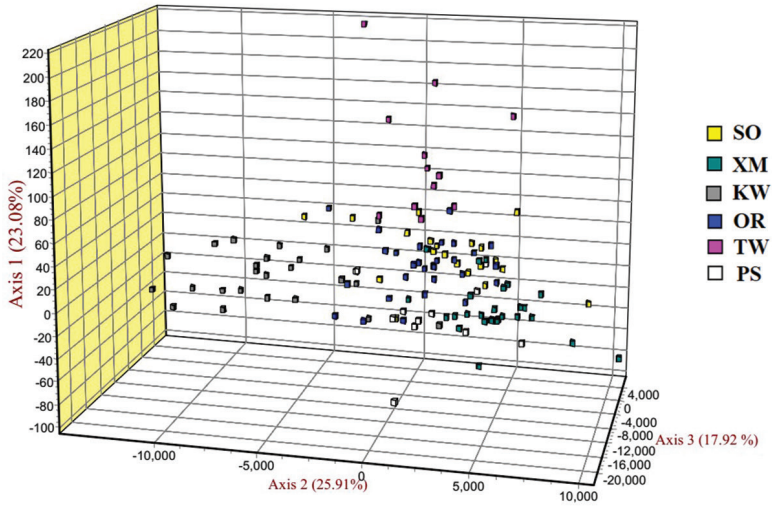

Figure 3. 3D-FCA showing relationships among six populations of *P. argenteus* based on seven microsatellite loci. Abbreviations: SO: Sonmiani Bay, OR: Ormara, PS: Pasni, KW: Kuwait, TW: Taiwan, XM: Xiamen.

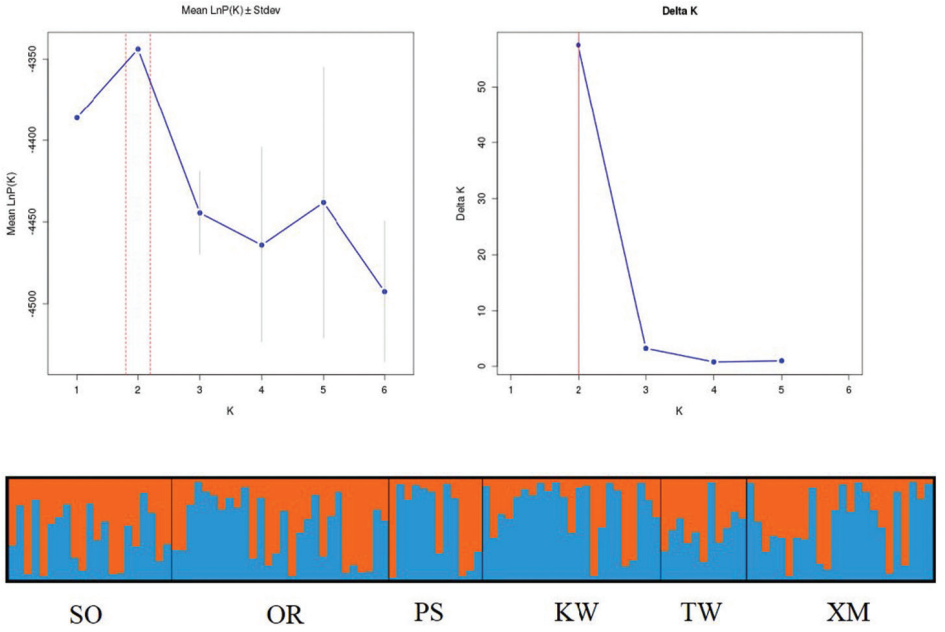

Figure 4. Results of the STRUCTURE analysis from seven microsatellite loci in *P. argenteus* (K = 2). Vertical lines are proportional to the probability of individual membership in the simulated cluster. Abbreviations: SO: Sonmiani Bay, OR: Ormara, PS: Pasni, KW: Kuwait, TW: Taiwan, XM: Xiamen.

Table 3. Proportion of six *P. argenteus* populations in each of the two inferred clusters.

Populations	Inferred clusters		Number of individuals
	1	2	
SO	0.568	0.432	21
OR	0.474	0.526	28
PS	0.419	0.581	12
KW	0.292	0.708	23
TW	0.494	0.506	11
XM	0.420	0.580	24

Abbreviatiosn: SO: Sonmiani Bay, OR: Ormara, PS: Pasni, KW: Kuwait, TW: Taiwan, XM: Xiamen.

Table 4. Results of Wilcoxon's heterozygosity excess test, Mode shift indicator for a genetic bottleneck in six *P. argenteus* populations.

Populations	Wilcoxon sign-rank test			Mode shift
	IAM	TPM	SMM	
SO	0.004	0.469	0.531	L
OR	0.004	0.531	0.711	L
PS	0.008	0.234	0.469	L
KW	0.148	0.961	0.996	L
TW	0.020	0.289	0.289	L
XM	0.004	0.004	0.945	L

Abbreviations: SO: Sonmiani Bay, OR: Ormara, PS: Pasni, KW: Kuwait, TW: Taiwan, XM: Xiamen.

Discussion

The degree of genetic variation is particularly important for the sustainability and evolution of species, and the strong correlation between genetic diversity and overall fitness has been reported (Reed and Frankham 2003; Vandewoestijne et al. 2008). Population genetic analyses could provide important insights on the genetic diversity of species and have directly informed fishery managers about the appropriate units of management (Ovenden et al. 2010; Dudgeon et al. 2012). Microsatellites are characterized by a high degree of length polymorphism (Zane et al. 2002), and they represent one of the most popular molecular markers in population genetic studies (Carlsson et al. 2004; Cheng et al. 2015). In this study, high average N_A, heterozygosity values and PIC of *P. argenteus* were detected by seven microsatellite loci, which is consistent with the mitochondrial DNA results of previous studies (Li et al. 2017b). High genetic diversity by mitochondrial DNA and microsatellite DNA may be related to a large effective population size, the immigration of new genes by the intermixing of different populations and/or low selection pressure. Although many marine organisms have been subjected to overfishing, *Pampus argenteus* presents a considerable yield, indicating a large population size. The wide distribution range of habitats indicates that *P. argenteus* faces limited natural selection pressure and can accumulate greater genetic variation. Significant excess H_O was not observed, which showed that *P. argenteus* has

not experienced bottleneck effect events. Moreover, the selection of loci with high PIC for the analysis can also lead to high genetic diversity.

Microsatellite markers have demonstrated to be highly sensitive for detecting the population structure of fish (Cheng et al. 2015; Stepien et al. 2017; Li et al. 2018). In this study, analyses based on seven microsatellite loci revealed low levels of genetic differentiation for *P. argenteus*. The Bayesian clustering analysis by STRUCTURE also suggested that the distribution proportions of two inferred clusters were not very different from each other. Similar level of genetic differentiation was detected in mitochondrial DNA (Li et al. 2017b). Marine fish populations usually show fluent gene flow and low levels of genetic differentiation because of their high dispersal potential of different life-history stages coupled with an absence of physical barriers to movement (Beheregaray and Sunnucks 2001). Physical distance has frequently been considered the main factor for isolation (Palumbi 1994). However, although long geographic distances occurred among the three countries, the expected genetic differentiation was not detected. Marine currents may play an important role in shaping the contemporary phylogeographic pattern of marine fishes (Xie and Watanabe 2007). For example, the eggs, larvae, or active adults of *Trachurus japonicus* can be transported over a long distance by the Kuroshio Current along the shelf slope of the East China Sea from areas northeast of Taiwan to the coastal waters of Japan (Cheng et al. 2015). The migratory behavior of *P. argenteus* during its entire life stage could increase the gene flow and weaken the genetic differentiation among geographic populations (Beheregaray and Sunnucks 2001).

In conclusion, high genetic homogeneity among six *P. argenteus* populations was detected, and the contemporary genetic structure of the species revealed in this study can preliminarily improve the genetic knowledge and provide a firm basis to guide fishery stock management in the Indo-Pacific Ocean. Unfortunately, only six geographical populations of *P. argenteus* were collected, which is not sufficient for an even sampling throughout its entire distribution in the Indo-Pacific Ocean. To describe the phylogeographic pattern of *P. argenteus*, additional representative populations should be collected for further analysis.

Acknowledgments

The present study could not have been performed without assistance from Dr Pengfei Li, Dr Fozia Khan Siyal, and Professor Weizhong Chen during the collection of *P. argenteus* specimens. We sincerely thank the reviewers and subject editor, whose comments greatly improved the manuscript. The work was supported by the National Natural Science Foundation of China (41776171), the International Science & Technology Cooperation Program of China (2015DFR30450), the National Programme on Global Change and Air-Sea Interaction (GASI-02-SCS-YSWspr/aut), and the Scientific Research Foundation of Third Institute of Oceanography, SOA (2016010). All authors declare that we have no conflict of interest.

References

Almatar SM, Lone KP, Abu-Rezq TS, Yousef AA (2004) Spawning frequency, fecundity, egg weight and spawning type of silver pomfret, *Pampus argenteus* (Euphrasen) (Stromateidae), in Kuwait waters. Journal of Applied Ichthyology 20: 176–188. https://doi.org/10.1111/j.1439-0426.2004.00546.x

Almatar S, Elah AA, Abu-Rezq T (2000) Larval developmental stages of laboratory-reared silver pomfret, *Pampus argenteus*. Ichthyological Research 47: 137–141. https://doi.org/10.1007/BF02684233

Beheregaray LB, Sunnucks P (2001) Fine-scale genetic structure, estuarine colonization and incipient speciation in the marine silverside fish *Odontesthes argentinensis*. Molecular Ecology 10: 2849–2866. https://doi.org/10.1046/j.1365-294X.2001.t01-1-01406.x

Belkir K, Borsa P, Chikhi L, Raufaste N, Bonhomme F (2004) GENETIX 4.05, logiciel sous Windows TM pour la génétique des populations. Laboratoire Génome, Populations, Interactions, Université de Montpellier II: Montpellier.

Bleeker P (1852) Bijdrage tot de kennis der Makreelachtige visschen van den Soenda-Molukschen Archipel. Bataviaasch Genootschap van Kunsten en Wetenschappen, 1–93.

Botstein D, White RL, Skolnick M, Davis RW (1980) Construction of a genetic linkage map in man using restriction fragment length polymorphisms. American Journal of Human Genetics 32: 314–331.

Boutin-Ganache I, Raposo M, Raymond M, Deschepper CF (2001) M13-tailed primers improve the readability and usability of microsatellite analysis performed with two different allele-sizing methods. Biotechniques 31: 24–28. https://doi.org/10.2144/01311bm02

Carlsson J, McDowell JR, Diaz-Jaimes P, Carlsson JE, Bole SB, Gold JR, et al. (2004) Microsatellite and mitochondrial DNA analyses of Atlantic bluefin tuna (*Thunnus thynnus thynnus*) population structure in the Mediterranean Sea. Molecular Ecology 13: 3345–3356. https://doi.org/10.1111/j.1365-294X.2004.02336.x

Cheng J, Yanagimoto T, Song N, Gao T (2015) Population genetic structure of chub mackerel *Scomber japonicus* in the Northwestern Pacific inferred from microsatellite analysis. Molecular Biology Reports 42: 37–382. https://doi.org/10.1007/s11033-014-3777–2

Davis P, Wheeler A (1985) The occurrence of *Pampus argenteus* (Euphrasen, 1788), (Osteichthyes, Perciformes, Stromateoidei, Stromateidae) in the North Sea. Journal of Fish Biology 26: 105–109. https://doi.org/10.1111/j.1095-8649.1985.tb04247.x

Divya PR, Mohitha C, Rahul GK, Shanis CPR, Basheer VS, Gopalakrishnan A (2017) Molecular based phylogenetic species recognition in the genus *Pampus* (Perciformes: Stromateidae) reveals hidden diversity in the Indian Ocean. Molecular Phylogenetics and Evolution 109: 240–245. https://doi.org/10.1016/j.ympev.2016.12.030

Dudgeon CL, Blower DC, Broderick D, Giles JL, Holmes BJ, Kashiwagi T, Krück NC, Morgan JAT, Tillett BJ, Ovenden JR (2012) A review of the application of molecular genetics for fisheries management and conservation of sharks and rays. Journal of Fish Biology 80: 1789–1843. https://doi.org/10.1111/j.1095-8649.2012.03265.x

Dulčić J, Jardas I, Pallaoro A, Lipeg L (2004) On the validity of the record of silver pomfret *Pampus argenteus* (Stromateidae) from the Adriatic Sea. Cybium 28: 69–71.

Euphrasén BA (1788) Beskrifning på 3:ne fiskar. Kongliga Vetenskaps-Academiens Handlingar 9: 51–55.

Fowler HW (1938) The fishes of the George Vanderbilt South Pacific Expedition 1937. Monographs of the Academy of Natural Sciences of Philadelphia 2: 1–349.

Goudent J (2001) FSTAT, Version 2.9.3: a program to estimate and test gene diversities and fixation indices. http://www.unil.ch/izea/softwares/fstat.html

Hashemi SAR, Safikhani H, Vahabnezhad A (2012) Growth, mortality parameters and exploitation rate of silver pomfret (*Pampus argenteus* Euphrasen, 1788) in Northwest of Persian Gulf (Khuzestan Coastal Waters, Iran). American Eurasian Journal of Agricultural and Environmental Sciences 12: 1095–1101. https://doi.org/10.5829/idosi.aejaes.2012.12.08.66127

Haedrich RL (1984) Stromateidae. In: Fischer W, Bianchi G (Eds) FAO Species Identification Sheets for Fishery Purposes. Western Indian Ocean (Fishing Area 51). Vol. 4. FAO, Rome.

Jia X, Li Y, Li C, Qiu Y, Gan J (2004) Environment and Fishery Resources in the Exclusive Economic Zone and the Continental Shelf of South China Sea. Science Press, Beijing, 378–380.

Kuronuma K, Abe Y (1972) Fish of Kuwait. Kuwait Institute of Scientific Research: University of California Press.

Lespinet O, Wolf YI, Koonin EV, Aravind L (2002) The role of lineage-specific gene family expansion in the evolution of eukaryotes. Genome Research 12: 1048–1059. https://doi.org/10.1101/gr.174302

Li Y, Lin L, Song N, Zhang Y, Gao T (2018) Population genetics of *Pampus echinogaster* along the Pacific coastline of China: insights from the mitochondrial DNA control region and microsatellite molecular markers. Marine and Freshwater Research 69: 971–981. https://doi.org/10.1071/MF17218

Li Y, Song N, Khan FS, Yanagimoto T, Gao T (2013) New evidence of morphological characters and DNA barcoding of *Pampus argenteus* (Euphrasen, 1788). Journal of Fisheries of China 37: 1601–1608. https://doi.org/10.3724/SP.J.1231.2013.38824

Li Y, Zhang Y, Gao T, Han Z, Lin L, Zhang X (2017a) Morphological characteristics and DNA barcoding of *Pampus echinogaster* (Basilewsky, 1855). Acta Oceanologica Sinica 36: 18–23. https://doi.org/10.1007/s13131-017-1124-x

Li Y, Zhang Y, Lin L, Gao T, Liu L (2017b) New genetic perspectives of the ambiguous pomfret as revealed by CR sequences. ZooKeys 719: 59–73. https://doi.org/10.3897/zookeys.719.19914

Li Y, Liu J (2018) Structure selector: A web based software to select and visualize the optimal number of clusters using multiple methods. Molecular Ecology Resources 18: 176–177. https://doi.org/10.1111/1755-0998.12719

Liu J, Li C (1998) Redescription of a stromateoid fish *Pampus punctatissimus* and comparison with *Pampus argenteus* from Chinese coastal waters. Chinese Journal of Oceanology and Limnology 16: 161–166. https://doi.org/10.1007/BF02845182

Luikart G, Allendorf FW, Sherwin B, Cornuet JM (1998) Distortion of allele frequency distributions provides a test for recent population bottlenecks. Journal of Heredity 12: 238–247. https://doi.org/10.1093/jhered/89.3.238

Meng Y, Zhang L, Zhao F, Shi Z, Zhuang P (2012) Prelimary study on the genetic diversity of four geographic populations of silver pomfret (*Pampus argenteus*). Marine Fishery 37: 48–52.

Morgan GR (1985) Stock assessment of the pomfret (*Pampus argenteus*) in Kuwaiti waters. ICES Journal of Marine Science 42: 3–10. https://doi.org/10.1093/icesjms/42.1.3

Nakabo T (2013) Stromateidae. In: Nakabo T (Ed.) Fishes of Japan with Pictorial Keys to the Species, Third Edition. Kanagawa: Tokai University Press, 1079–1080.

Narges A, Preeta K, Jasem M, Gholam-reza E, Vahid Y (2011) Stock assessment of silver pomfret *Pampus argenteus* (Euphrasen, 1788) in the Northern Persian Gulf. Turkish Journal of Fisheries and Aquatic Sciences 11: 63–65. https://doi.org/10.4194/trjfas.2011.0109

Ovenden JR, Morgan J, Kashiwagi T, Broderick D, Salini J (2010) Towards better management of Australia's shark fishery: genetic analyses reveal unexpected ratios of cryptic blacktip species *Carcharhinus tilstoni* and *C. limbatus*. Marine and Freshwater Research 61: 253–262. https://doi.org/10.1071/MF09151

Page RDM (1996) TREEVIEW: an application to display phylogenetic trees on personal computers. Computer Applications in the Biosciences Cabios 12: 357–358.

Palumbi SR (1994) Genetic divergence, reproductive isolation, and marine speciation. Annual Review of Ecology and Systematics 25: 547–572. https://doi.org/10.1146/annurev.es.25.110194.002555

Peng S, Shi Z, Hou J (2010a) Comparative analysis on the genetic diversity of cultured and wild silver pomfret populations based on mtD-loop and COI gene. Journal of Fisheries of China 34: 19–25. https://doi.org/10.3724/SP.J.1231.2010.06384

Peng S, Shi Z, Chen C, Hou J (2010b) Genetic diversity analysis of silver pomfret (*Pampus argenteus*) in the East China Sea based on mtDNA D-loop sequence. Marine Science 34: 28–32.

Pillai VN, Menon NG (2000) Marine Fisheries Research and Management. India: Central Marine Fisheries Research Institute, 364–373.

Piper R (2010) Re-occurrence of silver pomfret *Pampus argenteus* in the North Sea. Marine Biodiversity Record 3: e102. https://doi.org/10.1017/S175526721000093X

Piry S, Luikart G, Cornuet JM (1999) Bottleneck: a computer program for detecting recent reductions in the effective population size using allele frequency data. Journal of Heredity 90: 502–503. https://doi.org/10.1093/jhered/90.4.502

Pritchard JK, Stephens M, Rosenberg NA, Donnelly P (2000) Association mapping in structured populations. American Journal of Human Genetics 67: 170–181. https://doi.org/10.1086/302959

Raymond M, Rousset F (1995) GENEPOP: Population genetics software for exact test and ecumenism. Journal of Heredity 86: 248–249. https://doi.org/10.1093/oxfordjournals.jhered.a111573

Reed DH, Frankham R (2003) Correlation between fitness and genetic diversity. Conservation Biology 17: 230–237. https://doi.org/10.1046/j.1523-1739.2003.01236.x

Sami M, Rym E, Othman J, Hechmi M (2014) First record of *Pampus argenteus* (Euphrasen, 1788) (Osteichthyes: Stromateidae) in the Tunisian coast (Mediterranean Sea). Journal of Marine Biology and Oceanography 3: 1–2. https://doi.org/10.4172/2324-8661.1000123

Siyal FK, Li Y, Gao T, Liu Q (2013) Maximum sustainable yield estimates of silver pomfret, *Pampus argenteus* (Family: Strometidae [sic]) fishery in Pakistan. Pakistan Journal of Zoology 45: 447–452.

Song N, Liu M, Yanagimoto T, Sakurai Y, Han Z, Gao T (2016) Restricted gene flow for *Gadus macrocephalus* from Yellow Sea based on microsatellite markers: geographic block of Tsushima Current. International Journal of Molecular Science 17: 46. https://doi.org/10.3390/ijms17040467

Stepien CA, Karsiotis SI, Sullivan TJ, Klymus KE (2017) Population genetic structure and comparative diversity of smallmouth bass *Micropterus dolomieu*: congruent patterns from two genomes. Journal of Fish Biology 90: 2125–2147. https://doi.org/10.1111/jfb.13296

Vandewoestijne S, Schtickzelle N, Baguette M (2008) Positive correlation between genetic diversity and fitness in a large, well-connected metapopulation. BMC Biology 6: 46. https://doi.org/10.1186/1741-7007-6-46

Van Oosterhout C, Hutchinson WF, Wills DPM, Shipley P (2004) MICRO-CHECKER: Software for identifying and correcting genotyping errors in microsatellite data. Molecular Ecology Resource 4: 535–538. https://doi.org/10.1111/j.1471-8286.2004.00684.x

Williams SM, Bennett MB, Pepperell JG, Morgan JAT, Ovenden JR (2015) Spatial genetic subdivision among populations of the highly migratory black marlin *Istiompax indica* within the central Indo-Pacific. Marine and Freshwater Research 67: 1205–1214. https://doi.org/10.1071/MF14370

Wu R, He X, Zhuang Z, Liu S (2012) Mitochondrial COI sequence variation of silver pomfret (*Pampus argenteus*) from Chinese coastal waters. Acta Zootaxonomica Sinica 37: 480–488.

Xie S, Watanabe Y (2007) Transport-determined early growth and development of jack mackerel *Trachurus japonicus* juveniles immigrating into Sagami Bay. Marine and Freshwater Research 58: 1048–1055. https://doi.org/10.1071/MF06165

Yamada U, Tokimura M, Hoshino K, Deng S, Zheng Y, Li S, Kim Y, Kim J (2009) Name and Illustrations of Fish from the East China Sea and the Yellow Sea – Japanese-Chinese-Korean – Tokyo. Overseas Fishery Cooperation Foundation of Japan, 525–528.

Yang W, Li J, Yue G (2006) Multiplex genotyping of novel microsatellites from silver pomfret (*Pampus argenteus*) and cross-amplification in other pomfret species. Molecular Ecology Notes 6: 1073–1075. https://doi.org/10.1111/j.1471-8286.2006.01438.x

Yeh FC, Yang R, Boyle T (1999) POPGENE version 1.32, Microsoft Windows-based freeware for population genetic analysis. University of Alberta and Centre for International Forestry Research, Alberta, Canada.

Zane L, Bargelloni L, Patarnello T (2002) Strategies for microsatellite isolation: a review. Molecular Ecology 11: 1–16. https://doi.org/10.1046/j.0962-1083.2001.01418.x

Zeng L, Cheng Q, Chen X (2012) Microsatellite analysis reveals the population structure and migration patterns of *Scomber japonicus* (Scombridae) with continuous distribution in the East and South China Seas. Biochemical Systematics and Ecology 42: 83–93. https://doi.org/10.1016/j.bse.2012.02.014

Zhao F, Dong Y, Zhuang P, Zhang T, Zhang L, Shi Z (2011) Genetic diversity of silver pomfret (*Pampus argenteus*) in the Southern Yellow and East China Seas. Biochemical Systematics and Ecology 39: 145–150. https://doi.org/10.1016/j.bse.2011.02.002

Zhao F, Shi Z, Zhuang P (2010) Advances on reproductive biology and artifcial breeding technology of silver pomfret, *Pampus argenteus*. Marine Science 34: 90–96.